Universidade de Aveiro Departamento de Ambiente e Ordenamento
2009

Helena Margarida Gonçalves de Oliveira Martins

Estrutura urbana e qualidade do ar

Exploring the links between urban structure and air quality

Universidade de Aveiro Departamento de Ambiente e Ordenamento
2009

Helena Margarida Gonçalves de Oliveira Martins

Estrutura urbana e qualidade do ar

Exploring the links between urban structure and air quality

Dissertação apresentada à Universidade de Aveiro para cumprimento dos requisitos necessários à obtenção do grau de Doutor em Ciências Aplicadas ao Ambiente, realizada sob a orientação científica da Doutora Ana Isabel Miranda, Professora Associada do Departamento de Ambiente e Ordenamento da Universidade de Aveiro.

Apoio financeiro da Fundação para a Ciência e Tecnologia (FCT) e do Fundo Social Europeu (FSE) no âmbito do III Quadro Comunitário de Apoio pela Bolsa de Doutoramento Refª SFRH/BD/13581/2003.

Para a Rita e o João.

Para os meus Pais.

o júri

presidente

Doutor João Manuel Nunes Torrão
Professor Catedrático do Departamento de Línguas e Culturas da Universidade de Aveiro

Prof. Paulo Manuel Neto da Costa Pinho
Professor Catedrático da Faculdade de Engenharia da Universidade do Porto

Prof. Jose Antonio Souto Gonzalez
Professor Contratado do Departamento de Enxeñaría Química da Universidade de Santiago de Compostela

Prof. Ana Isabel Miranda
Professora Associada do Departamento de Ambiente e Ordenamento da Universidade de Aveiro

Prof. Jorge António Oliveira Afonso de Carvalho
Professor Associado Convidado da Secção Autónoma de Ciências Sociais, Jurídicas e Políticas da Universidade de Aveiro

Prof. Tiago Alexandre Abranches Teixeira Lopes Farias
Professor Auxiliar com Agregação do Instituto Superior Técnico da Universidade Técnica de Lisboa

Prof. Dr. Manuel Joaquim Sabença Feliciano
Professor Equiparado a Assistente do 2º Triénio do Departamento de Ambiente e Recursos Naturais do Instituto Politécnico de Bragança

Prof. Dr. Carlos Alberto Diogo Soares Borrego
Professor Catedrático do Departamento de Ambiente e Ordenamento da Universidade de Aveiro

agradecimentos

Disseram-me que seria melhor fazê-los, porque é assim que manda a tradição. Pensei em não o fazer… por escrito. Não quer isto dizer que não tenha a quem agradecer, muito pelo contrário. Pensei antes em fazê-lo pessoalmente, e a alguns o tenho feito durante este percurso.

E como se agradece àqueles para quem as palavras não são suficientes?

Até já…

palavras-chave Estrutura urbana, qualidade do ar, modelação atmosférica

resumo

A poluição atmosférica constitui actualmente um grave problema ambiental cujos efeitos se fazem sentir a diversas escalas, desde os efeitos imediatos e de longo termo na saúde humana e nos materiais, até fenómenos regionais, como a acificação, e fenómenos globais que durante este século poderão alterar as condições de vida no globo.

Apesar da redução das emissões de poluentes atmosféricos, conseguida através do uso de combustíveis mais limpos e tecnologias mais eficientes, as áreas urbanas continuam a evidenciar sinais de degradação ambiental. Para ser bem sucedida a cidade deve enfrentar as três dimensões da sustentabilidade: social, económica e ambiental.

O modo de utilização do solo numa zona urbana é uma característica fundamental da cidade, com influência directa no seu desempenho ambiental e na qualidade de vida que proporciona à população.

O presente trabalho explora a ligação entre a estrutura urbana e a qualidade do ar, um dos muitos aspectos do desenvolvimento urbano sustentável.

A perspectiva histórica sobre o desenvolvimento urbano, a poluição atmosférica e a sua interligação é abordada, bem como o trabalho de investigação que tem vindo a ser conduzido na área.

A aplicação de um sistema de modelação atmosférico a um caso de estudo idealizado demonstra a importância da estrutura espacial da cidade na sustentabilidade urbana, mostrando que cidades compactas com usos do solo misturados promovem uma melhor qualidade do ar quando comparadas com cidades dispersas, com baixa densidade populacional.

De modo a explorar a relação entre a estrutura urbana e a qualidade do ar numa zona urbana real, a região urbana do Porto é identificada como um caso de estudo adequado, e o processo de crescimento urbano nas últimas décadas é analisado, assim como os níveis de qualidade do ar da região.

De modo a definir a configuração do sistema de modelação mais adequada para a região de estudo, são efectuados diversos testes de sensibilidade com o modelo meteorológico. Relativamente ao modelo de qualidade do ar, é descrito e implementado um conjunto de acções de modo a melhorar o desempenho do modelo para a simulação das concentrações de poluentes na atmosfera urbana, no contexto de alterações do uso do solo.

Finalmente, são desenvolvidos e testados, através da aplicação do sistema de modelação, dois cenários alternativos de desenvolvimento urbano para a área de estudo. Estes cenários alternativos implicam diferentes emissões de poluentes e diferentes distribuições espaciais dessas emissões, e como consequência, diferentes níveis de qualidade do ar.

O estudo permite concluir que alterações nos padrões de uso do solo em áreas urbanas conduzem a alterações na meteorologia, emissões e qualidade do ar. As áreas urbanas dispersas, quando comparadas com estruturas urbanas compactas são responsáveis por temperaturas mais elevadas, emissões de poluentes para a atmosfera mais elevadas e maiores concentrações de poluentes.

keywords Urban structure, air quality, atmospheric modelling

abstract

Air pollution is enacted on all geographical and temporal scales, ranging from urban problems related to immediate and long-term effects on human health and material damage, over regional phenomena like acidification with a time horizon of decades, to global phenomena, which over this century may change living conditions in the entire globe.

Urbanization is certainly the future but a question mark hangs over what kind of future the city can look forward to. For it to be successfully realized, the city must tackle the dimensions of sustainability: social, economic and environmental.

In this study the link between urban structure and air quality, one of the many aspects of sustainable urban development, is explored. It starts by addressing the historical perspective on the subject, the currents of thought, and briefly refers the most important work conducted during the last decades in this field.

The application of a modelling system to an idealized study case demonstrates the importance of the city spatial structure on urban sustainability, showing that compact cities with mixed land-use provide better air quality compared to disperse cities with lower densities and segregated land-use or network cities equipped with intensive transport structures.

In order to explore the relation between urban structure and air quality in a real urban area, the Porto urban region is identified as a suitable subject for this study, and its process of urban growth in the last decades is analyzed, as well as the current air quality levels in the region.

Before proceeding to the atmospheric simulation it is firstly necessary to assemble an adequate modelling system. A series of meteorological modelling sensitivity tests are performed in order to define the most suitable meteorological model configuration for the study area. Regarding air quality modelling, a series of improvements are described and implemented in order to increase the model‘s performance in the simulation of air pollutant concentrations.

Finally, two alternative urban development scenarios for the study area are developed and tested through the application of the selected atmospheric modelling system. These alternative land use scenarios imply different emission totals and a different spatial distribution of emissions, and, as a consequence, different air quality levels.

In conclusion, it seems clear that changes in land use patterns in urban areas lead to changes in meteorology, emissions, air quality, and population exposure. The signal of the change is also clear: sprawling urban areas, when compared to contained urban development, are responsible for higher temperatures, higher emissions of pollutants to the atmosphere, and higher atmospheric pollutant concentrations.

Cities convey something special about civilization itself
that should not be reduced to banal, lifeless, endless sprawl.
Bob Giddings

TABLE OF CONTENTS

LIST OF FIGURES

LIST OF TABLES

1 INTRODUCTION

It is an indisputable fact that much has been done in the last decades to improve the quality of the air we breathe and live in. Policies, technology and increasing public awareness have taken us to an unprecedented level of protection. On the other hand, it is also a fact that not only our cities but also our countryside continue to show worrying and troubling signs of environmental stress, of which air pollution is one of many.

Air pollution is enacted on all geographical and temporal scales, ranging from urban problems related to immediate and long-term effects on human health and material damage, over regional phenomena like acidification and eutrophication with a time horizon of decades, to global phenomena, which over this century can change living conditions in the entire globe [Fenger, 1999]. Urban areas play a key-role in all these scales since they act as air pollution sources.

In 1900, 14% of the world's population lived in cities; fifty years later, the proportion had risen to 30%, and by 2003 to 48%. In 1900 there were 12 cities with one million inhabitants or more, and in 2000 there were 411 cities; today half the world's population lives in cities, 40 of them of up to 5 million inhabitants, also called mega-cities [UN, 2001, 2004]. In Europe, approximately 75% of the population lives in urban areas [EEA, 2006a]. The predictions are that by 2030, 60% of the population will be urban [UN, 2004]. Envisioning such a future is no easy matter.

Urbanization is certainly the future, but a question mark hangs over what kind of future the city can look forward to. To be successful, the city must tackle the dimensions of sustainability: social, environmental, as well as economic (and as some argue, cultural). Sustainable cities ensure well-being and a good quality of life for citizens, are environmentally friendly, and socially integrated and just.

The essence of cities is that they have always contained a myriad of diverse and intense connections and activities, where people live, work, shop and play, meeting the needs of economic production and

social reproduction [Smith, 2002]. The last two centuries have seen a transformation of cities from being relatively contained, to becoming widespread over kilometres of semi-suburban semi-rural land with commercial areas, office parks and housing developments that constitute neither city nor countryside. People often live miles from where they work, shop or go for leisure activities. This type of urban development has been named urban sprawl, and has its origins from the rapid low-density outward expansion of the United States of America cities in the beginning of the 20th century [Williams *et al.*, 2000]. In Europe, cities have traditionally been much more compact; however urban sprawl is now also a European phenomenon [EEA, 2006a; Kasanko *et al.*, 2006; Catalán *et al.*, 2008].

Historically, urban dispersion rose from the struggle against the 19th century industrial cities, which were congested, polluted, and foci of crime and disease [Neuman, 2005]. After that, the growth of cities has been driven by the growth of population; however, in Europe today there is little or no population growth, while sprawl shows no signs of slowing down. A variety of factors such as the negative environmental (pollution and noise) and social factors (poverty and insecurity) related to city cores, rising living standards, changing living preferences, and a new mobility paradigm are now driving sprawl [EEA, 2006a; Catalán *et al.*, 2008].

Since the mid-1950's, European cities have expanded on average by 78% whereas the population has grown by only 33%; also, more than 90% of the new residential areas are low density areas; inevitably European cities have become much less compact [Kasanko *et al.*, 2006]. According to the EEA's report on sprawl [2006a], the areas with the most visible impacts of urban sprawl are found in countries or regions with high population density and economic activity, such as Belgium, the Netherlands, or the Paris region, and/or rapid economic growth, such as Portugal, Ireland, and eastern Germany. In fact, Portugal is identified as presenting some of the highest sprawl growing rates, focused around major cities and in the coast. In Figure 1.1 it is possible to observe the Portuguese urban development polarized around the two metropolitan areas of Lisboa and Porto, and along the coastline.

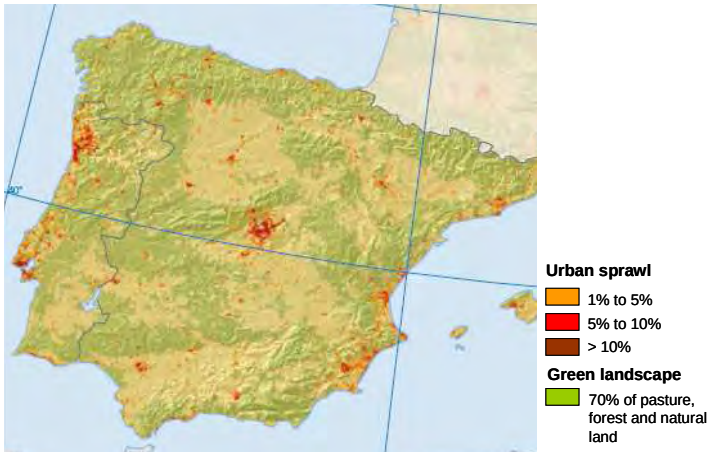

Figure 1.1 Polarised urban sprawl around major cities in the Iberian Peninsula (1990-2000) [EEA, 2006a].

The impacts of sprawl on natural areas are significant, impairing the land ability as a habitat for natural species, a source of food, recreation, water retention and storage. Even where the advance of urban land on natural areas is minimised, the indirect fragmentation impacts of transport and other urban related infrastructure developments create barrier effects that degrade the ecological functions of natural habitats [EEA, 2006a].

Urban development involves a substantial consumption of numerous natural resources, from which land and soil are the most evident. The capacity of soil to perform essential functions is dramatically reduced through loss of water permeability, loss of soil biodiversity and reduction of the capacity to act as a carbon sink. In addition, rainwater which falls on non-permeable soil is heavily polluted by particulate matter and heavy metals.

A further consequence of sprawl is the growing consumption of energy. Generally, compact urban areas, with higher population densities, are more energy efficient. Evidence from a number of studies [Newman and Kenworthy, 1999; Cameron *et al.*, 2003; EEA, 2006a] suggests that high energy consumption rates are associated with lower population densities, characteristic of sprawling environments. The extension of built-up areas is increasing mobility flows and increasing the distances covered. Transport related energy consumption in cities seems to increase as density falls [Newman and Kenworthy 1989a, 1989b; Newman, 1992; Breheny *et al.*, 1998; Cameron *et al.*, 2004], since the sprawling city is dominated by individual car use, which in turn, and in spite of the technological progress, leads to an increase of atmospheric emissions.

Problems with air pollution in urban areas have been known for long, but the attitude towards them was ambiguous since they were considered as a symbol of growth and prosperity. Nowadays, poor environmental management in general, noise, heavy traffic and congestion, poor air quality, and lack of strategic planning have lead to a perceived degradation of the urban environment. Not surprisingly, "pollution in towns and cities" is the issue Europeans most think of when talking about *Environment* [TNS, 2005]. Regarding air quality, 44% of Europe's urban citizens are exposed to air pollution levels that exceed the European Union quality objectives for tropospheric ozone, 14% for nitrogen dioxide and nearly all for particulate matter. It is estimated that approximately 20 million Europeans suffer from respiratory problems linked to air pollution [COM(2004)60 final]. As an example, Figure 1.2 presents PM10 (particulate matter with an equivalent aerodynamic diameter of less than 10 micrometers) annual average concentrations for Europe in 2005. The colours red and purple refer to values above the PM10 annual limit value (40 $\mu g.m^{-3}$), showing up at the Po Valley in Italy, and urban centres in some of the Balkan countries, Poland, Slovakia, Spain and Portugal.

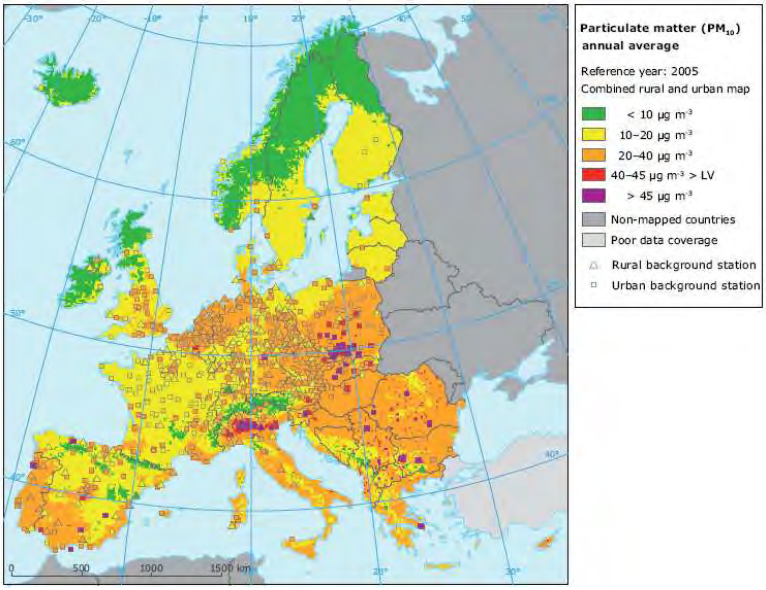

Figure 1.2 Map of PM10 annual averages for 2005, presented as spatial interpolated concentration fields and measured values at single monitoring sites [URL1].

Since the world's cities are the heart of most of the human activities, the major consumers of natural resources, and the major producers of pollution, it is obvious that the sustainability debate has an urban focus [Breheny, 1992a]. If cities are the source of the problem they must also be part of the solution.

In response to environmental sustainability issues, urban planners have focused their attention on the types of urban structure that will best serve our growing cities. In this thesis, by urban structure is understood not only the morphologic structures of the city, represented by its key-structures (road and rail networks, ports and airports, telecommunications and social infrastructures), but also the way how residential, industrial, services and recreational land uses are distributed throughout the city.

As Newton [1997] so well wrote, the city is a villain, a victim and a white knight with respect to air quality. A villain since its transport, residences and industries consume enormous amounts of energy, emitting enormous quantities of air pollutants and therefore contributing significantly to urban air pollution. A victim because its residents and image are affected negatively by the atmospheric pollution, which reduces the quality of life and health as well as the attractiveness of the city to tourists and potential new business and residents. But the city can also be a white knight since changes in its structure and development may lead to a substantial reduction of traffic, energy consumption and air pollutants levels.

For many years planners complained not of low-density settlements, but of high-density built environments. The low density urban developments derived from strong criticisms of crowding and pollution in the 19th century's industrial cities. Conversely, decades latter, the desire for the compact

city resurfaced after the myriad of problems associated with the dispersed form. Today, sprawling cities are the ones being rejected and classified as unhealthy and unsustainable, and the logical answer now seems to be compactness [Catalán et al., 2008].

Debates on the urban structure have become strongly polarized between the advocates and opponents of the compact and of the dispersed or sprawled city. Today it is widely accepted by the scientific community that there is a relation between the city's form, size, density and land use, and its sustainability; however, the consensus about the exact nature of this relation has not yet been reached [Williams *et al.*, 2000].

As it will be shown, several empirical and modelling studies have been performed, integrating land use, transport issues and even emissions, and its relationship with urban structure; however, few were found that explore the connection to air quality.

This brings us to the central concern of this thesis. Does energy inefficiency and increased emissions lead to a worst air quality in sprawling cities? Do compact cities, with mixed land uses, promote a better air quality?

In this study the link between urban structure and air quality, one of the many aspects of sustainable urban development, is explored. The topic is addressed according to the methodology presented in Figure 1.3.

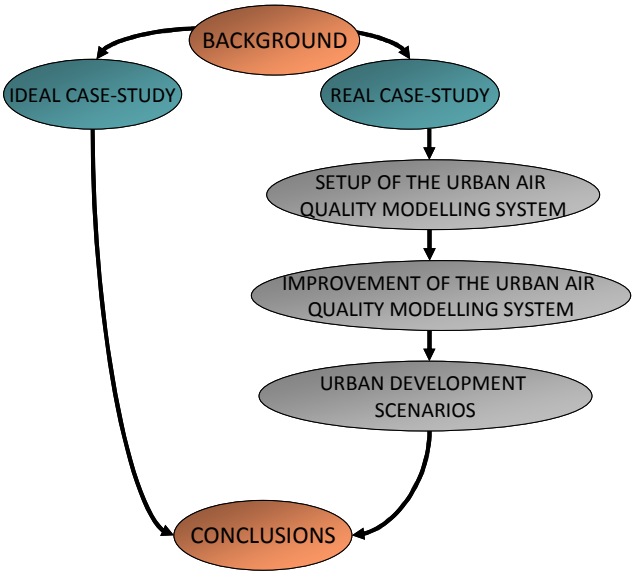

Figure 1.3 Methodology developed for the study of the relationship between urban structure and air quality.

First, the scientific and policy background is discussed; afterwards to answer the questions above, a two-folded study is conducted through the development of two case-studies, for which advanced atmospheric modelling tools are applied. As a first modelling approach, an idealized case-study is selected, based on typical city configurations. Then, to thoroughly explore the air quality

consequences of different urban land use scenarios under different meteorological conditions, the study of a real urban area is undertaken. For that purpose an air quality modelling system is implemented and improved, through the execution of a group of sensitivity tests. Finally, two urban development scenarios are defined and studied making use of the implemented modelling system, allowing the full assessment of the air quality impacts of distinct urban planning strategies.

This document is organized as follows. Chapter 2 presents the scientific background on the subject, characterizing the current state of knowledge on urban structure and its relation to energy consumption, emissions and air quality. It addresses the historical perspective, the currents of thought, and briefly refers the most important work conducted during the last decades. It also provides the state-of-the-art on atmospheric modelling tools available to further explore the topic.

In Chapter 3, this thesis first modelling application to investigate the influence of urban structure on air quality is presented. A mesoscale photochemical modelling system is applied to three idealized and distinct city structures, for an episodic air pollution situation, allowing the comparison of air quality levels in each urban structure.

In order to explore the relationship between urban structure and air quality in a real urban area, the Porto urban region is identified, in Chapter 4, as a suitable area for this study. Its process of urban growth in the last decades and the current air quality levels in the region are analysed. The modelling system selected for the air quality simulations is also presented and described.

Before proceeding to the atmospheric simulation it is firstly necessary to establish an adequate modelling system. In Chapter 5, a series of meteorological modelling sensitivity tests are performed, and their meteorological outputs are then fed into the air quality model in order to define the most suitable modelling configuration for the study area.

Chapter 6 describes and implements a series of improvements in the urban air quality modelling system, aiming to increase the model‘s performance in the simulation of air pollutant concentrations in the urban study area considering land use related aspects.

In Chapter 7, two alternative urban development scenarios for the study area are defined and tested through the application of the improved atmospheric modelling system. These alternative land use scenarios imply different emission totals and different emission spatial distribution and, as a consequence, different air quality levels.

Finally, Chapter 8 presents the main findings from the study cases and discusses them in the context of the main research questions identified throughout this thesis. The innovative character of the study is highlighted, as well as its limitations and future research.

2 SCIENTIFIC AND POLICY BACKGROUND

This chapter presents the scientific and policy background on the subject of the thesis - the relationship between urban structure and air quality - without forgetting energy consumption, traffic and pollutant emissions. Here the birth and growth of cities is briefly addressed, with a special attention to urban planning aspects related to urban structure. Next, the issue of urban air pollution is introduced, as well as the main air pollution problems that European cities are facing, and the European policies on the matter. The state-of-the-art on atmospheric modelling tools available to further explore the subject is also addressed. The most important research studies covering the relation between urban planning and air pollution during the last decades are then reviewed.

2.1 Urban planning

When the first cities emerged, they were created having defence in mind, resulting in compact forms of settlement [Thinh *et al.*, 2002]. With the advent of industrialization first and transport systems later, urban structures have changed dramatically, with an unprecedented process of urbanization that has persisted so far.

2.1.1 Brief history of the city

Early humans led a nomadic existence, relying on hunting and gathering for sustenance. In southern Mesopotamia, around 4000 B.C., the abundance of food, a system of writing, and a more complex social organization allowed cities to develop. This area, between the Tigris and the Euphrates rivers, has often been named the cradle of civilization, home of the world's first cities. It was the two rivers that became the basis upon which the wealth of the region was based, allowing a relatively easy irrigation of the land and yielding heavy crops [URL2].

The ever existing diversity of urban forms is connected to the functions that cities perform: centres of storage, trade, and manufacture, often founded at the intersections of transportation routes, or near rivers and oceans. Ancient cities displayed both regular and irregular types of urban form: the constrained area devoted to the activities of the elite (religious, political, and military) was often highly planned and regular in form, whereas residential areas often grew by a slow process of build-up, producing complex and irregular patterns [Saraiva, 2007].

During the Roman period a number of cities were created; theses were carefully planed, generally in flat areas, square or rectangle shaped [Saraiva, 2007]. After the fall of the Roman Empire, European cities became smaller and unplanned; medieval cities are usually associated with narrow winding streets converging on a market square with a cathedral and city hall.

In the Renaissance, architects began to study the shaping of urban space, in the search for a functional order. Parts of old cities were rebuilt to create elegant squares, long street views, and symmetrical building arrangements. The baroque city is characterized by large dimensions: palaces, long avenues, radial street networks, monumental squares, geometric parks and gardens.

With the Industrial Revolution cities changed dramatically. Technological innovations powered profound impacts on urban form: rail tracks, cable and electric cars converged on the centre of the city, and the development in communications allowed formerly concentrated urban activities to disperse across a wider area. The city centre contained the business district, defined by large office buildings and the first shopping establishments, as well as factories and storehouse structures. In the beginning, the working class lived in crowded neighbourhoods close to the city centre, but latter the increasing crowding, pollution, and disease originated the desire to escape to healthier environments in the outskirts of the city.

Today cities are made up of two distinct parts: an inner zone or city centre, and the suburbs. In the centre two distinct realities co-exist: the office buildings, mainly administrative and finance related rather than manufacturing; and a neglected large group of old mixed-use and residential buildings which are home to the low-income families and elderly, many times characterized by crime and social problems, and inadequate housing. These inner city areas were left behind by a massive migration to the suburbs, which began in the late 19th century but accelerated in the 1920s with the generalization of motorized transport.

2.1.2 Urban planning perspectives

People have imagined ideal cities since ever; urban planners in particular have directed their attention to the types of urban structure that can provide a greater quality of life and environmental protection.

In the 20th century, Le Corbusier, Frank Lloyd Wright, and other architects have designed cities on paper, many times proposing radical changes in the form of the city [Kuhn, 2003]. Le Corbusiers's 'Radiant City' and Frank Lloyd Wright's 'Broadacre City' represent two extremes in a broad spectrum between urban density and dispersal.

Le Corbusier (1887-1965) proposed high-density urban areas, with high office and apartment buildings, detached from the traffic lines, and placed within green open spaces (Figure 2.1). Different land uses would be located in separate districts, with distinct functions - residential, commercial areas, churches - forming a geometric pattern with a sophisticated transit system [Saraiva, 2007].

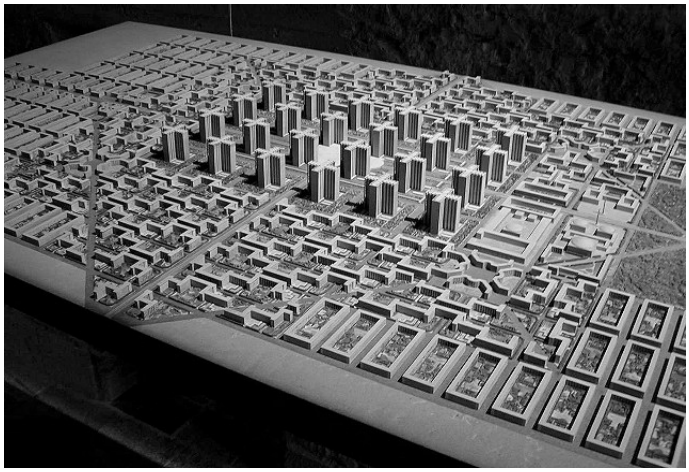

Figure 2.1 Le Corbusier "City for three million people" [URL3].

In opposition, Frank Lloyd Wright (1867-1959) defended the need for a closer contact with nature, and defended decentralized low-density cities, composed of single-family homes on large pieces of land, small farms, light industry, orchards, recreation areas, and other urban facilities [Saraiva, 2007; Kuhn, 2003]. In Broadacre City each family would be given one acre (4000 m²) of land, and travel needs would be almost entirely dependent on the automobile (Figure 2.2).

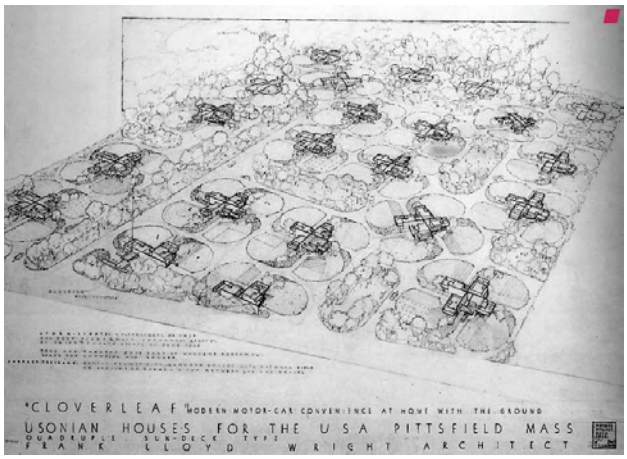

Figure 2.2 Frank Lloyd Wright "Broadacre City Plan" [URL4].

Ebenezer Howard (1850-1928) proposed the association between the advantages of the city and the country, in what he named a garden city (Figure 2.3), arranged in several concentric circles. He established an ideal number of 32 000 inhabitants, and each time the number was exceeded, a new nucleus should be formed. Each town would be surrounded by a belt of agricultural land, preventing the town from growing into adjacent countryside [Breheny, 1996].

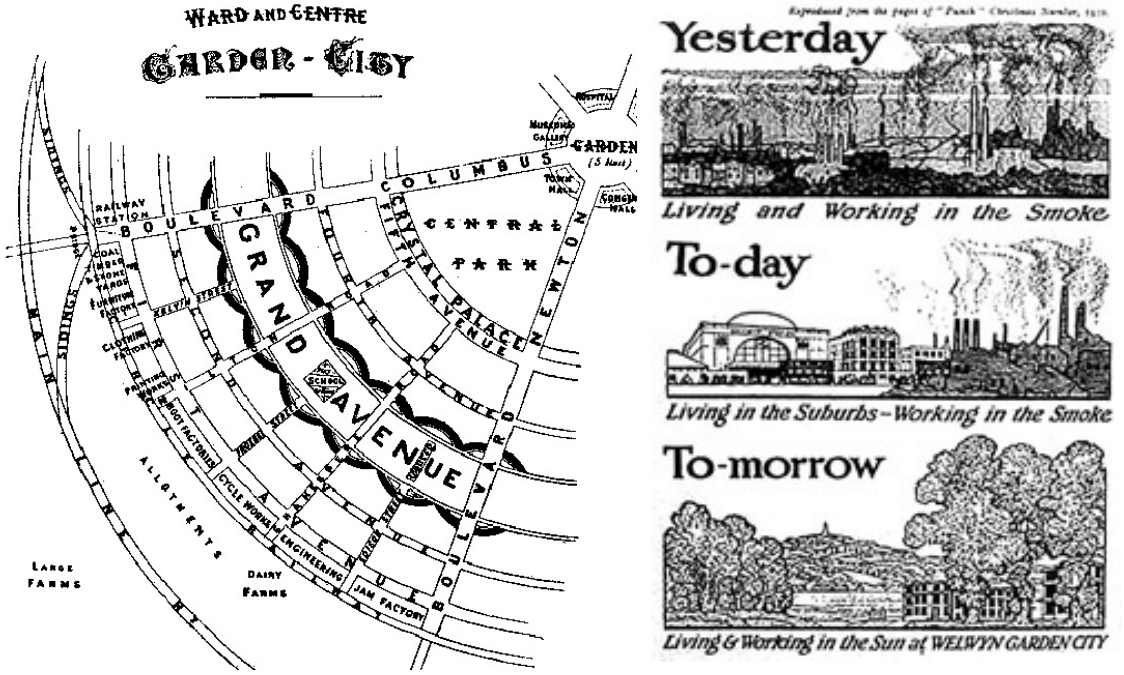

Figure 2.3 Ebenezer Howard's garden city diagram [URL5] and advertising [URL6].

Twenty years after the mid 1970's oil crisis which incited the first search for urban forms that conserved resources, the idea of sustainability has re-emerged, due to the growing awareness of urban problems related with resources depletion, energy consumption, pollution and waste [Schoffman and Vale, 1996]. Therefore, the role of urban planning in urban sustainability, namely which urban structure will provide higher environmental protection, is today still under discussion.

The scope of the debate can be summarized by classifying positions in two groups: the "decentrists", in favour of urban de-centralization, defending the dispersed city characterized by low population densities and large area requirements; and the "centrists", who believe in the virtues of high density cities with low area requirements, defending the compact city. Table 2.1 presents a list of possible characteristics of the compact city and of the dispersed city (or urban sprawl), compiled by Neuman [2005] and Burchell *et al.* [1998], respectively.

Table 2.1 Compact city [Neuman, 2005] and urban sprawl [Burchell *et al.*, 1998] characteristics.

Compact city characteristics	Urban sprawl characteristics
1. High residential and employment densities	1. Low residential density
2. Mixture of land uses	2. Unlimited outward extension of new development
3. Fine grain of land uses (proximity of varied uses and small relative size of land parcels)	3. Spatial segregation of different types of land uses through zoning
4. Increased social and economic interactions	4. Leapfrog development
5. Contained urban development, demarcated by legible limits	5. No centralized ownership of land or planning of land development
6. Multimodal transportation	6. Transportation dominated by privately owned motor vehicles
7. High degrees of accessibility: local/regional	7. Fragmentation of governance authority of land uses among many local governments
8. High degrees of street connectivity (internal/external), including sidewalks and bicycle lanes	8. Great variances in the fiscal capacity of local governments
9. High degree of impervious surface coverage	9. Widespread commercial strip development along major roadways
10. Low open-space ratio	
11. Unitary control of planning of land development, or closely coordinated control	
12. Sufficient government fiscal capacity to finance urban facilities and infrastructure	

Defenders of dispersal and low density development claim that low densities can be sustainable and that the quality of life within them is much higher, in comparison with contained high density developments. The argument against the dispersed city is that low densities, and the consequent large area needs and land use segregation, result in a high dependence from motorized vehicles. This argument is strengthened under the current climate change context, not only regarding the greenhouse gas (GHG) emissions but also because of the level of resources consumption.

The compact city is characterized by a high density, mixed use city, where growth is encouraged within the boundaries of existing urban areas, and with no development beyond its periphery. Those in favour of the compact city defend that urban containment, with mixed land use, will reduce the need for motorized trips, therefore reducing traffic emissions, and promoting public transport, walking and cycling [Breheny, 1992b; ECOTEC, 1993; Masnavi, 2000; Titheridge *et al.*, 2000]. Other cited benefits are the reuse of infrastructure and previously developed land, the rejuvenation of existing urban areas and urban vitality, a high quality of life and the preservation of green space [Thomas and Cousins, 1996]. It is also claimed that higher densities will help to make the supply of infrastructures and leisure services economically feasible, also increasing social sustainability [Jenks *et al.*, 1996].

The two dominant motives in favour of the compact city are the reduction of pollution, and the reduction of the loss of open countryside to urban uses. The reason behind the first motive is that urban containment will reduce the need for travel – which is the fastest growing and least controlled contributor to atmospheric emissions, and hence global warming – by facilitating shorter journeys and inducing greater supply and use of public transport. The second motive is that urban containment might deliver other environmental benefits, such as reductions in loss of open land and valuable habitats.

It has been demonstrated that sprawl elevates the cost of urban services by increasing the distance between new development and the established infrastructure of roads, sewer lines, and transit systems [Burchell *et al.*, 2002]. Other authors have associated sprawling urban development patterns with increased vehicle travel and congestion [Ewing *et al.*, 2003; Downs, 1992], increased volumes of storm-water runoff [Stone and Bullen, 2006], loss of prime agricultural lands [Heimlich and Anderson, 2001], and, even, increased rates of obesity in children and adult populations [Frumkin *et al.*, 2004].

Other authors [Breheny, 1992a, 1992b, 1996; Thomas and Cousins, 1996] however, claim that the environmental benefits resulting from urban compaction are doubtful and that higher urban densities are unlikely to bring about the high quality of life that centrists promise. Although some reduction in energy consumption might be expected from compaction, they argue that a large centralised city can often result in greater traffic congestion, and fuel efficiency is greatly reduced through increasing travel times and slower traffic speeds; congestion and dangerous traffic leads to a worse pedestrian environment, public transport is often caught up in congested streets, and parking is a serious problem, affecting the character and function of city streets. Another important aspect mentioned is that even if vehicle emissions are reduced, they may be concentrated in the precise areas where they cause most damage and adversely affect most people [Barret, 1996].

There is a wide variety of studies concerning the effects of land use changes in motorized trips and in urban emissions, but the results are not always consistent, and the exact extension of the cause-effect relationship is not conclusive [Marshall and Lamrani, 2003]. In §2.3. these studies will be further discussed.

In their book “Achieving sustainable urban form”, Williams *et al.* [2000] concluded that there are both benefits and costs associated with urban compaction: the main benefits are related to land efficiency and travel, and the main cost to quality of life. The book includes contributions from several authors, highlight the importance of behavioural and socio-economic criteria in explaining differences in travel patterns, and therefore in energy consumptions and emissions.

Jenks *et al.* [1996] and Williams *et al.* [2000] also concluded that instead of searching for a definitive sustainable urban form, the emphasis should be on how to determine which forms are suitable for a given city, defending that there are a variety of urban forms which are more sustainable than the typical recent development patterns. These are characterised by compactness (in various forms), mix of uses and interconnected street layouts, supported by strong public transport networks, environmental controls and high standards of urban management.

2.1.3 Global awareness and European Union urban planning initiatives

The pursuit of sustainability has been placed on the agenda of governments and non-governmental organizations after the 1972 United Nations Conference on the Human Environment, whose Principle 1 states that “Man has the fundamental right to freedom, equality and adequate conditions of life, in an environment of a quality that permits a life of dignity and well-being, and he bears a solemn responsibility to protect and improve the environment for present and future generations”.

In 1987, the World Commission on Environment and Development (WCED) [1987] was responsible for the best-known definition of sustainability or sustainable development, which is defined as a "form of progress that meets the needs of the present without compromising the ability of future generations to meet their needs”. In its report *Our common future* [WCED, 1987], urban areas were recognized as a “common” problem, accounting for a high share of the world's resource use, energy consumption, and environmental pollution.

The publication of *Our Common Future* and the work of the WCED laid the groundwork for the convening of the 1992 Earth Summit and the adoption of the Agenda 21. The Summit’s objective – the need to rethink economic development and halt the destruction of natural resources and pollution - and its message - that only the transformation of our attitudes and behaviour would bring about the necessary changes – were object of an unprecedented level of journalistic cover. This raised global awareness on environmental problems, which received a remarkable response through the adoption of sustainable development policies [Jenks, 2000].

The Commission of the European Communities’ Green Paper on the Urban Environment [COM(90) 218 final] constituted the first step towards an European-level debate and reflection on the problems of the cities, addressing environmental, social and economic aspects. This document identifies the “spatial arrangement” of urban areas as one of the main factors causing urban environmental problems. In particular, the physical separation of land uses is recognized as a reason for increased mobility needs, and for the reliance in motor vehicles to satisfy those needs. It states that there is a need for Community action since pollution generated in urban areas has international implications,

also urban problems are common to cities all over Europe, and potential impacts of Community policies on the urban environment have to be considered.

Regarding urban planning, the Green Paper encourages strategies which emphasize mixed uses and denser development, therefore avoiding urban sprawl. It is suggested that the Commission, in cooperation with Member States and local authorities, should develop guidelines for the incorporation of environmental considerations into city planning strategies. It was the first time it was assumed that urban planning issues and the urban environment should be put under the scope of the EC strategy.

Although not absorbed or included in any Directive, the Green Paper on the Urban Environment had a considerable impact and has become one of the base documents in any discussion of urban structure, and in particular of the compact city [Welbank, 1996].

The 5th Environmental Action Programme, 'Towards Sustainability', approved in 1993, advocated the integration of the environmental dimension in all major policy areas, and considered seven 'Themes and Targets', including Urban Environment, and seven types of policy instruments, including Spatial Planning, which is explicitly identified as one of the key mechanisms for working towards sustainable development.

Moreover, in 1993, together with the European Commission, the EC Expert Group on the Urban Environment launched the first phase of the Sustainable Cities Project. One of its main aims was to formulate recommendations to influence policy at the European Union, Member State, regional and local levels. This project sought to take a holistic approach to planning and management of cities, and advocated the ecosystem approach, through the consideration of the city as a living organism, characterizing its metabolism [Welbank, 1996].

In 1994 the Conference on Sustainable Cities in Aalborg (Denmark) brought together local and regional authorities to discuss the development of network activities as well as the exchange of information. The conference adopted the Charter of European Cities & Towns Towards Sustainability, also known as Aalborg Charter, which was signed by 80 different municipalities. The signatories recognize the importance of effective landuse and development planning policies by local authorities, assuming that higher densities and mix of functions offer efficient public transport and energy, as well as reduce the need for mobility, and therefore should be pursuit.

In 1997, the European Commission engaged directly in the debate on urban issues, through its communication “Towards an urban agenda in the European Union” [COM 97(197) final]. It recognizes the need for an integration of Community policies relevant to urban development, due to the range of social, environmental and economic problems experienced by cities and towns. The document clearly

states that it is not the Commission's intention to develop Europe wide urban policies for "matters which are best dealt at a local or regional level".

The Communication originated a lively response from the EC Expert Group, composed not only of independent experts but also of national representatives, demanding a clearer and stronger position from the EC. The Group's *Agenda for the Sustainable City* [1998] defended a "radical new approach setting sustainability requirements above those of free trade". Regarding urban structure two urban models were identified:

i) The compact city model, based on the reduction of urban expansion to protect the surrounding environment, through intensive land use based on urban regeneration, high densities, mixed uses, with increased accessibility of residential and business areas and services, resulting in higher use of public transport systems;

ii) The green city model, an alternative sustainable city, based on ecological design and the development of more or less self sufficient communities which, in comparison with the compact city, integrates urban and rural areas.

The Expert Group urged the Commission to encourage the containment of urban sprawl since it impedes the ability of cities to become more sustainable, by undermining its functions, inducing additional traffic, and contributing to social inequality. It also recommended the EC to include several aspects in its research agenda, including the development of sustainability scenarios, based on compactness and multi-functional use, and models for the renewal of existing urban areas and their expansion.

In 1998 the European Commission adopted the Communication *Sustainable Urban Development in the European Union: A Framework for Action* [COM(98)605], setting out objectives for urban areas and a range of existing and proposed actions to address them. The framework was organized under four independent policy aims: i) strengthening economic prosperity and employment; ii) promoting equity, social inclusion and regeneration; iii) promoting and improving the urban environment; iv) contributing to good urban governance and local empowerment. No mention was made to urban structure and its influence on urban sustainability.

In the scope of the 6th Environment Action Programme (EAP), which establishes the framework for environmental policy-making in the European Union for the period 2002-2012, the Commission presented a policy document called "Towards a Thematic Strategy on the Urban Environment" [COM(2004)60], defining four priority themes: sustainable urban management, sustainable urban transport, sustainable urban construction, and sustainable urban design. Actions proposed for the Thematic Strategy included the encouragement of all Member States to:

- ensure that their land use planning systems achieve sustainable urban settlement patterns and take into account environmental risks;
- develop incentives to encourage the reuse of abandoned land within the cities and set challenging targets for its reuse;
- set minimum residential land use densities to encourage higher density use and limit urban sprawl;
- evaluate the consequences of climate change for their cities so that inappropriate developments are not initiated and adaptations to the new climatic conditions can be incorporated into the land use planning process.

The document recognizes urban sprawl as the most urgent of the urban design issues. It was also stated that the Commission would prepare guidelines on "high density, mixed use" spatial planning, and explore the possibility of developing other guidelines on specific urban design issues.

However, after a period of consultations, all the considerations relating to sustainable urban design were removed from the final *Thematic Strategy on the Urban Environment* [COM(2005)718 final]. The Commission decided that legislation would not be the best way to achieve the objectives of the Strategy, "given the diversity of urban areas and existing national, regional and local obligations, and the difficulties linked to establishing common standards on all urban environment issues". Instead, the Strategy sets in place a framework to contribute to the better management of the urban environment and the widespread adoption of best practice, and seeks to discourage unsustainable approaches and promote the more sustainable alternatives.

It is fair to say that the *Thematic Strategy on the Urban Environment* falls short of the objectives of the 6th EAP, whose aim was defined as "contributing to a high level of quality of life and social well being for citizens by providing an environment where the level of pollution does not give rise to harmful effects on human health and the environment and by encouraging a sustainable urban development" [URL7]. It relies on voluntary and therefore, almost always, sector-based initiatives to promote sustainable urban areas, the same that have not resulted so far and have led us to today's situation. In order to set urban development priorities into the right direction, the Commission should instead adopt directives containing obligations for environmental management plans and sustainable urban transport. Additionally, in order to establish a clear link to EU environmental policies, objectives for decreasing atmospheric emissions at the urban level should also be set.

2.1.4 Urban sprawl in Europe

The urban future of Europe is today a matter of great concern, since approximately 75 % of the European population lives in urban areas, a number predicted to rise to 80 % by 2020 [EEA, 2006a]. More than a quarter of the European territory is now directly affected by urban land use; between 1990 and 2000, urban areas have expanded 5.5 % in average, with rates varying regionally from 0.7 % to 40 % [EEA, 2009].

Throughout Europe, urbanization is evident in many different forms, sometimes in concentrated compact centres but mostly in low density developments associated with urban sprawl [PBL, 2008]. This is raising concerns about the potential negative impact on urban sustainability [EEA-JRC, 2002; Kasanko et al., 2006; EEA, 2006a; Catalán et al., 2008; PBL, 2008]. Figure 2.4 shows the European areas with higher urbanization rates, where urban land cover has been increasing between four to six times faster than the European average, but the population density in residential areas declined six times faster [PBL, 2008]. Clearly for these areas the term sprawl is well fitted. Regions of this type can be found along the Portuguese coastline, in Madrid and its surroundings as well as in some coastal regions in Spain, in the north of the Netherlands, north-western Ireland, Italy (especially Sardinia) and Greece. Sprawl is particularly evident in countries or regions that have benefited from EU regional policies, such as Portugal, Ireland, and Spain.

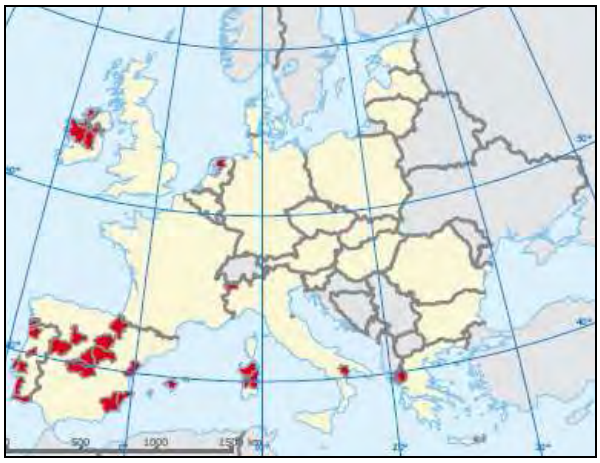

Figure 2.4 European areas with very rapid urbanization [PBL, 2008].

Historically, in comparison with North-American cities, European cities have traditionally been much more compact, with a dense historical core shaped before the emergence of modern transport systems; however, urban sprawl is now a common phenomenon throughout Europe [EEA, 2006a], even in Mediterranean urban areas, which are now experiencing a change towards more dispersed and horizontal growth at the expense of agricultural, forested and natural environments [Catalán et al., 2008].

Kasanko et al. [2006] analysed 15 European urban areas in respect to urban land use and population, from the mid 1950's to the late 1990's, using land use data stored in the MOLAND database from the Joint Research Centre of the European Commission. Five indicator sets were used: built-up area, residential land use, land taken by urban expansion, population density and urban density. The authors concluded that although very different in terms of population densities and land use, the studied cities presented some common trends: built-up areas have grown considerably in all the studied cities; the most rapid growth dates back to the 1950's and 1960's, with rates slowing down in the 1990's. However, during the 12 years from the mid 1980's to the late 1990's, the urban population declined 2.8 % and built-up areas have grown by approximately 9 %. Another important feature was the growth of discontinuous residential areas: in half of the studied cities more than 90 % of all residential areas built after the mid 1950's were low density areas. These features lead the authors to state "It is a mere question of taste whether to call it urban sprawl or urban expansion".

Kasanko et al. [2006] also identified a distinct group formed by Southern European cities (Palermo, Milan, Bilbao and Porto). Until the 1960's these were very compact in structure and densely populated; still at the end of the 1990's they remained the most compact and dense, however the distance to the remaining cities has shrunk.

In fact, in Southern Europe many large cities experienced strong rates of growth between the 1950s and the 1980s [Catalán *et al.*, 2008], with urban dispersion advancing very rapidly at much faster rates than population growth [Chaline, 2001]. Examples of this trend can be found in Porto [EEA, 2006a]; Marseille and the nearby Rhône valley [Pinson and Thomann, 2001], Milan [Cagmani *et al.*, 2002], Bologna [Anderlini, 2003], Venice and the Veneto region [Indovina, 1990], Athens [Leontidou, 1990] and Barcelona [Catalán *et al.*, 2008].

Hence, European urban areas are experiencing urban sprawl. Particularly at risk are the cities of Southern and Eastern Europe, historically more compact, but which in the past few decades have started to expand rapidly outwards.

2.2 Urban air pollution

Natural air pollution has occurred on Earth since the planet's formation; fires, volcanic eruptions, meteorite impacts, and high winds, all cause natural air pollution. Human-made urban air pollution problems have existed for centuries and have resulted from burning of wood, vegetation, coal, oil, natural gas, waste and chemicals [Jacobson, 2002].

2.2.1 The birth of urban air pollution awareness

Problems regarding air pollution in urban areas have been known for millennia, but the attitude towards them was ambiguous, since they were even considered a symbol of growth and prosperity, and the attempts to combat them were scattered and ineffective. It was only after the occurrence of a few major air pollution episodes in the 20th century that a greater awareness and the consequent development of air pollution policies took place [Fenger, 1999]. The first was the disaster in Meuse Valley in Belgium, between the 1st and 5th of December 1930: under the influence of stable meteorological conditions (lack of wind and low temperature), the 15-mile valley trapped pollutants released by local industries, leading to an increase of air pollutant concentrations, which caused a large number of people to suffer from respiratory tract problems, out of which about 60 died. The air pollution episode in Meuse Valley revealed a problem that until then had received little attention; fog episodes had previously been associated with increased mortality in London and Glasgow, but cold weather and viral epidemics could not be ruled out as contributory factors [Nemery *et al.*, 2001]. The Meuse fog disaster provided incontrovertible evidence that air pollution could kill and therefore it attracted the attention of the scientific community.

The London episode of December 1952 is the best known and most discussed in the literature, and would lead to modern air pollution legislation and abatement. The disastrous outcome was due to a combination of various factors. The most important one was a slowly moving anticyclone coming to halt above the city and giving low winds and damp air. This required more heating in the cold winter climate and thus gave further pollution, causing the build-up of higher pollutant concentrations [Fenger, 2009]. The monitoring equipment of that time was fairly primitive, but the peak values of sulphur dioxide and smoke were about 14 000 $\mu g.m^{-3}$ compared with the current air quality standards of a few hundred $\mu g.m^{-3}$ (Figure 2.5).

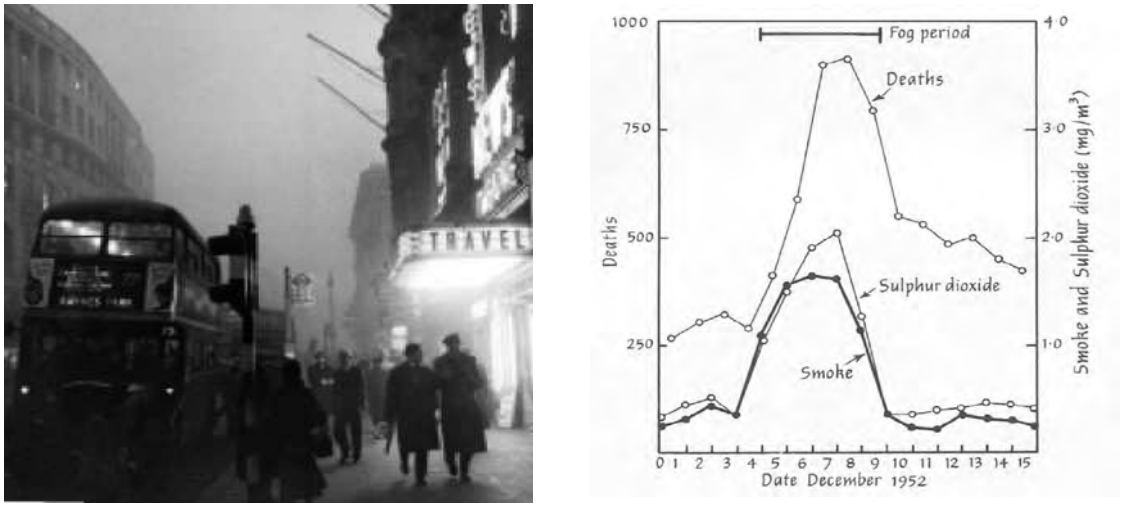

Figure 2.5 London December 1952 at noon [URL8] and London smog episode data [Wilkins, 1954].

Admissions to hospitals for the treatment of respiratory diseases were increased and so were admissions for heart diseases; shortness of breath, cyanosis, fever and evidence of excess fluid in the lungs were registered [Nemery *et al.*, 2001]. A significant increase in mortality was observed during this episode, the total excess was between 3500 and 4000. The event led to a public outcry and a strong political reaction; an increase in the number of monitoring stations and extensive legislation followed [Fenger, 2009].

Air pollution concentrations in London and most other major western cities have fallen markedly over the last century. In London, the last winter air pollution episode to cause major public health concern was in 1991, when the city experienced a winter temperature inversion with air stagnation, typical of the conditions previously associated with air pollution episodes. The pollutants that accumulated were not those from domestic fuel burning as in 1952, but from mobile sources with a contribution from space heating using natural gas [Anderson, 2009]. Although the relative increase in air pollution was quite similar to that observed in the 1952 episode the absolute levels were very much lower; a 10% increase in mortality attributable to air pollution was found, compared to 400% increase in mortality observed in the week of the 1952 fog [Anderson *et al.*, 2005].

2.2.2 Main atmospheric pollutants and sources

The driving forces behind air pollution are directly associated with human activity; energy consumption, industrial activities, transport demand and agriculture are the specific forces most directly linked to air pollutant emissions. While population growth in Europe has been minimal since 1990, the number of households grew rapidly by approximately 11% between 1990 and 2000 whilst total energy consumption increased by about 12% to 2004 [EEA, 2006a].

The transport sector has grown to become the largest energy consuming sector, accounting for approximately 31% of the European final energy consumption in 2004. In comparison, the industrial sector used 28% and households 27% [EEA, 2007]. The potential for transport-related air pollution caused by road vehicles has, therefore, increased.

Atmospheric pollutants (gaseous and particulate) can be divided in primary pollutants, which are directly emitted to the atmosphere by a natural or anthropogenic emission source, and secondary pollutants, which result from primary pollutants transformation through chemical reactions highly dependent on meteorological conditions and/or solar radiation [Alley *et al.*, 1998]. Currently, the two air pollutants of most concern for public health are surface particulate matter and ozone, therefore receiving special attention in this review and also throughout this thesis.

There is increasing evidence that fine dust particles, measured in microns or even nanometres, have deleterious effects on human health, causing premature deaths and reducing quality of life by

aggravating respiratory conditions such as asthma [WHO, 1999]. One reason why particulate matter is of such concern is the absence of any concentration threshold below which there are no effects. Since PM10 penetrates into the human thorax, air quality objectives have up to now been set in relation to the total mass concentration of such particles. Evidence suggests that fine particulates, with an equivalent aerodynamic diameter less than 2.5 micrometers (PM2.5), do most damage to human health, and that effects depend further on the chemical composition or physical characteristics of the particle [Samet *et al*., 2000; Burnett *et al.*, 2000].

Particulate matter (PM) includes as principal components sulfate, nitrate, organic carbon, elemental carbon, soil dust, and sea salt. The first four components are mostly present as fine particles (PM2.5), and these are of most concern for human health. Sulphate, nitrate, and organic carbon are produced within the atmosphere by oxidation of sulphur dioxide (SO_2), nitrogen oxides (NO_x) and non-methane volatile organic compounds (NMVOC); carbon particles are also emitted directly by combustion. Nitrate and organic carbon exchange between the particle and gas phases, depending in particular on temperature. The seasonal variation of PM is complex and location-dependent; in general, PM needs to be viewed as an air quality problem year-round [Jacob and Winner, 2009]. PM is efficiently scavenged by precipitation and this is its main atmospheric sink, resulting in atmospheric lifetimes of a few days in the boundary layer and a few weeks in the free troposphere. Export of PM from the source continents is limited by the precipitation scavenging, and therefore the PM background in the free troposphere is generally unimportant for surface air quality [UNECE, 2007]. Exceptions are plumes from large dust storms and forest fires which can be transported on intercontinental scales [Jacob and Winner, 2009].

While ozone (O_3) in the upper atmosphere provides an essential screen against harmful UV radiation, at ground level it is lung irritant causing many of the same health effects as particulate matter, as well as attacking vegetation, forests and buildings. Observed effects on human health are inflammation and morphological, biochemical, and functional changes in the respiratory tract, as well as decreases in host defence functions. Effects on vegetation include visible leaf injury, growth and yield reductions, and altered sensitivity to biotic and abiotic stresses. Ozone also acts both directly and indirectly—as part of a pollution "cocktail"—to accelerate the degradation of materials [Jacobson, 2002].

Ozone is produced in the troposphere by photochemical oxidation of carbon monoxide (CO), methane (CH_4), and NMVOC by the hydroxyl radical (OH) in the presence of reactive nitrogen oxides. The relation between O_3, NO_x and VOC is driven by complex nonlinear photochemistry, with the existence of two regimes with different O_3-NO_x-VOC sensitivity: in the NO_x-sensitive regime (with relatively low NOx and high VOC), O_3 increases with increasing NO_x and changes little in response to increasing VOC; in the NO_x-saturated or VOC-sensitive regime O_3 decreases with increasing NO_x and increases with

increasing VOC [Seinfeld and Pandis, 1998]. Also, in the vicinity of large nitrogen monoxide (NO) emissions, ozone is destroyed according to the reaction $NO + O_3 = NO_2 + O_2$, generally referred as O_3 titration by NO. This situation usually takes place in heavily polluted areas, with ozone consumption taking place immediately downwind of the sources, and becoming elevated as the plume moves further downwind [Seinfeld and Pandis, 1998; Derwent, 1999]. NMVOC, CO, and NO_x are emitted by large combustion sources and motor vehicles; vegetation is a large NMVOC source and CH_4 has a number of biogenic and anthropogenic sources. OH originates mainly from atmospheric oxidation of water vapour and cycles in the atmosphere with other hydrogen oxide (HOx) radicals [Jacob and Winner, 2009].

Ozone pollution is in general mostly a summer problem because of its photochemical nature [Seinfeld and Pandis, 1998]. The main sinks for tropospheric ozone are photolysis in the presence of water vapour, and uptake by vegetation (dry deposition); wet deposition is negligible as ozone and its major precursors have low solubility in water. The atmospheric lifetime of ozone ranges from a few days in the boundary layer to weeks in the free troposphere. Ozone and its anthropogenic precursors are transported on hemispheric scales in the free troposphere, therefore adding a significant background to surface ozone which is of increasing concern for meeting air quality standards [Holloway *et al.*, 2003].

2.2.3 Effects of meteorology on urban air pollution

With respect to urban air pollution, the region of the atmosphere governing transport and dispersion is the so-called planetary boundary layer (PBL), which extends from the surface to between 500 and 3000 m, representing the extent of influence of the Earth's surface on wind and structure of the atmosphere [Seinfeld and Pandis, 1998; Jacobson, 2002].

The concentration of pollutants (gaseous and particulate) in the atmosphere is affected by winds, temperature, clouds and relative humidity. In turn, these meteorological parameters are influenced by large scale and small scale weather systems [Jacobson, 2002], which can be categorized as [Seinfeld and Pandis, 1998]:

i) synoptic or macroscale – phenomena occurring on scales of thousands of kilometres, such as semi-permanent high and low pressure systems that reside over the oceans and continents;

ii) mesoscale – phenomena occurring on scales of hundreds of kilometres, such as land-sea breezes, mountain-valley winds and migratory high and low pressure fronts;

iii) microscale – phenomena occurring on scales of the order of 1 km, such as the meandering and dispersion of a stack plume and the complicated flow regime in the wake of a large building .

Each of these scales of motion plays a role in air pollution over different periods of time: microscale effects take place over scales on the order of minuts to hours, whereas mesoscale phenomena influence transport and dispersion of pollutants over hours to days, and synoptic phenomena are felt for days to weeks.

Low-pressure systems are associated with cloudy skies, stormy weather and fast surface wind; air rises and near surface pollutants are dispersed upwards, also the clouds block sun-light that would otherwise drive photochemical reactions, reducing pollution further. On the contrary, high-pressure systems are characterized by relatively low surface winds, sinking-air and cloud free skies; this horizontal and vertical dispersion of pollutants and the sunlight drives photochemical processes.

The stability of the air is a measure of whether pollutants will convectively rise and disperse, or instead build up in concentration near the surface. When the stability condition is such that air temperature increases with increasing height, a temperature inversion is present. Stable air and inversions trap pollutants, preventing them from dispersing into the troposphere and causing high pollutants surface concentrations; this was the case of the disaster in Meuse Valley in Belgium, already described.

Whereas large-scale pressure systems control the prevailing meteorology of a region, local factors also affect meteorology and therefore air pollution. Besides the temperature inversions, ground temperature affects air pollution through its effects on wind speeds: warm surfaces enhance convection, causing surface air to mix with air aloft, therefore speeding winds near the surface, which results in greater dispersion of near surface pollutants. On the other hand, higher surface wind speeds will also increase the re-suspension of particles from the ground. Also, air temperature affects rates of several processes such as rates of biogenic emissions from trees, carbon monoxide emissions from vehicles and chemical reactions [Jacobson, 2002].

The most widely recognized meteorological effect of urbanization is the *urban heat island effect* [Oke, 1988]. Defined as a differential in the air temperatures of urban centres relative to adjacent rural areas, the urban heat island effect is driven by the displacement of natural vegetation by the impervious surfaces of roads and buildings, as well as by the emission of vast quantities of waste heat from buildings, industry, and automobiles. In combination, these properties of urbanization can serve to raise by several degrees the average air temperature of large cities. Because regionalized air pollutants such as ozone and fine particulate matter are sensitive to temperature, the resulting urban heat island holds important implications for air quality.

The statistical correlation between the pollutant concentrations and the meteorological variables has been an active subject of study since it contributes to the understanding of the processes affecting pollutant concentrations [Jacob and Winner, 2009].

The influence of urban temperatures on regional ozone formation is well documented [Rao *et al.*, 1992, 1995]. In a study of temperature trends and ozone formation in large US cities, Stone [2005] has found a strong positive correlation between mean temperature and the average number of high ozone days per year. Ordonez *et al.* [2005] concluded that the dominant variables for summer ozone in Switzerland are temperature, morning solar radiation and the number of days since the last frontal passage. Camalier *et al.* [2007] estimated that 80% of the ozone variance in eastern United States can be explained by a linear model with temperature (positive) and relative humidity (negative) as the two most important predictor variables. The strong correlation of ozone and temperature is however limited to polluted conditions (O_3 > 120µg.m^{-3}); lower ozone concentrations more representative of background show no correlation with temperature [Sillman and Samson, 1995]. In the eastern United States high temperatures, large concentrations of water vapour, high solar radiation and stagnant conditions were the variables mostly correlated with high ozone levels [Vukovich and Sherwell, 2003]. In the southwest US temperature and mixing height most strongly influence ozone conditions [Wise and Comrie, 2005].

Observed correlations of PM concentrations with meteorological variables are weaker than for ozone [Wise and Comrie, 2005], reflecting the diversity of PM components. No significant correlations with temperature have been reported in the literature. Cheng *et al.* [2007] in their study of four Canadian cities have encountered a strong correlation of PM with stagnation; Wise and Comrie [2005] have obtained a negative correlation of PM with relative humidity in the south-western US.

Veloso *et al.* [2004] studied the metropolitan areas of Lisbon and Porto and concluded that relative humidity, maximum daily temperature and wind speed were found to be the meteorological variables with higher correlation with air quality data. For ozone a positive strong correlation with temperature was found; negative correlations with relative humidity and wind speed were obtained. For PM, wind speed and precipitation present higher negative correlation factors, while for temperature the correlation is positive.

In Portugal, it is recognized by several authors, both in modelling and field research, that coastal mesoscale meteorology is strongly connected with ozone production and transport [Coutinho and Borrego, 1991; Borrego *et al.*, 1994; Barros *et al.*, 2003; Evtyugina *et al.*, 2006; Monteiro *et al.*, 2005; Carvalho *et al.*, 2006]. Studies on atmospheric circulations over the Iberian Peninsula have shown particularities concerning summer dynamics [Millan *et al.*, 1992]. Frequently, there is the development of a low thermal pressure region in the centre of the Peninsula, which allows mesoscale processes

enhancement such as land–sea breezes [Martín *et al.*, 2001]. In the presence of complex terrain near coastlines, these mesoscale phenomena may be combined with anabatic/katabatic winds creating recirculations along shore. This type of circulations encourages photo-chemical production of air pollutants leading to smog episodes, which can cause health problems to the population and environmental degradation [Barna and Lamb, 2000].

2.2.4 European Union air pollution policies

The European Union has a solid legislation, developed over 30 years, that establishes a common demand level for environmental norms and practices in all Member States. The need to deliver cleaner air has been recognised for several decades with actions taken at national and EU level and also through active participation in international conventions. EU action has focused on: i) developing limit or target values for ambient air quality; ii) developing integrated strategies to combat the effects of trans-boundary pollution (in particular acidification, ozone and eutrophication) through the adoption of national emission ceilings; iii) identifying cost-effective reductions in targeted areas through integrated programmes; iv) introducing specific measures to limit emissions or raise product standards. This has resulted in the reduction of pollutant emissions from large combustion plant and mobile sources, the improvement of fuel quality, and environmental protection requirements have been integrated into the transport and energy sectors.

In November 1996, the Air Quality Framework Directive was adopted with the general aim of defining the basic principles of a common strategy to: i) define and establish objectives for ambient air quality in the Community designed to avoid, prevent or reduce harmful effects on human health and the environment as a whole; ii) assess the ambient air quality in the Member States on the basis of common methods and criteria; iii) obtain adequate information on ambient air quality and ensure that it is made available to the public, *inter alia* by means of alert thresholds; and iv) maintain ambient air quality where it is good and improve it in other cases [96/62/EC, Article 1]. The following “daughter directives” established new limit values for sulphur dioxide, nitrogen oxides, particulate matter and lead [1999/30/EC], carbon monoxide and benzene [2000/69/EC], ozone [2002/3/EC], and polyaromatic hydrocarbons (PAHs), nickel, cadmium, arsenic and mercury [2004/107/EC]. Table 2.2 presents the limit values for the protection of human health, and the information and alert thresholds established for PM10 and ozone, respectively.

Table 2.2 PM10 and ozone values for the protection of human health, and the information and alert thresholds.

PM10		
Averaging period	Limit value	
One day	50 $\mu g.m^{-3}$, not to be exceeded more than 35 times a calendar year	
Calendar year	40 $\mu g.m^{-3}$	
O_3		
Purpose	Averaging period	Threshold
Information	1 hour	180 $\mu g.m^{-3}$
Alert	1 hour (to be measured for three consecutive hours)	240 $\mu g.m^{-3}$

The Air Quality Framework Directive defines the main air quality management tools, which include the elaboration of emission inventories, the implementation of monitoring networks and the use of air quality modelling techniques. It also sets the Member States obligation to evaluate and manage the air quality in every zone and agglomeration of the territory. As defined in 96/62/EC, *zone* is a part of the territory delimited by the Member State, and *agglomeration* is a zone with a population concentration in excess of 250 000 inhabitants or with a population density which, for the Member States, justifies the need for ambient air quality to be assessed and managed. For those zones and agglomerations where the air quality limits are exceeded, Member States have the responsibility of developing and implementing *Plans and Programs for the Improvement of the Air Quality*.

Despite significant improvements, serious air pollution impacts persist. The Community's 6th EAP called for the development of a thematic strategy on air pollution with the objective to attain "levels of air quality that do not give rise to significant negative impacts, and risks to human health and the environment" [Decision 1600/2002/EC]. For the natural environment achieving this objective means no exceedance of critical loads and levels; for human health, the situation is more complex as there is no known safe level of exposure for some pollutants such as particulate matter and ground level ozone.

The Commission embarked on a programme of technical analysis and policy development, the "Clean Air for Europe" (CAFE) programme, with the general aim of developing a long-term, strategic and integrated policy to protect against the effects of air pollution on human health and the environment. After that, the Commission examined whether current legislation would be sufficient to achieve the 6th EAP objectives by 2020. This analysis looked at future emissions and impacts on health and the environment and has used the best available scientific and health information. It showed that significant negative impacts will persist even with effective implementation of current legislation.

Accordingly, the *Thematic Strategy on Air Pollution* [COM(2005)446 final] established interim objectives for air pollution in the EU and proposed appropriate measures for achieving them. It recommended that the current legislation should be modernised, better focused on the most serious

pollutants and that more had to be done to integrate environmental concerns into other policies and programmes.

Meeting the targets set out in the Strategy will require efforts and commitments by other sectors, such as energy and transport. The EU has set the target of producing 12% of energy and 21% of electricity from renewable energy sources by 2010, as well as minimum targets for the share of biofuels. Several actions have been taken to curb energy demand including energy labelling, energy performance of buildings, and a Directive on cogeneration. In keeping with the commitments made in the White Paper on a common transport policy, the EC committed itself on the encouragement of shifts towards less polluting modes of transport, alternative fuels, reduced congestion and the internalisation of externalities into transport costs. However, the Strategy does not make any reference to the integration of urban planning policies, namely urban structure and its role in urban air pollution.

More recently, it was recognized the need to substantially revise the air quality directives [96/62/EC, 1999/30/EC, 2000/69/EC, 2002/3/EC and 2004/107/EC], and in the interest of clarity, simplification and administrative efficiency replace them by a single directive - Directive 2008/50/EC. A special attention is given to fine particulate matter (PM2.5) due to its significant negative impacts on human health. Due to the absence of any concentration threshold below which PM2.5 would not pose a risk, a different approach was followed aiming at a general reduction of concentrations in the urban background to ensure that large sections of the population benefit from improved air quality. However, to ensure a minimum degree of health protection everywhere, that approach was combined with a limit value, preceded in a first stage by a target value. The PM10 limit values for the protection of human health, and the O_3 information and alert thresholds presented in Table 2.2 were maintained equal in Directive 2008/50/EC.

2.2.5 Emissions and air quality trends in Europe and Portugal

Emissions of air pollutants decreased substantially during the period 1990–2006 across Europe, in particular, in EU-27 (Figure 2.6). The largest reductions (in percentage) have been achieved for SO_X emissions (which have decreased by almost 70 % since 1990), followed by CO (-53 %), NMVOC (-44 %) and NO_X (-35 %); NH_3 emissions decreased by 22 % and particulate matter emission trends, which have been compiled only for 2000 to 2006, indicate approximately 10 % reduction [EEA, 2008]. As a result of the introduction of three-way catalytic converters on cars and stricter regulation of emissions from heavy goods vehicles across Europe, NO_X emissions from road transport decreased 16% between 2002 and 2006 [EEA, 2008]. The CO and NMVOC emissions presented a similar behaviour.

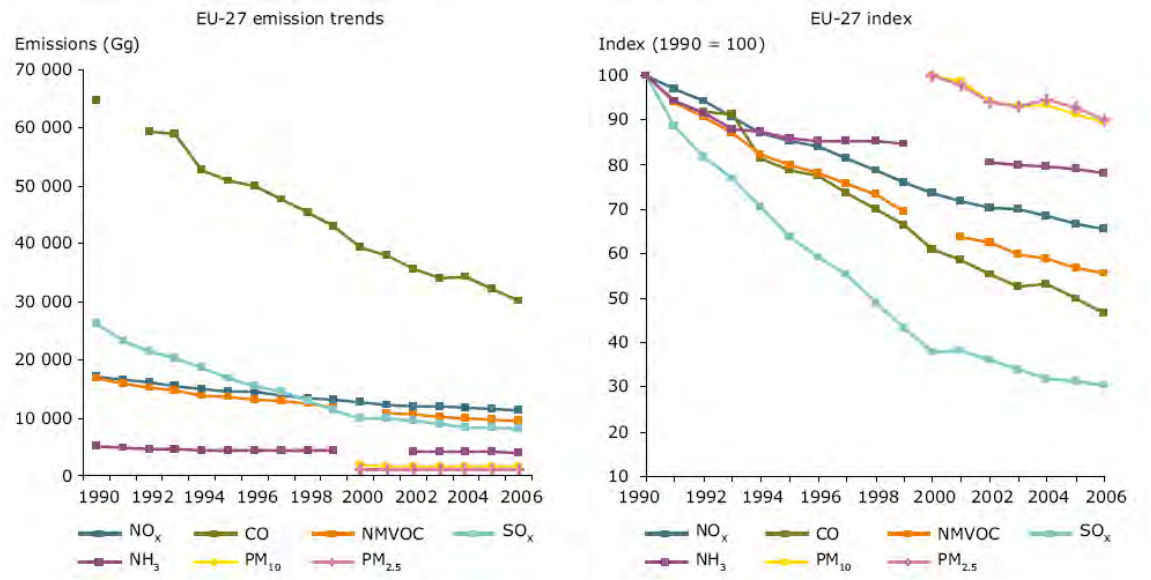

Figure 2.6 EU-27 emission trends for NO_x, CO, NMVOC, SO_x, and NH_3 in Gg between 1990 and 2006 (index year 1990 = 100) and for PM10 and PM2.5 between 2000 and 2006 (index year 2000 = 100) [EEA, 2008].

Although primary PM emissions have decreased in Europe in general, there is a wide variability in emission trends. In some countries reductions have been much larger than the average, whereas in other emissions have increased. The latter situation is especially due to emissions from the transport sector, where reductions resulting from a shift to lighter fuels are counteracted by an increasing share of diesel vehicles and rising traffic volumes [EEA, 2007].

In Portugal, between 1990 and 2007, with the exception of PM and NOx, the main air pollutant emissions have decreased, although in very different proportions [APA, 2009] (Figure 2.7).

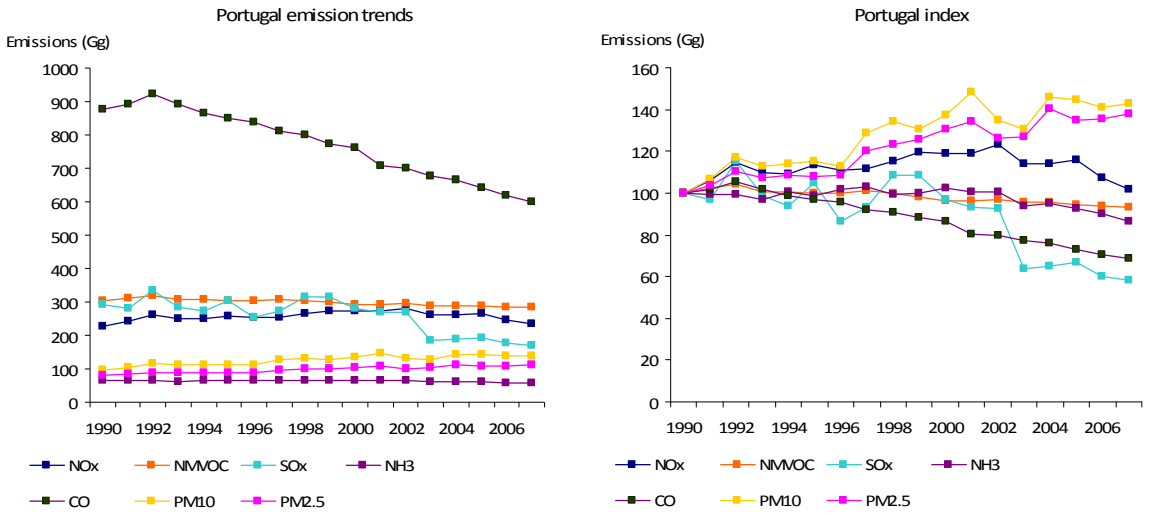

Figure 2.7 Portugal emission trends for NOx, CO, NMVOC, SOx, NH_3, PM10 and PM2.5 in Gg between 1990 and 2007 (index year 1990 = 100) (data from APA, 2009).

The SOx emissions, mainly generated in the energy industry sector and by the combustion in manufacturing industries, presented the largest decrease. The introduction of natural gas (1997), the installation of new combined cycle thermoelectric plants using natural gas (1999), the progressive installation of co-generation units, and the amelioration of energetic and technologic efficiency of industrial processes, are responsible for the verified tendency.

Transportation is responsible for the major share of CO, NOx, and NMVOC emissions. Despite the fast growing trends of the transport sector (mainly road) since the 90's, the introduction of new petrol-engine passenger cars with catalyst converters and stricter regulations on diesel vehicles emissions, limited the growth of these emissions.

NH_3 is primarily generated in biological systems, such as direct soil emissions, manure management systems, waste-water handling systems and decomposition of municipal and animal wastes. The overall evolution of NH_3 in the analysed period is downwards with a -13% change between 1990- 2007.

Particulate matter (Figure 2.8) is generated in a large extent in both energy and industrial processes, and the estimates show a significant positive trend since 1990 (> 35%). Between 1990 and 2006 PM10 emissions from industrial processes increased 142%, industrial combustion increased 74% and road transport increased 18% [EEA, 2008].

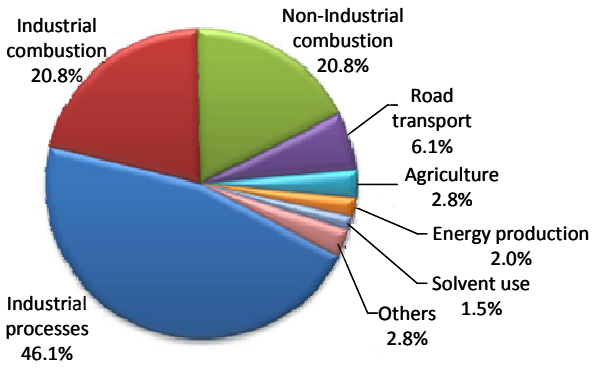

Figure 2.8 Portugal PM10 emissions contribution from different activities for 2005 [EEA, 2008].

When looking at the above emission data, it may seem that urban emissions are not important. For instance, PM10 transport emissions, which predominantly take place in urban areas, only account for a share of 6%. However, it is worth stressing that a great part of the overall emissions, such as emissions from industry, happen in urban areas, although that share is not known.

Notwithstanding the emissions decrease in Europe, ambient concentrations of particulate matter and ozone in the air have not shown any improvement since 1997 [EEA, 2007]. Across Europe, the population exposure to air pollution exceeds the standards set by the EU (Figure 2.9).

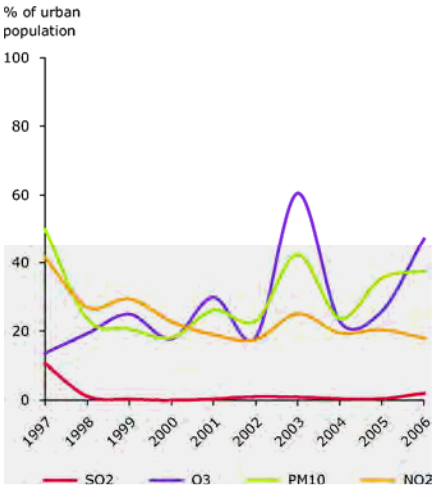

Figure 2.9 Percentage of urban population resident in areas where pollutant concentrations are higher than selected limit/target values, EEA member countries, 1997-2006 [URL1].

For ozone there has been considerable variation along the period 1997-2006, with 14% to 61% of the urban population exposed to concentrations above the target value [URL1]. In 2003, a year with extremely high ozone concentrations due to specific meteorological conditions, the exposure was higher. Concentrations in 2004 were lower, nevertheless, when, in accordance to the ozone directive, concentrations were averaged over a 3-year period, the eight-hour target value was not met over a large part of Europe (Figure 2.10). Current estimates point to approximately 21 400 premature deaths annually due to ozone exposure [EEA, 2007].

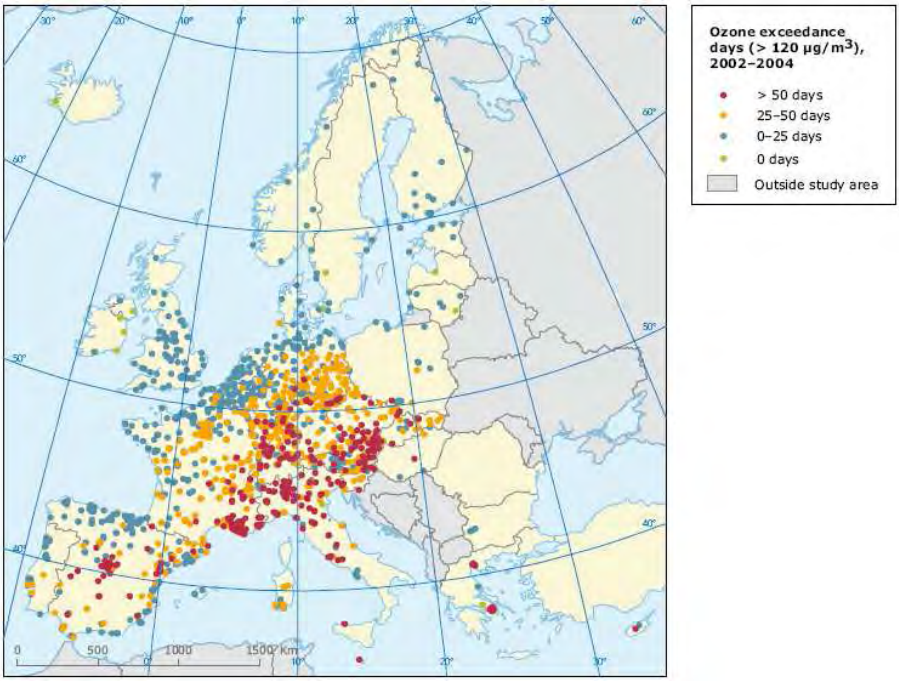

Figure 2.10 Days exceeding the ozone target value as 3-year average 2002–2004 [EEA, 2007].

Regarding PM10, in the period 1997-2006, 18 to 50% of the urban population was potentially exposed to ambient air concentrations higher than the EU limit value set for the protection of human health [URL1]. As an example, in 2004 limit values for daily and annual average PM10 concentrations were exceeded in hot spot, urban and rural locations across Europe, notably in southern and eastern Europe as well as the Benelux countries. The highest urban concentrations were observed in Italy, Czech Republic, Poland, Romania, Bulgaria and the Benelux countries as well as in cities in some other areas. Traffic hot spot stations were found to exceed the daily PM10 limit value in many countries, such as in Italy, Spain, Portugal, Bulgaria and Romania. Figure 2.11 displays the cities with hot spot stations coded against the limit value. In Portugal, it is clear that the 36th highest value is above the limit value in the urban centres of Lisbon and Porto, as well as in the NW coast (Aveiro, Estarreja and Coimbra).

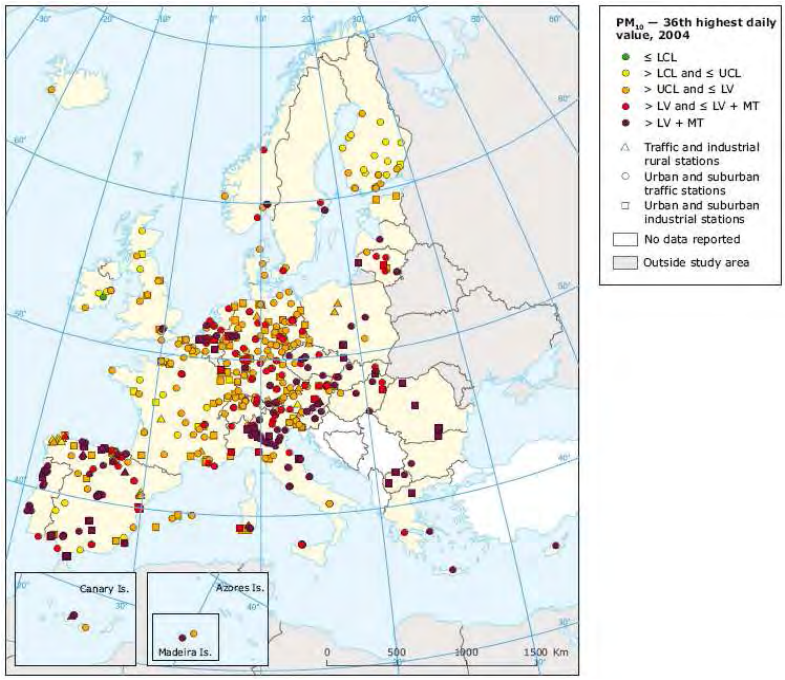

(LCL/UCL: Lower (30 µg.m^{-3})/Upper (50 µg.m^{-3}) LV/MT: Limit value/Margin of tolerance)

Figure 2.11 PM10 concentrations 36th highest daily value for 2004 [EEA, 2007].

In accordance to the established in the Air Quality Framework Directive, the Portuguese territory is divided in 25 zones and 13 agglomerations; therefore the air quality evolution presented here refers to these geographical units. As in Europe, in Portugal PM10 and ozone are the main reasons of concern. Figures 2.12 and 2.13 show the evolution of PM10 and ozone exceedances in Portugal in the period 2001-2005.

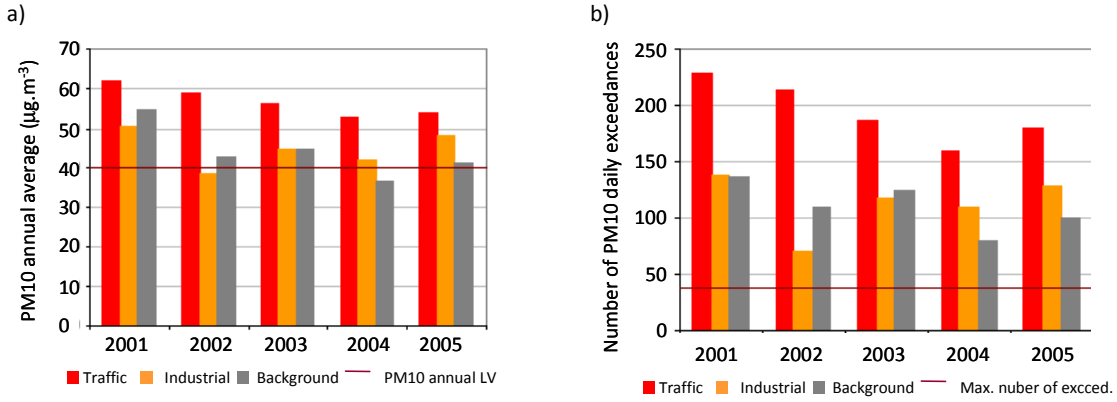

Figure 2.12 PM10 exceedances of a) annual and b) daily limit values for Portugal 2001-2005 [APA, 2008].

Limit values are exceeded mainly at traffic stations, although high concentrations are also found in background and industrial monitoring stations. All agglomerations presented more than 35 days above the daily limit value established for PM10; the annual limit value was mainly exceeded in the North Lisbon Metropolitan Area and Costal Porto agglomerations [APA, 2008].

Regarding ozone (Figure 2.13), the year of 2005 presented a significant increase in the number of hours exceeding the information and alert thresholds in background stations, due to the Lamas d'Olo new air quality station, which is a very particular case (Evtyugina et al., 2009). Maximum hourly ozone concentrations measured in background stations were above the information threshold for almost every zone and agglomeration. For background stations, ozone levels were higher in Coastal Porto agglomeration, followed by Lisbon Metropolitan Area [APA, 2008]. Ozone is a regional scale pollutant, therefore high concentrations occur across large areas. However, rural concentrations have generally been higher than urban and suburban, with the lowest values observed in traffic sites.

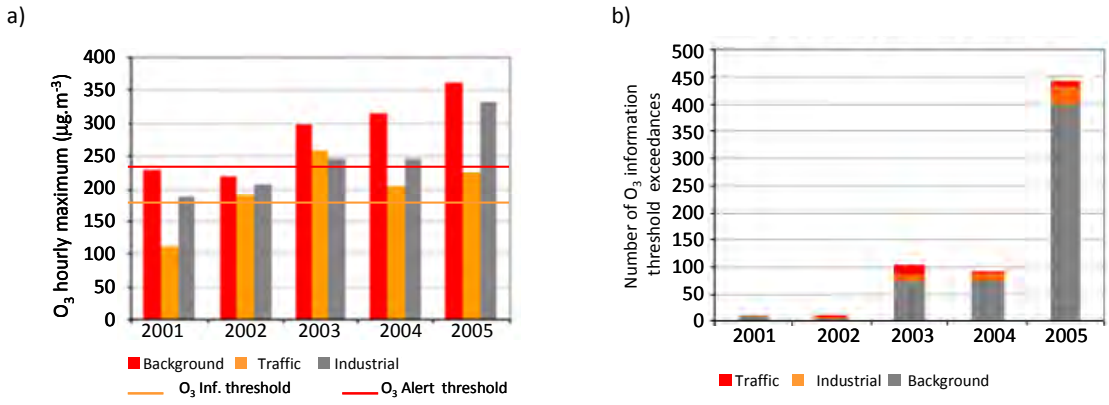

Figure 2.13 Ozone alert and information threshold exccedences for Portugal 2001-2005 [APA, 2008].

Photochemical and particulate matter air pollution problems in Portugal are evident from the above analysis, more precisely over specific urban areas. From 2001 to 2005, PM10 concentrations were consistently above the daily and the annual limit values; with persistent situations registered in

agglomerations from North to South [APA, 2008]. Regarding ozone the situation is more complex; exceedances are dispersed all over the territory, even in zones and not only in agglomerations, due to its secondary and regional pollutant characteristics.

However, air quality monitoring networks are unable to cover the entire territory; to estimate air pollutants concentration in any point of a given study area a variety of modelling tools are available; these will be addressed next.

2.2.6 Regional and urban air quality numerical models

Numerical air quality modelling is a powerful tool for air quality evaluation and management. Its application has been defined and recommended throughout EU's air quality legislation [96/62/EC, COM(2001)245 final, 2008/50/EC] to provide an adequate level of information on ambient air quality. In the framework of CAFE, modelling techniques have been used to study the repercussions of emission reduction scenarios in air quality levels, namely on ozone and particulate matter concentrations and their impacts on human health and vegetation [Thunis *et al.*, 2007; Vautard *et al.*, 2007].

An atmospheric numerical model is a computerized mathematical representation of the dynamical, physical, chemical and radiative processes in the atmosphere. Modern atmospheric science is a field that combines meteorology, physics, mathematics, chemistry, and computer sciences; other sciences such as geology, biology and oceanographic sciences are also involved to a lesser extent in the so called Earth System Models.

Until the 1940s scientific studies of the atmosphere were limited to the weather, since then the growing awareness of air pollution problems lead to a rapid increase of air pollution studies, and computer modelling of meteorology and air pollution initiated and slowly merged [Jacobson, 1999].

In the 1950's laboratory work was undertaken to better understand the formation of photochemical and London-type smog; also the emergence of computers allowed the implementation of box models for the simulation of atmospheric chemical reactions. Between the 1950's and the 1970's air quality models were expanded to three dimensions, and included the treatment of transport, deposition, emissions, and chemistry [Jacobson, 1999]. In the beginning these models used observed meteorological data as input; shortly after outputs from meteorological models were used as inputs to air quality models [Pielke *et al.*, 1992].

Nowadays the majority of the modelling systems for the study of air pollution comprise a meteorological model and an air quality model, and the respective pre-processors. The models can be linked off-line or on-line: the first meaning that the meteorological simulation is performed first and its

outputs are after that fed into the chemical model; the second meaning that meteorology and chemistry simulations are performed at the same time on the same grid, therefore existing feed-back mechanisms between the two models.

The main meteorological variables in a model are wind speed, wind direction, air temperature, air density, air pressure and water content. These variables are simulated by solving a set of partial differential equations and parameterized equations (equations in which one parameter is expressed in terms of at least two other parameters), including the momentum equation, the thermodynamic energy equation, the continuity equation of air and total water, and the equation of state. Changes in concentrations of gaseous and particulate species are found by solving ordinary differential equations that describe chemistry and physics, and partial differential equations that describe transport [Jacobson, 1999].

Over the past few years there has been a growing need to simulate meteorological fields for complex situations at higher spatial resolutions. This has been partly stimulated by the scientific and technological advances and partly by policy pressures requiring more detailed assessment of air pollution on urban to regional scales. As a consequence, complex dynamical models have been increasingly used in Europe and the USA for meteorological and air pollution applications [COST728, 2005].

Atmospheric problems can be simulated over a variety of spatial scales. Mesoscale studies spatial scales range from tens of kilometres (urban scale) to some thousands (regional scale); this is the scale representative of many of the air pollution problems, therefore is the most relevant and adequate for decision support [Moussiopoulos, 1996].

There is currently a wide variety of models steaming from the diversity in spatial and temporal scales, because different scales demand different approximations and parameterizations. For a classical Gaussian model, surface data from a single meteorological station is enough, since this type of model considers that these are applicable to the entire simulation domain and no variations with height are found. Lagrangean and Eulerian models, however, allow the variation of meteorological conditions along the domain, horizontal and vertically. For the simulation of complex meteorological conditions three-dimensional models are advised; these can be classified as diagnostic or prognostic models. Diagnostic models use available local meteorology to determine meteorological variables over the simulation domain through interpolation or extrapolation techniques; meteorological fields calculated for each time step are independent on previous time-steps results. Prognostic meteorological models are initialized by large scale synoptic analysis, and numerically solve atmospheric dynamics equations in order to determine local meteorological conditions [Seinfeld and Pandis, 1998]. Often these models have nesting capabilities that allow the consideration of a first regional domain (500–1000 km) with a

coarse resolution, and afterwards successive smaller nests to cover a specific area (1-10km) at higher resolutions.

Meteorological models able to resolve mesoscale processes (1-200 km) are considered to be the main tools in air pollution assessments because they allow sufficiently high spatial and temporal resolution and can trace back the linkages between sources and impacts of long travel distances and times. Additionally they can accommodate a wide range of specific local conditions. However, the meso-meteorological capabilities of meteorological models are generally not specifically optimized for pollution applications, namely in urban areas. For example, meteorological models contain options for treating processes which the users must select themselves, such as the boundary layer parameterization to use. Also, situations which present huge challenges for meteorological models include dispersion in very stable or low wind speed conditions, which generally lead to the production of secondary pollutants, such as ozone [COST728, 2005].

Meteorological mesoscale models have been developed in most European countries for flow simulations and for dispersion studies. Public/research versions are available from European and US National Weather Services and other agencies. Models such as MM5 [Dudhia *et al.*, 1993] are commonly employed as meteorological pre-processors/drivers for photochemical models and have demonstrated their usefulness for air pollution assessment down to spatial resolutions of 1 km and temporal resolutions of 1 hour [COST728, 2005]. Other research models which have been similarly employed include WRF [Grell *et al.*, 2005], ALADIN [URL9], RAMS [Pielke *et al.*, 1992], MEMO [Moussioupoulos *et al.*, 1994], MESO-NH [Cousin *et al.*, 2005], and METRAS [Schlünzen, 1988].

Based on meteorological model results air quality models simulate the transport, dispersion and chemical transformation of pollutants, providing the concentration and deposition of reactive and inert chemical species. Air quality models can be classified according to their mathematical formulation as Lagrangean or Eulerian models. Lagrangean models consider that the air parcel moves with the local wind and there is no mass exchange allowed to enter the air parcel and its surroundings (except of species emissions). The air parcel moves continuously and the length and direction of the dislocation are determined through the average wind speed and direction for each time step of the calculation [Draxier and Hess, 1998]. Eulerian models consider a fixed three-dimensional cartesian grid as a frame of reference rather than a moving frame of reference; these models are also known as grid models due to their three-dimensional grid. The emission of pollutants is considered for each cell, and the pollutants go through the grid under the influence of the atmospheric flow, undergoing physical and chemical transformations. Eulerian models are therefore more demanding in computational terms than Lagrangean models. The treatment of individual processes in Eulerian models can be more or less

complex, thus these vary widely in vertical resolution, used parameterizations, initialization methods and boundary conditions, and also in the used numerical techniques [Reid *et al.*, 2007].

Three-dimensional air quality Eulerian models were firstly developed and applied extensively to study ozone related pollution [Moussiopoulos, 1996]; more recently, developments have focused on the chemical simulation of aerossols [Hass *et al.*, 2003; Bessagnet *et al.*, 2004; Van Dingenen *et al.*, 2004]. The simulation of photochemical processes demands the inclusion of a group of chemical reactions responsible for ozone formation and the respective parameterization of reaction rates. These, together with the integration of transport, diffusion and deposition processes (dictated by meteorology) and anthropogenic and biogenic emissions, allow the estimation of air pollutant concentrations [Seinfeld and Pandis, 1998]. Modelling of aerosols has been more recently tackled due to the high complexity of the physical and chemical processes involved, many of them still unknown [Pio *et al.*, 2007; Pun *et al.*, 2007]. Implicated species are numerous, as well as its origin, primary and secondary (sulphates, nitrates, ammonia and secondary organic species). Besides its chemical composition, aerosols species must also be characterised in terms of size distribution, and dry and wet deposition cannot be neglected [Seinfeld and Pandis, 1998].

Currently, several air quality models are available for the simulation of gaseous and particulate chemistry at regional and urban scales. Some examples are the European models EMEP, LOTOS-EUROS and CHIMERE [Van Loon, 2004; Vautard *et al.*, 2007], the American models CMAQ and CAMx [Tesche *et al.*, 2006] or the Australian model TAPM [Hurley *et al.*, 2003].

Air quality models need to be evaluated to be used with confidence at the scientific and policy levels, therefore its application must always be accompanied by a set of quality control and quality assurance procedures, and preferably an uncertainty estimation analyses should be conducted [Borrego *et al.*, 2008a].

2.3 Integration of urban planning and air pollution

Since the world's cities are the major consumers of natural resources, the major producers of pollution and waste, and the focus of most other human activities, various governments realised that much of the sustainable debate has an urban focus [Breheny, 1992a]. Solving the problems of the city would be a major contribution to solving the most pressing global environmental problems, since it is in cities that we find the greatest concentration of population and economic activity, and it is in cities that the crucial long term and often irreversible decisions on infra-structure investments (related to energy supply and waste treatment) are made.

After the Brundtland Commission report [WCED, 1987] the notion that the natural environment should become a political priority, and the pursuit of sustainable development received a remarkable attention. In many countries there have been profound changes in policies and in political and popular attitudes, as the commitment to the sustainable development idea has increased [Breheny, 1996]. The question now is which urban form or structure will be likely to deliver more environmental benefits or will be less harmful to the human health and the environment. The most important work conducted in the field in the last two decades is reviewed next.

2.3.1 Data analysis studies

Much of the technical arguments for compact cities have revolved around the allegedly lower levels of travel, and hence lower levels of fuel consumption and emissions, associated with high urban densities. Newman and Kenworthy [1989a; 1989b] and Newman [1992] have done some work in the field. For a large number of cities around the world, they related fuel consumption per capita to population density, and found a consistent pattern with higher densities associated with lower fuel consumption. Figure 2.14 presents data for a number of world cities, revealing a consistent relationship between population density and energy consumption: high energy consumption rates are associated with lower population densities, characteristic of sprawling urban environments.

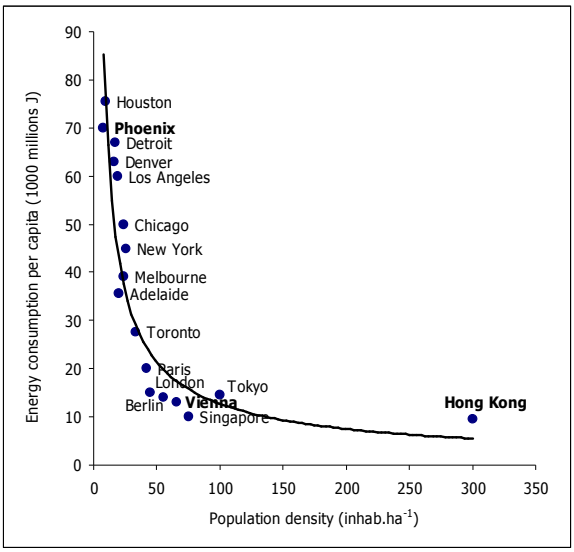

Figure 2.14 Energy consumption per capita and population density for several world cities (adapted from Newman and Kenworthy, 1999).

Energy consumption depends on a variety of factors such as climate, nature of transportation networks, energy sources and others, but a clear link with population density was found: US cities are on the top of energy consumption per capita; on the other extreme, are Asian cities like Hong Kong, with a per capita energy consumption 15% to 20% of the American cities and 30 times higher

population densities. The conclusion from this exercise was that, if fuel consumption and emissions are to be reduced, there is a need for policies to promote urban compaction and public transport.

Kenworthy and Laube [1996] compared a group of world cities over the period 1980 to 1990 regarding its land use and transport characteristics. The data revealed that metropolitan densities in the United States and Australia have remained very low and basically static between 1980 and 1990, while new development in European cities has spread out, although still occurring at densities significantly higher than in the US and Australia. In the wealthy Asian cities (Singapore, Tokyo and Hong Kong), development continued to occur at very high densities compared with the western world (12 times the US and Australia urban densities and over 3 times European densities). The study demonstrated the importance of urban density in explaining annual per capita auto use, with annual kilometres travelled per capita strongly inversely correlated (r^2=0.8) with urban density .

Conclusions similar to those of Newman and Kenworthy emerged from the ECOTEC [1993] study for the UK government, which found a clear inverse correlation between total distances travelled per week and population density. People living at the lowest densities were found to travel twice as far by car each week in comparison to those living at the highest densities.

The message coming from these studies remains controversial, and the studies by Newman and Kenworthy have been criticised for focusing on the single variable of density, when other factors are likely to be important in explaining travel behaviour. Gomez-Ibanez [1991] argues that household income and fuel price are important determinants of such behaviour, making it difficult to clearly identify the link between density and fuel consumption. He also addresses an important point: the costs of containment policies – in terms of economic losses, reduced quality of life, and others – have not been weighed against the supposed environmental gains.

A study from Ambiente Italia [2003] presents the relationship between CO_2 emissions and population density for several European cities (Figure 2.15). It seems that emissions decrease progressively with the increase of urban densities, although not as evidently as in the case of energy consumption, revealing that other factors such as climate, fuel mix and industrial activity are probably more important.

In addition to vehicle travel and emissions, the spatial structure of a region has been associated with meteorological phenomena that are important to regional air quality. As already mentioned, one of the most recognized meteorological effects of urbanization is the urban heat island effect. Rosenfeld et al. [1998] developed a model to assess the impact of various heat island management strategies on ozone formation in Los Angeles. The cooling benefits of a region-wide program designed to increase

the surface reflectivity of urban infrastructures and the extent of tree canopy cover could result in a reduction of the number of annual ozone exceedances by about 12%.

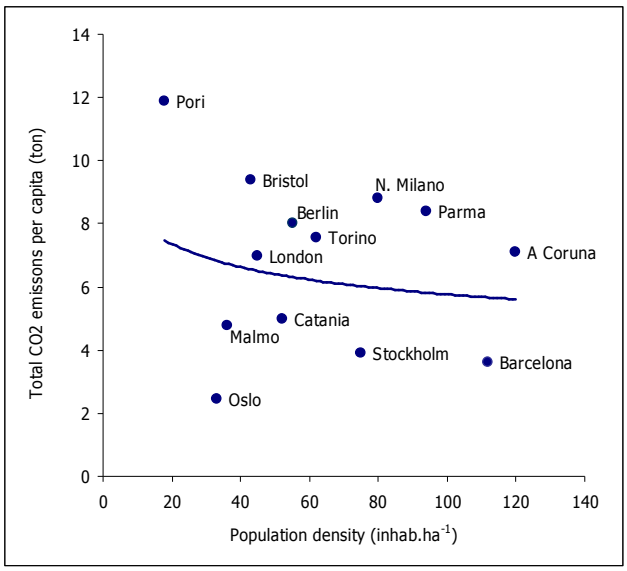

Figure 2.15 CO_2 emissions per capita and population density for several European cities (adapted from Ambiente Italia, 2003).

While several additional studies [Handy, 1996; Young and Bowyer, 1996; Cervero, 1988; Crane, 2000; Frank *et al.*, 2000; USEPA, 2001; Herala, 2003; Cameron *et al.*, 2004; Irving and Moncrieff, 2004; Handy *et al.*, 2005] have related travel behaviour, traffic, energy consumption and emissions with land use patterns, only few were found relating land use with air quality, i.e., with air atmospheric pollutant concentrations.

Emison [2001] examined the relationship between the degree of sprawl and ozone levels for 52 metropolitan areas in the United States. While there was evidence regarding the association between lower population densities and higher vehicle miles of travel, only moderate evidence was found relating sprawl and increased ozone levels. The author admits he would have expected a stronger and less ambiguous relation, therefore suggesting more research in order to explore the relationship between sprawl and photochemical pollution.

Marshall et al. [2005] analyse the impact of changes in land area and population on per capita exposure to motor vehicle emissions, through an exploratory analysis that considers a hypothetical, idealized representation of an urban area. The authors investigate, quantitatively and parametrically, how three changes in urban land area and urban population influence population inhalation of motor vehicle emissions: (1) increasing population while land area remains constant; (2) increasing land area while population remains constant; and (3) increasing land area and population while density remains constant. It was concluded that infill development has the potential to reduce motor vehicle emissions

yet increasing per capita inhalation of those emissions, while sprawl has the potential to increase vehicle emissions but reduce their inhalation.

More recently, Stone [2008] explored the implications of sprawl for air quality within the largest metropolitan regions of the Unites States. Through the integration of data on land use attributes and air quality trends recorded in 45 of the 50 largest US metropolitan regions, a quantitative index of urban sprawl was associated with the emissions of ozone precursors and the annual number of high ozone days in each region between 1990 and 2002. The work assessed the implications of sprawl for ozone in multiple cities while controlling for population, precursor emissions, and meteorological attributes important to ozone formation. The results of this study indicate that for the 45 surveyed US metropolitan regions, urban form is significantly associated with both ozone precursor emissions and ozone exceedances, during a 13-year study period. A positive association between sprawl and ozone exceedances was found to hold true when controlling for average ozone season (May through September) temperatures and annual emissions of ozone precursors. This suggests that the well-established linkage between decentralized development patterns and motorized transport use may be only one of multiple mechanisms through which sprawl influences air quality. Overall, the most sprawling cities experienced over 60% more high ozone days than the most compact cities.

Martins et al. [2007a] carried out a survey to relate population density with the atmospheric concentration of O_3 and PM10. In this scope, several reports from different sources, institutions and countries were analysed; in order to have comparable data, the analysed parameters were ozone one-hour maximum concentrations and PM2.5 annual average concentrations. Figure 2.16 relates the ozone one-hour maximum concentrations registered in 2003 (except for Phoenix with 2006 data, Adelaide 2004 data, and London 2005 data) for several world cities with each city's population density.

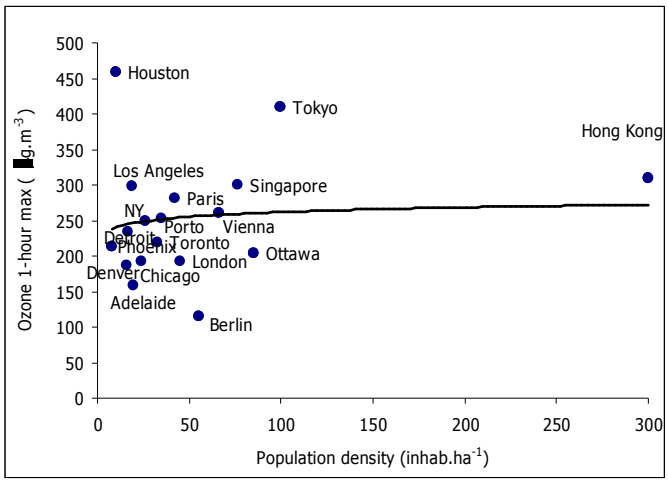

Figure 2.16 Ozone 1-hour maximum concentrations and population density for several world cities [Martins et al., 2007a].

Although it seems that maximum ozone concentrations tend to increase with population density, a conclusion cannot be drawn since the correlation factor is very low (r^2=0.1), suggesting that others factors, such as local climate, are more decisive. Figure 2.17 represents population density against PM2.5 annual average concentrations.

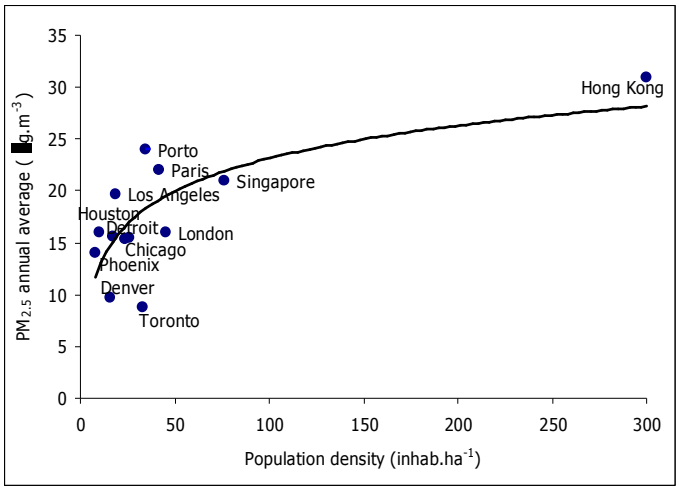

Figure 2.17 PM2.5 annual average concentrations and population density for several world cities [Martins et al., 2007a].

For PM2.5 it is evident that annual averages tend to increase with population density, with the two variables highly correlated (r^2=0.5). However, one should be cautious when comparing absolute values from different regions. Often data are based on one or few monitoring stations, placed in critical sites thus representing micro-environments. It should also be taken in to account that the coverage of stations is different for different countries and that average values can therefore be differently biased.

Most of the above work relied on empirical studies to provide descriptive comparisons of current cities and to find evidence that certain types of urban forms are correlated with desirable levels of energy consumption and emissions. For the most part, the debate has focused on urban densities - whether high urban densities reduce the need for travel and promote the use of mass transport systems - and on urban size - whether larger urban areas with higher densities are more energy efficient than smaller areas. Mathematical modelling studies have also been used to identify urban forms which minimise travel and energy consumption [Rickaby and De la Barra, 1989; Rickaby, 1991; Steadman and Barrett, 1991].

The approaches here presented integrate the land use and transport aspects of urban form, but lack the extra step that translates energy efficiency into indicators of air quality, via pollutant concentrations.

2.3.2 Numerical modelling studies

As just mentioned, several empirical and modelling studies integrate land use and transport issues and its relation with urban structure, however, few were found that explore the connection to air quality and human exposure. Conclusions from most of the studies done so far have been harmed by the lack of knowledge about the complex path between an initial action for the reduction of atmospheric emissions and the final benefit in terms of air quality and human exposure (Marquez and Smith, 1999).

Health effects of air pollution are the result of a chain of events, going from the release of pollutants leading to an ambient atmospheric concentration, over the personal exposure, uptake, and resulting internal dose to the subsequent health effect (Figure 2.18).

Figure 2.18 The source-effect chain of air pollution (adapted from Ferreira et al. 2005).

It is important to make a distinction between concentration and exposure; concentration is a physical characteristic of the environment at a certain place and time, whereas exposure describes the interaction between the environment and a living subject, referring to an individual's contact with a pollutant concentration.

Emissions reduction conducts to changes in atmospheric pollutant concentrations, but those changes will have different spatial and temporal magnitudes and signs, due to differences in emissions, weather patterns and population exposed to pollution according to the time of the day, day of the week or month of the year, and also according to the population age structure (children, adults and elderly suffer different effects due to their different respiratory frequencies). Exposure is the key factor in assessing the risk of adverse health effects, since high pollutant concentrations do not harm people if they are not present, while even low levels may become relevant when people are present [WHO, 1999].

Recent advances in computer technology have allowed the integration of land-use and traffic models with air quality models; these modelling tools assume a particular importance to the subject under study, since they allow the integration of the most important variables that have to be analysed. One of the earliest investigations in this field was carried out by Newton [1997] for Melbourne, using a framework developed by Marquez and Smith [1999] for linking urban form and air quality, integrating land use, transport and air quality models. The authors were responsible for one of the first integrations of land use and transport models, which represent complex, dynamic systems with large data requirements and intensive computing tasks, with even more demanding air quality models.

The framework consisted of five components, here briefly described: (1) a GIS/database, responsible by all mechanisms for managing data required by the other four components; (2) a land use – transport model, which generates and distributes trips through the study region's road network producing traffic flow; (3) an emissions interface, which calculates the distribution of emissions; (4) the meteorological component that receives mesoscale meteorological data, including three-dimensional time-varying vector wind fields, and two-dimensional time-varying fields of mixing depth, temperature, sensible heat flux and radiation; and (5) an air quality model which solves the mathematical equations that describe the transport and mixing of pollutants released into the atmosphere, producing as outputs a number of air quality metrics, including population exposure [Marquez and Smith, 1999].

In order to demonstrate the impact of urban form on future urban air quality, Newton (1997) developed six growth scenarios for 2011, following the six urban forms presented by Minnery [1992], which represent different spatial configurations, according to their shape and structure (Figure 2.19).

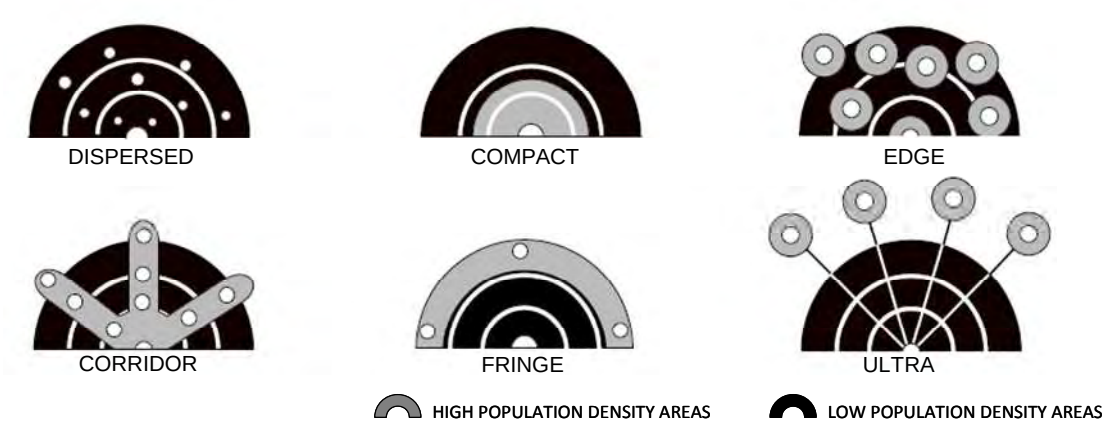

Figure 2.19 City types representing urban systems with different spatial configurations, according to their shape and structure (adapted from Minnery, 1992).

The dispersed city represents the current trend of many of our contemporary cities, with expansion of urban development at low densities, a well defined city centre and radial structure transport network. The compact city emerges as result of an effort for containing urban expansion, through the increase of population density in the city centre and in the adjacent suburbs. The edge city, or multi-nodal, is constituted by several high development central points (nodes), connected by highways and arterial roads, where jobs, commerce and leisure activities are concentrated. The corridor city is characterized by linear corridors originating from the city centre, served by high-quality transport infrastructures, along which growth takes place. In the fringe city, growth is accommodated in the suburbs and rural zones, away from the city centre. In the ultra-city the concept of metropolis is replaced by the concept

of metropolis-based region, extending some hundred kilometres from its historical origins; high-speed transport and communications provide the basis to this concept [Newton, 1997].

Land use and transport models were applied to a time horizon of 20 years, whilst the air quality model was applied for a typical summer day (with meteorological conditions favourable to the occurrence of photochemical smog, i.e. ozone) and a typical winter day (with meteorological conditions favourable to the occurrence of high PM10 concentrations). The results of the case study show that any of the several strategies designed to deliberately channel and concentrate additional population and industry into specific zones, when supported by simultaneous investments in transport infrastructure, will deliver environmental and efficiency benefits that consistently outperform those associated with the "business-as-usual" approach. Figure 2.20 presents some of the obtained results for human exposure.

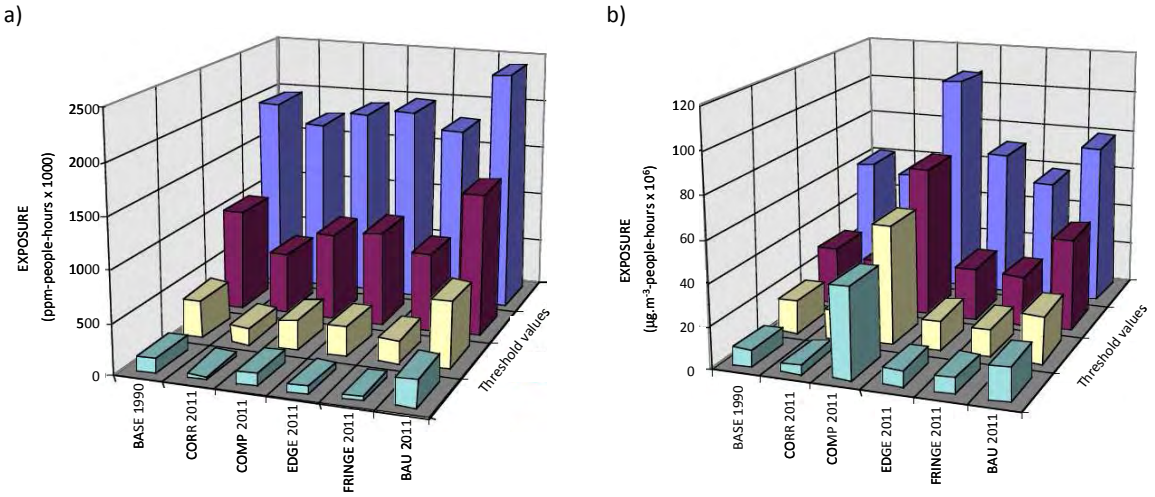

Figure 2.20 Predicted population exposure in Melbourne for a) a simulated summer photochemical smog event; and b) a simulated winter fine particle pollution event (exposure is calculated for predicted concentration above certain threshold values)[Newton, 1997].

In the case of population exposure to photochemical smog in Melbourne (Figure 2.20a), the corridor development scenario for 2011 results a 55% improvement over the 1990 base case. The compact and edge scenarios also delivered significant enhancements at 24% and 21% respectively. On the other hand, business-as-usual development produced an increase of 71% in human exposure to pollutant dosages above established air quality limits. For the winter episode (Figure 2.20b) the corridor city scenario results in a 14% improvement in human exposure to PM10, while the compact city scenario presents the worst situation, with a 160% aggravation. Despite the low levels of pollutant emissions and fuel consumption, the location of new residences and working places in the compact city centre, lead to the exposure of a greater number of residents and workers to high dosages of PM10. The study concludes that urban structure does matter, not just for urban air quality, but also for human exposure to pollutants.

Civerolo et al. [2007] investigated the potential effects of extensive changes in urban land cover, in the New York City (NYC) metropolitan region, on surface meteorology and ozone concentrations. A land-use change model was used to extrapolate urban land cover over the region from ''present-day'' conditions to a future year (2050), and the projections were subsequently integrated into meteorological and air quality simulations. The non-hydrostatic fifth-generation mesoscale model MM5 [Dudhia, 1993] was the regional-scale meteorological model used to simulate a 18-day episode. The emissions were processed using the SMOKE model [Houyoux *et al.*, 2000]. Air quality simulations were performed using the CMAQ air quality model [Byun and Schere, 2006]. Results from the study suggest that extensive urban growth in the NYC metropolitan area has the potential to increase afternoon near-surface temperatures by more than 0.6°C across the NYC metropolitan area. Simulation results indicate that future changes in urbanization, with emissions held constant, may lead to increases in episode-average ozone levels by about 1–5 ppb, and episode-maximum 8 h ozone levels by more than 6 ppb across much of the NYC area. However, spatial patterns of ozone changes are heterogeneous, presenting areas with decreasing ozone concentrations.

More recently De Ridder *et al.* [2008a, 2008b] investigated the effects of urban sprawl on road traffic, air quality and population exposure, at the scale of a large urban area (the German Ruhr area) for an air pollution episode. Starting from a high-resolution land use map established for the base case, spatial modelling techniques were applied to simulate changes in land use and employment density, in order to simulate urban sprawl. The scenario resulted in an increase of the built-up area from 28% to 50%, with an associated displacement of 12% of the urban population (which was kept constant) to the periphery. To simulate the effect of urban sprawl on traffic volumes and its distribution a traffic model was applied, yielding an increase of almost 17% for total vehicle-kilometres. Traffic flows and speed patterns were used to estimate emissions, revealing an increase of 12% in emission totals. Meteorological simulations were then performed with the ARPS model [Xue *et al.*, 2000], and used as input for the chemistry-transport model AURORA [Mensik *et al.*, 2001]. The sprawl scenario produced a temperature increase of about half a degree over significant portions of the domain, including beyond the area where the land use changes were implemented. The combination of increased temperature and emissions yielded ozone concentration pattern changes, from -1.5 to +4.5 $\mu g.m^{-3}$. Concerning PM10, concentration increases were small (less than 1 $\mu g.m^{-3}$). Regarding exposure it was found that the relatively small proportion of relocated individuals benefited of a decrease of exposure to particulate matter by almost 13%, due to their moving out of polluted areas; that came to the expense of an increase of exposure of 1.2% by the individuals that have not moved. Regarding domain average exposure, urban sprawl revealed a limited effect, with an increase amounting to 0.35% and 0.55% for PM10 and ozone, respectively.

Modelling studies seem to confirm the dilemma, well summarized by Cervero [2000]: “exposure levels, and thus health risks, are lower with sprawl, but tailpipe emissions and fossil-fuel consumption are greatly increased”. However, studies so far have only been conducted for episodic air pollution situations and only one of them, from Newton [1997], did compare alternative urban development scenarios; the other studies compared an urban sprawl development scenario with a starting point or reference situation, therefore were not able to compare alternative scenarios.

Next, the first modelling approach of this thesis is conducted for an idealized urban area.

3 AN IDEALIZED CASE STUDY

The present chapter constitutes this thesis first modelling approach to the study of the relation between urban structure and air quality, through the application of a modelling system to an idealized case study. This case study is developed around the creation of three imaginary cities, representing three alternative city structures. Differences between cities lay on a different land use distribution and different population densities, which are reflected in different total amounts and different spatial distribution of pollutants emitted to the atmosphere. A mesoscale photochemical modelling system is then applied to an ozone pollution episode to estimate the air quality levels, namely ozone and nitrogen oxides concentrations, in the three cities, allowing the comparison of the air quality performance of each urban structure. As a complement to air quality modelling, and in order to explore the possible effects of different urban structures on human health, the population exposure in each urban area was determined, combining information on air pollutant concentrations at different microenvironments and population time-activity pattern data.

3.1 Idealized city structures

Following the description by Minnery [1992], presented in §2.3.2 (Figure 2.19), three idealized city structures were created, presenting different spatial configurations which reflect three alternative urban development philosophies - dispersed, compact and corridor [Borrego *et al.*, 2006a].

The Dispersed City represents urban sprawl, with low population density, large area requirements and separation of artificial land uses into distinct zones - residential, commercial and industrial - with the consequent high car use dependence. The Corridor City, conceived around axes and nodes, is characterised by growth in linear corridors with origin in the city centre, supported by high quality transport infrastructure (highways); it offers partly mixed and partly unmixed functions. The Compact City uses less area than the Disperse City due to its high population density, with mixed land uses and

complementary functions located close together, allowing the reduction of travel length and number of trips. A total area of 2500 km^2 was defined and data sets were created considering four different land use categories: urban, suburban, green urban areas and rural. The distribution of land uses in each city took into account the city development philosophies, already described; the resulting land use composition and distribution is presented in Figure 3.1.

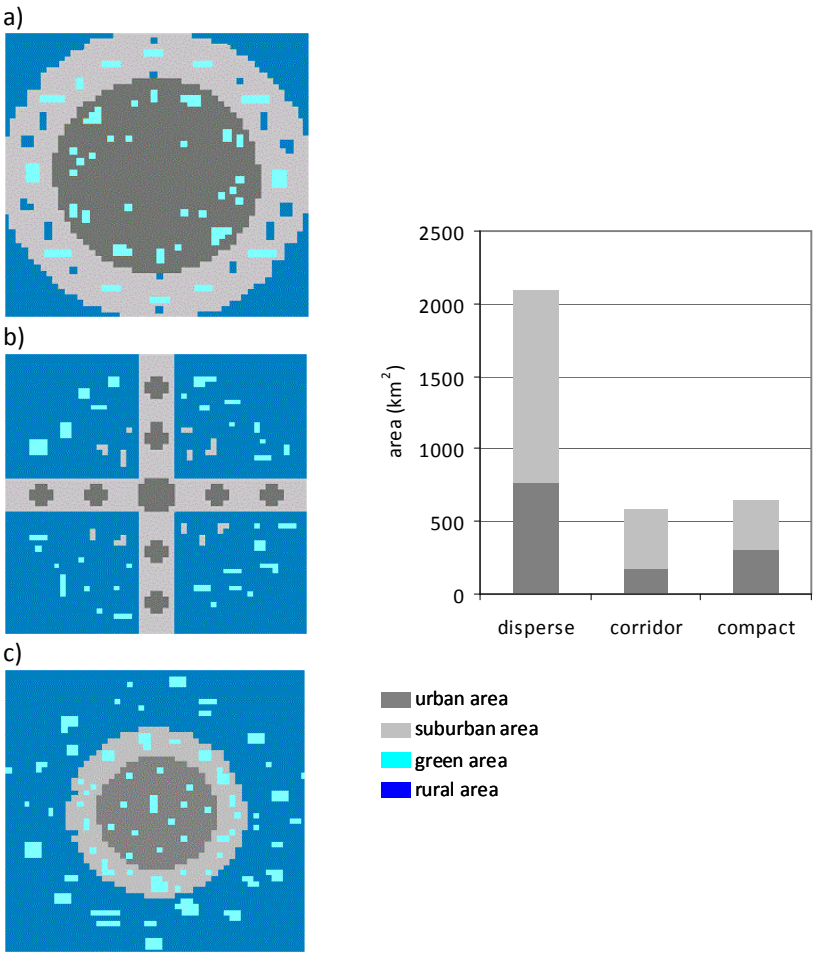

Figure 3.1 Land use in a) Disperse City, b) Corridor City, and c) Compact City, and the composition of artificial areas (urban and suburban) for each city.

The Disperse city presents an urbanized area more than three times greater than the other two cities, with suburban areas accounting for the greatest part of it (around 65%). Compact and Corridor cities show a similar urbanized area, but different shares of urban/suburban areas: in the Corridor city 70% of the urbanized area is suburban, while in the Compact the share is only 52%.

The created cities, or urban regions, intend to represent a large metropolis; therefore a number of three million inhabitants were distributed within the cities assuming different population densities for each land use class. These densities were based on data from André *et al.* [1999]: rural agglomerations present a population density below 100 inhabitants per square kilometre; for suburban

agglomerations the density varies between 101 and 1000 inhabitants.km^{-2}; and for the urban areas the value is higher than 1001 inhabitants.km^{-2}. The distribution of population was done using the SURFER software, namely its radial basis function, and considering the defined population density intervals. As a result, the highest population density is attributed to the urban zone of the Corridor city with 3000 inhab.km^{-2}. The maximum population density in the Compact city is 2000 inhab.km^{-2} and in the Disperse city this parameter reaches 800 inhab.km^{-2}.

3.2 Emissions

As already discussed, more dispersed city developments with discrete land uses increase distances between destinations, and consequently travel needs and trip lengths. According to this argument, traffic demand is the principal distinction between the constructed idealized cities, and therefore special attention is given to traffic emissions.

The further construction of the idealized cities made use of a set of statistical data collected under the framework of the MEET Project (Methodologies for estimating air pollutants emissions from transport), presented in a report from André *et al.* [1999]. The report assembles several driving statistics, essential for the estimation of air pollutants emissions from traffic (Table 3.1).

Table 3.1 Traffic data used for estimating air pollutants emissions from transport [André *et al.*, 1999].

		Private passenger cars	Public transport (buses and coaches)
average occupancy rates:			
	urban	1.8	31.2
	suburban	-	27.3
vehicle mileage (km.y^{-1}):			
	urban	7500 -12800	20700 - 35250
	suburban	8500 - 13900	7800 – 27000
	rural	14700	13140
average speed (km.h^{-1}):			
compact city	urban	30	16
	suburban	50	47
	rural	70	65
corridor city	urban	30	16
	suburban	95	90
	rural	70	65
disperse city	urban	30	16
	suburban	50	47
	rural	70	65

Figure 3.2 illustrates the traffic emission calculation methodology. Starting from population density, with private and public transport occupancy rates, it was possible to determine the total number of vehicles in each city. Then, using the vehicle mileage according to land use category, the total kilometres travelled were estimated.

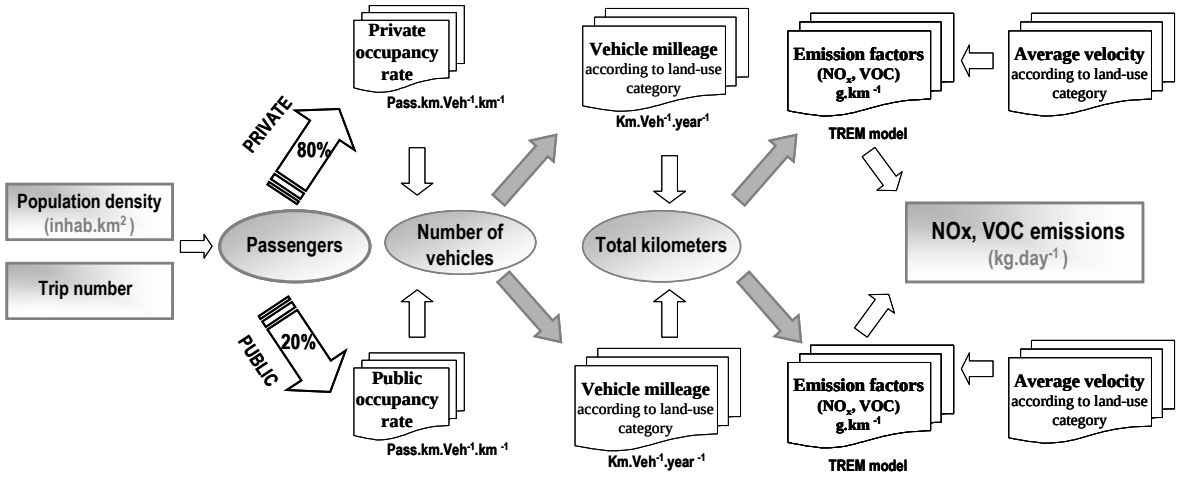

Figure 3.2 Methodology for traffic emission calculation.

Emission factors were calculated by TREM model [Borrego *et al.*, 2003], considering all vehicles as EURO 1 technology (for sake of simplification) and assuming different average velocities according to land use categories (presented in Table 3.1). TREM was developed at the University of Aveiro, based on MEET/COST methodology and its prime objective is the estimation of road traffic emissions, with high temporal and spatial resolution, to be used in air quality modelling. Roads are considered as line sources and emissions induced by vehicles are estimated individually for each road segment considering detailed information on traffic flux. Total emission of the pollutant p (E_p) for each road segment is estimated by the model as follows:

$$E_p = \Sigma (e_{ip}(v) \times N_i) \times L$$

where $e_{ip}(v)$ is the emission factor for pollutant p and vehicle class i as a function of average speed v; N_i is the number of vehicles of class i; and L is the road segment length.

Other considered emission sources are related to residential, commercial and industrial combustion activities. These emissions are based on emissions for the Lisbon Metropolitan Area from the National Emission Inventory [URL10], since it presents a similar area and population size [URL11]. The emissions from residential sources were spatially disaggregated according to population density. Emissions from industrial and commercial combustion activities were equally distributed for the suburban and urban area cells, respectively.

Emissions from vegetation were also taken into account due to their importance in the ozone cycle. The monoterpenes were quantified using an estimated average emission rate for a typical summer day based on emission factors [Guenter *et al.*, 1997] for typical Portuguese vegetation characteristics, such as species and density [Tchepel, 1997].

Since the modelling system is applied to an ozone pollution episode, the emissions of its precursors, such as nitrogen oxides and volatile organic compounds, assume special importance. These emissions for each city are presented in Table 3.2.

Table 3.2 Daily traffic, other anthropogenic and biogenic emissions obtained for each city (ton.day^{-1})

Emissions (ton.day^{-1})	Traffic		Other Anthropogenic		Biogenic Monoterpenes
	NOx	VOC	NOx	VOC	
compact city	12 922	5 126	5 517	16 192	11 478
corridor city	25 821	8 494	5 545	15 843	2 370
disperse city	22 198	9 646	5 720	16 432	6 306

While industrial, commercial and residential emissions are in the same range for the three cities, the Corridor and Dispersed cities present, as expected, considerably higher traffic emissions when compared to the Compact city. On the other hand, the Compact city shows higher monoterpene emissions due to the larger presence of green areas. In Figure 3.3 the maximum daily emission rates per area and the average emission rates per inhabitant, for each city, are illustrated.

a)

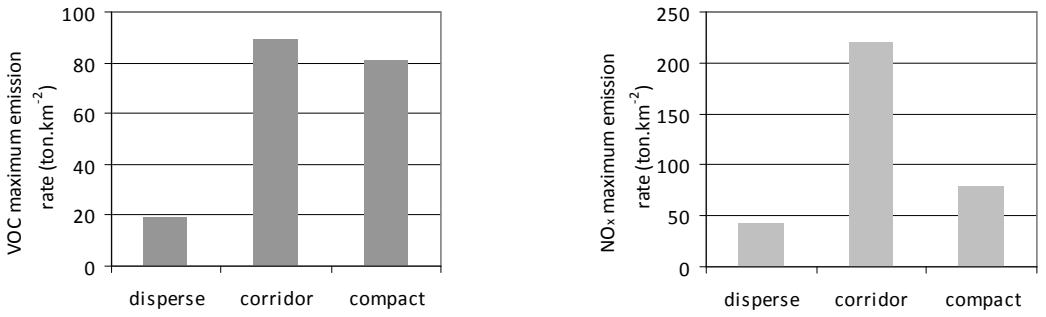

b)

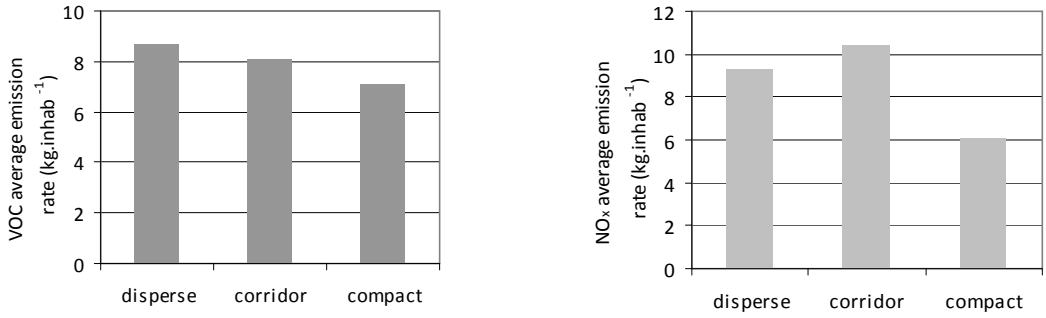

Figure 3.3 Daily VOC and NOx a) maximum emission rates per area and b) average emission rates per inhabitant for the disperse, corridor and compact cities.

The Corridor city is characterized by the highest maximum emission rates per area for both pollutants, as well as the highest NOx average emission rate per inhabitant. The Disperse city shows the lowest emission rates per area and the Compact city the lowest emission rates per inhabitant. It should be

also stressed that all the cities have different ratios of VOC to NOx emissions, which are relevant for ozone formation [Seinfeld and Pandis, 1998]. These differences are mainly related to the average vehicle speed selected for each land use category.

3.3 Air quality modelling

The air quality assessment for each idealized city structure was performed with the MEMO/MARS modelling system. MEMO/MARS has been successfully applied and verified for various European airsheds [Moussiopoulos *et al.*, 1994; Coutinho *et al.*, 1994; Lopes, 1997]; it has also been tested and validated for different areas of Continental Portuguese territory [Borrego *et al.*, 1999; Martins *et al.*, 2004]. Although the system does not belong to the most recent generation of models, the vast experience in the use of this system together with its good performance in the study of episodic situations of photochemical pollution [Borrego *et al.*, 2004; Ferreira *et al.*, 2003; Miranda *et al.*, 2002], justify and support its application to the present case-study.

3.3.1 MEMO/MARS modelling system

The MEMO/MARS system includes two main modules: the meteorological model MEMO (Mesoscale Model) and the photochemical model MARS (Model for the Atmospheric Dispersion of Reactive Species), both developed by the Aristotle University of Thessaloniki in collaboration with the University of Karlsruhe. Figure 3.4 presents a simplified scheme of the modelling system and the necessary data for its application.

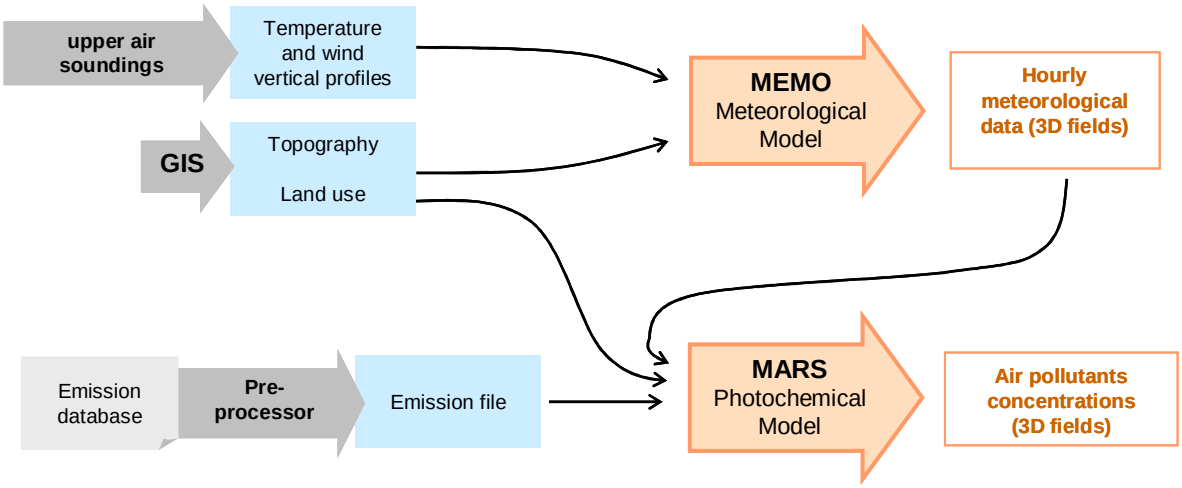

Figure 3.4 MEMO/MARS modelling system used in the study-case (adapted from Lopes, 1997).

The mesoscale model MEMO [ITT, 1994] is a non-hydrostatic prognostic model developed to simulate the atmospheric flow over complex terrain, allowing the description of the air motion and the

dispersion of inert pollutants. Within MEMO, the conservation equations for mass, momentum, and scalar quantities as potential temperature, turbulent kinetic energy and specific humidity are solved in terrain-following coordinates, allowing for non-equidistant mesh sizes to achieve a higher resolution near the ground. The model initialization is performed with diagnostic methods.

Necessary input data for the application of MEMO includes:

- orography height and surface type (MEMO includes 7 surface types: water, arid land, few vegetation, farmland, forest, suburban area and urban area) have to be provided for each grid location, as well as the corresponding thermo-physical data (albedo, volumetric heat capacity and heat conductivity);
- meteorological data (upper air soundings and/or surface measured temperature and wind data)
- time dependent boundary conditions (one dimensional profile of temperature and wind data must be provided to be used either for the initial state or time-dependant boundary conditions).

As output quantities MEMO produces for each grid location wind velocity components, potential temperature, pressure, turbulence data soil moisture profile and optionally concentrations of inert pollutants.

The photochemical model MARS is a three-dimensional Eulerian dispersion model for reactive species that describes the dispersion and chemical transformation of air pollutants [Moussiopoulos, 1995]. This model is oriented towards the photo-oxidants simulation, from which ozone is the major component. Processes of emission, dispersion, transformation and deposition of pollutants are calculated on a staggered grid in terrain-following co-ordinates. The version used in the study presents two chemical mechanisms: KOREM and EMEP. EMEP [Simpson *et al.*, 1993] describes the tropospheric gas-phase chemistry with 66 species, 139 photochemical reactions including 34 photolysis reactions; and the KOREM mechanism, which is simpler, including 39 chemical reactions and 20 reactive pollutants. KOREM is the combination of anorganic reactions of the CERT mechanism [Atkinson *et al.*, 1982] and of organic reactions of the compact mechanism of Bottenheim and Strausz [1982]. The chemistry of methane is also taken into account by including the reaction of methane with the hydroxyl radical. In KOREM mechanism the VOCs are lumped in five classes [Flassak *et al.*, 1992]. On the other hand, the EMEP mechanism considers 13 categories as VOC speciation (including ketones, alcohols and isoprene).

Meteorological data such as wind speed, turbulent kinetic energy, surface roughness, Monin-Obukhov length, and friction velocity are required as input at pre-defined times during the model simulation; these can be supplied by MEMO. Emission data must include information about the diurnal cycle of pollutants considered in the reaction scheme and the composition of every pollution source, allowing

the construction of an appropriate emission inventory for the air quality calculations. Information about the initial state in the whole domain and about the development of pollutant concentrations at the lateral boundaries is also required. MARS outputs include hourly concentrations of chemically reacting pollutants for each grid location.

3.3.2 Model application and results

Tthe MEMO/MARS modelling system was applied to a domain of 200 km x 200 km, with a horizontal grid resolution of 2 km x 2 km. A direct correspondence between the land uses urban, suburban, and rural, defined for the construction of the cities and the land uses defined in MEMO/MARS was made; urban green areas were translated in MEMO/MARS as few vegetation land use category. The KOREM mechanism was selected due to its smaller computing time requirements in comparison with EMEP, based on conclusions from a study by Miranda *et al.* [2002] concerning the two mechanisms, which point to a non-significant improvement of results associated to a more complete description of the photochemical reactions.

Simulations were performed for the three cities for an Iberian Peninsula summer day favourable to the occurrence of photochemical air pollution episodes. The 29th June 2001 was selected for the simulation, as representative of the typical Iberian Peninsula summer synoptical situation, characterized by an almost inexistence of surface pressure gradients and consequently low winds in the low troposphere, clear skies and high temperatures [Coutinho *et al.*, 1994]. The emission file was built with the data obtained by the methodology previously described (see §3.2), considering all emissions as area sources which were represented by a regular matrix. Constant background concentrations (initial and boundary conditions) were equally defined for the three cities: 60 $\mu g.m^{-3}$ for ozone and 2 $\mu g.m^{-3}$ for nitrogen dioxide [Barros, 1999].

Results were analysed considering the O_3 and NO_2 concentrations in relation to its background values and not the absolute concentrations, since this is an idealized study case and the subject under analysis is the relation between the three cities and not the concentrations *per se*. Figures 3.5 and 3.6 present the hourly variation of the two pollutants maximum concentrations (relative to the background value) estimated for each city. Results are shown only from 8:00 to 22:00, since for the remaining hours, corresponding to the night period, concentrations for the three cities are very similar.

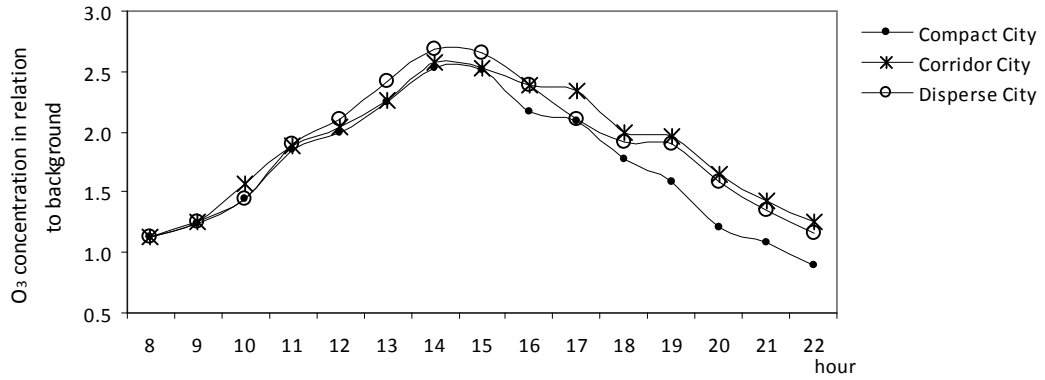

Figure 3.5 Hourly variation of O_3 maximum concentrations for each city.

Although there is a similar behaviour of O_3 concentrations for the three cities, the Disperse city shows the highest concentration levels at the most critical hours (between 12:00 and 16:00). After this period, and during the evening, the Corridor City presents O_3 concentration values similar to the Disperse City. The Compact City reveals the lowest maximum O_3 concentrations, even in the morning when no significant differences among the three cities were estimated. As expected from photochemistry, the highest concentrations in all the three cities are reached at around 14:00.

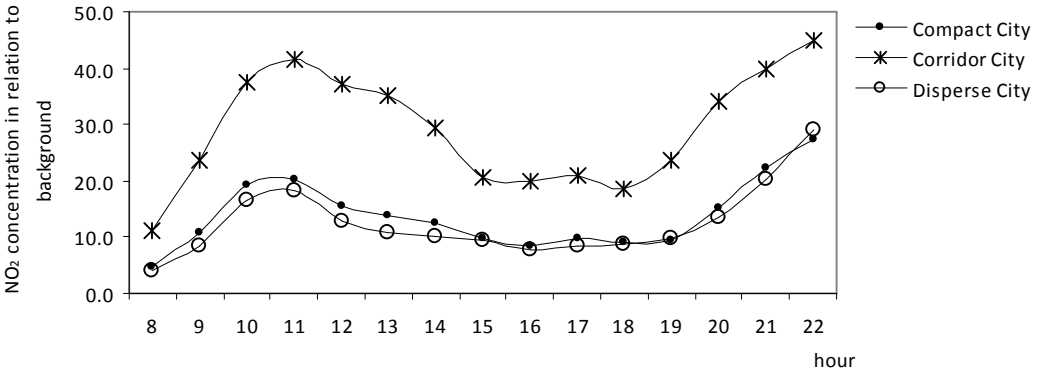

Figure 3.6 Hourly variation of NO_2 maximum concentrations for each city.

The NO_2 hourly variation is similar for the three cities, but the Corridor city reaches higher concentrations in comparison with the other two cities, which have concentrations of the same order of magnitude. Higher NO_2 concentration values are calculated in the morning and at the end of the day as a result of the photochemical cycle and the traffic emissions daily profile.

A comparison between the hourly maximum ozone value within the domain and the corresponding concentration in the city centre is presented in Figure 3.7 a), (b) and (c) for each city. In all the city cases, ozone concentrations are lower in the city centre, with a minimum value between 15:00 and 17:00 showing that ozone consumption occurs at hours of maximum solar radiation in the presence of high levels of nitrogen oxide traffic emissions.

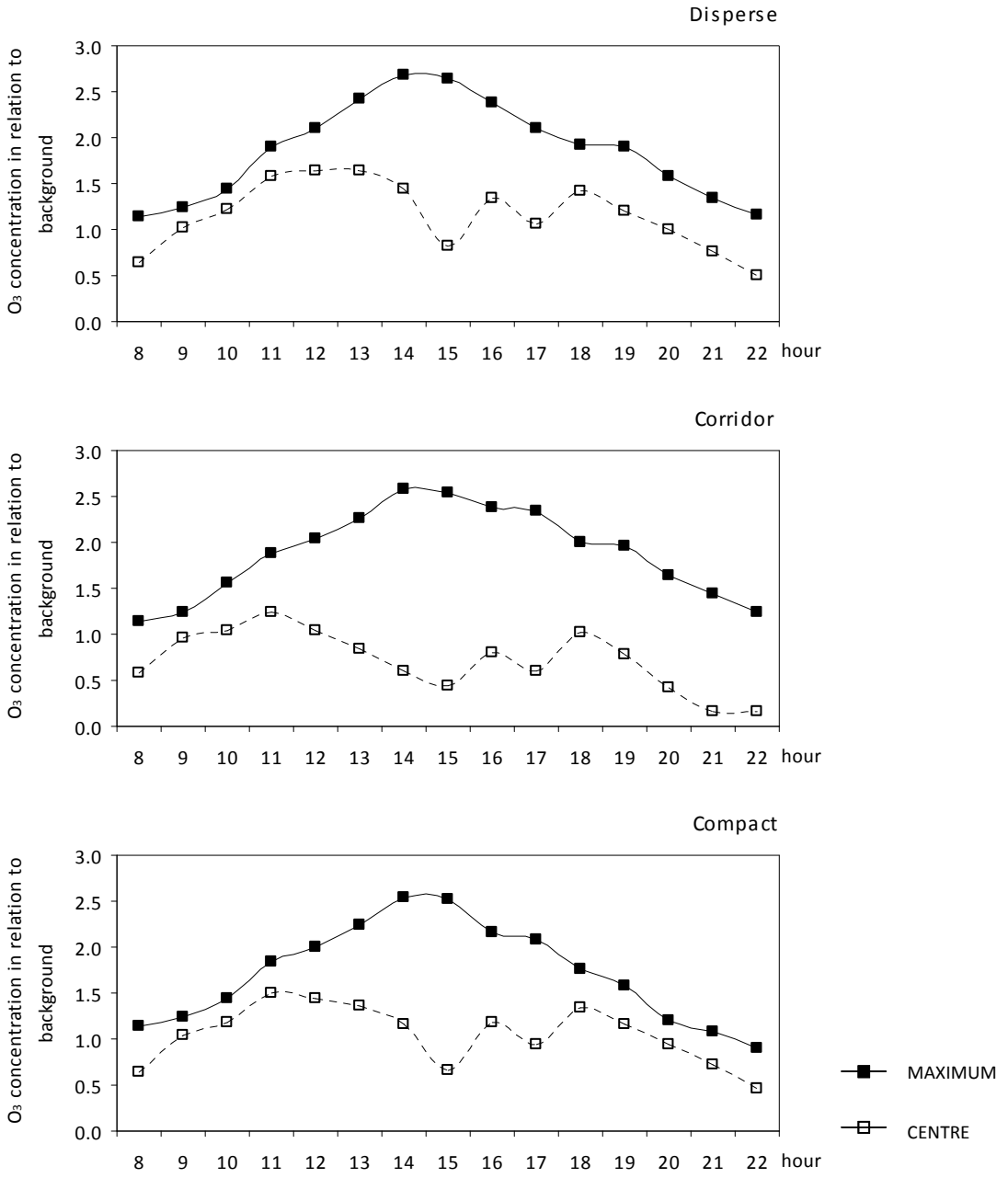

Figure 3.7 Comparison between O_3 concentration in the centre of the city and the maximum domain value for each city.

The same comparison for NO_2 is presented in Figure 3.8 showing that, in opposition to what happens with O_3 concentrations, NO_2 levels reached in the city centre are very close to the maximum domain values, meaning that the highest concentrations are located near the city centre.

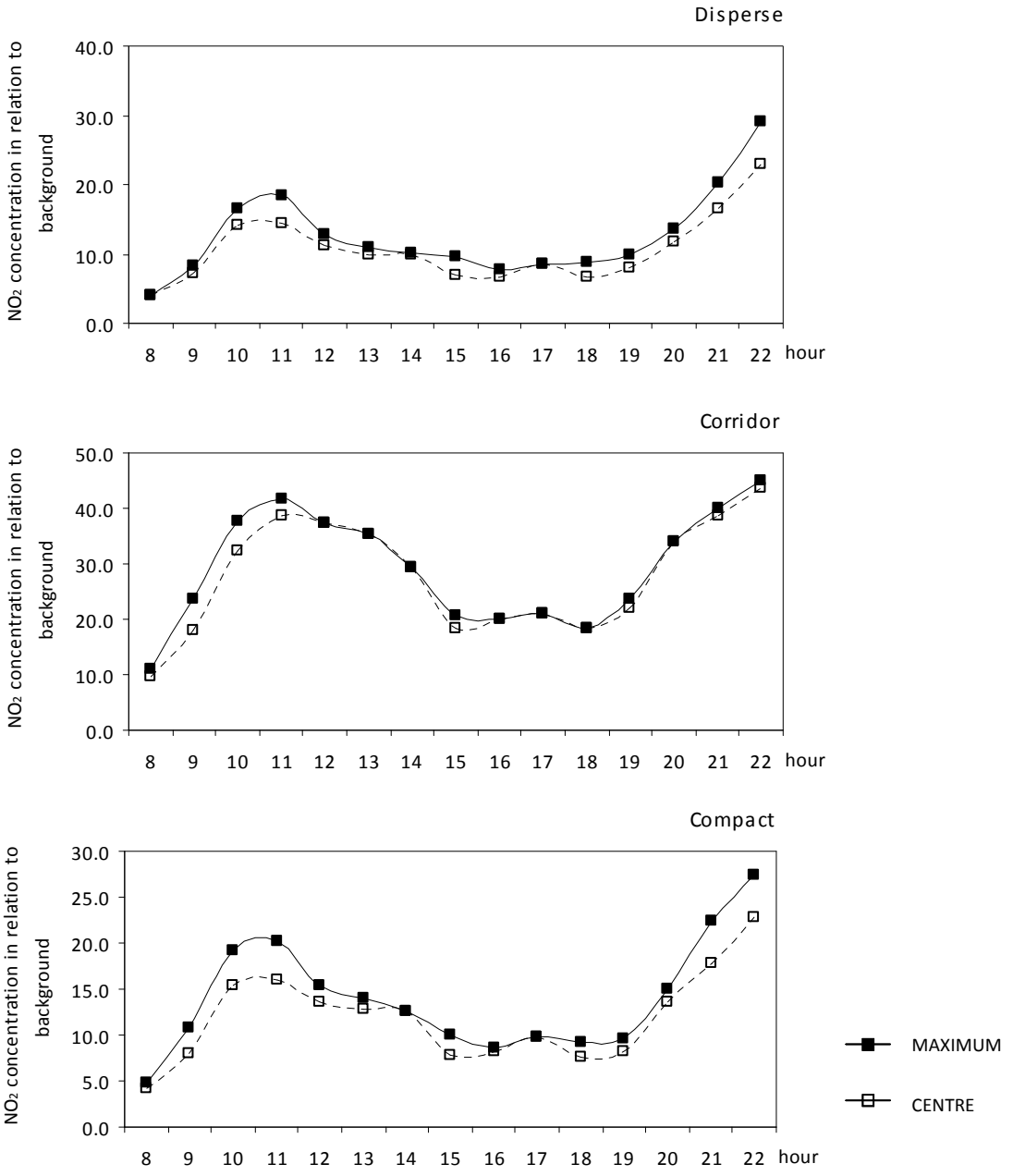

Figure 3.8 Comparison between NO_2 concentration in the centre of the city and the maximum domain value for each city.

To better understand the spatial distribution of concentrations for each city, Figure 3.9 presents an example of the O_3 concentration temporal evolution for 12:00, 13:00 and 14:00, three consecutive hours that show the growth of the ozone plume until it reaches its maximum value at 14:00. All the cities present ozone consumption in the city centre, due to the O_3 titration by NO. However, while the Compact and Corridor cities present the ozone plume formation outside the city centre limits, the Disperse city's plume covers a greater urbanized area. The compact city presents the smallest plume and with lower concentrations.

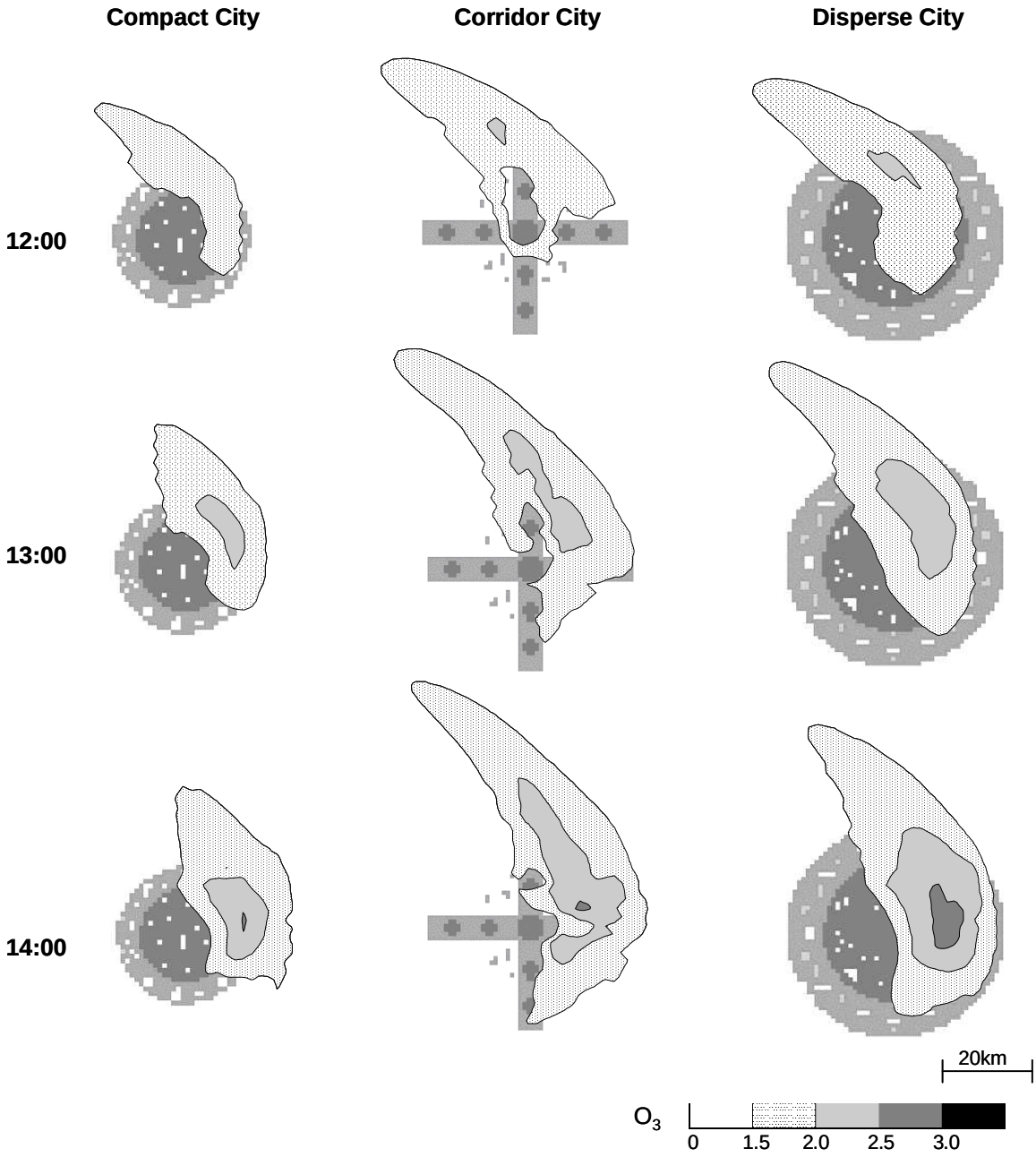

Figure 3.9 O_3 concentrations fields (relative to background concentration) at 12:00, 13:00 and 14:00.

Figure 3.10 presents the same evolution for NO_2,, this time from 20:00 to 22:00, corresponding to the maximum concentration hours. Again, the Compact city presents the smallest plume and lower concentrations, reflecting the emissions presented in Table 3.2. The Disperse city presents a similar behaviour with slightly higher concentrations. The Corridor presents the most severe NO_2 plumes, reaching concentrations twice as high as the other two cities.

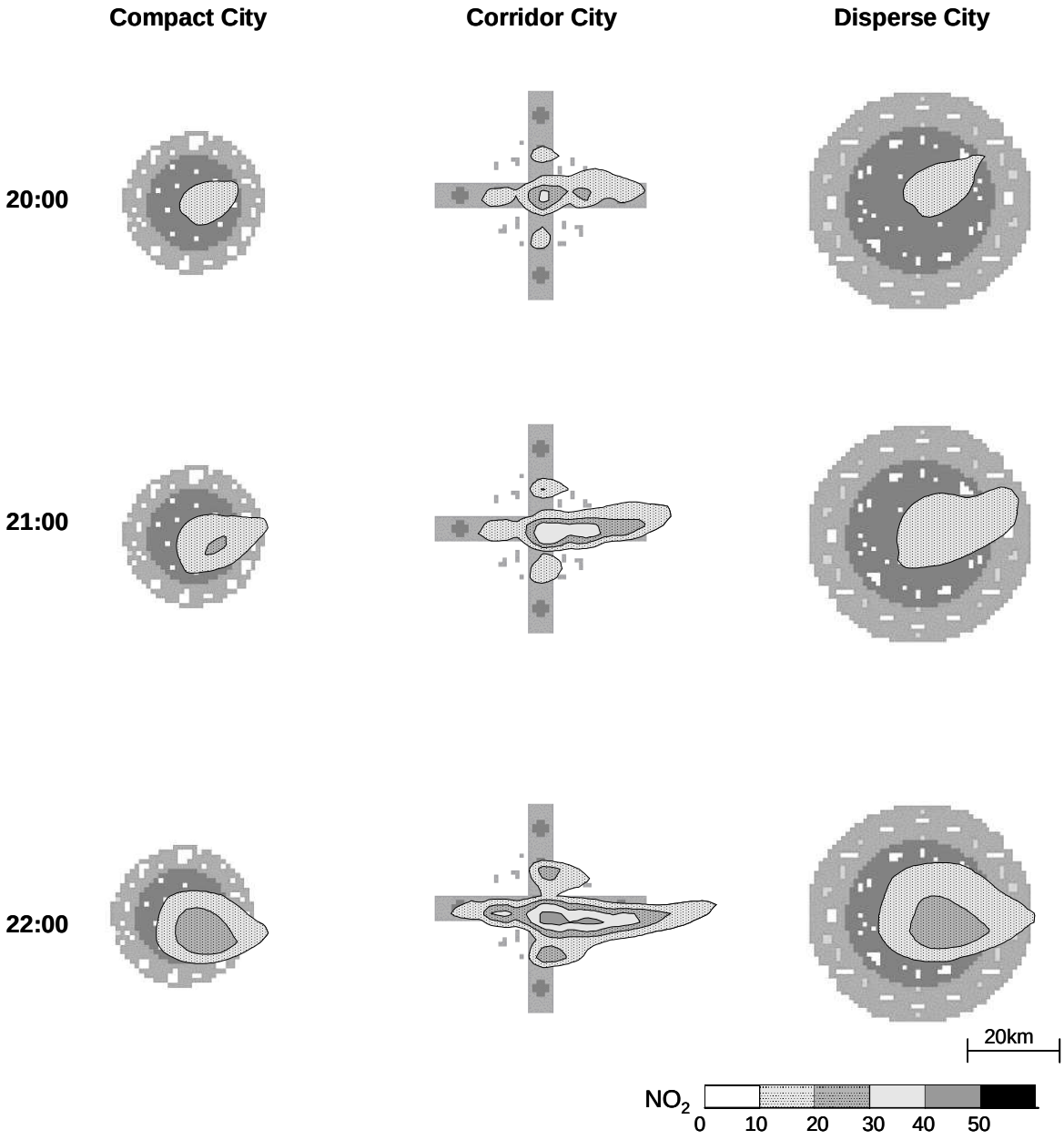

Figure 3.10 NO_2 concentrations fields (relative to background concentration) at 20:00, 21:00 and 22:00.

3.4 Exposure modelling

Taking into account that air quality is different from population exposure to air pollutants, the population exposure to O_3 and NO_2 in each urban area was determined [Ferreira et al., 2005].

The exposure can be obtained from direct measurements on individuals, either a total population or selected persons (direct method), or it may be determined from model calculations (indirect method) where the exposure is determined by combining information about concentrations at locations with

information about the time spent in specific microenvironments [Hertel *et al.*, 2001]. A microenvironment is defined as a three-dimensional space where the pollution concentration at some specified time is spatially uniform or has constant statistical properties. It can be the interior of a car, inside a house, or urban, suburban, and rural areas, etc. Integrated exposure is the exposure that a specific person experiences over a given period of time:

$$E_i = \sum_j^J C_j t_{ij}$$

where: E_i is the total exposure for person i over the specified period of time, C_j is the pollutant concentration in microenvironment j, t_{ij} is the residence time of the person i in microenvironment j, and J is the total number of microenvironments. The total exposure is, therefore, the sum of exposures during a given time. To obtain the total exposure of a population E_{pop} of N persons, it is necessary to sum the individual exposures E_i of all the persons in the population.

3.4.1 Exposure modelling methodology

A methodology was developed combining the air pollutants concentrations simulated by MEMO/MARS with information on population distribution and occupation in order to estimate the population exposure. Integrated population exposure was calculated based on O_3 and NO_2 concentrations, population distribution over the city and their time-activity patterns, i.e. the fraction of the day time spent in indoor and outdoor microenvironments.

Although the total population is the same for the three cities, the different structures allowed distinct distributions of the population by land use class, and also temporal variation of the number of people allocated to each land use category. It was considered that during the night (from 22:00 to 7:00) the population remains at its corresponding land use. Along the day (subdivided into two periods, one working period from 9:00 to 12:00 and 14:00 to 18:00, and the circulation period, at 8:00, 13:00 and 19:00 to 21:00) 20% of the rural population and 70% of suburban people move to urban areas. Population in suburban land use is increased by 30% coming from rural areas and 10% from urban sites.

Aiming to define the microenvironments to be considered for population exposure estimation, rural, suburban and urban land use categories were subdivided into residences, other indoors (offices, commercial places), traffic (inside vehicles) and outdoors. The number of people assigned to each land use class was distributed per microenvironment accordingly to the typical diurnal pattern associated with rural, suburban and urban areas, and considering the characteristics of each city structure. For example, during the night there are less people outdoors and in traffic in rural and suburban areas

than in urban areas, and on the other hand, in rural areas people spend more time outdoors during the day, due to agriculture related activities.

The microenvironments occupation in the urban land use areas differs among the cities. The smaller number of vehicles in the compact cities implies a greater occupation of the outdoors microenvironment, since the fraction of walking people, specially during circulation period, is higher in the compact city than in the disperse and corridor cities.

Indoor concentrations were obtained by the application of indoor/outdoor relations for O_3 and NO_2 derived from literature (Table 3.3) (Baek *et al.*, 1997; Monn, 2001; Wu *et al.*, 2005).

Table 3.3 Indoor/outdoor relations for O_3 and NO_2, for each microenvironment.

	Residence	Other indoors	Traffic
O_3	$C_{in} = 0.4\ C_{out}$	$C_{in} = 0.6\ C_{out}$	$C_{in} = 0.2\ C_{out}$
NO_2	$C_{in} = 0.5\ C_{out}$	$C_{in} = 0.7\ C_{out}$	$C_{in} = 3\ C_{out}$

For each city, the estimation of integrated population exposure was performed for the 24 hours of the simulated day, considering the population present at each hour in each microenvironment. A total daily population exposure was also calculated as a sum of the hourly-obtained exposures.

3.4.2 Results and Discussion

In order to assess the influence of the city structure in the human exposure, Figures 3.11 and 3.12 present the O_3 and NO_2 population exposure obtained for each city, at 14:00 and 22:00, respectively, corresponding to the maximum hourly simulated concentrations of each pollutant.

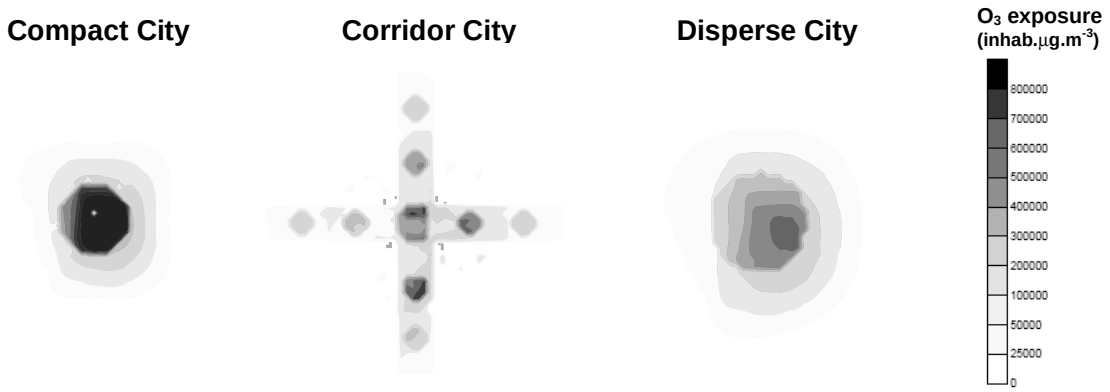

Figure 3.11 O_3 population exposure (inhab.μg.m^{-3}) for each city at 14: 00.

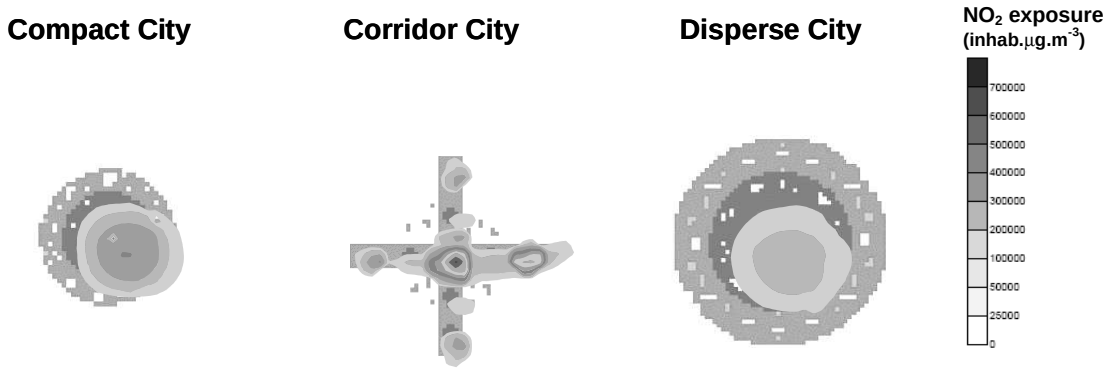

Figure 3.12 NO_2 population exposure (inhab.µg.m^{-3}) for each city at 22: 00.

Regarding O_3 exposure, although the maximum value was obtained for the Corridor city, the Compact city evidences a larger area of higher population exposures, because the urban land use of this city has the highest population density. Regarding NO_2, the Corridor city is clearly the one that presents the worst situation, with maximum exposures. The Disperse and Compact cities present similar exposure levels.

Figure 3.13 shows the total integrated population exposure for the simulated day, calculated by the sum of hourly population exposures for each city.

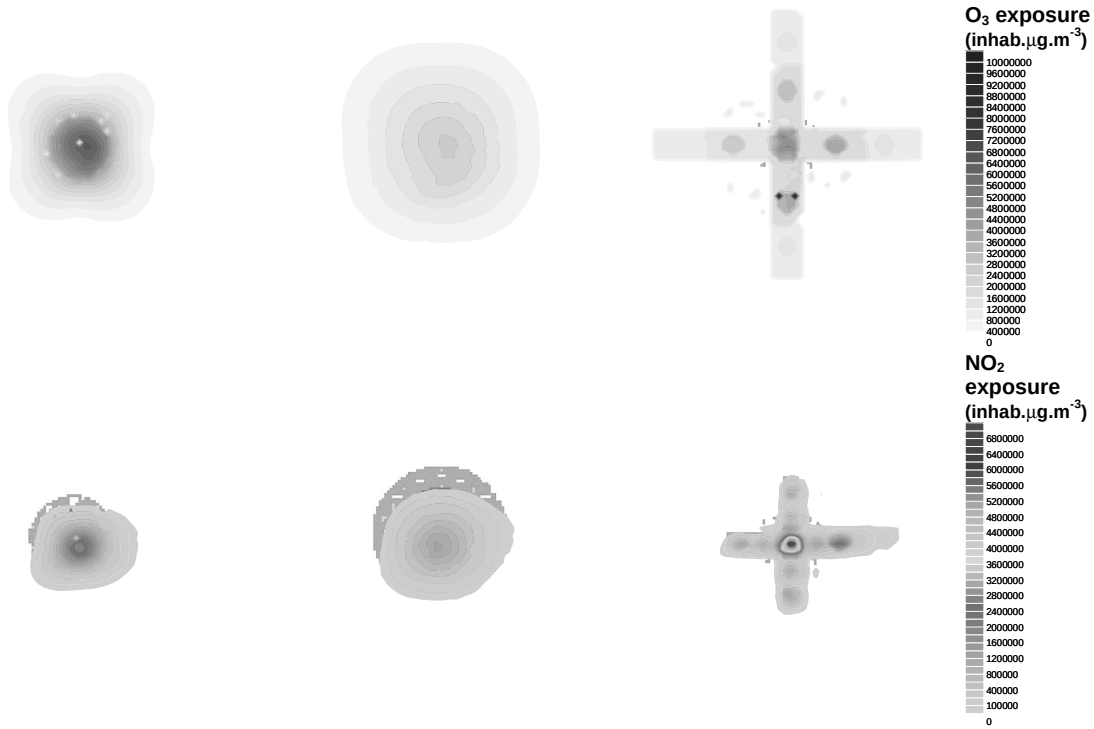

Figure 3.13 Total population exposure for a) O_3 and b) NO_2 accumulated during the simulation day for each city [inhab. µg.m^{-3}].

For both pollutants, the total integrated population exposure for the simulated day, achieves maximum values for the corridor city, but larger areas of higher levels for the compact city, similarly to what was verified in the hourly exposures for peak simulated concentrations.

3.5 Final remarks

The study here presented demonstrates the importance of the city spatial structure on urban sustainability, showing why air quality should be considered as an important indicator for urban planning. Emission rates and air pollution concentration fields were analysed for three imaginary cities with different urban structure but with the same population: the Corridor city is characterized by highest emission rates, while the Disperse city has the lowest emissions per area and the Compact city the lower emission rates per inhabitant. According to the photochemical simulations results, it is possible to conclude that compact cities with mixed land-use provide better air quality compared to disperse cities with lower densities and segregated land-use or network cities equipped with intensive transport structures. Although presenting the lower concentrations, and therefore the lowest individual exposures, if the entire population is considered, the compact city presents the worst scenario, due to the higher number of people exposed to the higher concentrations.

4 CASE STUDY PRESENTATION

The study of a real urban area is necessary to thoroughly explore the air quality consequences of different urban land use scenarios; also, it is important to extend the air quality modelling simulation over a full-year of different meteorological conditions to cover a wide range of air pollution conditions. This chapter begins with the identification of the Porto urban region as a suitable case for this study. Since the methodology involves the definition of different scenarios for the future of this urban region, it is essential that the starting-point, i.e. the base situation, is well known and characterized. For that purpose, the process of urban growth in the last decades is analyzed, as well as the current air quality levels in the region. Afterwards, the models to be used in the atmospheric simulation of the Porto study region are presented and described.

4.1 Why Porto

As already discussed, Southern Europe's urban areas are experiencing a change towards more dispersed and horizontal growth at the expense of agricultural, forested and natural land. Porto, located in Portugal's northern region, is currently cited as an example of this trend; in the report "Urban sprawl in Europe" [EEA, 2006a], Porto urban area is identified as one of the European cities where sprawl is growing faster. In the last decades, the Porto area has experienced an accelerated process of land occupation, with the urban area increasing at much faster rates than the population [EEA-JRC, 2002].

According to the air quality reports for Portugal's Northern region, the assessment of pollutant concentrations measured in the air quality monitoring network shows that Porto metropolitan region presents a poor air quality, with ozone thresholds and PM10 limit values exceeded [Borrego *et al.*, 2005, 2006b, 2008b].

It seems therefore that the Porto region is an interesting and challenging case to be studied in the framework of the topic urban structure and air quality.

The Porto urban region is complex to define; several classifications exist, such as the Porto district (composed of 18 municipalities), the Porto Metropolitan Area (16 municipalities from Porto and Aveiro districts) or even the Great Porto (11 municipalities from two districts). However, none of these artificial divisions is adequate for this study and the methodology to be applied, i.e., the study area must include the municipalities which show important relations with Porto, mainly in terms of mobility. Moreover, the region has to be suitable to the application of the regional air quality modelling system: this system has to be applied to a vaster area, firstly with lower resolution, to be then focused on a more particular region of interest with a higher resolution.

The region selected for the detailed analysis is showed in Figure 4.1 and includes 21 municipalities: 16 from the Porto district (Felgueiras, Gondomar, Lousada, Maia, Marco de Canavezes, Matosinhos, Paços de Ferreira Paredes, Penafiel, Porto, Póvoa de Varzim, Santo Tirso, Trofa, Valongo, Vila do Conde and Vila Nova de Gaia), four from the Aveiro district (Espinho, Castelo de Paiva, Santa Maria da Feira and São João da Madeira) and one from Braga district (Vila Nova de Famalicão); the total area reaches almost 240 000 hectares. The Porto municipality constitutes the study region's centre around which a first metropolitan ring is formed by the municipalities of Matosinhos, Maia, Gondomar and Vila Nova de Gaia; the municipalities of P. Varzim, V.N. Famalicão, Lousada, Felgueiras, Penafiel, M. Canavezes, C. Paiva and S.J. Madeira can be considered part of a peripheral ring, while the remaining intermediate municipalities constitute a second metropolitan ring.

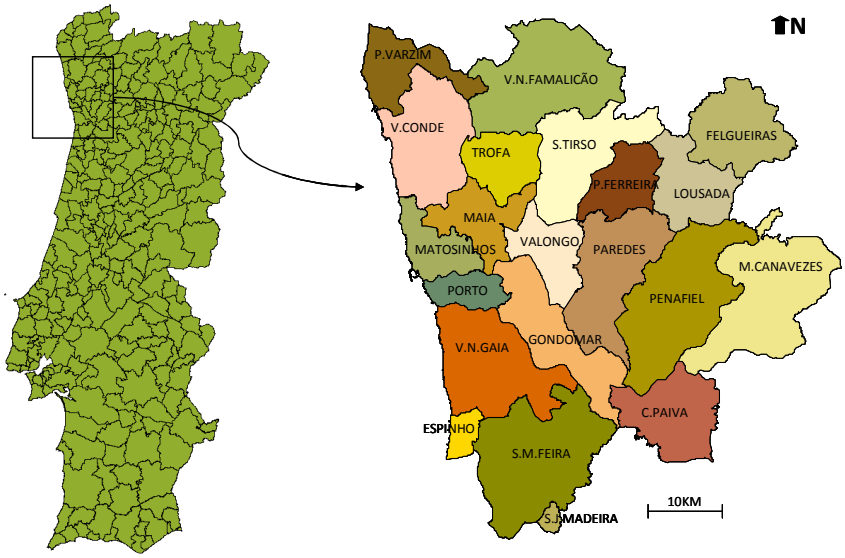

Figure 4.1 Study region, including 21 municipalities.

After the study region definition it is now necessary to select the study period. The year 2006 was chosen due to different factors: the number of available air quality monitoring stations increased to 24 in 2006, and the data have been validated and object of detailed analysis in the most recent air quality report for the region [Borrego *et al.*, 2008b]; concerning meteorology, 2006 is considered an "average" year, as opposed to 2003, 2004 and 2005, which were abnormally dry and/or warm [URL12, Trigo *et al.*, 2006; Viegas *et al.*, 2006].

4.2 Patterns of urban growth and change in the Porto region

In this section, the process of urban growth and change in the Porto region is analysed, starting with a brief overview of the evolution of the Porto urban area in the second half of the 20th century, and followed by a more detailed analysis of the study region based on two land use datasets from the EEA's Corine Land Cover, referring to the years 1987 and 2000.

4.2.1 Porto's urban area evolution in the 1950's – 1990's

The evolution of the Porto urban area in a 40-year period, from 1958 to 1997, is here described based on the land use data collected by the European Commission Joint Research Centre (EC-JRC) MOLAND database [EEA-JRC, 2002].

Figure 4.2 presents the land use evolution for a selected part of the Porto urban area (Porto, Matosinhos, and part of Vila Nova de Gaia, Maia and Gondomar municipalities), from 1958 to 1997, according to the EEA-JRC [2002] report. The evolution of the percentage of built-areas (these include residential, commercial and industrial areas, transport areas, dump sites, construction sites and mineral extraction sites) is also indicated.

As the maps and the magnitude of the numbers reveal, the built area has grown considerably from 1958 to 1997, at the expense of agriculture lands and forested areas. In this period, while built-up areas have grown 98%, the population growth was only 23% [EEA-JRC, 2002].

Since each of the various built-up land use classes has its own development dynamics and drivers, it is useful to split up the built-up class into more detailed sub-classes. Kasanko *et al.* [2006] took a closer look into two classes: residential land use, and the aggregation of industrial, commercial and transport land use. In the late 1990's, 61% of the built up area in Porto corresponded to residential land use, and 25% to the aggregation of the other three classes. Regarding the growth of these two groups, from the mid 1950's to the late 1990's, while the residential class increased by 91%, the three aggregated classes increased by almost 300%, revealing therefore a greater dynamic.

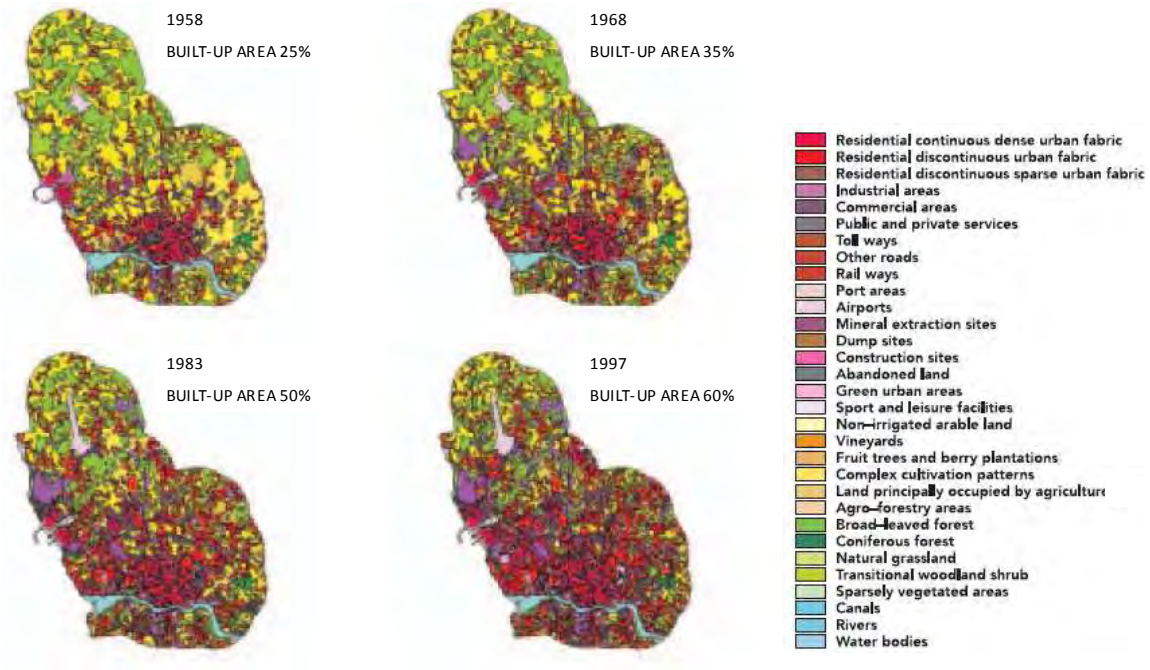

Figure 4.2 Land use and built-up area evolution for a part of the Porto urban area, 1958-1997 (EEA-JRC, 2002).

When dealing with urban sprawl it is important to further classify residential areas in two sub-classes: continuous (buildings and related structures covering more than 80% of the total surface) and discontinuous (covering between 10 and 80%). According to Kasanko *et al.* [2006], in Porto the proportion of continuous-discontinuous residential land is 38%-62%; it is also important to stress that 63% of the residential areas built after the mid 1950's are discontinuous, revealing a clear trend towards less intensive residential areas.

It is also essential to combine land use data with data on population evolution. Kasanko *et al.* [2006] computed the residential population density, which according to them, is the number of inhabitants per residential square kilometre. This measure is considered a more reliable indicator of urban density than the population density *per si*, especially when comparing data from different time periods, and consequently different land use occupation. In Porto this indicator has decreased progressively in the 50-year period, from 14734 to 9531 inhabitants per square kilometre (-35%), meaning that the growth of residential areas has outpaced the population growth, revealing the existence of urban sprawl.

Figure 4.3 presents a comparison of the population growth and the built-up area growth for a group of European cities including Porto [Kasanko *et al.*, 2006]. The linear growth line (for which population growth equals built-up area growth) divides the cities in two groups: cities above the line have experienced a faster built-up area growth, while for cities below the line the population growth was faster. The further the city is located from the line, the larger the difference between both growth rates.

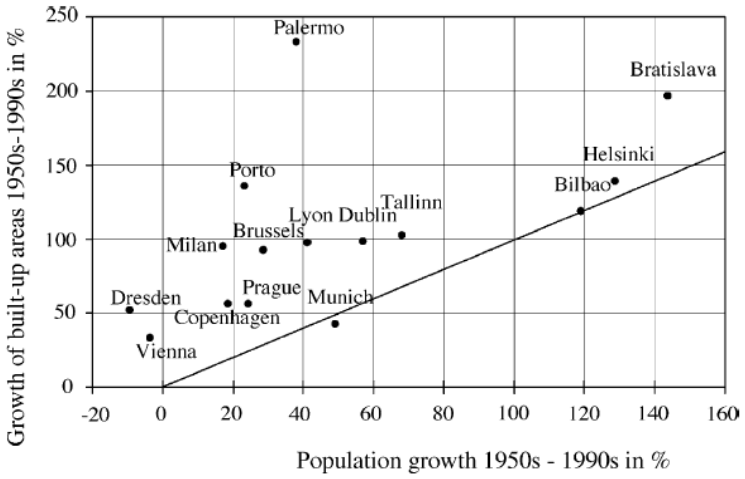

Figure 4.3 Population growth and built-up area growth in Porto and in a group of European cities, from the mid-1950´s to the late 1990's [Kasanko *et al.*, 2006].

Munich, Bilbao and Helsinki are the only cities for which population growth has accompanied urban growth; on the other hand, Porto, together with Palermo (Italy), is one of the cities where the built-up area has grown faster and where population growth has not been equally rapid. Reasons advanced by Kasanko *et al.* [2006] to explain this variation include a lower than average starting level of urbanization, rising living standards, and developing commercial and transport services. It is also interesting to note that in this group, no cities are found bellow the line, i.e., there is not a single case for which population growth has outcome urban area growth.

4.2.2 Porto's regional evolution in the period 1987- 2000

In the previous section, the evolution of a limited area of Porto's region was presented, as well as it comparison with other European urban areas. This section explores the path of the recent urban expansion in the Porto area, deepening the previous brief characterization above. For that purpose the process of urban growth in this area is analysed in detail, with the use of two digital Corine Land over (CLC) maps – CLC90 (data from 1987) and CLC2000 (data from 2000).

The CORINE (COordination of INformation on the Environment) programme of the European Commission includes a land cover project - CORINE Land Cover (CLC) [EEA, 2000] intended to provide consistent localized geographical information on the land cover of the Member States of the European Community. CLC is a standardised land cover inventory derived from satellite imagery for two median dates (1990 and 2000) for 24 countries, with 250 m resolution. For Portugal, CLC 1990 (CLC90) was produced with satellite images from 1985 to 1987, depending on the region, while CLC2000 concerns the year 2000 [Painho and Caetano, 2006]. CLC is organized in three levels, with a total of 44 classes, which are presented in Table 4.1.

Table 4.1 Corine Land Cover classes [EEA, 2000].

Level 1	Level 2	Level 3
1. Artificial Surfaces	1.1. Urban fabric	1.1.1. Continuous urban fabric
		1.1.2. Discontinuous urban fabric
	1.2. Industrial, commercial and transport units	1.2.1. Industrial or commercial units
		1.2.2. Road and rail networks and associated land
		1.2.3. Port areas
		1.2.4. Airports
	1.3. Mine, dump and construction sites	1.3.1. Mineral extraction sites
		1.3.2. Dump sites
		1.3.3. Construction sites
	1.4. Artificial non-agricultural vegetated areas	1.4.1. Green urban areas
		1.4.2. Sport and leisure facilities
2. Agricultural areas	2.1.Arable land	2.1.1. Non-irrigated arable land
		2.1.2. Permanently irrigated land
		2.1.3. Rice fields
	2.2. Permanent crops	2.2.1. Vineyards
		2.2.2. Fruit trees and berry plantations
		2.2.3. Olive groves
	2.3. Pastures	2.3.1. Pastures
	2.4. Heterogeneous agricultural areas	2.4.1. Annual crops assoc. with permanent crops
		2.4.2. Complex cultivation
		2.4.3. Land principally occupied by agriculture
		2.4.4. Agro-forestry areas
3. Forests and semi-natural areas	3.1. Forests	3.1.1. Broad-leaved forest
		3.1.2. Coniferous forest
		3.1.3. Mixed forest
	3.2. Shrub and/or herbaceous vegetation association	3.2.1. Natural grassland
		3.2.2. Moors and heathland
		3.2.3. Sclerophyllous vegetation
		3.2.4. Transitional woodland shrub
	3.3. Open spaces with little or no vegetation	3.3.1. Beaches, dunes, and sand plains
		3.3.2. Bare rock
		3.3.3. Sparsely vegetated areas
		3.3.4. Burnt areas
		3.3.5. Glaciers and perpetual snow
4. Wetlands	4.1. Inland wetlands	4.1.1. Inland marshes
		4.1.2. Peatbogs
	4.2. Coastal wetlands	4.2.1. Salt marshes
		4.2.2. Salines
		4.2.3. Intertidal flats
5. Water bodies	5.1. Inland waters	5.1. 1. Water courses
		5.1.2. Water bodies
	5.2. Marine waters	5.2.1. Coastal lagoons
		5.2.2. Estuaries
		5.2.3. Sea and ocean

The two datasets are here analysed for the study region, in order to produce a thorough characterization of the land use evolution in the period between 1987 and 2000. Figure 4.4 presents the study region land cover maps for 1987 and 2000, resulting from the processing of CLC90 and CLC2000 data, respectively. To obtain a clearer picture of the land cover, the 44 CLC classes were grouped in 5 large categories:

1) artificial surfaces – corresponding to CLC category 1 (see table 4.1), which includes urban fabric (continuous and discontinuous), industrial, commercial and transport units, and other artificial areas;

2) agricultural areas – corresponding to CLC category 2, including arable land, crops, pastures and other agricultural areas;

3) forests and shrub areas – corresponding to CLC categories 3.1 and 3.2;

4) other non artificial surfaces – corresponding to CLC categories 3.3 and 4, including areas of little or no vegetation, and inland and coastland wetlands;

5) water bodies, corresponding to CLC category 5, including inland and marine waters.

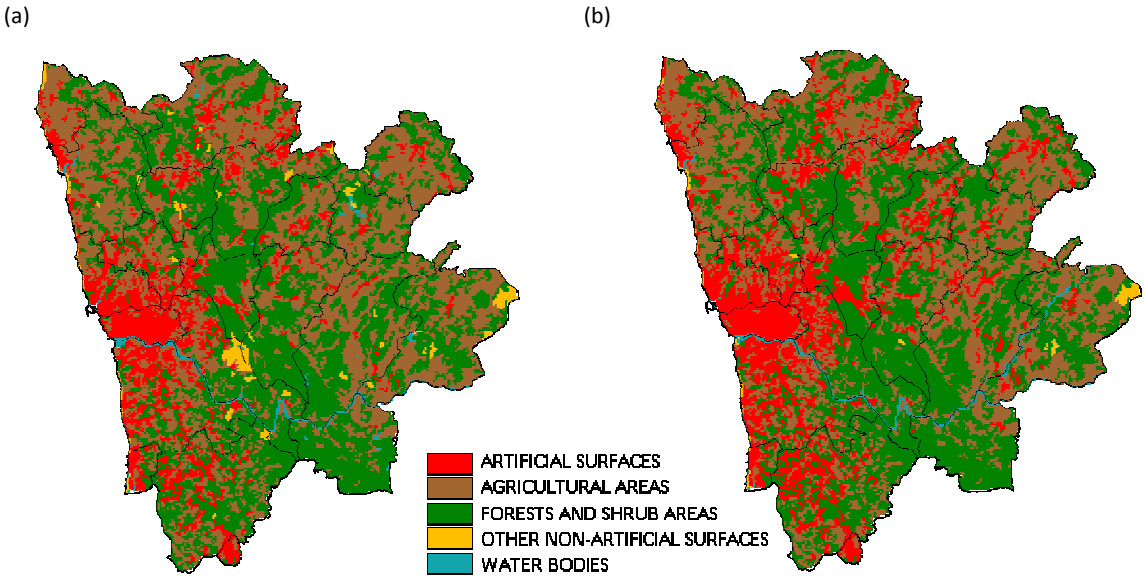

Figure 4.4 Study region land cover maps for (a) 1987 and (b) 2000.

The land cover maps reveal the expansion of artificial areas throughout the study region, mainly occupying land previously dedicated to agriculture, due to its proximity to the already existent urban areas. In order to have a clearer picture of the magnitude and nature of this growth, Table 4.2 presents the numbers behind the maps, including the total area for each of the 4 large land use categories and corresponding share (%) for each dataset, as well as the magnitude of the change between 1987 and 2000. Furthermore, artificial surfaces area is analysed with more detail by looking at its composition: continuous urban fabric (CLC 111 class); discontinuous urban fabric (CLC 112); industrial or commercial units (CLC 121); other artificial surfaces (remaining CLC category 1 classes, including transport units, mineral, dump and construction sites, and artificial vegetated areas).

Table 4.2 Study region land cover data for 1987 and 2000.

Land uses	CLC90 (1987 data)		CLC2000		Change	
	hectares	%	hectares	%	hectares	%
Artificial surfaces	30908.2	12.9	43727.9	18.3	+ 12819.7	+41.5
Continuous urban fabric	3369.0	10.9	4059.2	9.3	+690.2	+20.5
Discontinuous urban fabric	23583.0	76.3	32895.0	75.2	+9312.0	+39.5
Industrial or commercial units	2719.9	8.8	4973.1	11.4	+2253.2	+82.8
Other artificial surfaces	1236.3	4.0	1800.7	4.1	+564.3	+45.6
Agricultural areas	101350.1	42.3	93766.2	39.1	-7584.0	-7.5
Forests and shrub areas	101598.7	42.4	98319.4	41.0	-3270.3	-3.2
Other non-artificial surfaces	5750.4	2.4	3784.9	1.6	-1965.4	-34.2
TOTAL AREA	239598.4	100	239598.4	100	-	-

From 1987 to 2000, built-up land uses increased 41.5%, nearly 3% annually. Around 13 000 new hectares have become artificial during this period, with urbanized land rising from 13% of the total area of the region in 1987 to 18% in 2000. The analysis by municipality (presented in Appendix A) shows that the largest increases (in absolute and relative area) are particularly observed outside the urban centre, i.e. outside Porto municipality, confirming the previous assertions about the existence of urban sprawl processes in the region. Municipalities in the first metropolitan ring around Porto – Maia, Gondomar and Vila Nova de Gaia – as well as Santa Maria da Feira, which already presented in 1987 a high share of urbanized areas (21%, 12%, 29% and 15% respectively), reveal the largest absolute increases of artificial surfaces. Municipalities outside the first metropolitan ring, such as Lousada, Penafiel, Marco de Canavezes and Castelo de Paiva, with very low shares of urbanised areas in 1987 (2.1%, 1.8%, 1.4% and 0.4%, respectively) presented the highest growth rates between 1987 and 2000: 240%, 230%, 150% and 190%. As expected, Porto municipality presents the highest percentage of artificial land uses, with 91.5% of the total area in 2000 (83% in 1987).

As urbanization advanced, many non-urban hectares disappeared. The municipalities of the first metropolitan ring, already identified above, and Vila Nova de Gaia presented the largest relative losses; Santa Maria da Feira, Maia, Vila Nova de Gaia and Valongo exhibited the highest absolute losses of natural and semi-natural areas. The municipalities beyond the first urban ring experienced the lowest non-urban decrease, as a result of its high initial non-urban area. Some municipalities, such as Penafiel, Gondomar, Paredes and Castelo de Paiva, showed an increase in forested areas, which, together with the urbanization increase, also contributed to the loss of agricultural areas. Considering the entire study area, agriculture land loss represents more than half of the entire non-urban losses (12820 ha); forest and shrub areas come next with 26%.

A more detailed analysis of the new artificial uses between 1987 and 2000 reveals little changes in the urbanization trends. The discontinuous or low density urban fabric ranks first for both years, summing around 75% of the total artificial area. While in 1987 continuous urban fabric was the second land use category, with 11% of the total artificial area, in 2000 the industrial and commercial units took over the second place, with 11%. This land use category showed the highest growth rate between 1987 and 2000 (83%, corresponding to an average annual growth of 6%), followed by other artificial surfaces (46%). Although the discontinuous urban fabric shows only the third growth rate (40%), it is the first in terms of area growth, almost 10 000 hectares, representing 73% of the new artificial areas. The land use category compact or continuous urban fabric showed the lowest growth.

The analysis by municipality reveals that more than half of the municipalities have an insignificant share of continuous urban fabric (less than 2% of the total artificial area), nine of them presenting no continuous fabric at all. These municipalities are the same that exhibited the highest growth rates of artificial surfaces. Only Porto has a significant share of continuous urban fabric (46.5%).

Evidence therefore suggests that Porto region is undergoing a process of urban sprawl; to further confirm it, it is important to look at the relation between the artificial areas growth and the population growth in the same period. Unfortunately no data were available for resident population in 1987 for all the municipalities in the study region. Therefore Figure 4.5 presents the comparison between population change and artificial area change between 1987 and 2000 only for a limited group of municipalities.

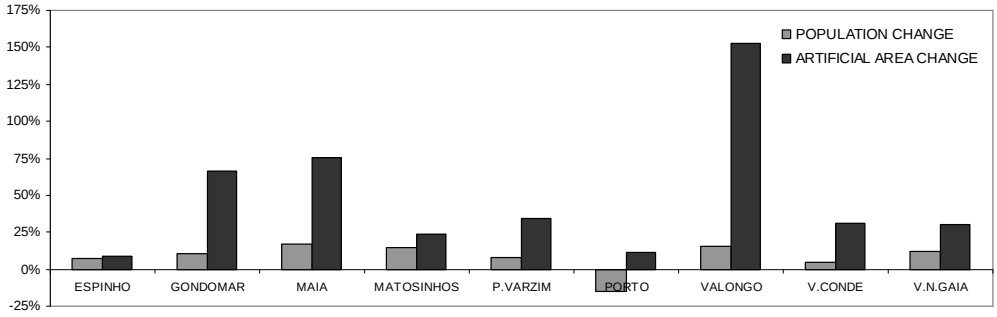

Figure 4.5 Population change and artificial areas change between 1987 and 2000 for a group of municipalities in the study region.

The graph shows that for the time period 1987-2000 the artificial area growth was much higher than the population growth. Valongo reveals an artificial area growth ten times larger than its population growth, for Maia and Gondomar the growth was six times larger. Porto registers a decrease in population (less 47500 residents), but still presents an artificial area growth of 11%.

Making use of the population data and of the residential area, obtained through the sum of continuous and discontinuous urban fabric, for each of the municipalities from the previous figure, the

residential density (number of residents per residential square kilometre) was calculated for 1987 and for 2000 (Figure 4.6).

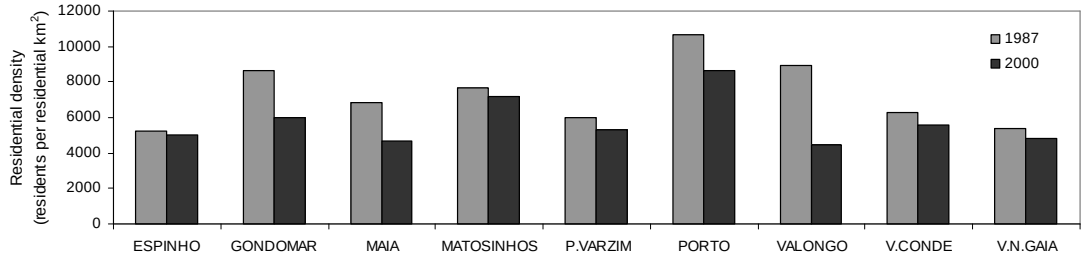

Figure 4.6 Residential density calculated for 1987 and 2000 for a group of municipalities in the study region.

A trend towards lower residential densities is observed, revealing that the population growth has lost importance as an explanatory factor of the urbanization process, while the generalization of dispersed urban patterns has risen, claiming more and more land necessary to accommodate the same number of people. An important sprawl process in the region is the proliferation of new industrial and commercial areas. Extensive industrial areas and mega commercial structures punctuate the Porto region, with the traditional tendency of locating commercial uses within the urban fabric rapidly fading. There is no longer a real mixture of uses; instead, commercial activities are now segregated and concentrated in large portions of land orientated to commercial and leisure activities.

4.3 Mobility and attractiveness in the study region

In metropolitan areas, the need for daily-travel or commuting is a reality steaming from the progressive distancing between residential areas and work and study areas. Hence, in a study whose aim is to link urban structure with emissions and air quality, it is essential to look not only at the number of residents per municipality but also at the population flow between municipalities. It was therefore necessary to characterize the commuting characteristics of the region and the relative attractiveness/ repulsiveness of each municipality in the study area. For that purpose, a study from the National Statistics Institute (INE, 2003) focusing on commuting in Lisbon and Porto Metropolitan areas for the year 2001 was the main source of data. The study demonstrates the existence of important commuting movements in the Porto Metropolitan Area, through the analysis of the main interaction axis and the accounting of workers and student's flows between municipalities. Of great significance are the interactions between Porto, the centre of the region, and the municipalities of the first metropolitan belt, namely Vila Nova de Gaia, Matosinhos, Gondomar, Maia, and also Valongo; these interactions are strongly unbalanced in favour of Porto [INE, 2003]. Other features worth mentioning are:

- the residents of the more peripheral municipalities, such as Espinho, Póvoa de Varzim and Vila do Conde do not have Porto as the main destination; Espinho's residents move preferably towards Vila Nova de Gaia, while the other two have each other as the main destiny;

- outside the Porto Metropolitan Area, the residents from Trofa, Paredes and Penafiel exhibit a high polarization towards the region centre, namely towards Porto and Maia.

The mentioned study compiled all these relations between municipalities, producing maps and tables that translate these relationships into attraction and repulsion rates; these rates relate the number of individuals entering/ exiting a given municipality with the number of individuals residing in the municipality. The described data, referring to the year 2001, from the INE study, is here processed and attraction and repulsion rates re-calculated for the municipalities in the case study region. As an example, Figure 4.7 presents the data for Porto municipality, with a net attraction rate of 38.2%; Appendix B presents the numbers for the remaining municipalities.

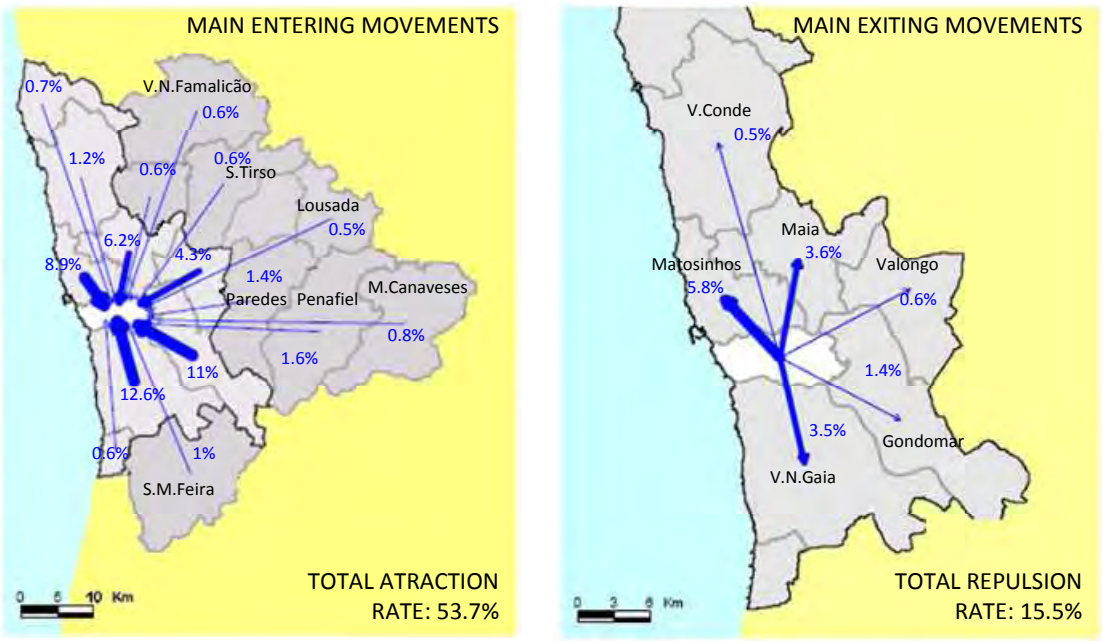

Figure 4.7 Porto main entering and exiting movements and attraction and repulsion rates for 2001 (maps from INE[2003]; numbers computed by manipulation of INE data).

Taking into account all the available data, it was assumed that the study region acts as a tight zone, and the possible interactions between it and the surrounding areas are not considered. For the municipalities of Paços de Ferreira, São João da Madeira, Lousada and Castelo de Paiva, there was no data available concerning attraction and repulsion rates; for the first two the same rates of Santa Maria da Feira were assumed, due to the common peripheral character of the three municipalities; for the last two the rates of Penafiel were assumed, since the three municipalities present very similar characteristics in terms of land use and population.

These attraction and repulsion rates are essential for the definition and construction of the urban development scenarios for the region since, in order to determine the total amount and distribution of atmospheric pollutant emissions in the study region, it is necessary to consider not only the number of inhabitants or residents per municipality but also the flow between municipalities.

4.4 Air quality levels in Porto urban region

Portugal's northern region, in accordance to the established in the Air Quality Framework Directive [96/62/EC], was classified [IA, 2001] in two zones (Interior North and Coastal North) and four agglomerations (Coastal Porto, Braga, Vale do Ave and Vale do Sousa) (Figure 4.8).

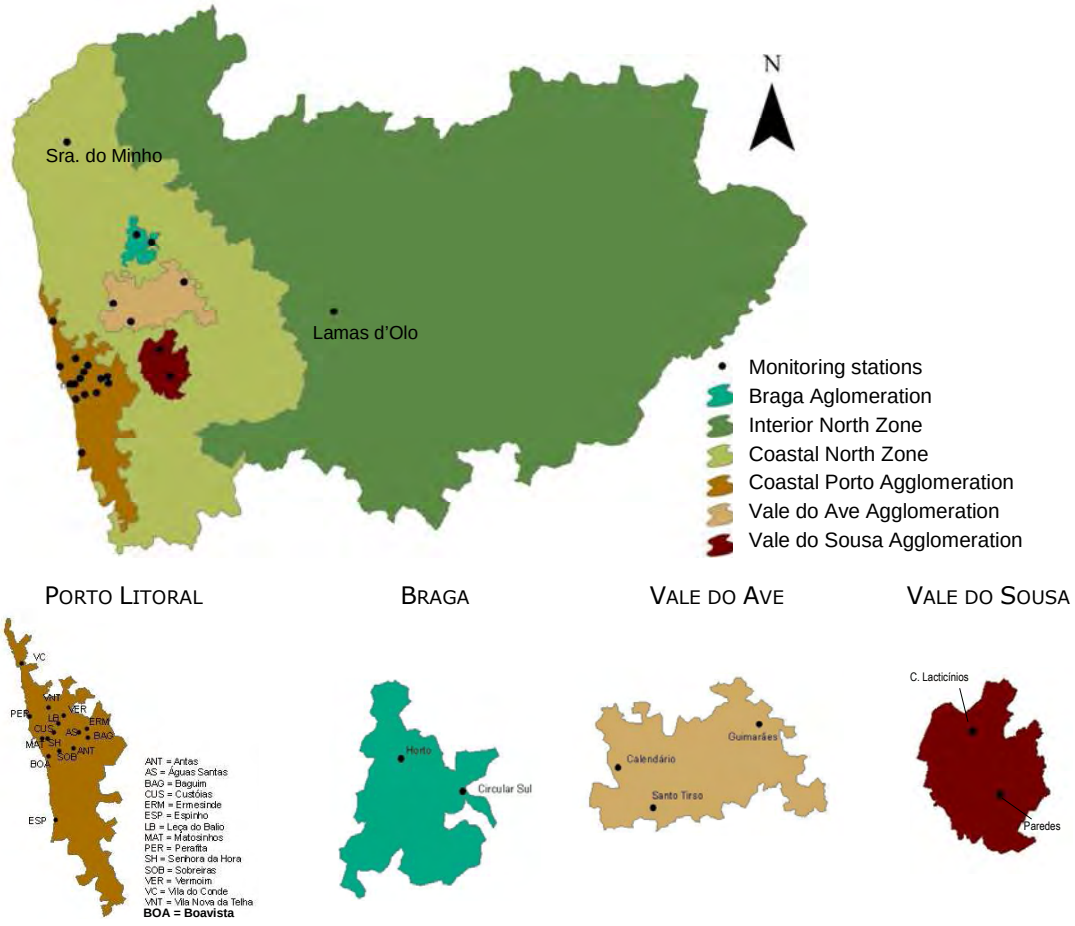

Figure 4.8 Portugal's Northern Region: zones and agglomerations, and air quality monitoring stations location (adapted from Borrego *et al.*, 2008b).

Since 2005, the air quality monitoring network covers all the zones/agglomerations, with a total of 24 stations in 2006, the large majority of them (15) located in Coastal Porto due to the high number of inhabitants. Table 4.3 lists the monitoring stations existing in the study area (Figure 4.1), as in 2006, and their characteristics, including, type of environment, influence and measured pollutants.

Table 4.3 Study area air quality monitoring stations identification and characterization.

Agglom.	Municipality	Station	Environment	Influence	Measured Pollutants
Coastal Porto	Espinho	Espinho (ESP)	urban	traffic	CO, NOx, SO_2, PM10
	Gondomar	Baguim (BAG)	urban	traffic	CO, NOx, O_3
	Maia	Águas Santas (AS)	urban	traffic	CO, NOx, SO_2
	Maia	Vermoim (VRM)	urban	traffic	CO, NOx, SO_2, PM10,PM25, O_3
	Maia	V.N.Telha (VNT)	suburban	background	CO, NOx, SO_2, PM10, O_3
	Matosinhos	Custóias (CST)	suburban	back/ind	CO, NOx, SO_2, PM10, O_3, BTX
	Matosinhos	Leça Balio (LB)	suburban	background	CO, NOx, SO_2, PM10, O_3
	Matosinhos	Matosinhos (MAT)	urban	traffic	CO, NOx, SO_2, PM10
	Matosinhos	Perafita (PRF)	suburban	back/ind	CO, NOx, SO_2, PM10, O_3
	Matosinhos	S.Hora (SH)	urban	traffic	CO, NOx, SO_2, PM10
	Porto	Antas (ANT)	urban	traffic	CO, NOx, PM10, O_3
	Porto	Boavista (BOA)	urban	traffic	CO, NOx, SO_2, PM10
	Valongo	Ermesinde (ERM)	urban	background	NOx, SO_2, PM10, O_3
	V.Conde	V.Conde (VC)	suburban	traffic	CO, NOx, SO_2, PM10
Vale do Sousa	P.Ferreira	C.Lacticínios (CL)	urban	background	NOx, SO_2, PM10, O_3
	Paredes	Paredes (PAR)	urban	traffic	CO, NOx, PM10, BTX
Vale do Ave	S.Tirso	S.Tirso (ST)	urban	background	CO, NOx, SO_2, PM10, O_3
	V.N.Famalicão	Calendário (CLD)	suburban	background	NOx, SO_2, PM10, O_3

As already mentioned, Porto metropolitan region presents a poor air quality, with ozone thresholds and daily and annual PM10 limit values exceeded. Figures 4.9 and 4.10 show the air quality monitoring stations for which PM10 daily and annual legal requirements, respectively, were not fulfilled [Borrego et al., 2008c]. High PM10 concentrations are measured in urban and suburban monitoring stations. Daily and annual limit values are exceeded for almost all monitoring stations; regarding the daily limit value the number of annual exceedances goes well beyond the allowed 35.

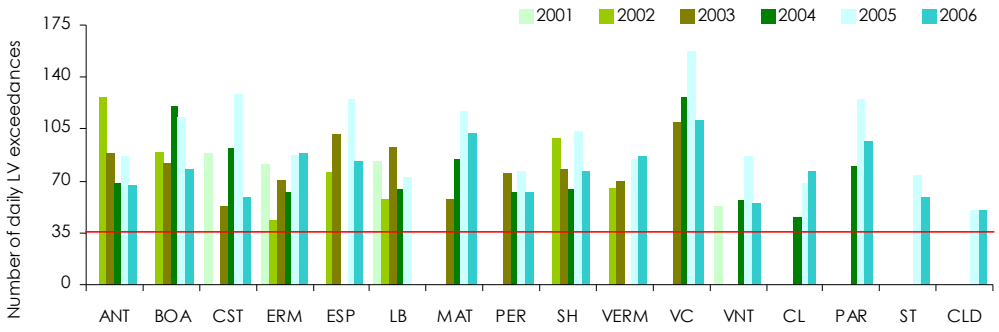

Figure 4.9 Monitoring stations not fulfilling PM10 legal requirements for daily LV + MT in 2001-2006 in the study area (the red line indicates the allowed number of daily exceedances) (data from Borrego et al., 2008c).

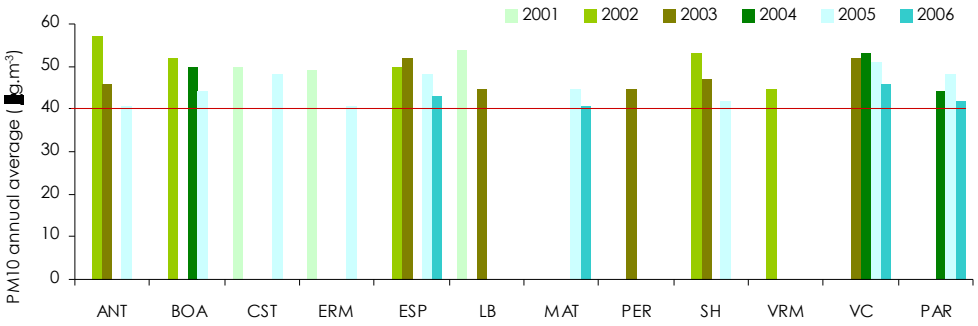

Figure 4.10 Monitoring stations not fulfilling the PM10 legal requirements for annual LV + MT in 2001-2006 in the study area (based on Borrego et al., 2008c).

As already mentioned, particulate matter can be emitted from a variety of sources, including natural ones, such as forest fires and deserts. Borrego *et al.* [2008c] studied the origin of PM10 episodes in Portugal's Northern region from 2001 to 2006. The results are summarized in Figure 4.11 (note: days with simultaneous fire and desert dust events may exist, therefore the sum of the three origins can be greater than 100%). For 2001, natural sources were responsible for the majority of the PM10 episodes; this can be explained by the low number of PM10 episodes registered in 2001 intimately related to the small number of PM10 monitoring stations at that time (only six). From 2002 to 2006 anthropogenic sources were identified as the major causes for this type of pollution. Still, natural sources, particularly dust blown from the North African deserts, were responsible for a significant share of PM10 pollution episodes. Directive 1999/30/EC acknowledges the existence of these natural events, and accepts their subtraction to the total number of PM10 episodes, to verify the compliance with legislated values. However, after the implementation of this procedure it was demonstrated that none of the agglomerations in non-compliance had a change in its situation [Borrego *et al.*, 2008c].

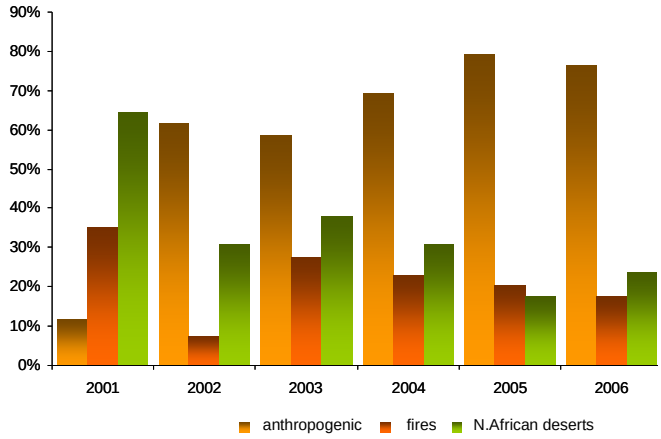

Figure 4.11 Causes for PM10 daily LV exceedancees in North Portugal, 2001-2006 [Borrego *et al.*, 2008c].

As a result of these exceedances, and accordingly to the determined in the Air Quality Framework Directive, the Northern Region of Portugal, as well as the Lisbon Metropolitan region, are currently under the obligation of developing and implement *Plans and Programs for the Improvement of the Air Quality* [Borrego *et al.*, 2008c].

These Plans and Programs will also be mandatory for ozone from 2010 onwards; and accordingly to the air quality reports for the northern region it is likely that the northern region will have to develop and implement them. The analysis of ozone measured data confirms that concentration values are higher outside the urban centre of the region, i.e. outside Porto municipality. Nevertheless the ozone information threshold is exceeded in the majority of the monitoring stations, and often along a high number of hours per year. As an example, Figure 4.12 shows the exceedances to the O_3 information threshold in 2006 in the study area, and their monthly distribution. Concerning the seasonal occurrence of exceedances, ozone limit values are generally higher between April and September, while for PM10 high concentrations have been found both in summer and winter.

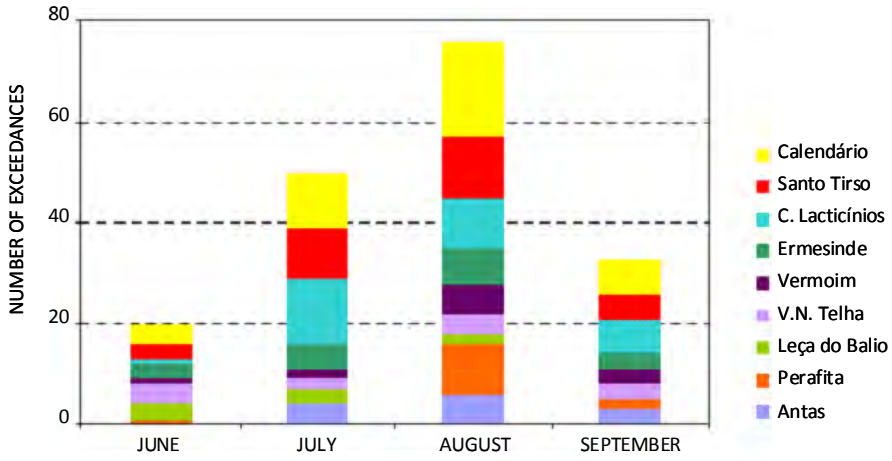

Figure 4.12 Monthly distribution of exceedances to the O_3 information threshold in 2006 (Borrego *et al.*, 2008b)

The air quality monitoring data for the Porto area, obtained from the National Air Quality Database [URL13] for 2006, was analysed in order to identify air pollution episodes (an episode was defined as a period for which PM10 and/or O_3 limit values are exceeded in three or more air quality monitoring stations simultaneously, according to Martins *et al.* [2007b]. Firstly, all PM10 and O_3 episodes were identified (Appendix C); for ozone the hourly information threshold (180 $\mu g.m^{-3}$) was considered, for PM10 the daily limit value was selected (50 $\mu g.m^{-3}$). The analysis illustrates the air quality degradation over the study area, mainly for particulate matter for which a total of 36 episodes were identified, summing up 122 days, i.e. one third of the year with PM10 values exceeded simultaneously in at least three monitoring stations. These exceedances took place throughout the year, with the months January/February and August being specially critic. Regarding ozone, nine episodes were identified, with the information threshold exceeded for a total of 116 hours, and the alert threshold exceeded 4 hours; for the year under analysis, ozone episodes occurred between June and September.

The Portuguese Environmental Agency (APA) has identified the occurrence of dust events from North Africa or forest fire activity which might help to explain or justify the occurrence of some of the air pollution episodes. These events over the Portuguese territory for the year 2006 were presented in a report from APA [2007].

PM10 and O_3 anthropogenic episodes were identified based on the information concerning natural events and the total events presented in Appendix C. While for ozone the elimination of the days with natural events results in a significant reduction (around one third) of the number of hours with exceedances of probable anthropogenic origin, for PM10 episodes this reduction is very small.

4.5 Atmospheric modelling

This section describes the numerical models, meteorological (MM5) and chemical (CAMx), used in the atmospheric simulations for the Porto study region. Both models are freely available, and have been extensively used and validated worldwide, being subject of constant improvement and update. These facts, together with the good performance of the models obtained for different regions, including the present study region, justify their selection. Moreover, these models are ready to be applied in long-term simulations, as it is the case of the one-year simulation carried out in this study, with acceptable computing times. This was not the case of the modelling system applied in the idealized case-study presented in the previous chapter; as already mentioned the MEMO-MARS system belongs to a previous generation of models, very useful for the study of pollution episodes (1 to 3 days) but not prepared to perform long-term simulations.

4.5.1 Meteorological model MM5

The PSU/NCAR mesoscale model was developed at the Pennsylvania State University and the National Centre for Atmospheric Research (NCAR). The model is supported by several pre- and post-processing programs, which are referred to collectively as the MM5 modelling system [Dudhia, 1993; Dudhia *et al.*, 2005]. The MM5 modelling system software is freely provided and supported by the Mesoscale Prediction Group in the Mesoscale and Microscale Meteorology Division at NCAR, therefore it is widely used internationally [Vautard *et al.*, 2004; Minguzzi *et al.*, 2005; Jiménez *et al.*, 2006; Civerolo *et al.*, 2007; among others].

The MM5 is a three-dimensional non-hydrostatic prognostic model that simulates mesoscale atmospheric circulations. Important features in the MM5 modelling system include: (i) a multiple-nest capability; (ii) non-hydrostatic dynamics; (iii) a four-dimensional data assimilation (Newtonian nudging) capability; (iv) increased number of physics options; and (v) portability to a wide range of computer platforms [Dudhia et al., 2005]. A simplified flow-chart of the modelling system is depicted in the schematic diagram in Figure 4.13 (features not used in the presented study are not depicted).

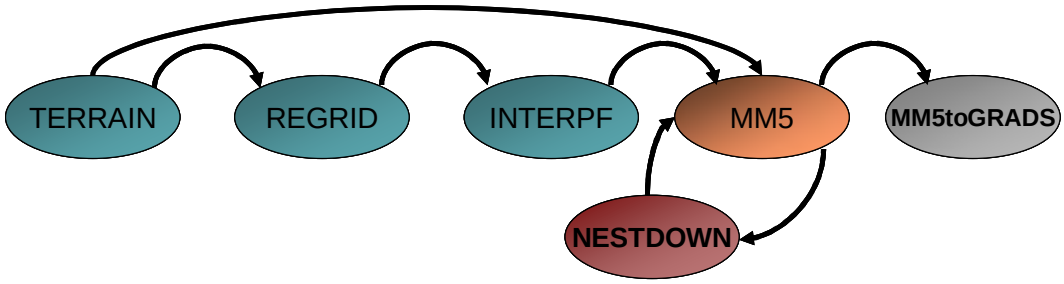

Figure 4.13 A simplified flow chart of the MM5 modelling system.

The program beginning any simulation in MM5 is TERRAIN. It horizontally interpolates (or analyzes) the regular latitude-longitude terrain elevation, and vegetation (land use) onto the chosen mesoscale domains. Currently the MM5 modelling system has two types of land use data with global coverage available from the United States Geological Survey (USGS): 13-category, with a resolution of 1 degree, 30 and 10 minutes; and 24-category, with a resolution of 1 degree, 30, 10, 5 and 2 minutes, and 30 seconds. The USGS 24-category data is referred to 1990, and some of the components are originated from a dataset compiled in the 1970s [Dudhia et al., 2005]. Table 4.4 presents the description of the 24 USGS categories, including the physical parameters for the Northern Hemisphere summer and winter.

Table 4.4 Description of 24-category USGS vegetation categories and physical parameters for Northern Hemisphere summer and winter [Dudhia *et al.*, 2005].

Vegetation Identifier	Vegetation Description	Albedo		Moisture avail. (%)		Emissivity (% at 9 μm)		Roughness length (cm)		Thermal inertia ($calcm^{-2}K^{-1}s^{-1/2}$)	
		sum	win	sum	win	sum	win	sum	win	sum	win
1	Urban and Built-Up Land	18	18	10	10	88	88	50	50	0.03	0.03
2	Dryland Crop. and Pasture	17	23	30	60	92	92	15	5	0.04	0.04
3	Irrigated Crop. and Pasture	18	23	50	50	92	92	15	5	0.04	0.04
4	Mixed Dry./Irrig. Crop. Past.	18	23	25	50	92	92	15	5	0.04	0.04
5	Cropland/Grassland Mosaic	18	23	25	40	92	92	14	5	0.04	0.04
6	Crop./Woodland Mosaic	16	20	35	60	93	93	20	20	0.04	0.04
7	Grassland	19	23	15	30	92	92	.12	.10	0.03	0.04
8	Shrubland	22	25	10	20	88	88	10	10	0.03	0.04
9	Mixed Shrubland/Grassland	20	24	15	25	90	90	11	10	0.03	0.04
10	Savanna	20	20	15	15	92	92	15	15	0.03	0.03
11	Deciduous Broadleaf Forest	16	17	30	60	93	93	50	50	0.04	0.05
12	Deciduous Needlel. Forest	14	15	30	60	94	94	50	50	0.04	0.05
13	Evergreen Broadleaf Forest	12	12	50	50	95	95	50	50	0.05	0.05
14	Evergreen Needlel. Forest	12	12	30	60	95	95	50	50	0.04	0.05
15	Mixed Forest	13	14	30	60	94	94	50	50	0.04	0.06
16	Water Bodies	8	8	100	100	98	98	0.1	0.1	0.06	0.06
17	Herbaceous Wetland	14	14	60	75	95	95	20	20	0.06	0.06
18	Wooded Wetland	14	14	35	70	95	95	40	40	0.05	0.06
19	Barren or Spars. Vegetated	25	25	2	5	85	85	10	10	0.02	0.02
20	Herbaceous Tundra	15	60	50	90	92	92	10	10	0.05	0.05
21	Wooden Tundra	15	50	50	90	93	93	30	30	0.05	0.05
22	Mixed Tundra	15	55	50	90	92	92	15	15	0.05	0.05
23	Bare Ground Tundra	25	70	2	95	85	85	.10	5	0.02	0.05
24	Snow or Ice	55	70	95	95	95	95	5	5	0.05	0.05

The purpose of REGRID is to read archived gridded meteorological analyses and forecasts on pressure levels and interpolate those analyses from some native grid and map projection to the horizontal grid and map projection defined by the MM5 pre-processor program TERRAIN. It expects input from files of gridded meteorological analyses, besides the TERRAIN program, and creates files ready for INTERPF.

The INTERPF program handles the data transformation required to go from the analysis programs to the mesoscale model. This entails vertical interpolation of pressure levels to terrain-following sigma levels, diagnostic computation, and data reformatting. INTERPF takes REGRID output data as input to generate a model initial, lateral boundary condition and a lower boundary condition.

The MM5 program is the numerical weather prediction part of the modelling system. It can be used for a broad spectrum of theoretical and real-time studies, and in the smaller meso-beta and meso-gamma scales (2-200 km), MM5 can be used for studies involving mesoscale convective systems, fronts, land-sea breezes, mountain-valley circulations, and urban heat islands. The program numerically solves the pressure, mass, momentum, energy and water conservation equations; it presents different parameterization schemes for clouds, planetary boundary layer and diffusion, moisture, radiation, and surface.

MM5´s nesting capability allows the consideration of several domains in a single simulation or in consecutive simulations; therefore, the first domain can present a more regional dimension with a coarser mesh, while the next domain will cover a smaller area but with a higher resolution. In MM5 two nesting options are available:

- One-way nesting: when a single-domain or multiple-domain run completes, its domain output can be put into NESTDOWN to create an input file with higher resolution and new lateral and lower boundary files; this is known as a one-way nest because it is forced purely by the coarse mesh boundaries, and has no feedback on the coarse-mesh run.
- Two-way nesting - multiple domains can be run in MM5 at the same time, each domain takes information from its parent domain every time-step, and runs three time-steps for each parent step before feeding back information to the parent domain on the coincident interior points. The feedback distinguishes two-way nesting from one-way nesting, and allows nests to affect the coarse mesh solution, usually leading to better behaviour at outflow boundaries. However there is a significant overhead cost associated with the boundary interpolation and feedback at every time-step.

Finally, MM5toGrADS is a utility program from the MM5 modelling system that converts MM5 binary outputs to temporal series, and bi- and three dimensional fields for all meteorological variables; this program therefore allows the visualization and posterior analysis of the results of the meteorological simulation.

More details about the MM5 modelling system can be easily accessed through its webpage [URL14].

Since MM5 includes several parameterizations, users can choose among the multiple options of model physics and parameterization schemes; some are based on the scale of the motion, such as the cumulus parameterizations, while others are dependent on users preferences, such as the planetary boundary layer schemes [Mao *et al.*, 2006].

Several authors [Zhang and Zheng, 2004; Mao *et al.*, 2006; Han *et al.*, 2008; among others] have studied the implications of the use of different MM5 PBL parameterizations in the meteorological and

air quality predictions, concluding that different PBL schemes may cause considerable differences in model results for meteorological variables and air pollutants concentrations.

Here, the parameterizations that will be used in this study are described. A study from Aquilina *et al.* [2005] tested several MM5-PBL schemes for the West Coast of Portugal, particularly for the Lisbon area, and concluded that the MRF [Hong and Pan, 1996] scheme provided in general the best meteorological results. The MRF scheme, named after the model where it was implemented (the NCEP Medium Range Forecast Model), is suitable for high-resolution in PBL; the PBL height is determined from critical Bulk-Richardson number. However, considering that the air quality model to be applied (CAMx, described ahead), requires turbulent kinetic energy (TKE) as an input parameter, which is not provided when MRF-PBL scheme is used, this scheme will only be applied to the coarser MM5 domain, since the remaining domains (defined ahead) will provide information for the air quality modelling.

In previous MM5- CAMx applications for Portugal, the ETA PBL scheme has been used [Salmim *et al.*, 2005; Miranda *et al.*, 2006; Borrego *et al.*, 2008d]. The ETA - PBL scheme is the Mellor-Yamada scheme as used in the Eta model [Janjic, 1990, 1994]. It predicts TKE, and calculates exchange coefficients using similarity theory, and vertical fluxes with an implicit diffusion scheme. The PBL height is diagnosed from the TKE profile.

Aquilina et al. [2005] also observed that the Gayno-Seaman PBL scheme [Gayno, 1994], yielded particularly good results for higher resolution applications over the Lisbon area; therefore, this scheme is also used in the present study. This scheme is also based on Mellor-Yamada TKE prediction, but it is distinguished from others by the use of liquid-water potential temperature as a conserved variable, allowing the PBL to operate more accurately in saturated conditions [Ballard *et al.*, 1991; Shafran *et al.*, 2000].

4.5.2 Air quality model CAMx

The Comprehensive Air quality Model with extensions (CAMx) was developed by ENVIRON International Cooperation, from California, United States of America. CAMx [Morris *et al.*, 2004] is an Eulerian photochemical dispersion model that allows the integrated “one-atmosphere” assessment of gaseous and particulate air pollution over many scales ranging from sub-urban to continental.

CAMx simulates the emission, dispersion, chemical reaction, and removal of pollutants in the troposphere by solving the pollutant continuity equation for each chemical species on a system of nested three-dimensional grids. The Eulerian continuity equation describes the time dependency of the average species concentration within each grid cell volume as a sum of all of the physical and chemical processes operating on that volume. The continuity equation is numerically marched forward

in time over a series of time steps. At each step, the continuity equation is replaced by an operator-splitting approach that calculates the separate contribution of each major process (emission, advection, diffusion, chemistry, and removal) to concentration change within each grid cell [ENVIRON, 2008].

CAMx carries pollutant concentrations at the centre of each grid cell volume, representing the average concentration over the entire cell. Meteorological fields are supplied to the model to quantify the state of the atmosphere in each grid cell for the purposes of calculating transport and chemistry. CAMx incorporates two-way grid nesting, which means that pollutant concentration information propagates into and out of all grid nests during model integration. Any number of grid nests can be specified in a single run, while grid spacing and vertical layer structures can vary from one grid nest to another. The nested grid capability of CAMx allows cost-effective application to large regions in which regional transport occurs, yet at the same time providing fine resolution to address small-scale impacts in selected areas [ENVIRON, 2008].

The CAMx chemical mechanisms are based on Carbon Bond version 4 (CB4) [Gery *et al.*, 1989] and SAPRC99 [Carter, 2001]. There are four specific mechanisms currently supported, along with a plug-in that allows a simple user-defined chemical mechanism to be employed (referred to as "Mechanism 10"); these are listed in Table 4.5.

Table 4.5 Chemistry mechanisms currently implemented in CAMx [ENVIRON, 2008].

Mechanism ID	Description
3	CB4 [Gery et al., 1989] gas-phase chemistry with revised radical-radical termination reactions and updated isoprene chemistry; 96 reactions and 37 species (25 state gases and 12 radicals).
1	Mechanism 3 with reactive chlorine chemistry [Tanaka *et al.*, 2000]; 110 reactions and 48 species (34 state gases and 14 radicals).
4	Mechanism 3 with additional inorganic gas-phase reactions, including aerosol and mercury chemistry: secondary organic aerosol formation from condensable gases, aqueous PM chemistry, inorganic PM thermodynamics, and aerosol size evolution; 117 reactions and up to 67 species (37 state gases, 18 particulates, and 12 radicals).
5	The fixed parameter version of the SAPRC99 gas-phase mechanism [Carter, 2001]; 217 reactions and 77 species (59 state gases and 18 radicals).
10	A user-defined simple chemistry mechanism can be developed for any gas and/or particulate species.

CAMx requires input files that configure each simulation, define the chemical mechanism, and describe the photochemical conditions, surface characteristics, initial/boundary conditions, emission rates, and various meteorological fields over the entire modelling domain. Table 4.6 summarizes the input data requirements of CAMx, as well as the various pre-processors, made available by ENVIRON and adapted for the most common uses by the scientific community.

Table 4.6 Data requirements of CAMx [ENVIRON, 2008] and respective pre-processors.

Data class	Data type	Pre-processor
Meteorology (supplied by a meteorological model)	3-Dimensional Gridded Fields: - Vertical Grid Structure - Horizontal Wind Components - Temperature - Pressure - Water Vapor - Vertical Diffusivity - Clouds/Precipitation	MM5CAMx
Air Quality (obtained from measured ambient data)	Gridded Initial Concentrations Gridded Boundary Concentrations Time/space Constant Top Concentrations	ICBCPREP
Emissions (supplied by an emissions model)	Elevated Point Sources Combined Gridded Sources: - Low-level Point - Mobile - Area/Non-road Mobile - Biogenic	PT_EMISS AREA_EMISS
Geographic (Developed from terrain and landuse/landcover maps, drought index maps, modeled or satellite derived snow cover)	Gridded Surface Characteristics: - Land Use/Vegetative Cover - UV Albedo - Snow Cover - Land/Water Mask - Roughness Length - Drought Stress - Terrain Elevation	AHOMAP
Photolysis (Derived from satellite measurements and radiative Transfer Models)	Atmospheric Radiative Properties: - Gridded Haze Opacity Codes - Gridded Ozone Column Codes - Photolysis Rates Lookup Table	PHOTOLYSIS

Preparing this information requires several pre-processing steps to translate "raw" emissions, meteorological, air quality and other data into the final input files for CAMx [Monteiro *et al.*, 2007a]. Some changes have been performed over the last years in order to implement MM5-CAMx system for Portugal [Miranda *et al.*, 2002; Ferreira *et al.*, 2003; Ferreira, 2007]. Figure 4.14 presents the structure of the model, including the pre- and post-processors, and relations between them.

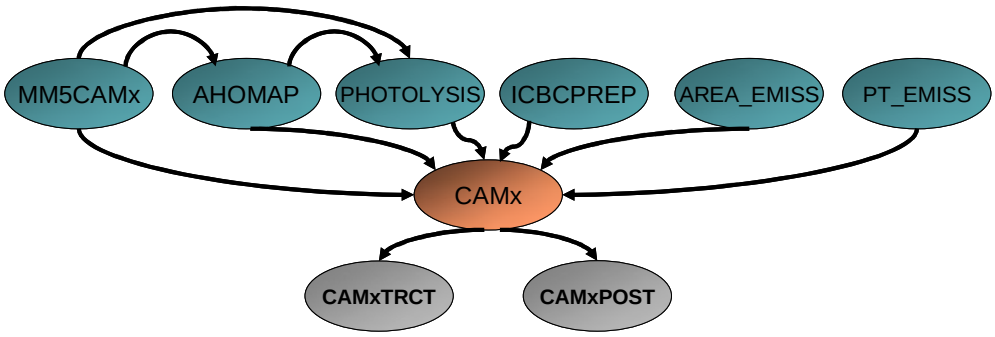

Figure 4.14 The CAMx modeling system.

The MM5CAMx pre-processor generates CAMx meteorological input files from the MM5 output files, including land use, altitude/pressure, wind, temperature, moisture, clouds/rain and vertical diffusivity. The vertical structure in CAMx will be defined from the MM5 sigma layers, and therefore will vary in space, also vertical layer structures can vary from one grid nest to another. The vertical diffusivity fields are obtained from MM5 outputs directly from TKE .

Topographic and land use information is also provided by the MM5 model through the MM5CAMx pre-processor. The 24 land use classes from MM5, presented in Table 4.4, are aggregated in the 11 categories considered by CAMx and presented in Table 4.7.

Table 4.7 CAMx land use categories, surface roughness and albedo [ENVIRON, 2008] and correspondent MM5 categories.

Land cover category	Surface roughness (m)				UV albedo	MM5 land categories
	spring	summer	fall	winter		
1. Urban	1.00	1.00	1.00	1.00	0.08	1. Urban and built-up land
2. Agricultural	0.03	0.20	0.05	0.01	0.05	-
3. Rangeland *	0.05	0.10	0.01	0.001	0.05	7. Grassland 8. Shrubland 9. Mixed shrubland/grassland 10. Savanna 20. Herbaceous tundra
4. Deciduous forest	1.00	1.30	0.80	0.50	0.05	6. Cropland/woodland mosaic 11. Deciduous broadleaf forest 12. Deciduous needleleaf forest 21. Wooden tundra
5. Coniferous forest, wetland	1.30	1.30	1.30	1.30	0.05	13. Evergreen broadleaf forest 14. Evergreen needleleaf forest 18. Wooded wetland
6. Mixed forest	1.15	1.30	1.05	0.90	0.05	15. Mixed forest 22. Mixed tundra
7. Water	0.0001	0.0001	0.0001	0.0001	0.04	16. Water bodies
8. Barren land	0.002	0.002	0.002	0.002	0.08	19. Barren or sparsely vegetated 24. Snow or ice
9. Non-forested wetlands	0.20	0.20	0.20	0.05	0.05	17. Herbaceous wetland
10. Mixed agricultural/range	0.04	0.15	0.03	0.006	0.05	2. Dryland cropland and pasture 3. Irrigated cropland and pasture 4. Mixed dryl./irrig. Crop. and past. 5. Cropland/grassland mosaic
11. Rocky	0.30	0.30	0.30	0.15	0.05	23. Bare ground tundra

*rangeland – North-American term for lands on which a significant proportion of the natural vegetation is native grasses, grass-like plants, forbs, and shrubs; includes natural grasslands, savannas, shrublands, many deserts, tundra, alpine communities, coastal marshes, and wet meadows.

The land use grid together with TOMS ozone column data files [URL15] constitutes the input for AHOMAP, which prepares albedo, haze, and ozone column input files for PHOTOLYSIS. This pre-processor determines the photolysis rates for each grid cell as a function of five variables: the solar zenith angle, height above ground, UV albedo, haze turbidity and ozone column depth.

There are numerous approaches for defining initial, boundary, and top concentration inputs for CAMx. The level of detail ranges from time- and space-constant values for all pollutants, to specific time and space profiles for each pollutant. The level of detail depends on available measurements, and focus and detail (spatial and temporal resolution) of the modelling exercise. ENVIRON provides one simple program, ICBCPREP, which prepares CAMx initial condition (IC) and boundary condition (BC) files from existing air quality data for the study region, allowing the definition of top concentrations, constant in space and time, for each chemical species to be modelled. Another approach gaining popularity is to extract initial and boundary conditions from large regional applications of global-scale chemical transport models. Interface programs have been developed for this purpose, but are not distributed by ENVIRON. This issue is further discussed in the next chapter.

Finally the pre-processors PT_EMISS and AREA EMISS calculate the hourly variation of emissions from point and area sources, respectively. More details about the area emissions pre-processor are discussed in the next chapter, since it will be subject of improvements.

The post-processors, CAMxPOST e CAMxTRCT, allow the extraction of time series simulated concentrations for predefined locations, and bi-dimensional concentration fields for a given pollutant, respectively. These tools permit the comparison between simulated and observed data and also the evaluation of concentrations all over the study area.

4.5.3 Case study domain definition

Figure 4.15 presents a simplified scheme of the MM5-CAMx modelling system applied to the simulation of the atmospheric flow and air quality in the study region.

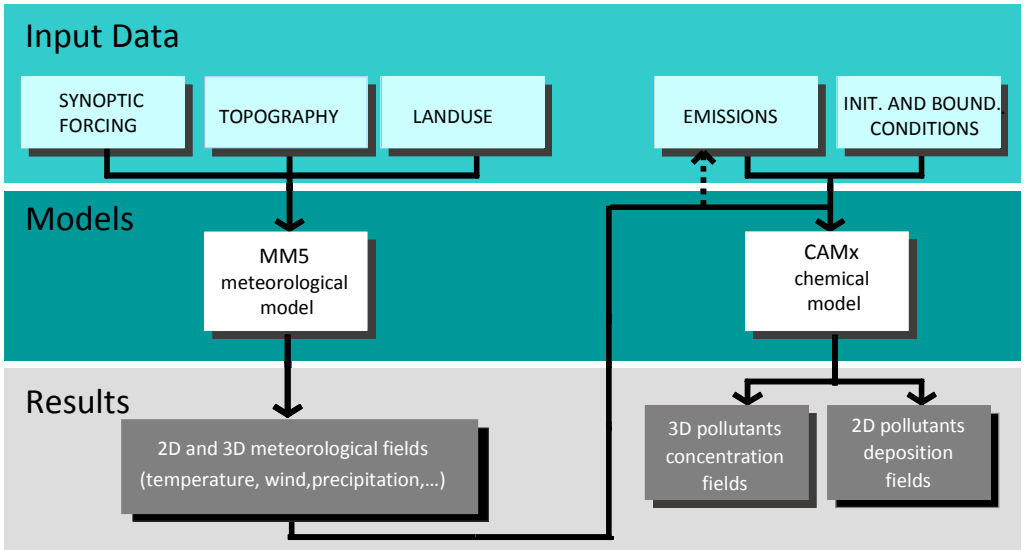

Figure 4.15 Simplified scheme of the MM5-CAMx modelling system.

For the meteorological simulation, the MM5 capability of doing multiple nesting is used, and the model is applied for five domains, using the two-way nesting technique. Figure 4.16 shows the model domain setup and the location of the meteorological stations to be used in the validation process: domain 1 (D1) at 27 km resolution covering the Iberian Peninsula and France; D2 at 9 km resolution over Portugal; D3 at 3 km resolution over NW Portugal; and domains D4 and D5 with 1 km resolution over Great Porto Area and Aveiro coastal region, respectively.

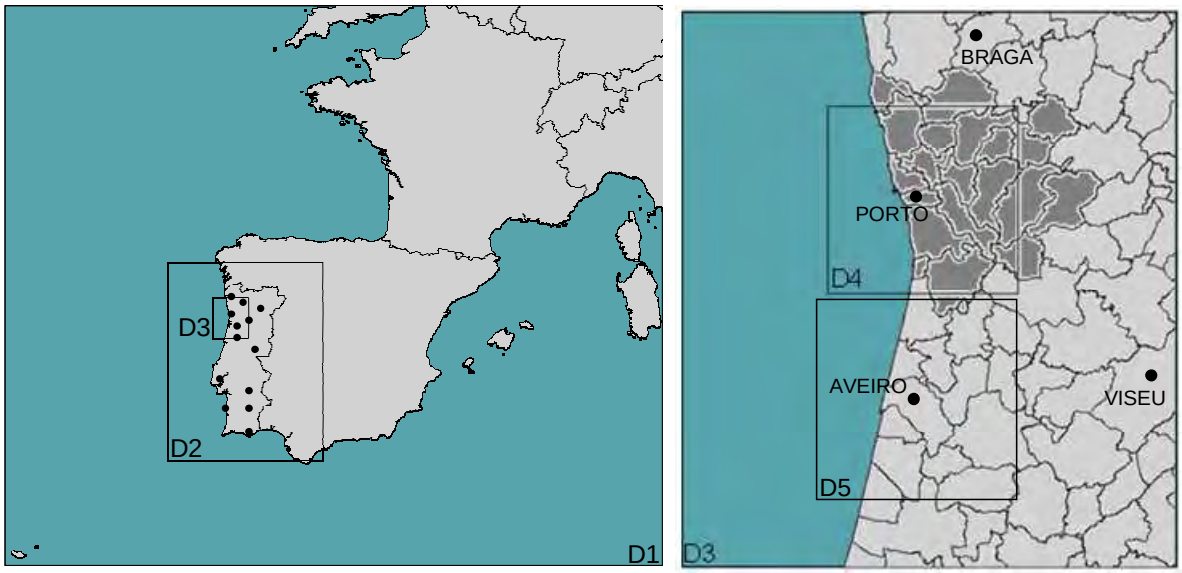

Figure 4.16 Meteorological model domains.

Table 4.8 summarizes the corresponding grid configurations. Considering previous research studies performed for NW Portugal (Carvalho *et al.*, 2006), 25 unequally spaced σ levels are used in order to optimize the simulation through the increase of vertical resolution near the surface.

Table 4.8 Meteorological domains configuration

Domain	No. of cells in x-direction	No. of cells in y-direction	Z levels	Resolution (km)
D1	91	77	25	27
D2	63	81		9
D3	45	51		3
D4	51	51		1
D5	54	54		1

Regarding the air quality simulations, CAMx is applied for three domains, slightly smaller than the corresponding MM5 domains, using its two-way nesting capability. Figure 4.17 shows the model domain setup: domain 1 (D1) at 9 km resolution covering Portugal; D2 at 3 km resolution over NW Portugal; and D3 with 1 km resolution over Great Porto Area. A fourth domain (Aveiro coastal region)

was not judged necessary because D3, which includes the agglomerations of Portugal's Northern region, has a high number of air quality stations.

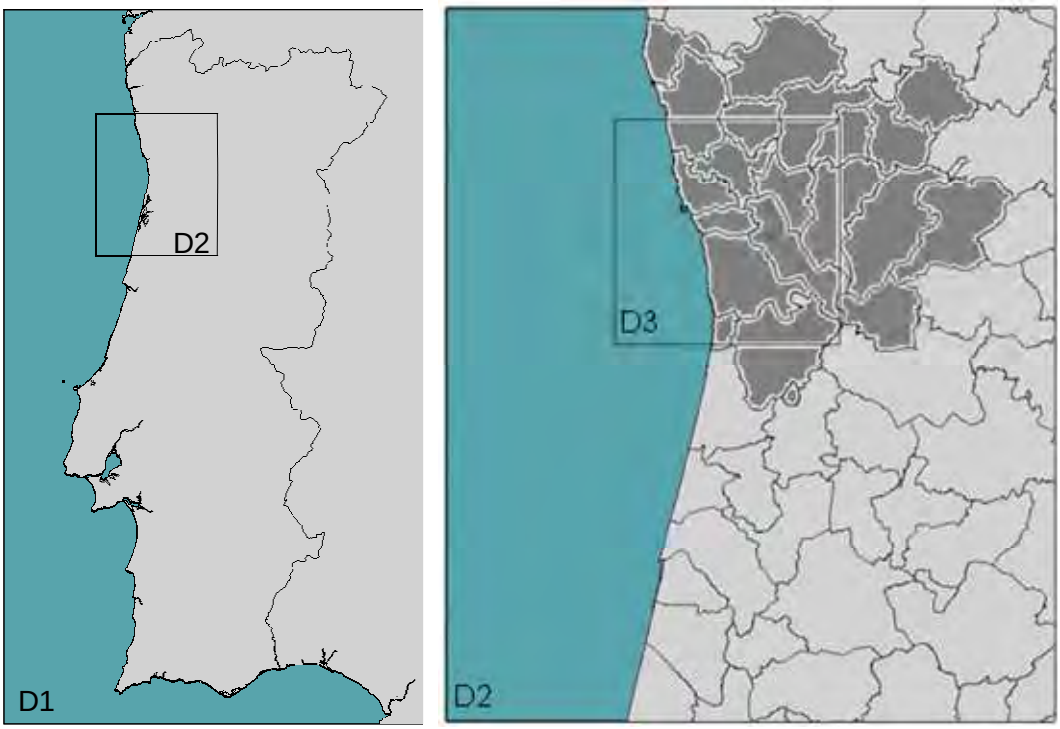

Figure 4.17 CAMx simulation domains.

Table 4.9 summarizes the corresponding grid configurations. Considering previous research studies performed for Portugal (Ferreira, 2007; Ferreira *et al.*, 2003), 17 unequally spaced σ levels are used.

Table 4.9 CAMx domains configuration

Domain	No. of cells in x-direction	No. of cells in y-direction	Z levels	Resolution (km)
D1	40	70	17	9
D2	35	41		3
D3	38	38		1

In order to apply the modelling system to the study area it is firstly necessary to determine the most adequate model configuration and to improve some aspects already identified in previous studies; this will be the subject of the next two chapters. Only after that it will be possible to correctly simulate the air quality and assess the consequences of different urban land use scenarios.

5 SETUP OF THE URBAN AIR QUALITY MODELLING SYSTEM

Before applying the selected air quality modelling system to the Porto area it is important to determine the most appropriate model setup for the study case. For that purpose two air pollution episodes are selected in order to perform a group of meteorological modelling sensitivity tests. The meteorological model outputs are then fed into the air quality model with the objective of defining the most suitable model configuration for the study area.

5.1 Episodes selection

The selection of an adequate study period is part of the model configuration setup process. This period should be short, to allow the conduction of a group of simulations and sensitivity tests, and should also include air pollution situations, in order to evaluate the capability of the modelling system to reproduce observed data.

As already discussed, in 2006, as in previous years, the air quality monitoring network of the Portuguese Northern Region registered high levels of ozone and particulate matter. The crossing of all the air pollution episodes of these two pollutants, with information relative to the occurrence of natural events (forest fires, and dust from North African deserts) allowed the identification of anthropogenic episodes. Since summer and winter pollution episodes present different characteristics, two air pollution episodes are selected, one for each season. For the selection of the summer episode, a period with O_3 and PM10 simultaneous exceedances was searched for; for the winter episode, since a large number of days were available, only those with a period not inferior to three days were analysed. Table 5.1 presents the identified episodes.

In order to decide which episodes to simulate, a graphic representation of the measured concentrations at the several monitoring stations in the study area was made. Figures 5.1 and 5.2

present O_3 and PM10 concentrations observed in Coastal Porto air quality network for the two identified summer periods.

Table 5.1 Anthropogenic PM10 and O_3 episodes in the study area, for 2006.

Summer episodes	Winter episodes
3-6 June	3-5, 7-12, 17-20 January
22 August	30 January – 9 February
	13-16 March
	11-14 November
	16-24 December

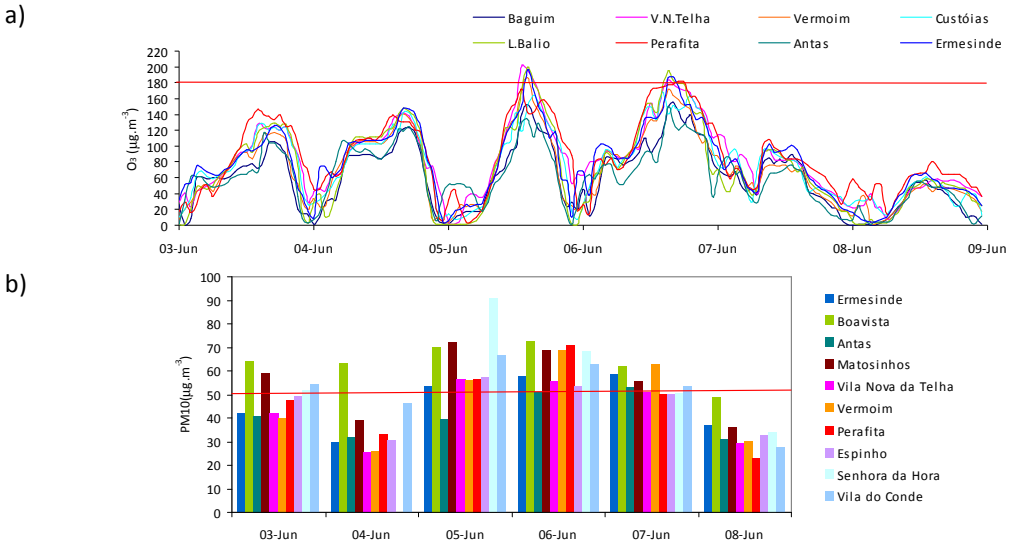

Figure 5.1 Pollutant concentrations for 3-9 June a) O_3 hourly average (the red line is the population information threshold, 180 µg.m^{-3}) and b) PM10 daily average (the red line is the daily limit value, 50 µg.m^{-3}).

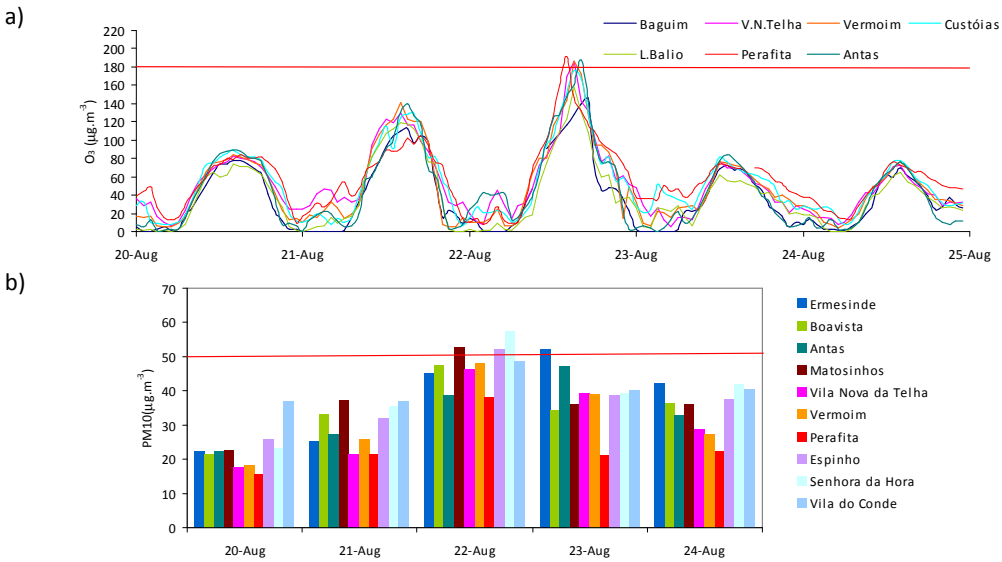

Figure 5.2 Pollutant concentrations for 20-24 August a) O_3 hourly average (the red line is the population information threshold, 180 µg.m^{-3}) and b) PM10 daily average (the red line is the daily limit value, 50 µg.m^{-3}).

Figure 5.3 presents PM10 concentrations observed in Coastal Porto air quality network for the seven identified winter periods.

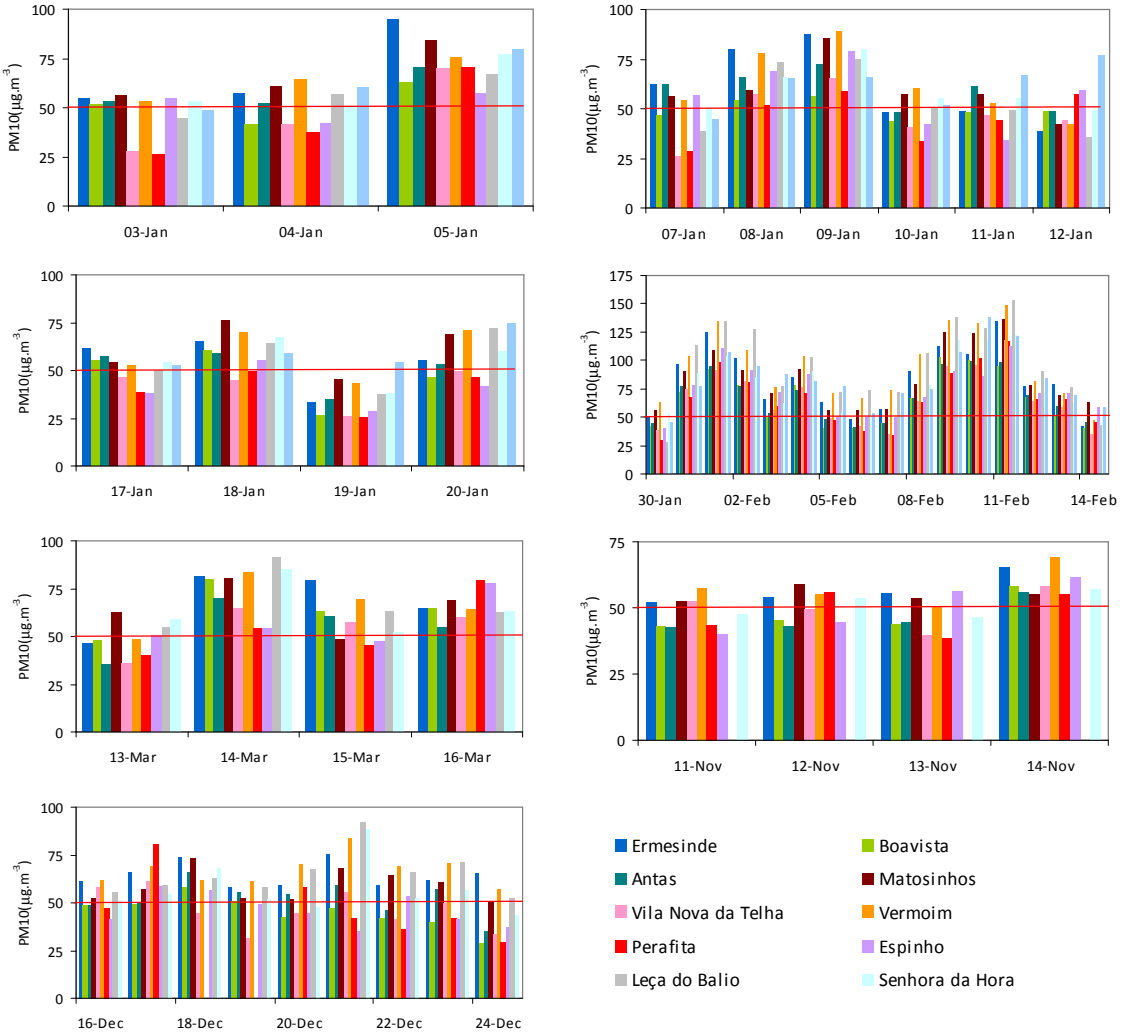

Figure 5.3 PM10 daily average concentrations for the winter episodes (the red line indicates the daily limit value - 50 µg.m^{-3}).

The periods 3 to 6 June and 16-24 December show high pollutants concentrations for a considerable time period and in a large number of air quality stations. Therefore they were selected as the summer and winter episode, respectively, for the sensitivity tests.

A brief meteorological characterization of the pollution episodes is here presented, with the aid of the 500 hPa pressure maps presented in Appendix D. The selected summer period, 03 to 08 June 2006, can be divided in two distinct periods: from 3 to 6 June a thermal low is developing and intensifying over the Iberian Peninsula (Figure D1); in the 7 and 8 June a frontal surface is approaching the NW coast of Portugal (Figure D2). The first situation is a typical summer situation in the region, and is generally favourable to photochemical production [Hoinka and Castro, 2003]. For the selected winter episode,

from 16 to 18 December, an anticyclone is present in surface and in altitude, with strong subsidence conditions which lead to a highly stable atmosphere and therefore low dispersion (Figure D3). From 19 December on the situation is similar although subsidence conditions are not so strong (Figure D4).

5.2 Meteorological modelling sensitivity tests

A series of numerical MM5 sensitivity experiments are performed, over the summer and winter episodes, allowing the determination of the best, or most well suited, model setup for the case-study. Questions to be answered are: (1) what differences exist between MM5 outputs resulting from the change in various factors?; and (2) is there a preferred configuration for MM5 that produces improved results?

The meteorological sensitivity tests help to understand the effects of using different MM5 configurations for the simulated meteorological conditions, which in turn are essential inputs for the air quality simulations. The applied MM5 physical options common to all the sensitivity tests include: Grell cumulus scheme [Grell *et al.*, 1994] at the 27-km resolution domain and no cumulus parameterization for the smaller grids, RRTM [Mlawer *et al.*, 1997] radiation scheme, Reisner-Graupel moisture scheme [Reisner *et al.*, 1998], and MRF PBL [Hong and Pan, 1996] scheme at the 27-km resolution domain. The used land surface model is the five-layer soil model [Dudhia, 1996]. The initial and boundary conditions are from the National Centre for Environmental Predictions (NCEP) global 1-degree reanalysis data, updated every 6-hours [URL16]. These options correspond to the configuration generally used in previous MM5-CAMx modelling system applications for Portugal [Ferreira *et al.*, 2003; Ferreira *et al.*, 2004; Carvalho *et al.*, 2006; Ferreira, 2007; among others].

Table 5.2 presents the matrix of the MM5 sensitivity experiments, which are designed to compare effects on meteorological simulations resulting from: different spatial resolutions; different land use data; different PBL parameterizations; and different urban roughness length. More details regarding each of the sensitivity tests are given further ahead.

Table 5.2 MM5 model configuration for the sensitivity tests

	Land use dataset	PBL scheme (D2-D5)	URBAN z_0
test 1	USGS24	ETA	0.5m
test 2	CLC24	ETA	0.5m
test 3	CLC24	GAYNO-SEAMAN	0.5m
test 4	CLC24	GAYNO-SEAMAN	1.0m

The results of the several MM5 simulations are evaluated against each other but also against data from a group of national meteorological stations, covering Continental Portugal (Figure 5.4).

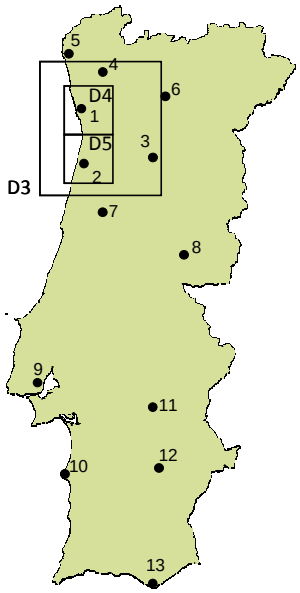

Meteorological stations

1 – Porto / Pedras Rubras (PT)
2 – Aveiro / University (AV)
3 – Viseu / Airfield (VS)
4 – Braga (BR)
5 – Viana do Castelo (VC)
6 – Vila Real (VR)
7 – Coimbra / Geophysical Institute (CBR)
8 – Castelo Branco (CB)
9 – Lisboa / Gago Coutinho (LS)
10 – Sines (SN)
11 – Évora (EV)
12 – Beja (BJ)
13 – Faro / Airport (FR)

Figure 5.4 Meteorological stations and their location in domains 3 to 5.

It is worth referring that Porto's meteorological station is not located in Porto municipality but in Matosinhos municipality, near the Airport. Therefore this station is neither representative of Porto city's characteristics nor of an urban area. This justifies the definition of an additional 1 km x 1 km resolution domain, over Aveiro urban area (D5), which includes an urban meteorological station; this "extra" domain allows obtaining more results for the thinner resolution, and therefore to explore the possible benefits of using a more refined resolution and to explore the differences between the sensitivity tests.

Besides the qualitative analysis of results, the statistical analysis is considered a key-factor for the analysis of the model performance [Hanna *et al.*, 1993; Elbir, 2003]; also it constitutes the second step from the "Basic Recommendations for modelling uncertainty estimation" [Borrego *et al.*, 2008a].

The MM5 skill is evaluated through the application of the quantitative error analysis introduced by Keyser and Anthes [1977] and widely used in model validation exercises [Eastman *et al.*, 1998; Miranda *et al.*, 2002; Ferreira *et al.*, 2003; Carvalho *et al.*, 2006]:

$$E = \left(\sum_{i=1}^{N} (\phi_i - \phi_{iobs})^2 \Big/ N \right)^{1/2}$$

$$E_{UB} = \left(\sum [(\phi_i - \phi_0) - (\phi_{iobs} - \phi_{0obs})]^2 \Big/ N \right)^{1/2}$$

$$S = \left(\sum_{i=1}^{N} (\phi_i - \phi_0)^2 \Big/ N \right)^{1/2}$$

$$S_{obs} = \left(\sum_{i=1}^{N} (\phi_{iobs} - \phi_{0obs})^2 \Big/ N \right)^{1/2}$$

The parameter E is the root mean square error (rmse), E_{UB} is the rmse after the removal of a certain deviation and S and S_{obs} are the standard deviation of the modelled and observed data. If ϕ_i and ϕ_{iobs} are individual modelled and observed data in the same mesh cell, respectively; ϕ_0 and ϕ_{0obs} the average of ϕ_i and ϕ_{iobs} for some sequence in study, and N the number of observations, then the simulation presents an acceptable behaviour when $S \approx S_{obs}$, $E < S_{obs}$ and $E_{UB} < S_{obs}$. In addition to these parameters the correlation coefficient was also determined for each simulation:

$$r = \frac{\sum_{i=1}^{N}(\phi_{iobs} - \phi_{0obs})(\phi_i - \phi_0)}{\sqrt{\sum_{i=1}^{N}(\phi_{iobs} - \phi_{0obs})^2 \sum_{i=1}^{N}(\phi_i - \phi_0)^2}}$$

5.2.1 Test1 – Reference setup

The physical option selected for this test include default MM5 setups for land use dataset and urban roughness height, as well as ETA PBL scheme for domains 2 to 5; these, together with the above described options, common to all tests, complete the MM5 reference setup already mentioned.

Table 5.3 lists the statistical measures obtained for MM5-test1 simulation, at the two meteorological stations with results for the three spatial resolutions (Porto/Pedras Rubras and Aveiro). Results for the remaining meteorological sites are presented in Appendix E (Table E.1). However, in order to have a broader perspective, the analysis presented is performed for all meteorological sites.

Table 5.3 Statistical measures for temperature and wind components obtained for MM5-test1 simulation - summer (3-8 June 2006) and winter (16-24 December 2006) episodes.

	T				u				v			
	r	S/S_{obs}	E/S_{obs}	E_{ub}/S_{obs}	r	S/S_{obs}	E/S_{obs}	E_{ub}/S_{obs}	r	S/S_{obs}	E/S_{obs}	E_{ub}/S_{obs}
PT	0.59	0.46	1.27	0.82	0.77	0.99	0.77	0.67	0.55	2.24	2.07	2.06
9km	0.46	0.79	1.14	0.94	0.21	1.30	1.79	1.48	0.13	1.54	2.31	2.20
3km	0.85	0.86	0.80	0.53	0.70	0.71	0.72	0.72	0.65	0.96	0.82	0.81
	0.72	1.00	1.23	0.75	0.17	0.38	1.03	1.04	0.13	0.37	1.39	1.12
1km	0.86	0.88	0.77	0.52	0.69	0.59	0.73	0.73	0.62	0.75	0.79	0.79
	0.72	1.04	1.32	0.76	0.14	0.33	1.12	1.05	0.02	0.29	1.37	1.06
AV	0.29	0.32	1.43	0.97	0.65	0.99	0.87	0.84	0.55	1.58	1.34	1.34
9km	0.27	0.67	1.19	1.05	0.41	1.60	2.01	1.53	0.38	3.18	3.04	2.88
3km	0.84	0.81	0.71	0.55	0.75	0.97	0.73	0.69	0.58	0.87	0.87	0.86
	0.67	1.02	1.28	0.89	0.25	0.78	1.14	1.12	0.40	0.90	1.08	1.02
1km	0.84	0.77	0.79	0.55	0.69	0.83	0.71	0.67	0.64	0.87	0.81	0.81
	0.74	1.02	1.28	1.07	0.21	0.81	1.33	1.24	0.41	1.09	1.12	1.11

For surface temperature at Porto, Aveiro, and Braga, the best skill is obtained for the finer resolution both in summer and winter, although in summer the skill record is better. This last observation is valid for the three meteorological variables at all sites and spatial resolutions. Regarding the wind

components, Aveiro, Viseu and Braga present better results for the thiner resolutions; for Porto the 1-km resolution presents slightly lower skills; the zonal wind component, u, is generally better simulated than the meridional component, v. Looking at the 9 km resolution, coastal cities (PT, AV, BR, VC, SN) present the worst results, due to the lack of high resolution land-use data, which places these cities in the water or very near it.

As an example of the obtained results, Figure 5.5 shows the time series obtained for Porto for the surface temperature and wind components (zonal and meridional), from test1 simulations and measurement data, for the summer episode.

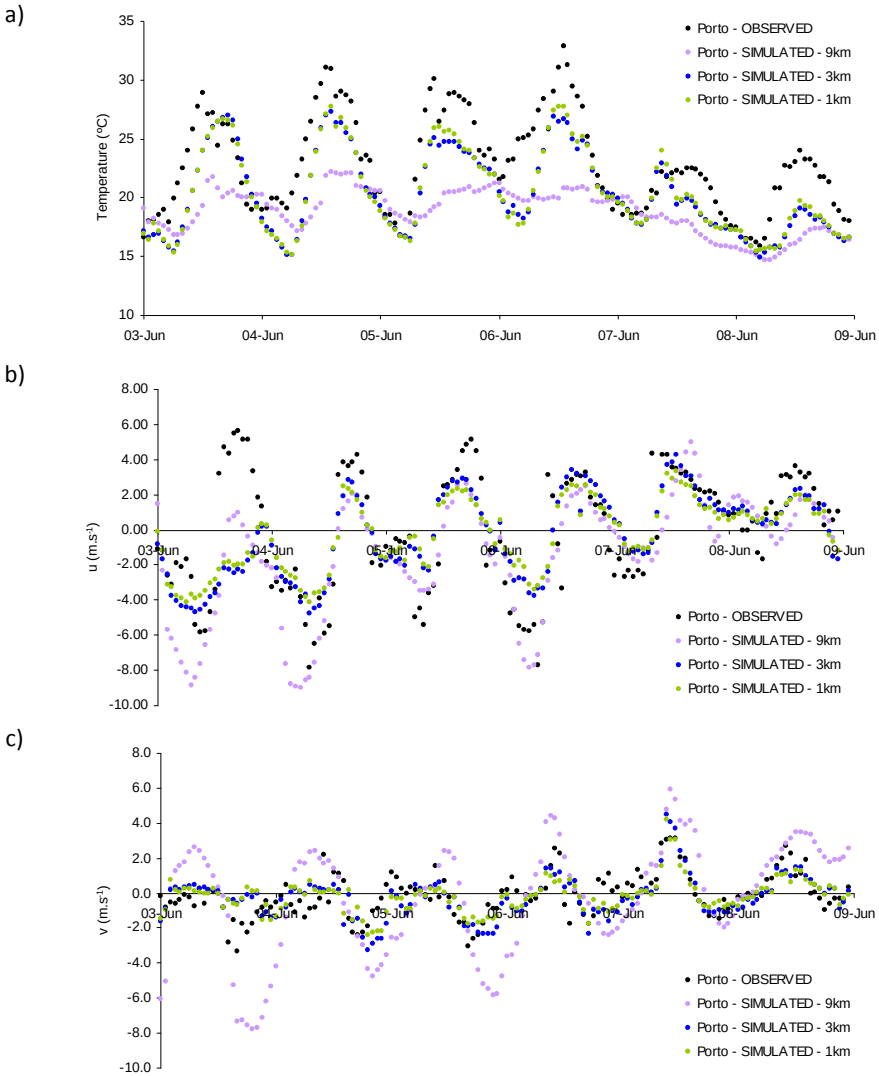

Figure 5.5 Summer episode time series comparison of surface a) temperature, b) zonal wind component, and c) meridional wind component from MM5-test1 simulations at 9 km, 3 km and 1 km, and surface measurements at Porto.

For the 9 km resolution, the simulation shows a clear underestimation of temperature. The underestimation was reduced in the finer resolutions simulations. Wind components also show

significant differences for the different resolutions, with a better agreement for the finer one. Also, results are clearly better for the second half of the episode.

In Appendix E, the same evolution is presented for the winter episode (Figure E.1); for wind components, results are similar to those obtained for summer; for temperature, differences between resolutions are not so evident, but larger differences are found between the 3 km and 1 km resolutions, with the last presenting a better performance.

5.2.2 Test2 – High resolution land use data

The goal of this sensitivity test is to understand the effects of using different land use datasets in MM5 on the simulated meteorological conditions; therefore, the original USGS24 dataset is replaced by a new one based on Corine Land Cover 2000 [EEA, 2000], within domains 3 to 5 of the simulation. Next, the two land use datasets are described, compared and discussed, in order to evaluate the benefits of using a higher resolution and higher-confidence land use dataset.

The previous chapter already mentioned and described the USGS 24-category land use database existent in MM5 modelling system (§ 4.5.1, Table 4.4), as well as the CORINE Land Cover 44-classes data base (§4.2.2, Table 4.1).

In order to compare datasets for the study area, Figure 5.6 presents CLC2000 and USGS land use classes for NW Portugal domain (D3), with 3 km resolution. The CLC2000 original dataset, with 250 m resolution, was processed in a geographical information system (GIS) software in order to transform it to a raster format with the desired resolution, in this case 3 km.

The differences between both data sets are evident, with CLC2000 presenting 30 classes for D3, and USGS24 presenting only 6 classes. However, since CLC2000 is much more detailed than USGS24, a direct and clear comparison is difficult. In this sense, the 44 classes in CLC2000 were converted to the 24 USGS categories, according to the correspondence given in Table 5.4, which results from the careful analysis of the description of each land use class for each dataset.

a) USGS24

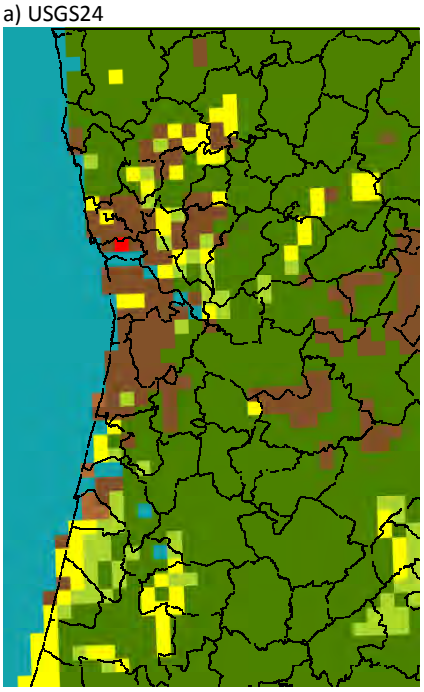

1 Urban
2 Dryland Cropland Pasture
6 Cropland Wood Mosaic
9 Mix Shrubland/Grassland
10 Savanna
11 Deciduos Braodleaf
16 Water Bodies

b) CLC2000

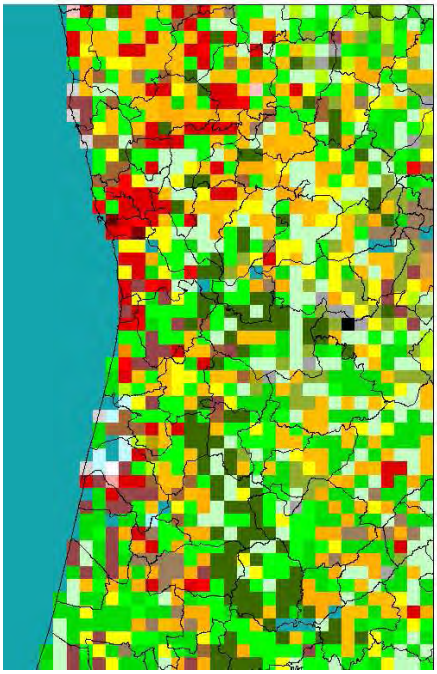

111 Continuous urban fabric
112 Discontinuous urban fabric
121 Industrial or commercial units
123 Port areas
124 Airports
133 Construction sites
211 Non-irrigated arable land
212 Permanently irrigated land
221 Vineyards
222 Fruit trees and berry plantations
231 Pastures
241 Annual crops associated with permanent crops
242 Complex cultivation
243 Land principally occupied by agriculture...
311 Broad-leaved forest
312 Coniferous forest
313 Mixed forest
321 Natural grassland
322 Moors and heathland
324 Transitional woodland shrub
331 Beaches, dunes, and sand plains
333 Sparsely vegetated areas
334 Burnt areas
411 Inland marshes
421 Salt marshes
422 Salines
511 Water courses
512 Water bodies
521 Coastal lagoons
523 Sea and ocean

Figure 5.6 Comparison between a) USGS24 and b) CLC2000 land use categories for D3.

Table 5.4 Correspondence between CLC2000 and USGS-24 land use categories.

CLC2000	USGS-24
1.1.1. Continuous urban fabric	1. Urban and built-up land
1.1.2. Discontinuous urban fabric	
1.2.1. Industrial or commercial units	
1.2.2. Road and rail networks and associated land	
1.2.3. Port areas	
1.2.4. Airports	
1.3.3. Construction sites	
1.4.2. Sport and leisure facilities	
2.1.1. Non-irrigated arable land	2. Dryland Cropland and pasture
2.1.2. Permanently irrigated land	3. Irrigated Cropland and pasture
2.4.1. ANNUAL CROPS ASSOCIATED WITH PERMANENT CROPS	5. Cropland/grassland mosaic
2.4.2. COMPLEX CULTIVATION	
2.2.2. Fruit trees and berry plantations	6. Cropland/woodland mosaic
2.2.3. OLIVE GROVES	
2.4.3. LAND PRINCIPALLY OCCUPIED BY AGRICULTURE, WITH SIGNIFICANT AREAS OF NATURAL VEGETATION	
2.4.4. Agro-forestry areas	
1.4.1. Green urban areas	7. Grassland
2.3.1. Pastures	
3.2.1. Natural grassland	
2.2.1. Vineyards	8. Shrubland
3.2.2. MOORS AND HEATHLAND	
3.2.3. SCLEROPHYLLOUS VEGETATION	
3.2.4. Transitional woodland shrub	
3.1.1. BROAD-LEAVED FOREST	11. Deciduous broadleaf forest
3.1.2. CONIFEROUS FOREST	14. Evergreen needleleaf forest
3.1.3. MIXED FOREST	15. Mixed forest
5.1. 1. WATER COURSES	16. Water bodies
5.1.2. WATER BODIES	
5.2.1. COASTAL LAGOONS	

5.2.2. ESTUARIES	
5.2.3. SEA AND OCEAN	
	17. Herbaceous wetland
2.1.3. RICE FIELDS	
4.1.1. INLAND MARSHES	
4.1.2.PEATBOGS	
4.2.1. SALT MARSHES	
4.2.2. SALINES	
4.2.3. Intertidal flats	
1.3.1. Mineral extraction sites	19. Barren sparse vegetation
1.3.2. DUMP SITES	
3.3.1. BEACHES, DUNES, AND SAND PLAINS	
3.3.2. BARE ROCK	
3.3.3. SPARSELY VEGETATED AREAS	
3.3.4. BURNT AREAS	
3.3.5. Glaciers and perpetual snow	

Figure 5.7 presents the CLC2000 land use converted into the 24 USGS categories (from now on designated by CLC24), in comparison with the original MM5 USGS24 dataset, for D3.

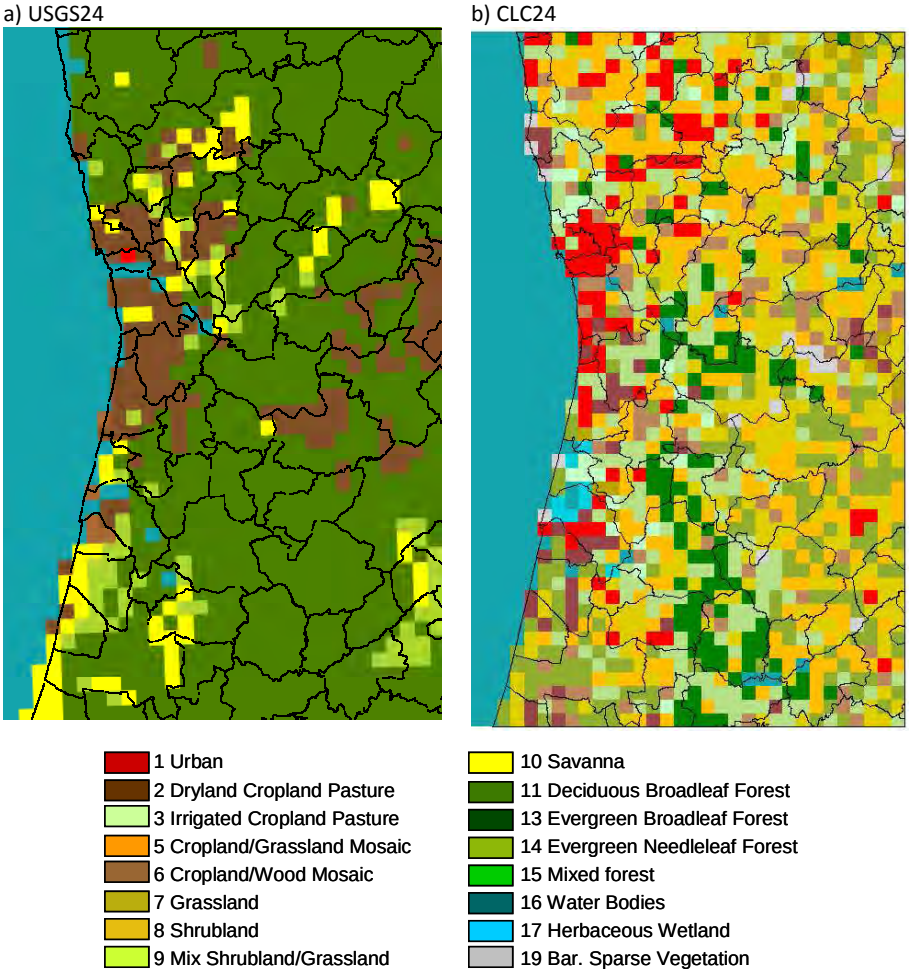

Figure 5.7 Comparison between a) USGS24 and b)CLC24 land use categories for D3.

Once more, the differences between both data sets are evident, with CLC24 presenting 13 classes in D3, and USGS-24 presenting only 6 classes. Besides the diversity of land use classes, a major difference of great importance for the meteorological modelling, as well as for the air quality modelling, is the representativeness of the urban land use class (in red): in the USGS-24 dataset only one cell is found in Porto municipality, while in the new CLC24 a group of urban cells is found in Porto and adjacent municipalities, and also smaller groups are found over the simulation domain, representing smaller cities.

Table 5.5 presents the number of grid cells for each land use class for each dataset (one grid cell corresponds to 9 km x 9km).

Table 5.5 Number of grid cells for each land use class for each dataset (one grid cell - 9 km x 9 km).

Land Use Classes	USGS24	CLC24
1.Urban and built-up land	1	93

2. Dryland cropland and pasture	154	44
3. Irrigated cropland and pasture	0	32
5. Cropland/grassland mosaic	0	262
6. Cropland/woodland mosaic	4	92
7. Grassland	0	23
8. Shrubland	0	269
9. Mixed Shrubland/grassland	62	-
10. Savanna	76	-
11. Deciduous broadleaf forest	812	112
14. Evergreen needleleaf forest	0	173
15. Mixed forest	0	213
16. Water bodies	1186	956
17. Herbaceous wetland	0	8
19. Barren or sparsely vegetated	0	18

It is possible to observe that not only the classes are distinct but also the representativeness of each class is different:

- in CLC24 the urban land use (class 1) presents 93 cells (837 km^2) while in the USGS24 it has only 1 cell;
- the most important land use class in USGS24 (besides water bodies) 11-deciduous broadleaf forest (812 cells), assumes a much smaller importance in the CLC24 dataset (only 112 cells for class11, with a total of 498 cells for the forest classes -11, 14 and 15);
- the most important land use class in CLC24 (besides water bodies) is class 8-shrubland (269 cells), a class that is not present in the USGS24 dataset.

Figures 5.8 and 5.9 present USGS24 and CLC24 land use classes for D4 and D5, 1 km resolution. In CLC24 dataset the centre of D4, constituted by Porto municipality and its surroundings (part of Matosinhos, Maia, Vila Nova de Gaia and Gondomar), is represented as a large urbanized area (represented in red), while in the USGS24 original MM5 data, the urbanized area is much more restricted and concentrated in Porto municipality. Considering the entire simulation domain, in CLC24 the urban land use is responsible for an area over 15 times larger in comparison with USGS24.

The misrepresentation of land use from USGS-24 is also clear for the Aveiro region, with a large part of the coastal region represented as water. Looking at Aveiro urban region, only two urban cells are represented in USGS24, while CLC24 presents a larger urban area (151 km^2).

a) USGS24 b) CLC24

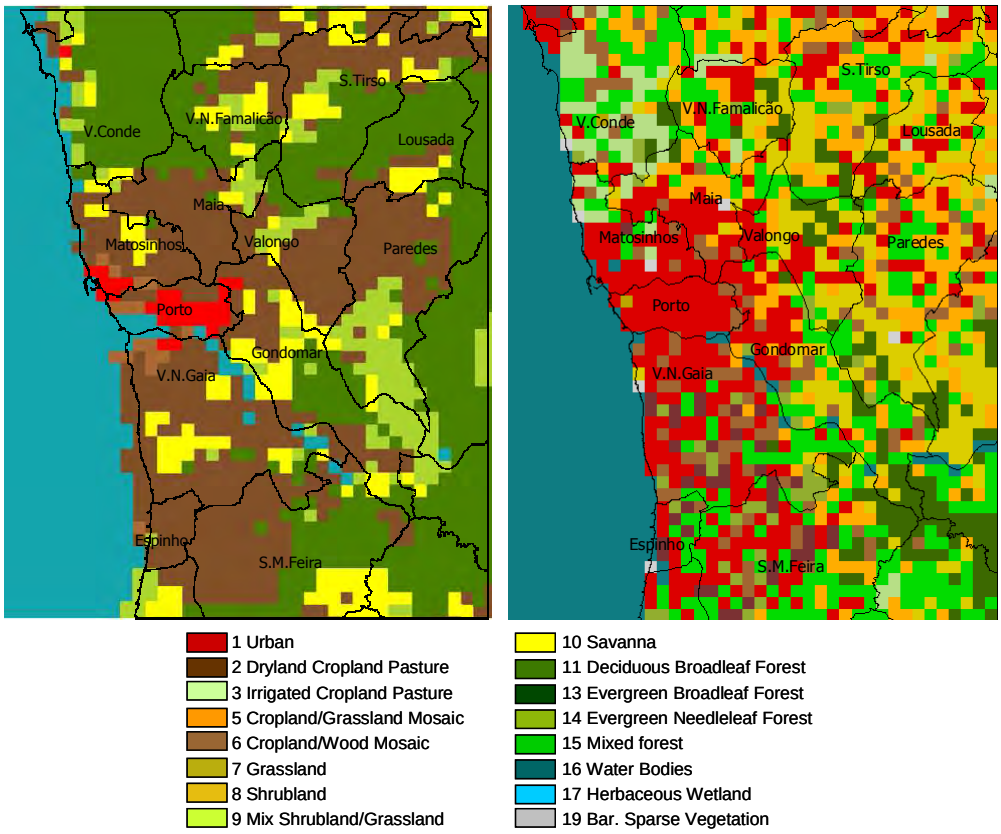

Figure 5.8 Comparison between (a) CLC24 and (b) USGS24 land use categories for D4.

a) USGS24 b) CLC24

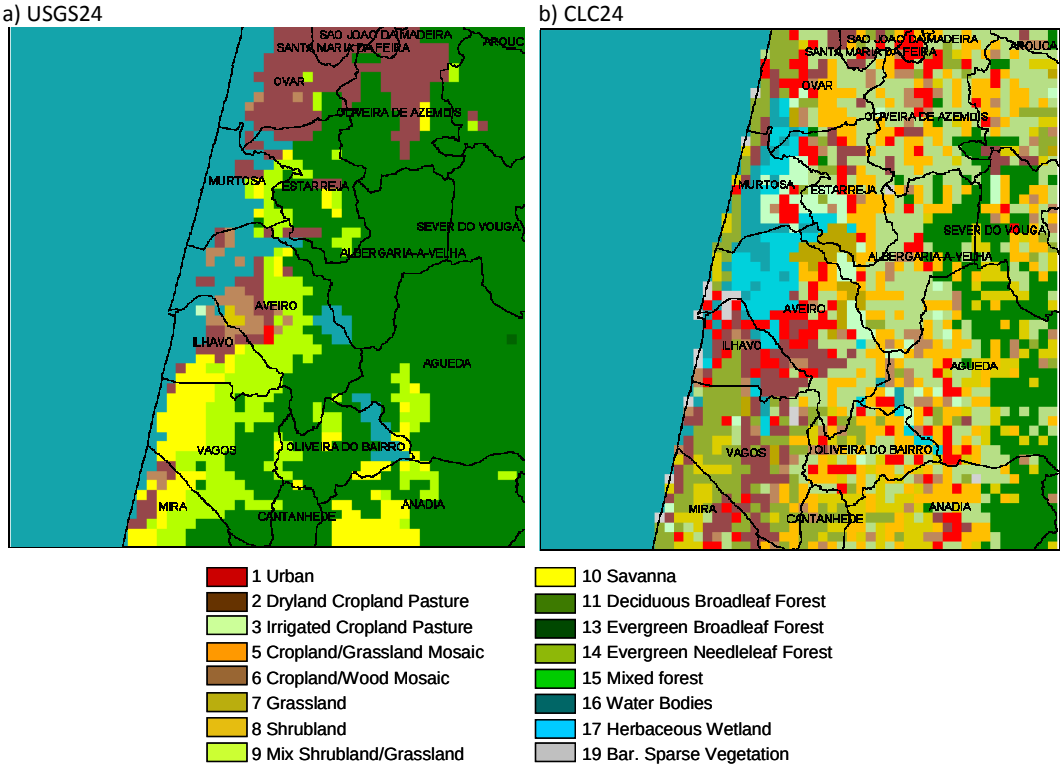

Figure 5.9 Comparison between CLC24 and USGS-24 land use categories for D5.

It is possible to conclude that the land use in the study area is weakly represented in the USGS24 original dataset. The upgrading of the land use representation in general, and the more realistic representation of urban areas, through the consideration of a greater number of urban cells, in particular, may prove to be important to the improvement of the modelling system's performance.

In order to test the new land use dataset and its effects on the simulation results, the current MM5 land use (USGS24) was replaced by the developed CLC24, for domains 3, 4 and 5 of the simulation.

Table 5.6 lists the statistical measures obtained for MM5-test2 simulation at Porto and Aveiro. Results for the remaining meteorological sites are presented in Appendix E (Table E.2).

Table 5.6 Statistical measures for temperature and wind components obtained for MM5 – test2 simulation - summer (3-8 June 2006) and winter (16-24 December 2006) episodes.

	T				u				v			
	r	S/S_{obs}	E/S_{obs}	E_{ub}/S_{obs}	r	S/S_{obs}	E/S_{obs}	E_{ub}/S_{obs}	r	S/S_{obs}	E/S_{obs}	E_{ub}/S_{obs}
PT	0.60	0.46	1.27	0.81	0.78	1.03	0.76	0.67	0.56	2.43	2.05	2.05
9km	0.48	0.85	1.11	0.95	0.22	1.30	1.79	1.47	0.13	1.52	2.27	2.18
3km	0.87	0.95	0.75	0.50	0.69	0.70	0.73	0.73	0.66	0.88	0.80	0.79
	0.73	1.07	1.27	0.77	0.17	0.42	1.07	1.01	0.12	0.35	1.37	1.11
1km	0.87	0.99	0.70	0.50	0.66	0.64	0.75	0.75	0.63	0.80	0.81	0.81
	0.77	1.12	1.24	0.73	0.14	0.40	1.11	1.01	0.06	0.31	1.35	1.08
AV	0.26	0.32	1.43	0.98	0.64	1.01	0.89	0.86	0.56	1.56	0.32	0.95
9km	0.27	0.70	1.19	1.06	0.42	1.58	2.00	1.50	0.36	3.14	3.00	2.94
3km	0.86	0.82	0.69	0.59	0.75	0.99	0.73	0.66	0.62	0.81	0.84	0.82
	0.66	1.08	1.44	0.84	0.26	0.82	1.11	1.12	0.39	0.90	1.07	1.05
1km	0.87	0.85	0.66	0.50	0.76	0.94	0.69	0.65	0.76	0.76	0.73	0.73
	0.73	1.07	1.27	0.76	0.26	0.96	1.15	1.11	0.44	0.94	1.06	1.05

For temperature at Porto, Aveiro, and Braga, the best skill is obtained for the finer resolution both in summer and winter, as verified for test1; again better skills are obtained for summer. Regarding the wind components, best results for Porto are obtained at 9 km and 3 km resolutions for u and v, respectively; for Aveiro, wind is better simulated at 1 km resolution; Viseu and Braga do not present significant differences between resolutions. For the remaining sites, with simulated values only for the 9 km resolution, skills are high except for the coastal locations of Viana do Castelo and Sines.

In Appendix E the time series of temperature and wind components from test2 simulations and measurement data at Porto are presented for both episodes (Figures E2 and E3). All resolutions show an underestimation of temperature during the greatest part of the simulation periods; the best agreement between measured and simulated temperature is found at 1 km resolution. For wind components, the 3 and 1 km resolutions present lower simulated values and therefore better results.

In order to better analyse the possible benefits of using a high-resolution land use dataset, results from test1 and test2 are now confronted. Figure 5.10 presents the spatial distribution of differences in

daily average temperature obtained for D4 (Porto Great Area), resulting from the use of the different land use datasets, for the summer episode.

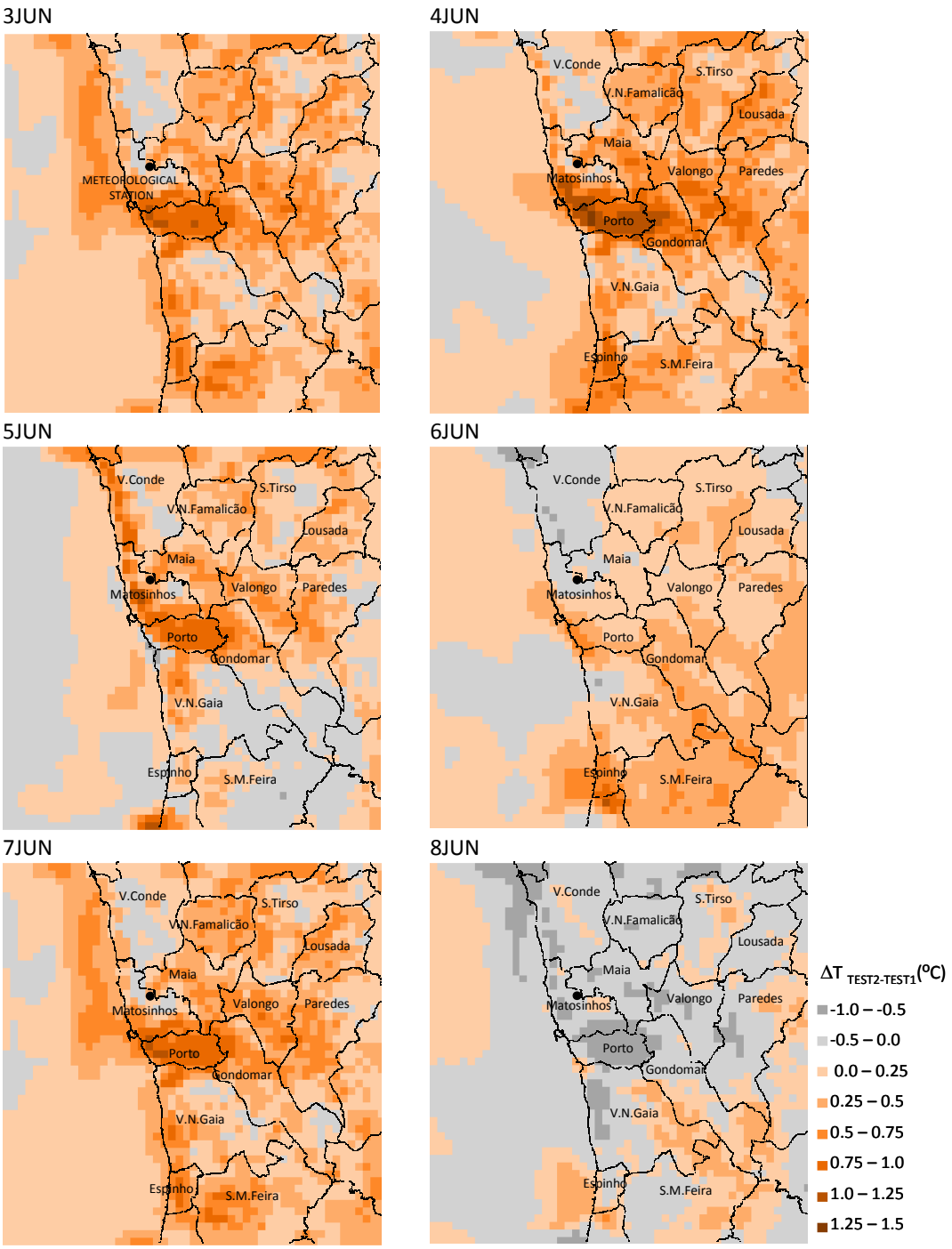

Figure 5.10 Spatial plot of daily average temperatures differences (test2 minus test1) for D4, summer episode.

A positive ΔT is found over Porto city for all days of the episode except June 8. Average daily temperatures differences reach values as high as 1.5°C over Porto, with hourly maximums of 3°C. Other significant positive temperature differences are found in the coastal cells and in the near coast sea cells. Negative differences are found in cells corresponding to forest (land uses 11, 14 and 15) in

the CLC24 land use dataset (test2), formerly corresponding to pastures and shrubland/grassland (land uses 2 and 9) in USGS24 (test1).

At this point, an obvious question emerges: does this temperature increase over Porto correspond to a closer representation of the reality? Unfortunately, the available meteorological station is located in Matosinhos municipality, and not in Porto. Still, the comparison between test2 and test1 temperature values for Porto/Pedras Rubras meteorological station is presented in Figure 5.11. The slight increase in temperature obtained with test2 corresponds to a closer representation of the observed values; this is also confirmed by the comparison of statistical parameters presented in Tables 5.3 and 5.8, which are better for test2.

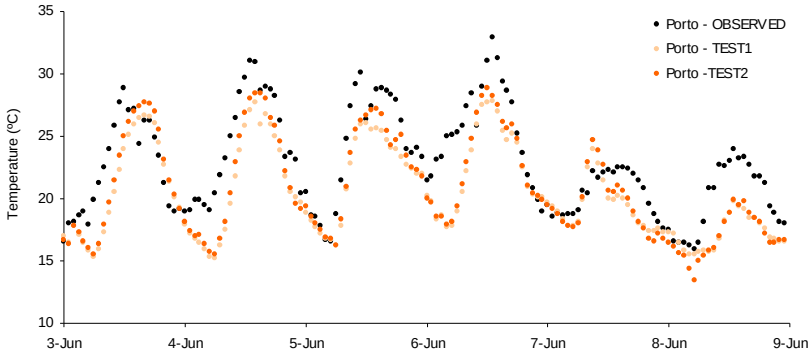

Figure 5.11 Summer episode D4 time series comparison of surface temperature for test2 and test1 in Porto/Pedras Rubras.

Figure 5.12 presents the same comparison, now for the winter episode. Here the difference between the two tests are evident, with the higher temperature obtained for test2 being almost always closer to the observed values; this is confirmed by Tables 5.3 and 5.8 which are consistently better for test2.

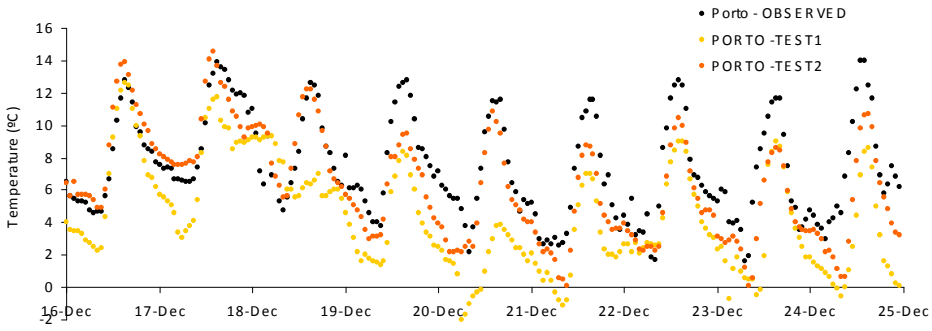

Figure 5.12 Winter episode D4 time series comparison of surface temperature for test2 and test1 in Porto/Pedras Rubras.

Results from D5 simulations, corresponding to Aveiro area, where the meteorological station located in the University is inside the urban area help answering the question above. Figure 5.13 presents the

spatial distribution of differences in daily average temperature between test2 and test1 for D5, for the last three days of the summer episode.

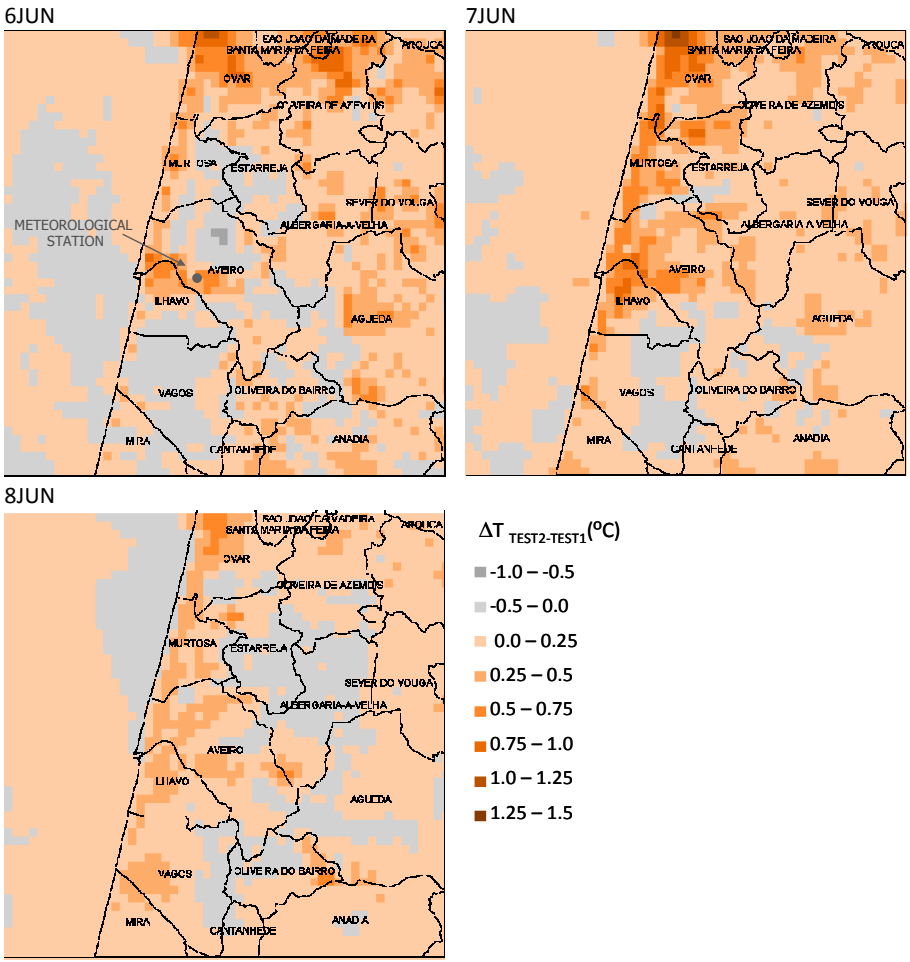

Figure 5.13 Spatial plot of daily average temperatures differences (test2 minus test1) for D5, the summer episode (6-8 June).

A positive ΔT is found over a large part of the simulation domain; increases over Aveiro city (in the area of the meteorological station), in the order of 0.5 to 1°C, are clear in the cells corresponding to urban areas in the new land use. Positive temperature differences are also estimated near the coast in the border between Ílhavo and Aveiro municipalities, formerly water in USGS-24, and now in land and even urban cells.

Figure 5.14 present the time series comparison of temperature for test1 and test2 simulations and measurement data at Aveiro.

a)

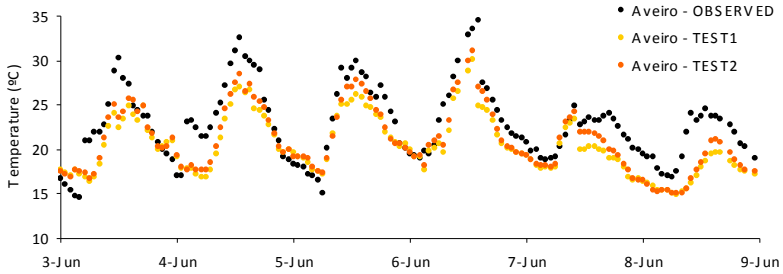

b)

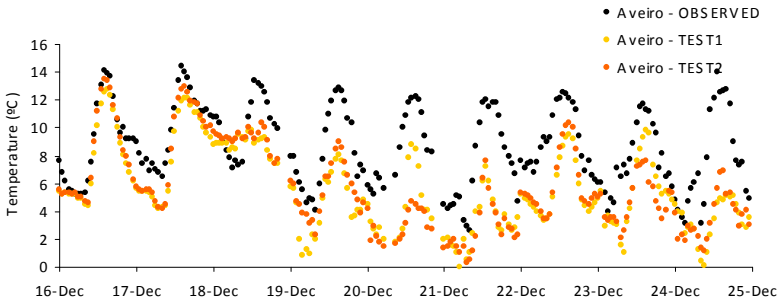

Figure 5.14a) Summer and b) winter, episode time series comparison of surface temperature for test2 and test1 in Aveiro, for D5 (1 km resolution).

The time series for Aveiro for the summer episode confirms that test2 fits best the observed values, during the entire simulation period, but especially for higher temperatures. For the winter episode, however, results are not so clear: for the first half of the episode test2 seems to yield a better agreement with observed values, while for the second half test1 looks better.

Considering the former analysis for Aveiro and the fact that it is a small urban area when compared to Porto, it is expected that the larger temperature increases presented in Figure 5.11 correspond to a closer representation of the reality.

The same analysis is performed for wind speed in Appendix E. Figures E.4 and E.5 present the time series comparison of wind speed obtained with test 1 and test 2 and the observed wind speed for the summer and winter episodes, for Porto and Aveiro, respectively. The graphs, as well as the statistical parameters presented in Tables 5.3 and 5.8, show that differences between simulations are not clear. However, test2 results are closer to the observed values. For both episodes, wind speeds for Porto are highly underestimated by both tests.

Figure E.7 shows the spatial distribution of differences in daily average wind speed obtained for D3 for the summer episode. For the majority of the episode the Porto municipality presents a decrease in wind speed in the order of 1 $m.s^{-1}$, as a result of the land use dataset improvement: the larger urban area implies higher friction, therefore influencing (decreasing) the wind speed calculation in the model. Wind speed increases are found in a confined area in the mouth of Douro River. The statistical

parameters presented in Tables 5.3 and 5.8, consistently better for test2, confirm that test2 results are closer to the observed values.

5.2.3 Test3 – PBL parameterization

This test intends to verify the influence of a different PBL parameterisation in MM5 results, because, as already mentioned in §4.5.1, different PBL schemes significantly influence the model results. For domains 2 to 5, the previous tests (tests 1 and 2) used the ETA scheme parameterization [Janjic, 1990]; for test3 the Gayno–Seaman scheme [Gayno, 1994] was used.

Table 5.7 lists the statistical measures obtained for MM5 – test3 simulation at Porto and Aveiro. Results for the remaining meteorological sites are presented in Appendix E (Table E.3).

Table 5.7 Statistical measures for temperature and wind components obtained for MM5 – test3 simulation - summer (3-8 June 2006) and winter (16-24 December 2006) episodes.

	T				u				v			
	r	S/S_{obs}	E/S_{obs}	E_{ub}/S_{obs}	r	S/S_{obs}	E/S_{obs}	E_{ub}/S_{obs}	r	S/S_{obs}	E/S_{obs}	E_{ub}/S_{obs}
PT	0.59	0.44	1.25	0.82	0.76	0.96	0.73	0.69	0.58	2.09	1.75	1.71
9km	0.46	0.64	1.36	0.91	0.31	1.01	1.34	1.19	0.12	1.19	1.99	1.89
3km	0.89	0.97	0.55	0.47	0.83	0.74	0.57	0.57	0.54	0.92	0.97	0.92
	0.85	1.09	0.70	0.58	0.23	0.52	1.05	1.02	0.10	0.48	1.46	1.22
1km	0.89	1.05	0.52	0.49	0.80	0.68	0.61	0.61	0.50	0.89	0.99	0.95
	0.86	1.13	0.67	0.58	0.24	0.51	1.05	1.01	0.08	0.44	1.43	1.19
AV	0.32	0.31	1.40	0.96	0.59	0.90	0.88	0.87	0.56	1.44	1.24	1.23
9km	0.24	0.45	1.45	1.02	0.50	1.23	1.54	1.16	0.39	2.74	2.54	2.52
3km	0.85	0.84	0.54	0.53	0.71	1.22	0.93	0.87	0.60	0.91	0.85	0.85
	0.84	0.93	0.67	0.56	0.31	1.08	1.33	1.23	0.31	1.10	1.29	1.24
1km	0.86	0.92	0.52	0.51	0.68	0.95	0.84	0.78	0.61	0.85	0.83	0.83
	0.84	0.99	0.63	0.56	0.32	1.04	1.33	1.19	0.35	1.05	1.17	1.17

For surface temperature the best skill is obtained for the finer resolution both in summer and winter, again with a better skill result for summer. Regarding wind components, Aveiro and Braga present better results for the thinner resolutions; Porto and Viseu do not present a clear trend, with better skills varying with resolution and wind components. For the 9 km resolution, coastal cities (PT, AV, BR, VC, SN) present the worst results, due to the lack of high resolution land-use data.

As an example, Figure 5.15 presents the time series comparison of the surface temperature and wind components, from test3 simulations and measurement data at Porto, for the summer episode. For temperature, the performance of the model increases with increased resolution; regarding wind components, the 3 and 1 km simulations are closer to the observed values, but the 9 km resolution seems to better follow the observed trend.

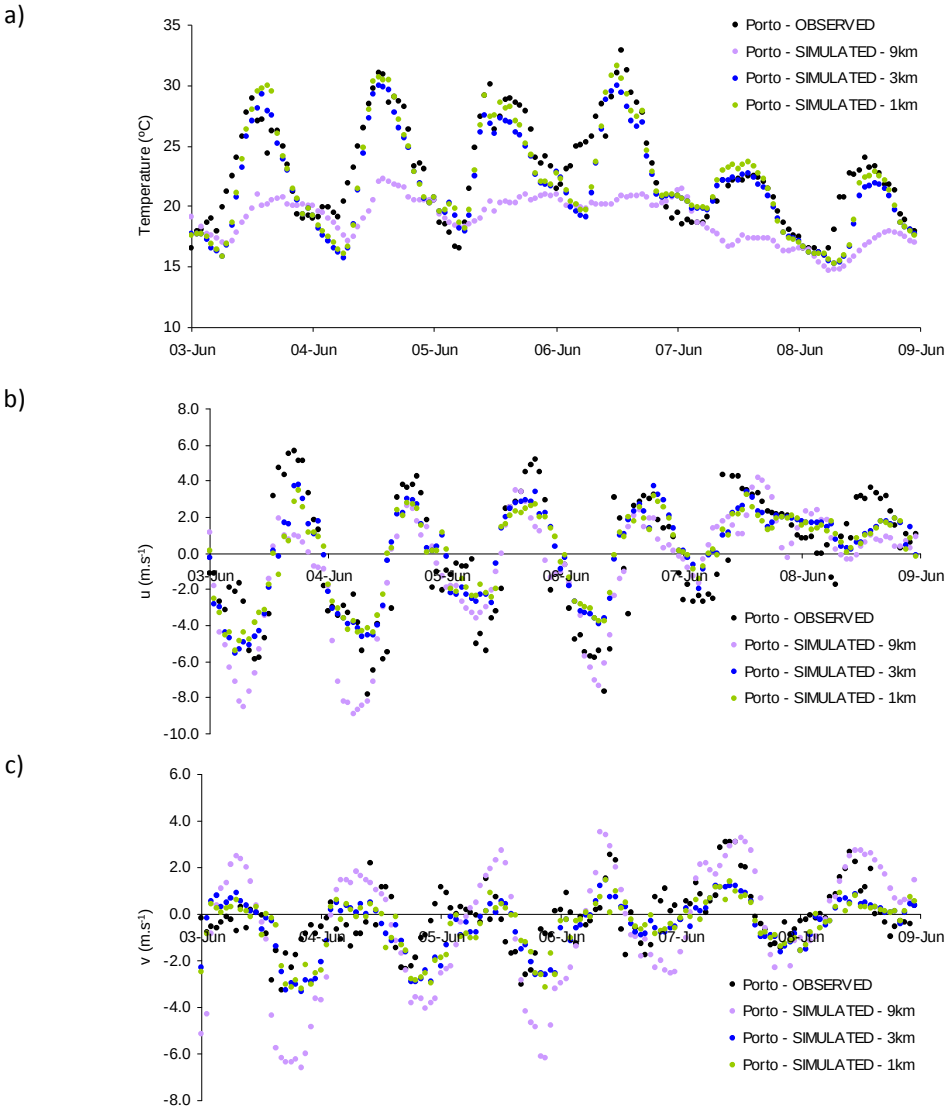

Figure 5.15 Summer episode time series comparison of surface a) temperature, b) zonal wind component, and c) meridional wind component from MM5-test2 simulations at 9 km, 3 km and 1 km, and surface measurements at Porto.

Appendix E presents the same graphs for the winter episode (Figure E.7). For temperature, the 3 and 1 km simulations present better results; regarding wind components, it is not possible to identify a resolution presenting better results.

Figure 5.16 shows the spatial distribution of differences between test3 and test2 in daily average temperature obtained for D4 (Porto Great Area), for the summer episode. A positive ΔT is calculated over the entire domain, with the exception of a part of the ocean cells. Over Porto, temperature increases between 1°C and 2°C. In hourly terms, positive differences reach +4.2°C over Porto and Vila Nova de Gaia cities, and +3°C over most of the land.

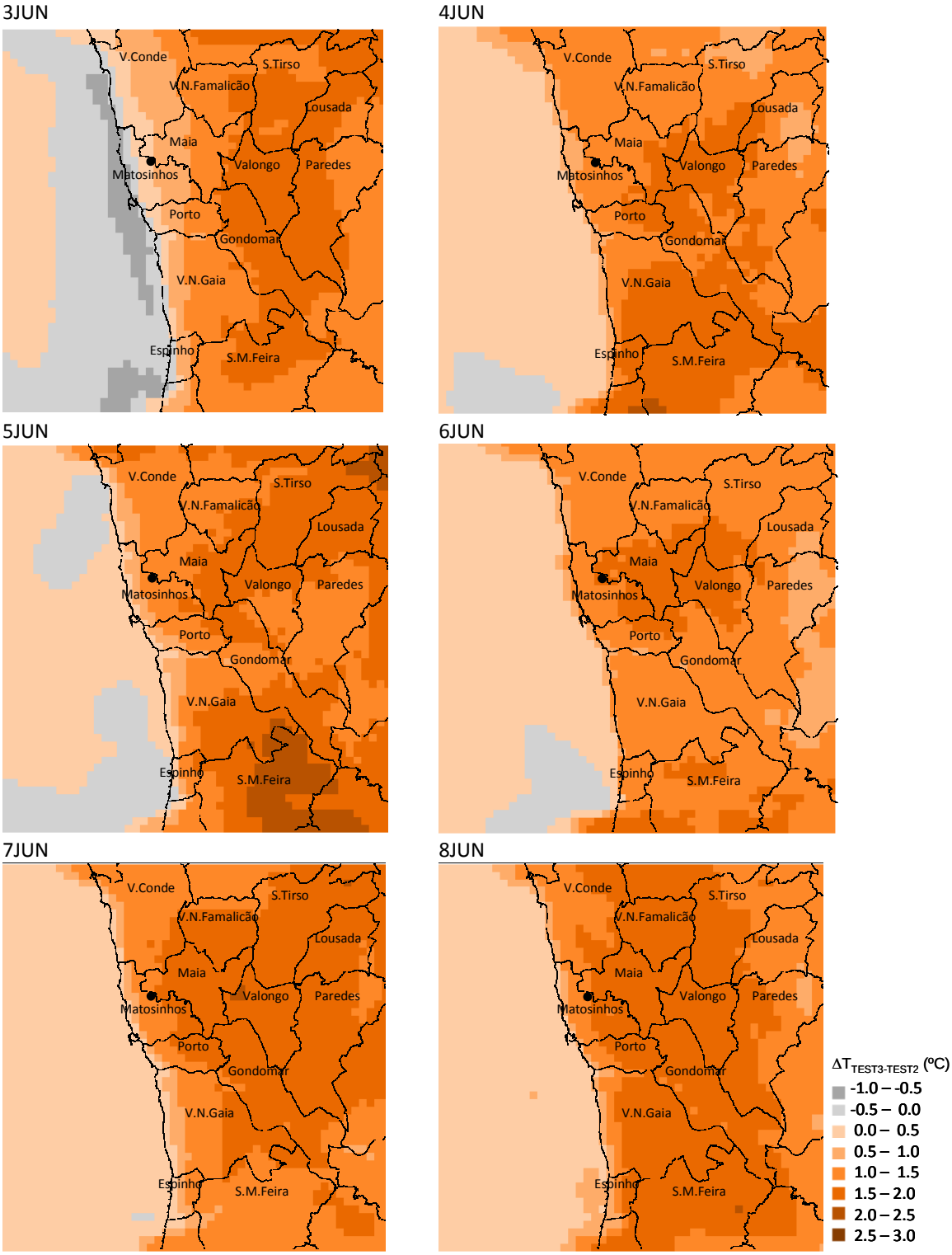

Figure 5.16 Spatial plot of daily average temperatures differences (test3 minus test2) between model simulations, for the summer episode.

At this point, it is clear that the significant temperature spatial differences between simulations are not translated into the statistical parameters; this is because there is a limited number of meteorological stations, namely for the 1 km resolution.

Figure 5.17 presents the time series comparison between test3 and test2 temperature values for Porto.

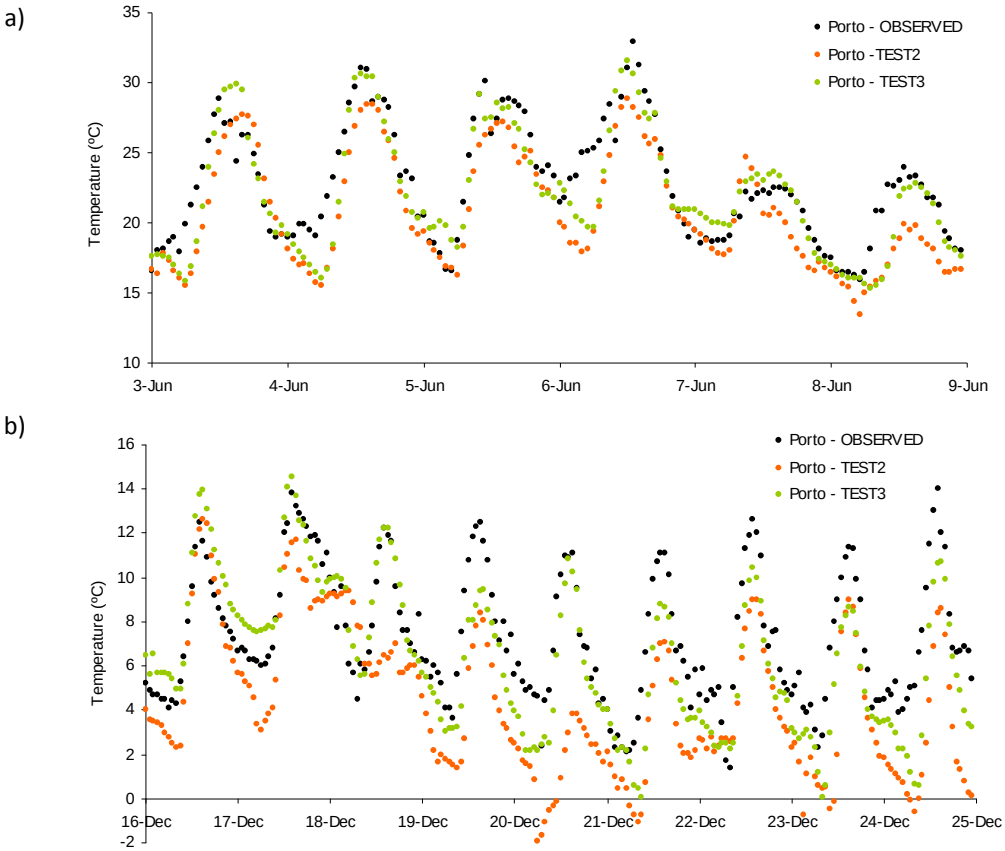

Figure 5.17 Time series comparison of surface temperature for test3 and test2 in Porto/Pedras Rubras for D4 a) summer episode and b) winter episode.

It is possible to conclude that test3 clearly presents better results, with smaller deviations in relation to the observed values and with a better correlation; these improvements are particularly important for the winter episode.

In Appendix E, Figure E.8 presents the spatial distribution of differences in daily average wind speed obtained for D3 (Porto Great Area) for the summer episode. For the first three days, the Porto municipality, as well as the majority of the simulation domain, presents a small increase in wind speed, ranging from 0.2 to 1.0 $m.s^{-1}$; in the second half of the episode, differences between the two tests are negative but in the same order of magnitude.

The main difference between ETA (test2) and Gayno-Seaman (test3) PBL schemes, is that the last one has the ability to provide cloud tendencies, allowing for the calculation of the sub-grid condensed-phase processes associated with fog [Gayno, 1994; Mao *et al.*, 2006]. This may help to understand the better performance of test3 in the study region.

5.2.4 Test4 – Urban roughness height

Another important parameter in the simulation of atmospheric flow over urban areas is the urban roughness height. Rougher surfaces, and therefore higher roughness heights, are likely to cause more intense turbulence and therefore to affect the dispersion of pollutants [Stull, 1998; Rotach, 1999]. With the objective of better characterizing urban areas for meteorological modelling purposes, besides the land use improvement introduced in test2 and the PBL parameterization from test3, this test replaces the default urban roughness height (0.5 m) by a higher value, 1 m, as suggested by Pielke [1984] for city centres. This value was tested in a former study for the Lisbon urban area, and yielded good results [Aquilina *et al.*, 2005]; therefore it was defined as part of the "optimum setup" for high-resolution simulations over that area.

Table 5.8 lists the statistical measures obtained for MM5 – test4 simulation at Porto and Aveiro; results for the remaining meteorological sites are presented in Appendix E (Table E.4). The confrontation of this table with table 5.9 reveals very similar numbers. However, Coimbra and Évora present slightly better results for test4 temperature in winter and summer, respectively. Porto and Aveiro show small differences in wind components between simulations, and for temperature results are identical.

Table 5.8 Statistical measures for temperature and wind components obtained for MM5 – test4 simulation - summer (3-8 June 2006) and winter (16-24 December 2006) episodes.

	T				u				v			
	r	S/S_{obs}	E/S_{obs}	E_{ub}/S_{obs}	r	S/S_{obs}	E/S_{obs}	E_{ub}/S_{obs}	r	S/S_{obs}	E/S_{obs}	E_{ub}/S_{obs}
PT	0.59	0.45	1.25	0.82	0.76	0.96	0.72	0.68	0.58	2.05	1.71	1.68
9km	0.46	0.64	1.36	0.90	0.30	0.98	1.33	1.18	0.08	1.19	1.99	1.88
3km	0.88	0.96	0.55	0.48	0.83	0.72	0.57	0.57	0.51	0.89	0.97	0.94
	0.85	1.09	0.70	0.58	0.22	0.48	1.05	1.01	0.10	0.46	1.46	1.22
1km	0.89	1.05	0.52	0.49	0.81	0.61	0.62	0.62	0.46	0.80	0.98	0.95
	0.86	1.13	0.67	0.58	0.26	0.44	1.05	0.99	0.11	0.40	1.44	1.18
AV	0.32	0.31	1.40	0.96	0.59	0.90	0.89	0.87	0.57	1.42	1.21	1.20
9km	0.24	0.45	1.46	1.02	0.50	1.24	1.53	1.16	0.40	2.72	2.52	2.50
3km	0.85	0.84	0.53	0.52	0.71	1.19	0.90	0.85	0.58	0.89	0.87	0.87
	0.84	0.92	0.66	0.56	0.33	1.08	1.30	1.21	0.28	1.09	1.32	1.26
1km	0.87	0.94	0.50	0.49	0.68	0.84	0.81	0.75	0.59	0.75	0.83	0.83
	0.84	0.98	0.63	0.56	0.34	0.92	1.22	1.11	0.33	0.98	1.16	1.14

No figures are presented for the time evolution and spatial distribution of temperature or wind differences between tests 4 and 3, because differences between the two tests results are minimal, with a maximum positive ΔT of 0.3°C in a confined area in Porto municipality. The differences in average daily means range from -0.4°C and +0.3°C; wind speed differences are irrelevant.

Once more, the limited number of meteorological stations in urban environments, namely for the 1 km resolution, does not allow the full assessment of possible benefits of using a higher urban roughness height value.

Next results from the sensitivity tests are compared.

5.2.5 Sensitivity tests inter-comparison

Results from the four MM5 sensitivity tests are now compared and analysed in order to select the most suitable model configuration. Figure 5.18 presents the summer episode temperature scatter diagrams and time series evolution of simulated and observed temperatures for Porto and Aveiro at 1 km resolution. Appendix E contains the same graphs for a selection of the remaining meteorological sites: Viseu and Braga (3 km resolution), and Lisboa and Faro (9 km resolution) (Figure E.9). In the case of overlapping of test 1 and test2 results, diagrams may not show the results for test1 (in violet) since these are underneath test2 results (in blue); the same is valid for test3 results (in orange) that can be found underneath test4 results (in green).

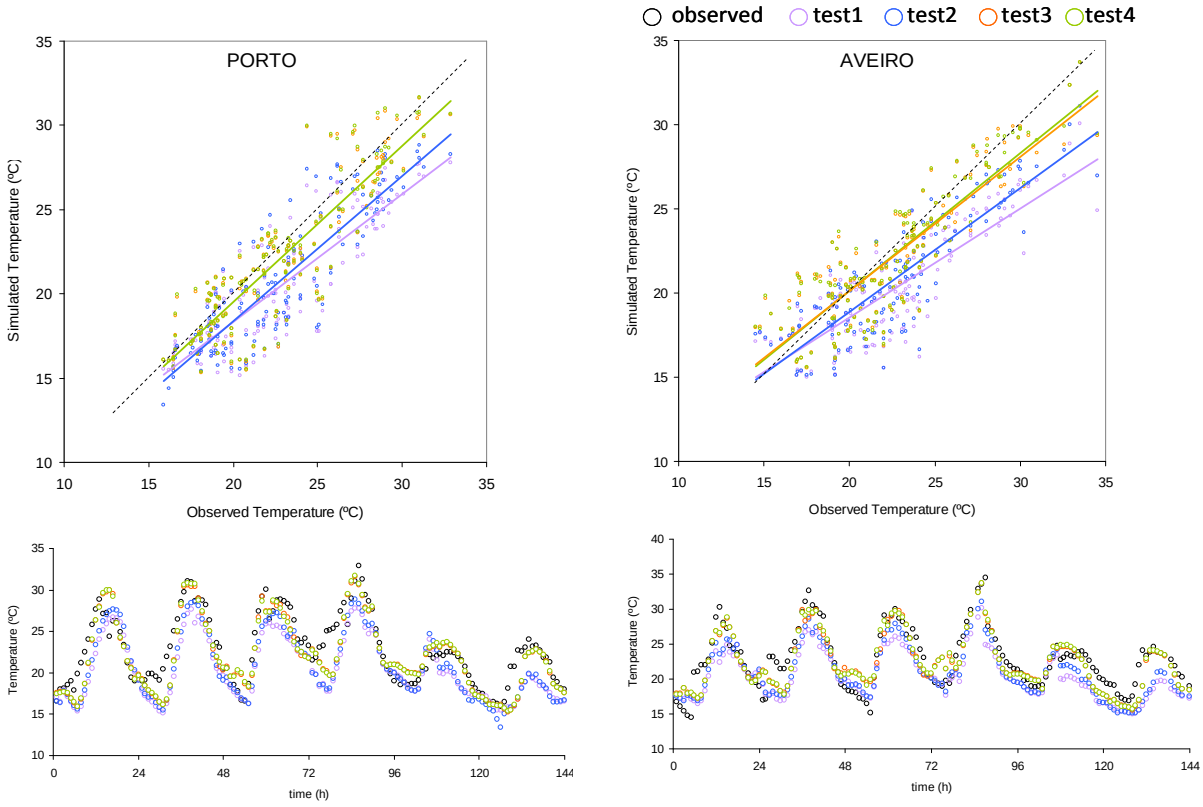

Figure 5.18 Scatter diagram of observed versus modelled temperature at Porto and Aveiro (1 km resolution), summer episode.

The first remark is that simulations can clearly be divided in two groups - simulations 1 and 2, and simulations 3 and 4. In general, tests 3 and 4 present the best results for all the analysed sites.

Temperature is almost always underestimated, and specially for higher temperatures; also higher differences between the four tests are found for higher temperatures. For Porto and Aveiro, test2 is clearly better than test1 due to the land use improvement; while Porto presents no differences between test3 and test4 (the meteorological station is located in a rural area), for Aveiro the last fits slightly better the observed values. Viseu and Braga do not present as good results as Porto and Aveiro, probably due to the lower resolution (3 km); tests 1 and 2 results are very similar with the last one slightly better, indicating that differences in land use datasets are bigger for the higher resolution (1 km). Lisboa and Faro simulated values are not so good due to the coarser resolution (9 km), for this reason also differences between tests 1 and 2 and between tests 3 and 4 are not perceivable.

The same graphs for winter are presented in Figure 5.19 (and E.10 in Appendix E). The analysis is similar to the one presented for the summer period, with the exception of Braga which presents an over-estimation of the winter episode temperatures. As observed previously, namely through the statistical analysis, winter results are not as good as summer results.

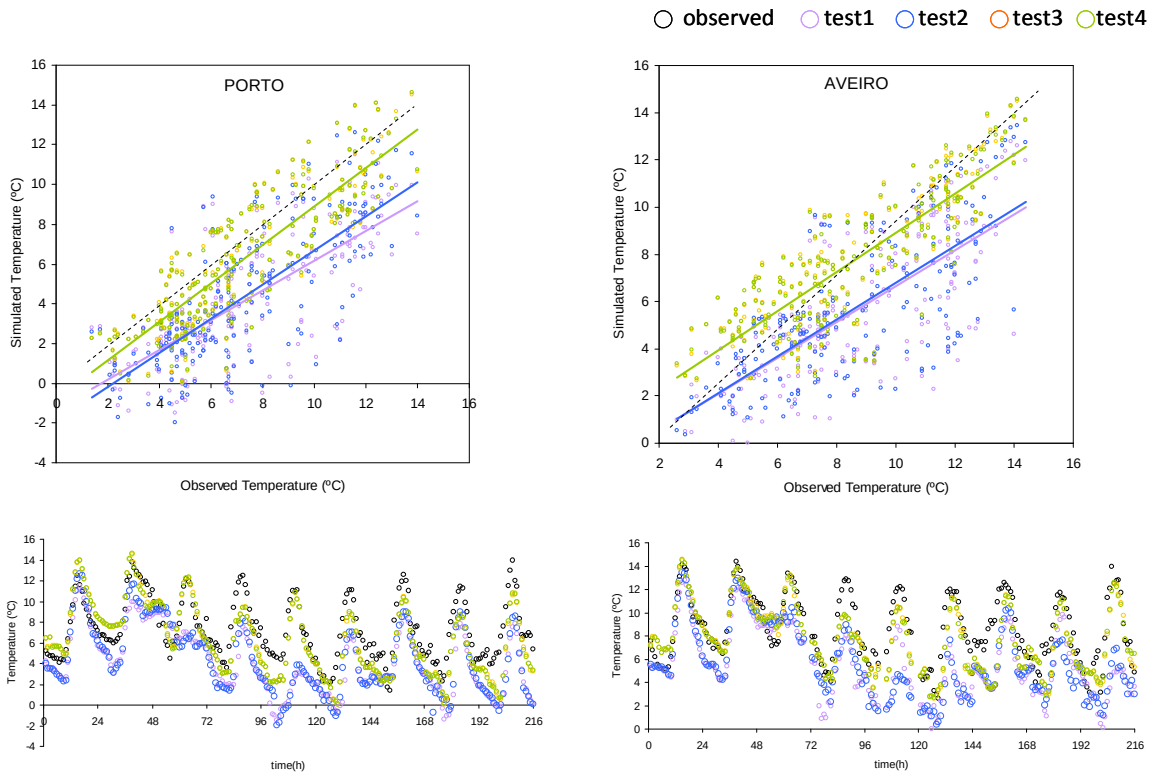

Figure 5.19 Scatter diagram of observed versus modelled temperature at Porto and Aveiro (1 km resolution), summer episode.

The inter-comparison continues with the graphical analysis of the statistical parameters (r, S/Sobs and Eub/Sobs) obtained for all meteorological sites; for the sites which have results for more than one resolution, only the best resolution(s) is(are) presented. Figure 5.20 presents the statistical parameters

calculated for temperature through the four sensitivity tests, for the studied episodes. Again, for the majority of sites, simulations can be divided in two groups - simulations 1 and 2, and simulations 3 and 4 – since statistics are very similar. Both episodes show better results for tests 3 and 4, with higher correlation factors, S/S_{obs} closer to 1 and smaller deviations (smaller E_{UB}/S_{obs}), for the majority of analysed sites. Also it is clear that differences between tests are higher for the winter episode.

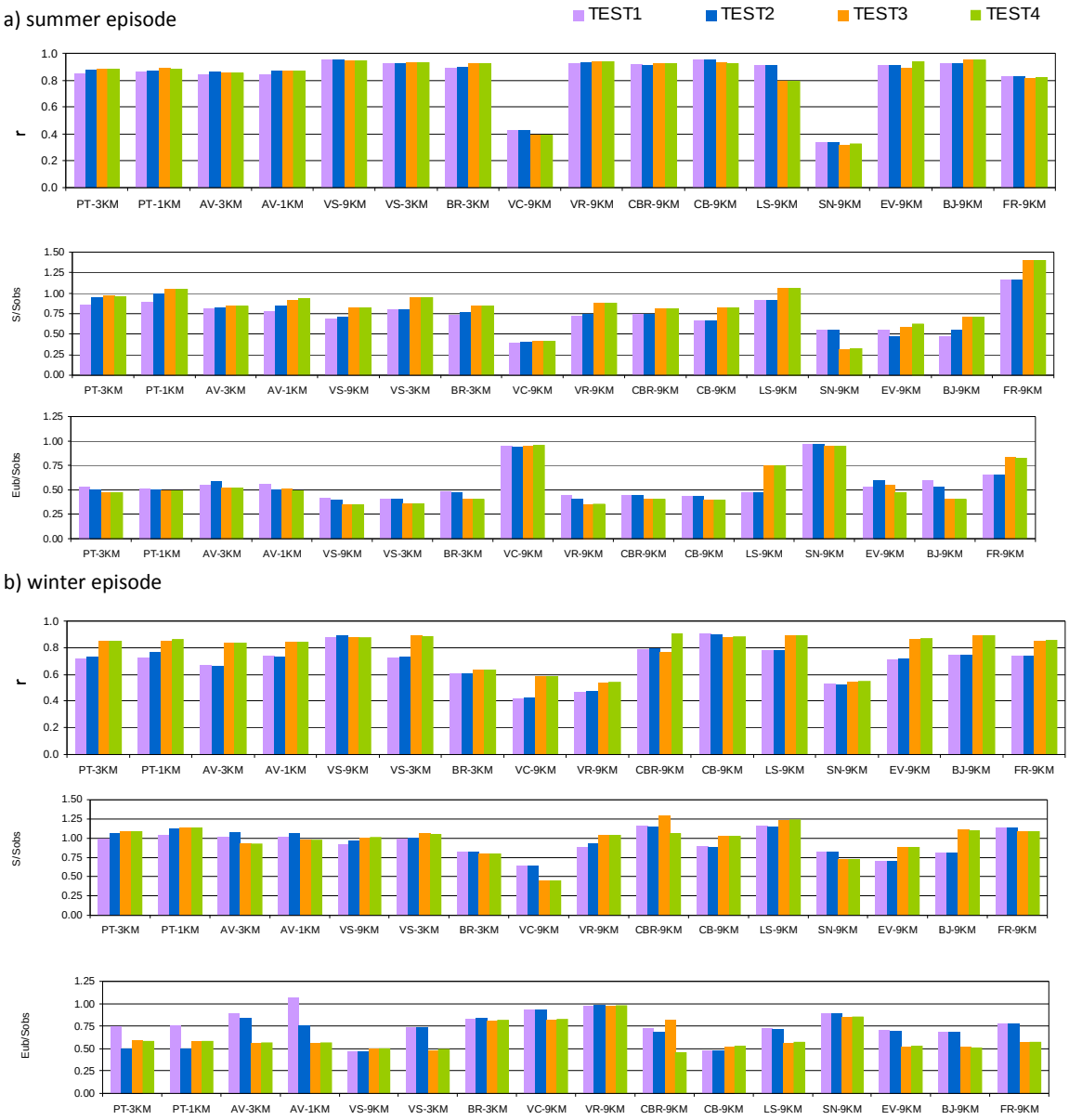

Figure 5.20 Sensitivity tests statistical comparison for temperature, for the a) summer episode and b) winter episode.

Figure 5.21 presents the statistical parameters the wind components, for the summer episode. The statistical parameters r and Eub/S_{obs} present higher skills for simulations 1 and 2; the parameter S/S_{obs} is not conclusive since there is a clear equilibrium between the two simulation groups. For Porto

meteorological station in particular tests 3 and 4 present better results for *u*, while test2 is the best for *v*. For Aveiro, however test2 presents the best results for both wind components.

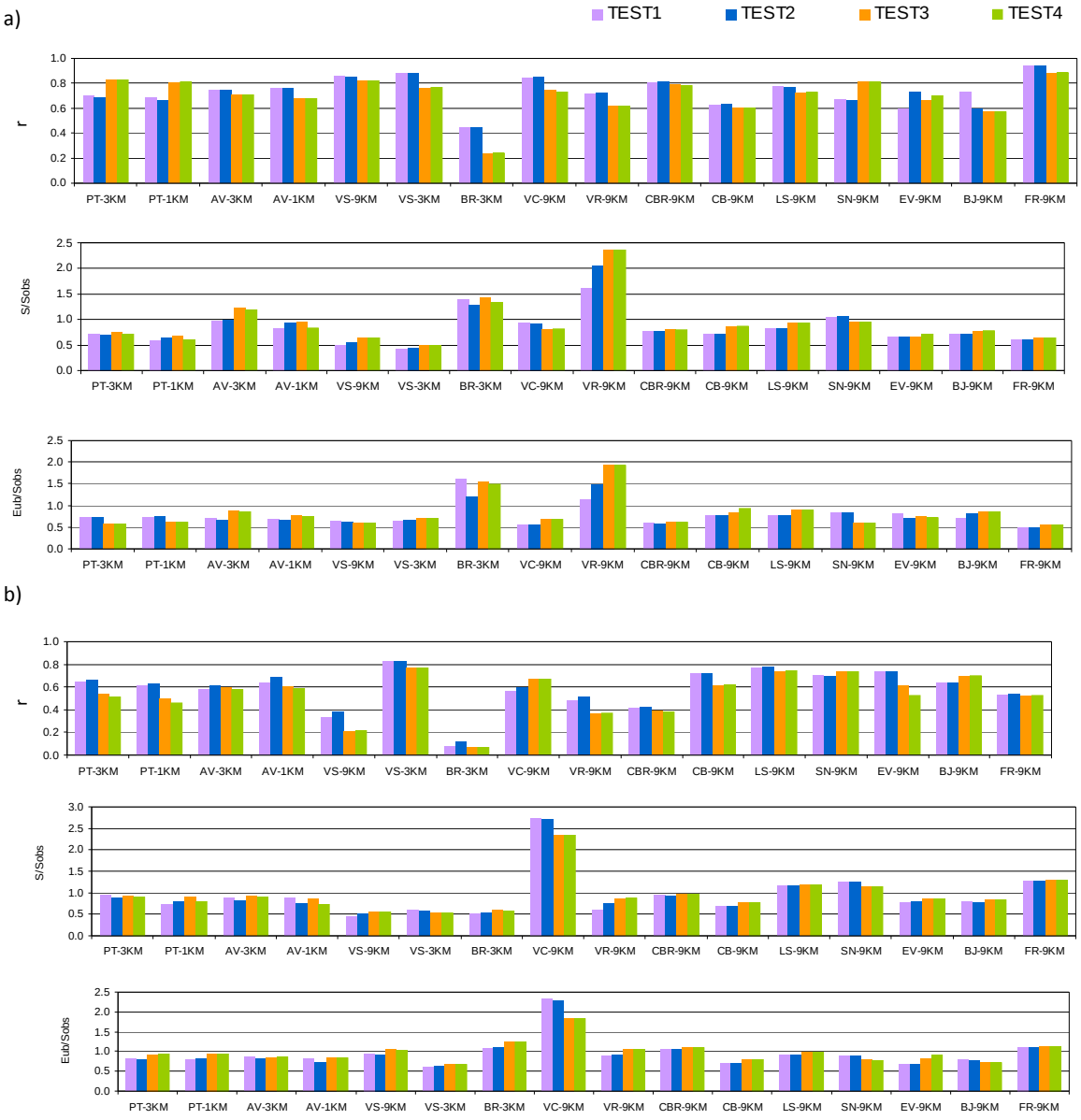

Figure 5.21 Sensitivity tests statistical comparison for a) *u* and b) *v*, for the summer episode.

Figure 5.22 presents the same for the winter episode; in this case the general statistical analysis is inconclusive. For Porto test3 results are the best for *u*, while for *v* it is not possible to draw any conclusion.

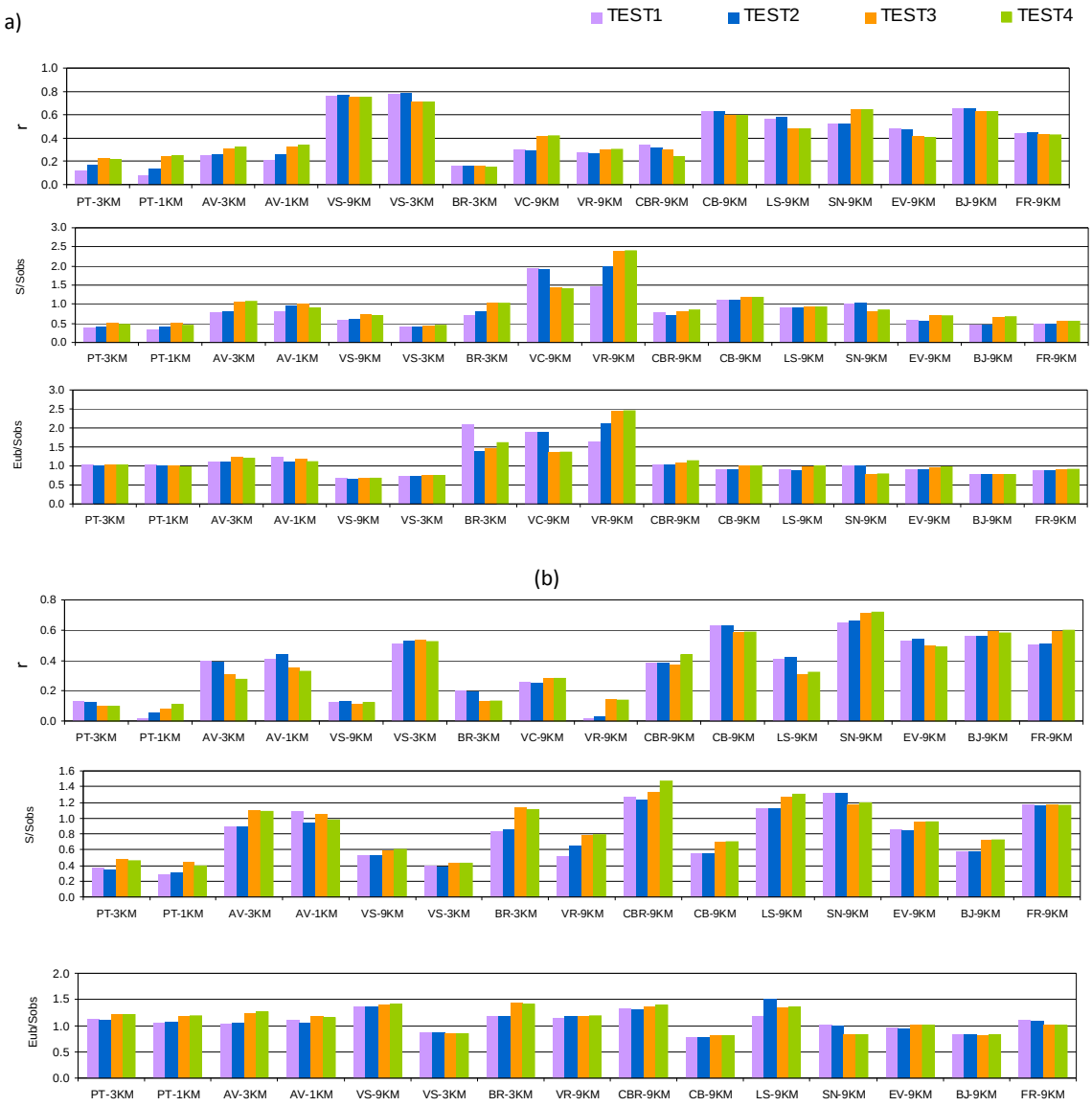

Figure 5.22 Sensitivity tests statistical comparison for a) *u* and b) *v*, for the winter episode.

Although the different tests yield distinct results for temperature and wind, especially for the thinner resolution, it is not possible to clearly identify the most adequate configuration. For temperature the best results are obtained with simulations 3 and 4; for wind components the best summer results are those from test2, and the winter episode is not conclusive. One of the reasons for the impossibility of choosing the best configuration concerns the reduced number of meteorological stations in the study area, namely in Porto; it was shown that differences between the tests are more significant when the simulation had a higher resolution. Therefore the choice is postponed to the following section, where the MM5 outputs are tested as CAMx inputs, and results for air pollutants concentrations are analysed to select the most well suited meteorological model configuration.

5.3 Air quality modelling setup

The skill of an air quality simulation depends on several factors, among which meteorological conditions, including meridional and zonal wind components, temperature, water vapour mixing ratio, surface pressure, solar radiation, cloud fraction, precipitation, boundary layer height, and turbulence are known to have direct impact on the simulation [Seaman, 2000]. Sensitivities and uncertainties in air quality modelling arise when gridded meteorological fields are generated by mesoscale atmospheric models using different physics and parameterizations, and spatial and temporal resolutions [Pielke and Uliasz, 1998].

Here, the CAMx reference-setup is described, and its sensitivity to the different MM5 inputs is analysed, in order to select the most suited MM5 configuration, i.e., the MM5 configuration that yields better air quality results. The results from CAMx simulations are evaluated against each other, but also against data from a group of air quality stations. Hourly data for particulate and gaseous species from the Northern Region Air Quality Network, for the periods 3-8 June and 16-24 December, were downloaded from the Air quality database website [URL13], to be used in the CAMx performance evaluation. The air quality monitoring network of the Northern region has already been presented in chapter 4 (Table 4.3). The air quality stations selected for the validation procedure include those located in CAMx domain 3 (over Porto urban area, with 1 km^2 resolution), i.e., those belonging to Coastal Porto agglomeration, with available data for the periods under study.

Hanna *et al.* [1993] recommend a group of statistical parameters that have been adopted as a reference method in the European Union for air quality models evaluation [Olesen, 2001]. Among the group, three main parameters, which have been used in a variety of studies [Borrego *et al.*, 2008a], were selected for a quantitative error analysis - the correlation coefficient (r), the mean quadratic error (MQE) and the bias (BIAS):

$$r = \frac{\sum_{i=1}^{n}\left(C_{obs\,i} - \overline{C}_{obs}\right)\left(C_{\mathrm{mod}\,i} - \overline{C}_{\mathrm{mod}}\right)}{\sqrt{\sum_{i=1}^{n}\left(C_{obsi} - \overline{C}_{obs}\right)^2 \sum_{i=1}^{n}\left(C_{\mathrm{mod}\,i} - \overline{C}_{\mathrm{mod}}\right)^2}}$$

$$MQE = \frac{1}{n}\sqrt{\sum_{i=1}^{n}\left(C_{obsi} - C_{\mathrm{mod}\,i}\right)^2}$$

$$BIAS = \frac{1}{n}\sum_{i=1}^{n}\left(C_{obsi} - C_{\mathrm{mod}\,i}\right)$$

where: n is the total number of sample pairs, C_{obsi} is the observed value at time i and C_{modi} is the respective simulated concentration. These three parameters offer complementary information: the correlation factor (r) translates the linear relation between concentrations, reflecting a better or worst

reproduction of physical and chemical atmospheric processes; MQE and BIAS give an indication of the deviation between observed and simulated concentrations, either in absolute (MQE) or in systematic terms (BIAS), allowing the inference of the magnitude and trend of the errors, respectively. For both the ideal value is zero.

These three parameters will be used for O_3 and PM10 results evaluation. For ozone, additional quality indicators given by the USEPA for the evaluation of photochemical models [USEPA, 1991] are used, namely the mean normalized bias error (MNBE), the mean normalized gross error (MNGE), and the unpaired peak prediction accuracy (UPA):

$$MNBE = \frac{1}{n}\sum_{i=1}^{n}\frac{C_{\mathrm{mod}}(x,t) - C_{obs}(x,t)}{C_{obs}(x,t)}$$

$$MNGE = \frac{1}{n}\sum_{i=1}^{n}\frac{\left|C_{\mathrm{mod}}(x,t) - C_{obs}(x,t)\right|}{C_{obs}(x,t)}$$

$$UPA = \frac{C_{\mathrm{mod}}(x,t)_{\max} - C_{obs}(x,t)_{\max}}{C_{obs}(x,t)_{\max}}$$

where: $C_{mod}(x,t)$ is the modelled concentration in site x at time t, $C_{obs}(x,t)$ is the observed concentration in site x at time t, $C_{mod}(x,t)_{max}$ is the maximum model concentration in site x at time t, $C_{obs}(x,t)_{max}$ is the maximum observed concentration in site x at time t, and *n* is the number of monitoring sites.

Although there is no objective criterion set forth for a satisfactory model performance, US EPA suggested values of ±5–15% for MNBE, 15–20% for UPA, and 30–35% for MNGE, to be met by modelling simulations being used for regulatory applications [Hogrefe *et al.*, 2001].

5.3.1 CAMx reference setup

CAMx version 4.5.1., released in May 2008, was used for this study. The setup here described can be considered the reference since it corresponds to the configuration established in previous MM5-CAMx modelling system applications for Portugal [Ferreira *et al.*, 2003, 2004; Ferreira, 2007]. The chemical mechanism 4 (CB-IV with additional reactions, including aerosol chemistry) was used. The meteorological input data for CAMx is generated by the MM5 mesoscale model, through the MM5CAMx pre-processor made available by ENVIRON [URL17].

5.3.1.1 Initial and boundary conditions

The initial and boundary conditions used were defined based on the results from a study conducted by Carvalho [2005], and already used by Ferreira [2007], which defined fixed top concentrations for each month of the year, for a group of species of CBIV mechanism. The determination of monthly top

concentrations resulted from the treatment of historical air quality data, with the identification of the annual average pattern for each air quality station considered in the study Carvalho [2006].

5.3.1.2 Emissions processing

The 2005 National Emission Inventory [URL10] was used as the anthropogenic emission inventory for the 2006 episode simulations, since no data are available for the year of the simulations. The inventory was elaborated according to the CORINAIR methodology [EEA, 2006b], and groups the emissions by the activity sector. For modelling purposes, in the reference setup, anthropogenic emissions are treated separately in two groups: large point sources (industrial facilities with high production levels and high emission levels), and area sources (diffuse pollutant activities). The pollutants considered include NOx, NMVOC, CO, NH_3, PM10 and PM2.5.

Figure 5.23 presents the distribution of large point sources, their location in terms of municipality, and additional information such as the fuel used and the production process.

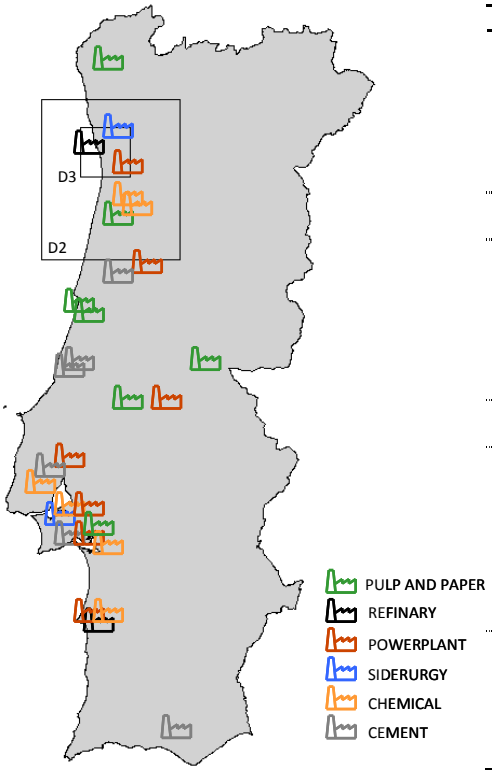

SOURCE TYPE	MUNICIPALITY	OBS.
PULP AND PAPER	AVEIRO	KRAFT
	CONSTÂNCIA	SULPHITE
	FIGUEIRA FOZ	KRAFT
	FIGUEIRA FOZ	SULPHITE
	SETÚBAL	KRAFT
	VIANA CASTELO	KRAFT
	VILA VELHA RODAO	KRAFT
REFINARY	MATOSINHOS	-
	SINES	-
POWER PLANT	ABRANTES	COAL
	ALENQUER	OIL/N.GAS
	BARREIRO	
	GONDOMAR	N.GAS
	MORTÁGUA	BIOMASS
	SETÚBAL	OIL
	SINES	COAL
SIDERURGY	MAIA	-
	SEIXAL	-
CHEMICAL	BARREIRO	UREA
	BARREIRO	PHOSPHATE
	ESTARREJA	PVC
	ESTARREJA	POLYURETHANE
	SETÚBAL	PHOSPHATE
	SINES	POLYETHYLENE
	SINES	CARBON BLACK
	VILA FRANCA XIRA	AMONIA
CEMENT	ALCOBACA	COAL
	COIMBRA	COAL
	LEIRIA	COAL
	LOULÉ	COAL
	SETÚBAL	COAL
	VILA FRANCA XIRA	COAL

Figure 5.23 Large point emission sources.

For the large point sources, 32 installations were considered at the national level according to the industrial processes: refineries, power plants, pulp and paper, cement and chemical products. Data requirements for these emission sources include the stack parameters (location, height and diameter) and the effluent parameters (output temperature and speed, flow and emissions) of all sources and all pollutants emitted (gaseous and particulate).

The National Inventory only contains annual totals. Because atmospheric modelling requires a higher temporal resolution, preferably hourly, further processing of the inventory was needed. In the reference setup, the inventory was processed through a program, AREA_EMIS, previously developed for the UAM-IV model [USEPA, 1990], with some changes and improvements introduced for CAMx: Those include the temporal resolution in order to consider 4 typical days (weekend and week, for summer and winter) and therefore build 4 typical emission grids [Ferreira, 2007]. The differences between these 4 typical days are given by different traffic profiles, obtained through traffic counting for Porto, in the frame of SAPHIRE project [Oliveira *et al.*, 2004].

Because chemical mechanisms contain a simplified set of equations that use representative ''model species'' to represent atmospheric chemistry [Dodge, 2000], it is necessary to supply the model with the species profiles, namely for NOx, NMVOC and PM. For the reference setup, the NMVOC speciation was processed according to Zlatev *et al.* [1993]; for NOx, a constant non-specific NO/NOX ratio of 0.9 has been assumed for all the categories; for PM2.5 the speciation profile considered an equal contribution from the three species considered (POA, PEC and FPRM). Table 5.9 presents the profiles used in the reference set-up; no category-specific profiles were used, meaning that a single profile was used for every emission source category.

Table 5.9 NMVOC and PM speciation profiles for the CAMx reference setup.

Compound class	Species	Profile
NMVOC	Parafines	0.57
	Toluene	0.153
	Xylene	0.123
	Formaldehyde	0.025
	Ethene	0.056
	Other aldehydes	0.004
PM10	CPRM – other coarse primary aerosol	(1-PM2.5)
PM2.5	POA – primary organic aerosol	0.33
	PEC – primary elemental carbon	0.33
	FPRM – other fine primary aerosol	0.34

For biogenic emissions a bottom-up approach is used. The methodology for Portugal was developed by Tchepel [1997], and requires the knowledge of the temperature, solar radiation and forest area density. For the CAMx simulations, biogenic emissions are given as isoprene and monotherpenes.

5.3.2 Results

This section presents the results of CAMx simulations using meteorological input data from the four MM5 sensitivity tests carried out previously, in order to check their influence on the air quality simulation outputs. The analysis of the results is presented for the summer and the winter episodes.

5.3.2.1 Summer episode

Table 5.10 presents statistical results for ozone for the summer episode, averaged for the air quality monitoring sites of the domain, for each of the simulation domains, with the best results highlighted in bold.

Table 5.10 CAMx reference setup statistical results obtained for ozone, summer episode.

	r	BIAS ($\mu g.m^{-3}$)	MQE ($\mu g.m^{-3}$)	MNBE (%)	MNGE (%)	UPA (%)
MM5 INPUT	Ozone 9 km resolution (D1)					
test 1	0.61	28.1	3.83	-8.9%	21.2%	-5.8%
test 2	0.65	**27.4**	**3.67**	**-8.6%**	**18.8%**	**-0.1%**
test 3	**0.66**	35.2	4.04	-32.6%	26.2%	-21.6%
test 4	**0.66**	35.2	4.03	-33.5%	27.0%	-25.8%
	Ozone 3 km resolution (D2)					
test 1	0.60	32.65	4.09	-35.7%	28.7%	-8.8%
test 2	**0.66**	**31.44**	**3.93**	**-31.7%**	**19.9%**	**-5.0%**
test 3	0.65	39.47	4.31	-48.8%	23.2%	-21.0%
test 4	0.65	39.46	4.31	-49.4%	23.5%	-26.1%
	Ozone 1 km resolution (D3)					
test 1	0.60	34.17	4.16	-42.6%	26.0%	-22.1%
test 2	**0.64**	**33.17**	**4.00**	**-33.4%**	17.9%	**-14.1%**
test 3	0.63	41.54	4.49	-51.8%	**14.1%**	-30.9%
test 4	0.63	41.57	4.49	-52.4%	14.4%	-34.5%
USEPA guidelines	-	-	-	± 5-15%	15-20%	± 30-35%

Results reveal that the highest correlation coefficients are obtained for MM5 test2 for the 1 km and 3 km resolutions, and for tests 3 and 4 for the 9 km resolution. The other statistical measures, however, are better for test2 for all simulation domains: lower biases, lower average errors and a better peak prediction accuracy. Comparing the obtained parameters with the USEPA guidelines: all the simulations meet the UPA criteria; the MNBE criteria are met only for test1 and test2 9 km resolution; and for MNGE, test2 meets the criteria for every resolution. The positive biases, and the negative normalized biases, obtained with any MM5 output and for all resolutions reveals that O_3 is under-predicted. The analysis also indicates that the best over all results are obtained for the 9 km resolution: although correlation coefficients are not very different among resolutions, biases and errors are smaller for this resolution. This is not an outcome of the meteorological inputs since the MM5 performance increased significantly for the 3 km and 1 km resolutions when compared to the 9 km resolution. Hence, a possible explanation could be related with the current spatial allocation of emissions, revealing that the higher the resolution the lower the accuracy of the emissions disaggregation.

Figure 5.24 presents the graphical analysis of the statistical parameters (r, BIAS and MQE) for each air quality monitoring site for the 1 km resolution, for ozone.

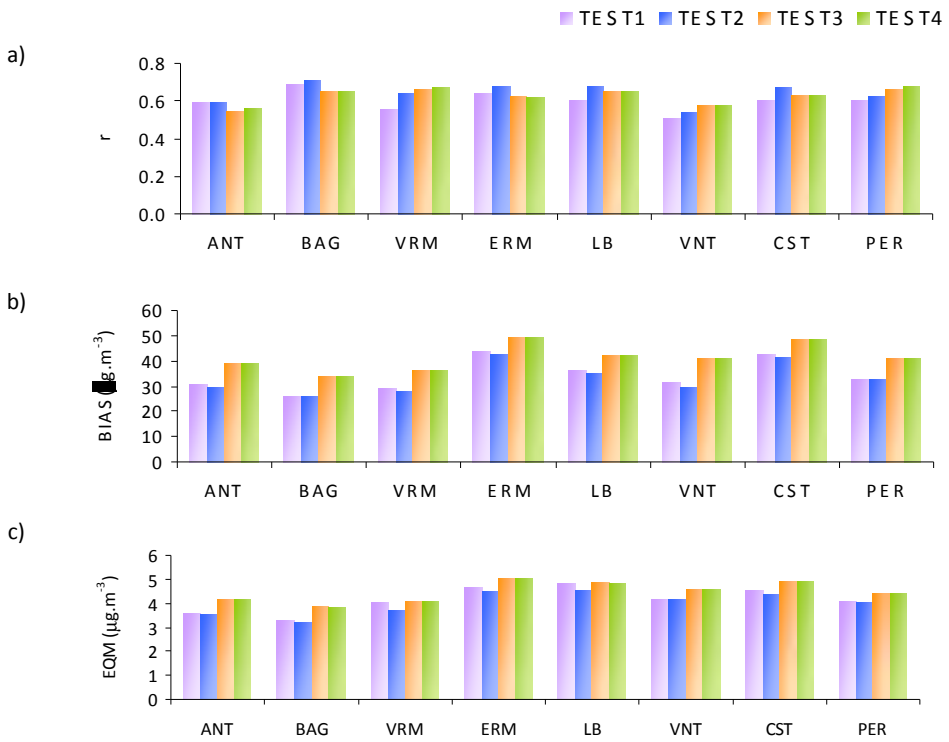

Figure 5.24 CAMx reference statistical results for ozone for the 1 km simulation (D3) a) r, b) BIAS, and c) MQE, for the summer episode.

Regarding the correlation coefficient, the highest values are generally obtained for test2, with the exception of Vermoim, Vila Nova da Telha and Perafita, for which tests 3 and 4 are better. The BIAS and MQE are smaller for test2 for all sites, with tests 3 and 4 presenting considerably worse results. No different tendency was detected between traffic (VRM, ANT, BAG), background (VNT, ERM, LB) and industrial (CST, PER) stations.

As an example of the spatial distribution of concentrations, Figure 5.25 shows the O_3 and NO_2 concentration fields obtained for the 06.06.06, from 12:00 to 15:00 (a period for which some of the highest ozone concentrations were observed) using MM5 test2 results as input for CAMx, for the 1 km resolution (D3); the coloured circles represent the concentrations observed in the air quality monitoring sites. From the figure, the ozone underestimation is clear mainly because of the misallocation of the ozone plume: where the monitored concentrations are showing higher values (such as Antas, Baguim and Ermesinde at 12:00) the simulation yields lower concentrations. Looking at the NO_2 concentration fields, it is also evident that while the simulation shows higher values in Matosinhos municipality, the monitored values are higher in Porto. The misallocation of NO_2 emissions, as well as the use of inadequate time profiles, can therefore help to explain the misallocation of the ozone plume.

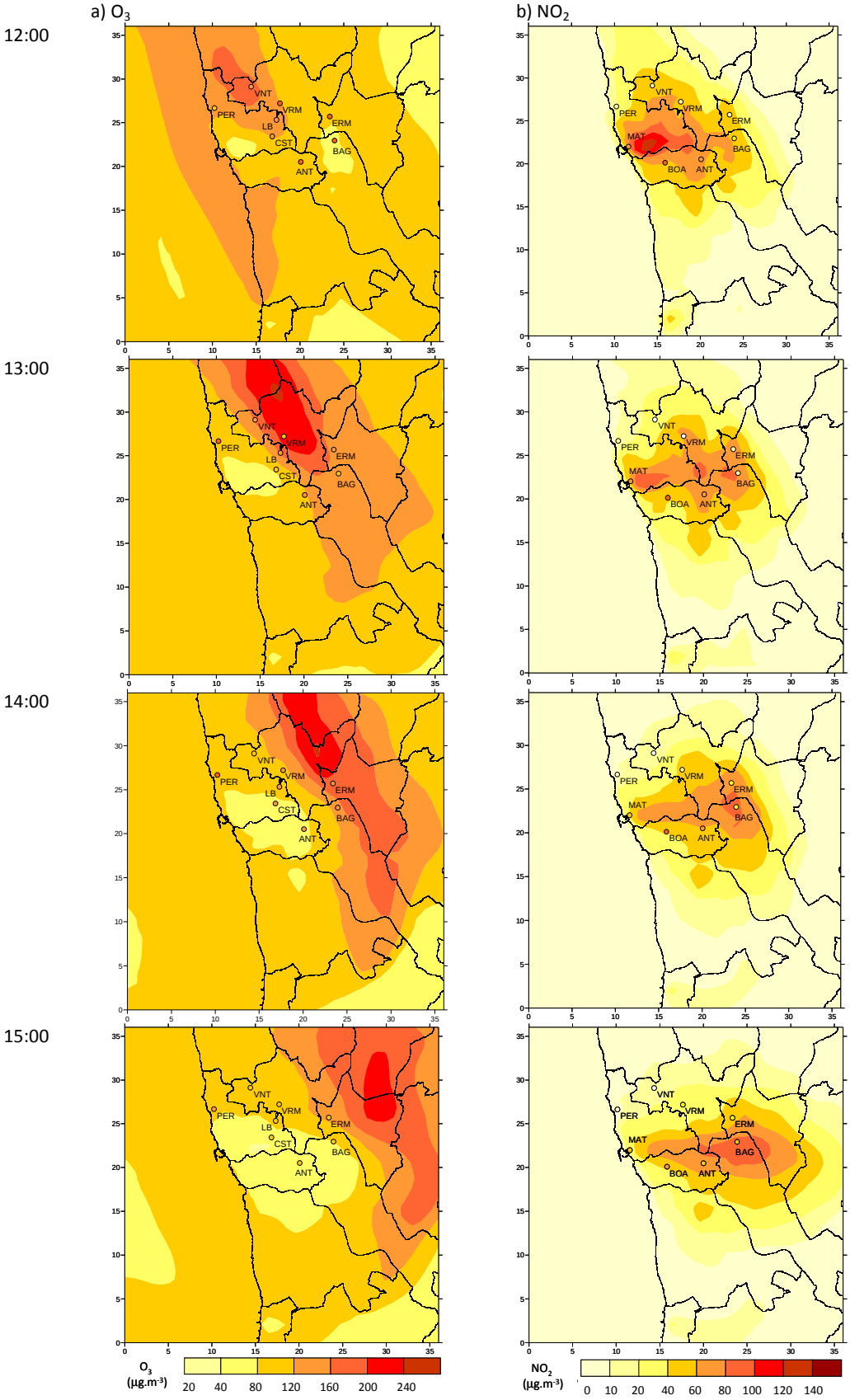

Figure 5.25 O_3 and NO_2 concentration fields (µg.m^{-3}) for 06.06.06, using test2 MM5 inputs, D3 (1 km resolution).

Table 5.11 shows the statistical results for PM10, averaged for the air quality monitoring sites of the domain, for the summer episode, for each of the simulation domains, considering hourly values.

Table 5.11 CAMx reference setup statistical results obtained for PM10, summer episode.

MM5 INPUT	r	BIAS ($\mu g.m^{-3}$)	MQE ($\mu g.m^{-3}$)	r	BIAS ($\mu g.m^{-3}$)	MQE ($\mu g.m^{-3}$)	r	BIAS ($\mu g.m^{-3}$)	MQE ($\mu g.m^{-3}$)
	PM10 – 9 km resolution (D1)			PM10 – 3 km resolution (D2)			PM10 – 1 km resolution (D3)		
test 1	0.19	23.5	2.71	0.17	22.2	2.76	0.16	21.3	2.80
test 2	**0.22**	21.5	**2.61**	**0.21**	20.5	**2.72**	**0.22**	19.3	**2.67**
test 3	**0.22**	**18.0**	2.62	0.18	**15.5**	2.91	0.17	**13.6**	2.97
test 4	0.21	18.3	2.63	0.17	15.8	2.93	0.16	14.0	3.01

Results show very low correlation coefficients, probably due to the use of inappropriate hourly emission profiles and a inadequate spatial distribution of emissions. The best correlations are those obtained with test2; the lowest BIAS are calculated with test3 and the lowest MQE with test2. The positive biases obtained for all MM5 outputs and for all resolutions indicate that PM10 is under-predicted. In opposition to what happened for ozone, the analysis does not reveal a better over all resolution, with the 9 km and 1 km resolutions presenting similar statistics.

Figure 5.26 presents the graphical analysis of the statistical parameters (r, BIAS and MQE) for each site for the 1 km resolution and the summer episode.

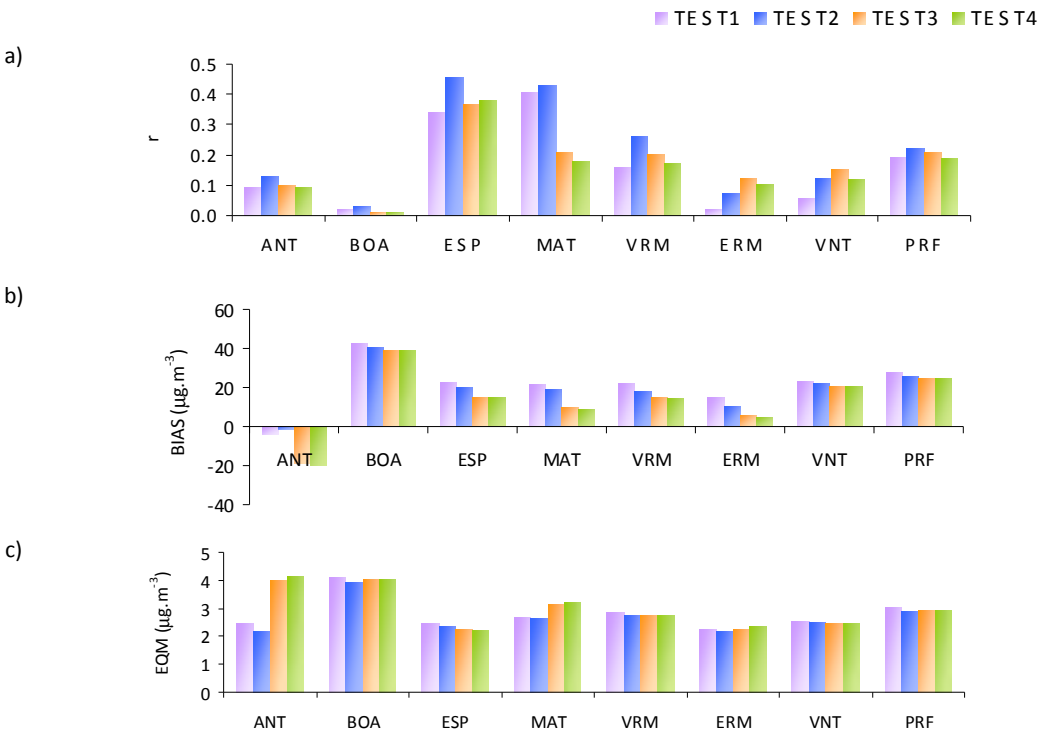

Figure 5.26 CAMx reference setup statistical results for PM10 for the 1km simulation (D3) a) r, b) BIAS, and c) MQE, for the summer episode.

Regarding the correlation coefficient, the highest values are obtained for Espinho and Matosinhos, two traffic stations; test2 presents the best results , with tests 3 and 4 presenting better skills only for two sites (Vila Nova da Telha and Ermesinde). The obtained BIAS is positive for all stations and lower for tests 3 and 4, except for Antas. Test2 can be identified as the best regarding the mean quadratic error.

To conclude the analysis for the summer episode, Figure 5.27 presents the PM10 daily average concentration fields, calculated using as meteorological inputs test2 and test3 MM5 results, for domain 3 (1 km resolution). The circles represent the concentrations measured in the air quality monitoring sites.

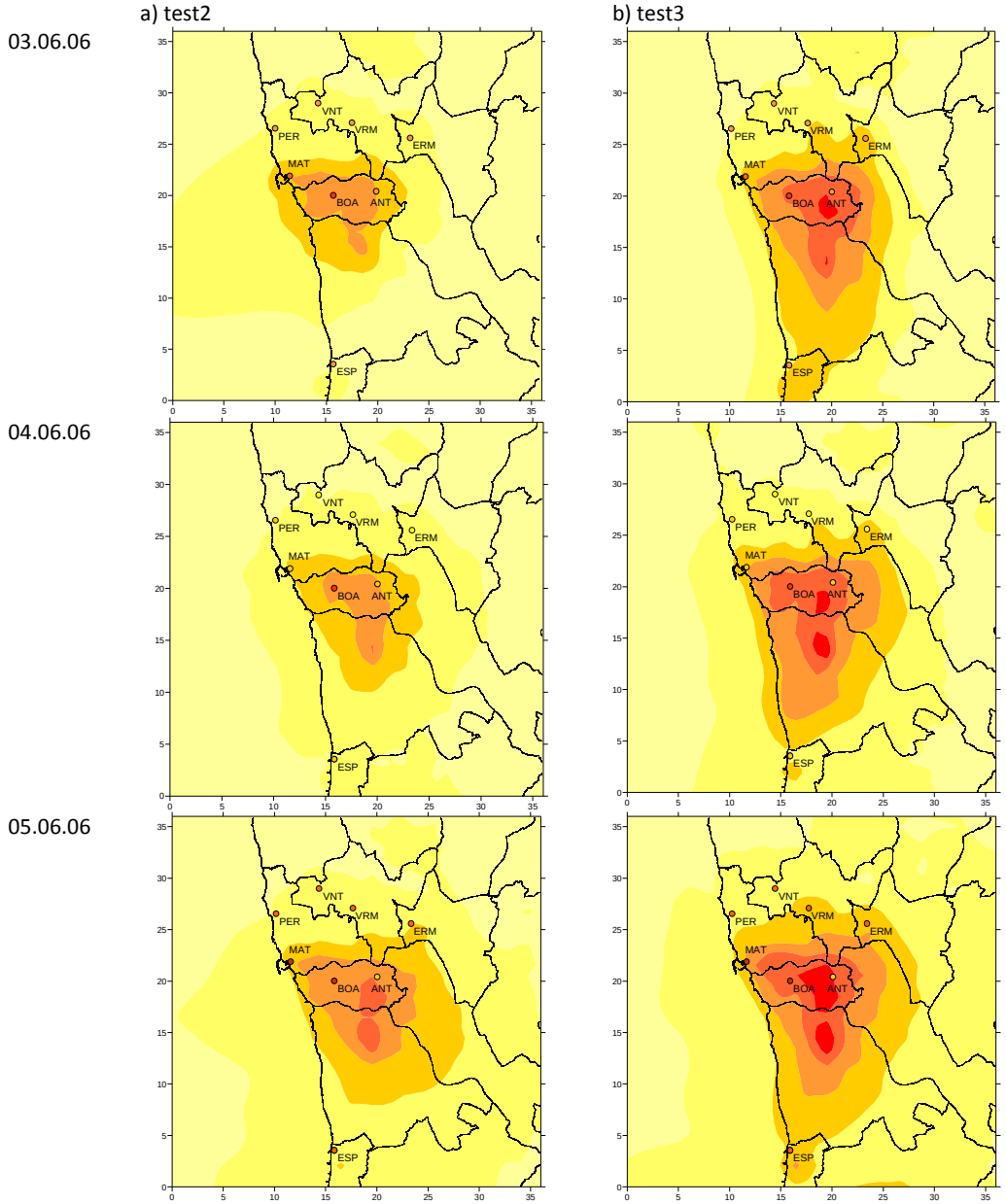

Figure 5.27 PM10 daily average concentration fields (µg.m^{-3}) for the summer episode, using a) test 2 and b) test 3 MM5 inputs, D3 (1 km resolution).

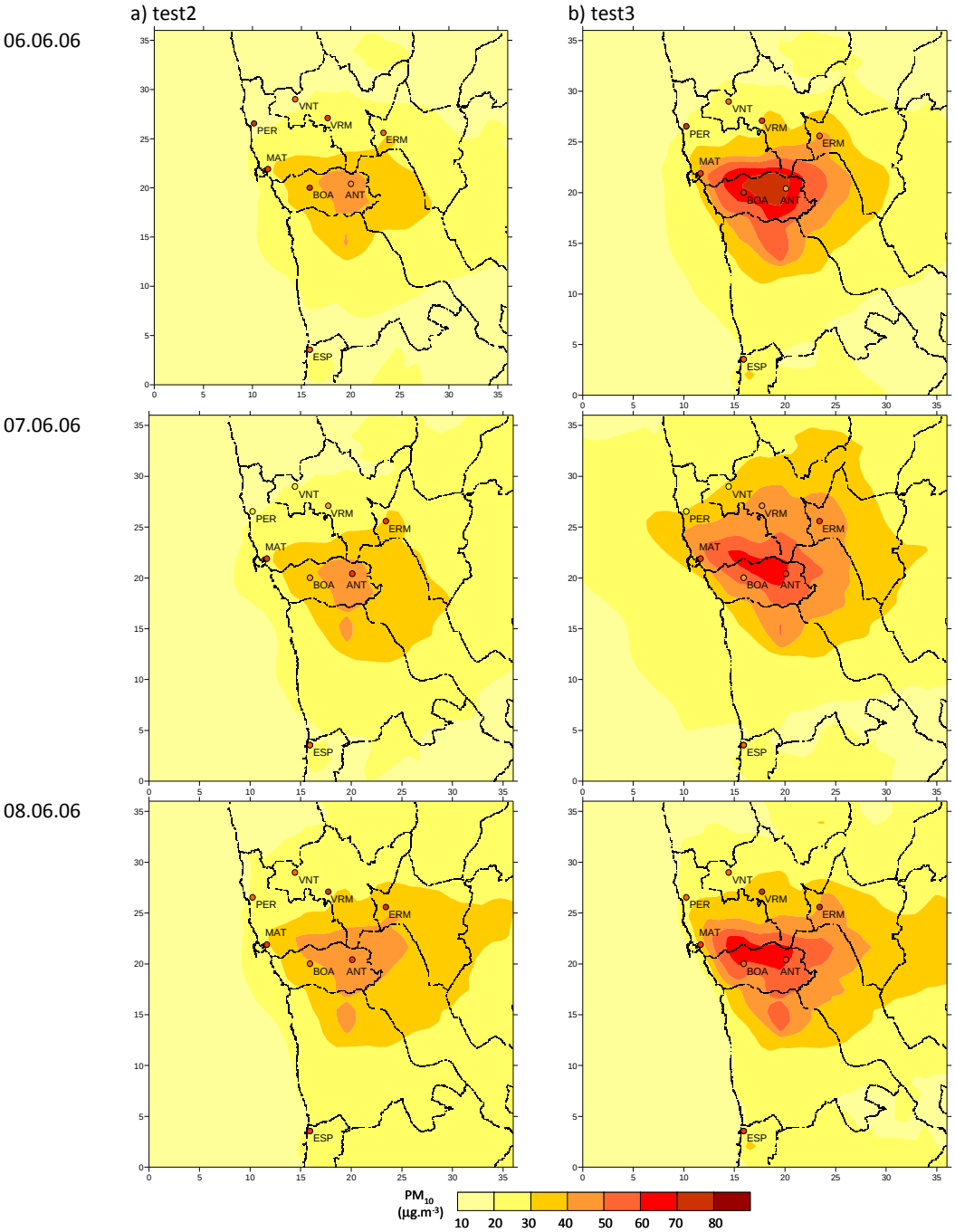

Figure 5.27 (cont.) PM10 daily average concentration fields (µg.m^{-3}) for the summer episode, using a) test 2 and b) test3 MM5 inputs, D3 (1 km resolution).

The shape of the PM10 plume is very similar for the two tests, however test3 presents higher PM10 concentrations over the entire simulation domain, which results in a better performance over certain sites, such as Boavista, Matosinhos, Ermesinde and Vermoim, and in a worst performance over Antas. Both tests fail to capture the high concentrations registered in the NW part of the domain; the PM10 plume seems to be displaced towards SE.

From the above, and for the summer episode, it is not easy to identify the best MM5 configuration for PM10 concentrations simulations, since test2 presents the greatest number of higher statistical skills but test3 seems to better spatially represent PM10 concentrations over Porto. However, test2 was clearly identified as the best MM5 configuration for ozone concentrations reproduction. Therefore, and in conclusion, test2 is identified as the most suitable MM5 configuration for the summer episode air quality simulations.

5.3.2.2 Winter episode

For the winter episode, only the results for PM10 are presented since in this period no considerable ozone concentrations were observed (hourly maximum of 70 $\mu g.m^{-3}$). Table 5.12 presents the statistical results for PM10, averaged for the air quality monitoring sites of the domain, for the winter episode, for each of the simulation domains, considering hourly values. Results reveal higher correlation coefficients in comparison to those obtained for summer, the best for tests 3 and 4. For the other statistical measures the best option is not clear, however tests 2 and 3 are the ones with a greater number of higher skills. In general, tests 1 and 2 present a positive bias, indicating an under-prediction of PM10 concentrations, on the other-hand, tests 3 and 4 tend to over-predict PM10.

Table 5.12 CAMx reference setup average statistical results obtained for PM10, winter episode.

MM5 INPUT	r	BIAS ($\mu g.m^{-3}$)	MQE ($\mu g.m^{-3}$)	r	BIAS ($\mu g.m^{-3}$)	MQE ($\mu g.m^{-3}$)	r	BIAS ($\mu g.m^{-3}$)	MQE ($\mu g.m^{-3}$)
	PM10 9 km resolution (D1)			PM10 – 3 km resolution (D2)			PM10 – 1 km resolution (D3)		
test 1	0.19	11.2	3.2	0.21	6.8	3.5	0.20	4.9	4.13
test 2	0.22	9.4	**3.1**	0.24	6.8	**3.4**	0.24	**4.2**	4.06
test 3	**0.36**	**0.1**	3.6	**0.35**	**-4.6**	4.2	**0.33**	-8.2	**3.4**
test 4	**0.36**	-0.7	3.6	**0.35**	-5.2	4.3	**0.33**	-8.5	3.5

Figure 5.28 presents the graphical analysis of the statistical parameters (r, BIAS and MQE) obtained for each site, for the 1 km resolution. The correlation factor is higher for tests 3 and 4 for all stations; regarding the BIAS and MQE it is not easy to identify the best option, but tests 3 and 4 seem to yield better scores. It is worth mentioning the high negative biases obtained for Antas and Boavista traffic sites, located in Porto municipality, indicating a significant over-prediction of PM10 concentrations for all tests.

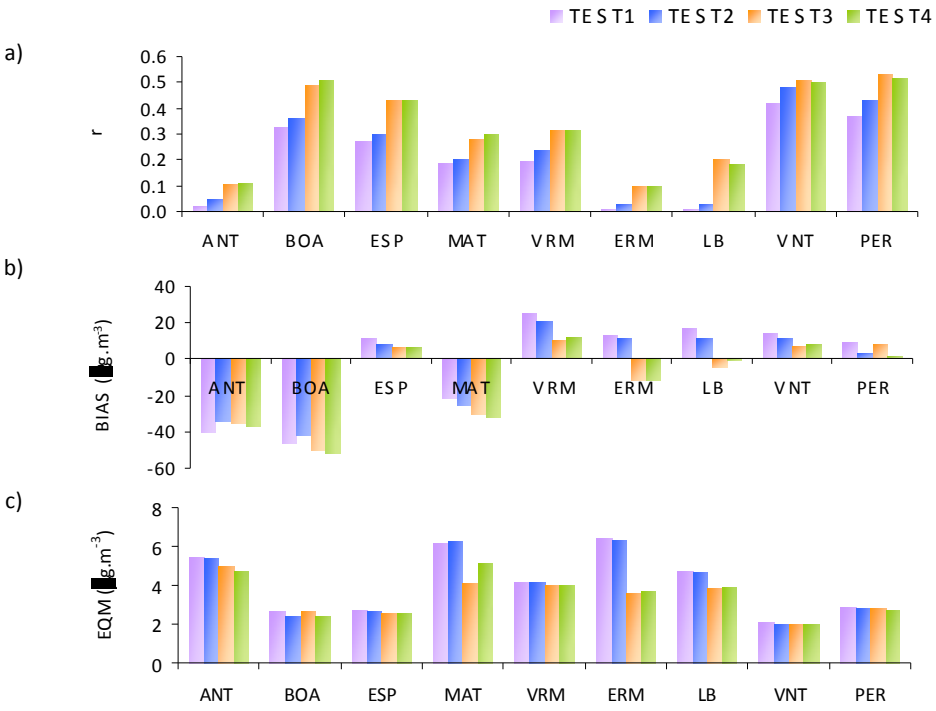

Figure 5.28 CAMx statistical results for PM10 for the 1 km simulation (D3) a) r, b) BIAS, and c) MQE, for the winter episode.

Figure 5.29 shows the PM10 daily average concentration fields for the winter episode, using tests 2 and 3 MM5 outputs as input for CAMx, for domain 3 (1 km resolution). Test3 yields higher PM10 concentration in comparison with test2, which has different implications in the model performance depending on the site that is analysed: in general, test2 is the best representing the PM10 daily average for Porto and Boavista; for the greatest part of the remaining monitoring sites, however, test3 better represents the high daily averages monitored, which test2 is not able to simulate.

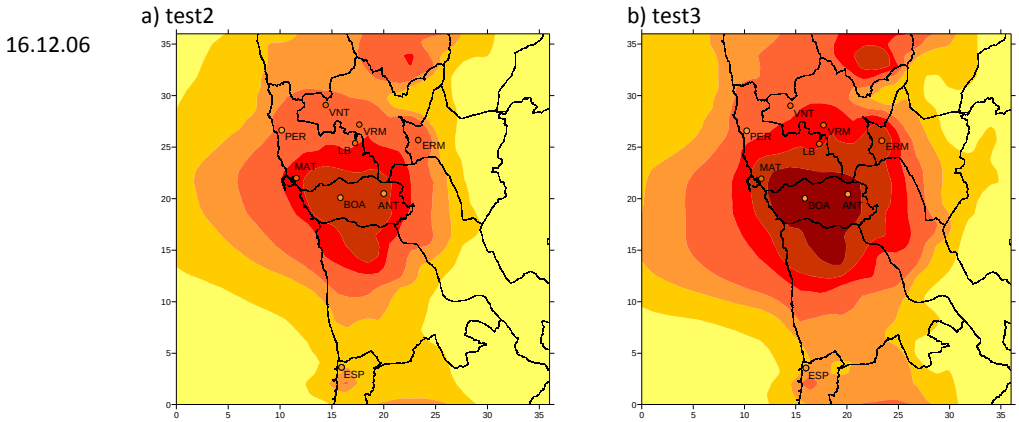

Figure 5.29 PM10 daily average concentration fields (µg.m^{-3}) for the winter episode, using a) test 2 and b) test 3 MM5 inputs, D3 (1 km resolution).

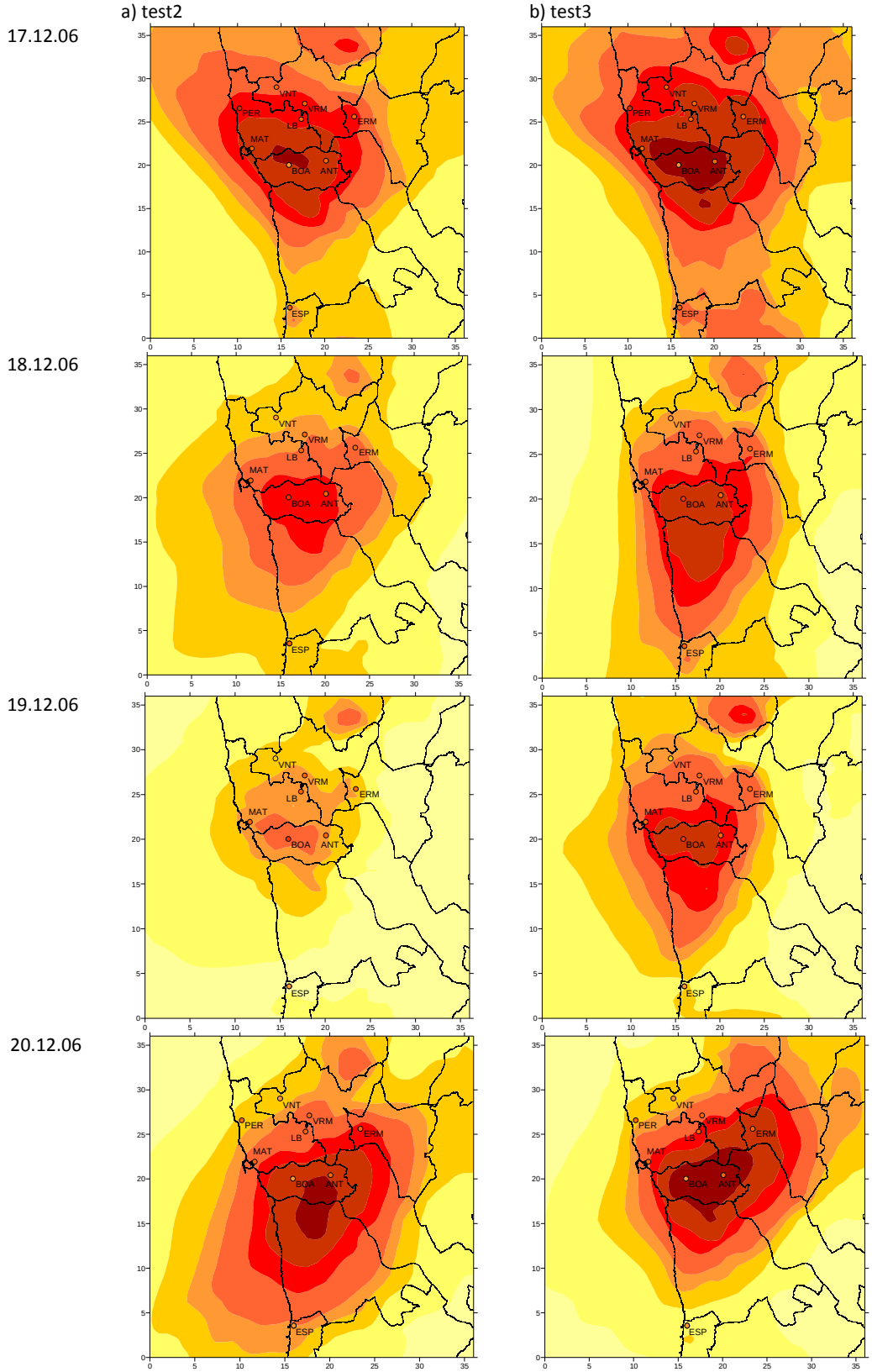

Figure 5.29 (cont.) PM10 daily average concentration fields (µg.m^{-3}) for the winter episode, using a) test 2 and b) test 3 MM5 inputs, D3 (1 km resolution).

a) test2 b) test3

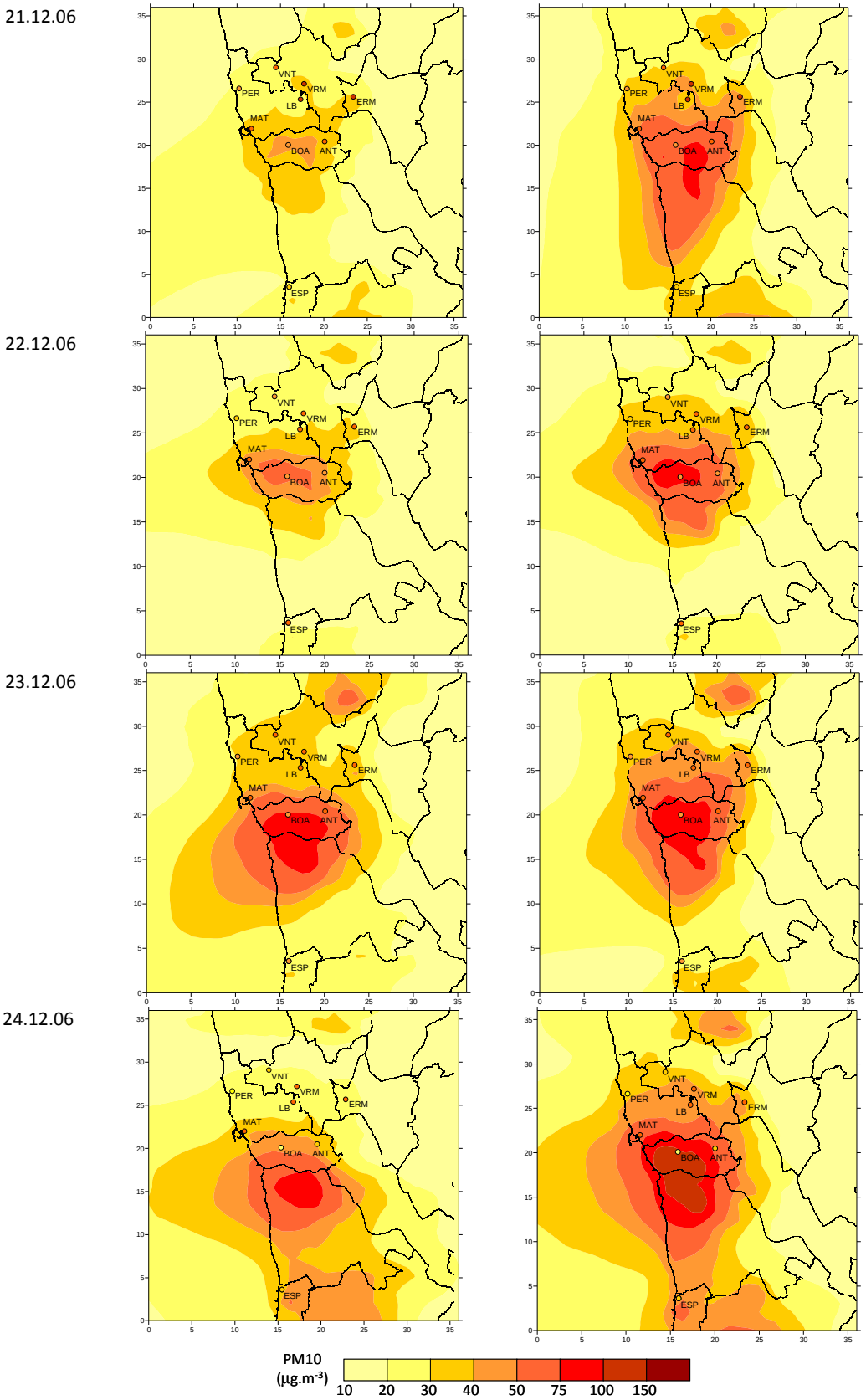

Figure 5.29 (cont) PM10 daily average concentration fields (µg.m^{-3}) for the winter episode, using a) test 2 and b) test 3 MM5 inputs, D3 (1 km resolution).

From the above analysis, test3 seems to be the most suitable MM5 configuration for the simulation of the winter episode PM10 levels, since it better represents the observed concentrations.

5.4 Final remarks

The results of the MM5 sensitivity tests were analysed and provided no clear conclusion about the most suitable meteorological model configuration. Next, MM5 outputs were fed to CAMx model and output concentrations were compared among each other and with observed O_3 and PM10 values. Different conclusions were then drawn for each episode and pollutant. In the summer period, test2 provided the best results for the simulation of ozone levels. For PM10 test2 also presented higher correlation factors and smaller errors, test3 however, produced smaller deviations, appearing to better represent spatial PM10 concentrations. For the winter episode, test3 provided the highest PM10 concentration correlations and the smaller errors and deviations, as a result of the better meteorological results obtained with Gayno-Seaman PBL scheme.

From the above it is decided that test2 shall be the MM5 configuration for the simulation of summer months (April to September) and test3 the configuration for the winter period (January to March, and October to December).

However, it is considered that modelling results should be improved, namely the correlation factors obtained for PM10 (in the order of 0.20 and 0.40, for the summer and winter episodes respectively), and the deviations for ozone (30 - 40 $\mu g.m^{-3}$). Therefore, a set of improvements and developments has implemented in the air quality model, before its application to the study case; this is the subject of the next chapter.

6 IMPROVEMENT OF THE URBAN AIR QUALITY MODELLING CONFIGURATION

Air quality models are subject to uncertainty resulting from inaccuracies in the meteorological inputs, as addressed in the previous chapters, as well as from parameterizations and approximations embedded in the model algorithms and chemical mechanisms, and uncertainties in emissions [Hanna *et al.*, 1998; Mallet and Sportisse, 2006; Appel *et al.*, 2007]. Emission inventories are crucial ingredients to successfully simulate atmospheric pollutants concentrations, although including substantial uncertainties related to the spatial and temporal allocation of emissions, as well as the chemical speciation [Mao *et al.*, 2006; Monteiro *et al.*, 2007b; Webster *et al.*, 2007].

In this chapter, the steps taken to improve the urban air quality modelling system performance for the study case are described. The developments introduced include the refinement of the spatial distribution of emissions, taking into account the new land use dataset for the region, and the consideration of region-specific temporal profiles and chemical speciation profiles. These developments result in the creation of a new emission pre-processor.

The outcome of this process is an improved MM5-CAMx configuration, to be applied in the study-case.

6.1 Initial and boundary conditions

A three-dimensional air quality model contains a set of differential equations, which are approximated and then solved to obtain the concentrations of a set of chemical constituents in time and space. Solving these differential equations, however, requires initial conditions (IC) and boundary conditions (BC) to be defined for all constituents [Liu *et al.*, 2001; Jiménez *et al.*, 2007; Samaali *et al.*, 2009]. IC are specified within the simulation domain at the beginning of simulation, while BC are prescribed throughout the simulation period.

Either observations or predictions from a larger-scale air quality model can be used to determine the chemical IC and BC values that are needed. In principle observations are preferred, but in practice it is

difficult or impossible to obtain measurements for all of the required species with the spatial and temporal resolution required by air quality models. This leads to uncertainties in the chemical IC and BC used (e.g., temporal non-representativeness, spatial interpolation errors), which then affect the model predictions [Berge *et al.*, 2001].

IC influence has been found to be significantly reduced (i.e., to 10% or less) after two days of model integration [Berge *et al.*, 2001]. Regarding BC, there are more difficulties in their characterization. Seinfeld and Pandis [1998] have suggested three methods to minimize the influence of chemical BC: (1) extend the modelling domain far enough to include all emission sources that affect atmospheric composition in the area of interest; (2) include the effect of these sources in the BC implicitly; and (3) use larger-scale simulations to provide BC for the smaller simulated domain.

The first method can require the use of very large modelling domains that may be very expensive computationally [e.g., Fiore *et al.*, 2009]; the second method employs time-independent BC during the model integration period [e.g., Hogrefe *et al.*, 2004]; whereas the third method uses time-dependent BC [e.g., Hogrefe *et al.*, 2006]. The time-dependent methods are often applied in multi-scale nested simulations and are potentially the most realistic treatment [Samaali *et al.*, 2009].

For the CAMx improved setup, initial concentrations and hourly boundary conditions were created from output concentration files from the LMDz-INCA chemistry-climate global circulation model [Hauglustaine *et al.*, 2004] for gaseous species, and from the global model GOCART [Ginoux *et al.*, 2001] for aerosols. In order to use the output files from the global models, an interface program developed specifically for this purpose, within a collaboration between the University of Santiago de Compostela and the University of Aveiro, was used. The program was based in an existent application for CHIMERE model [Vautard *et al.*, 2001], which allows the reading of the global model's output data and the writing of these data in a CAMx-compatible format. This program executes all the interpolation operations necessary to adapt the data given by the global models (with a grid resolution between 0.5 and 1 degree) to those needed for the air quality simulations (a few kilometres resolution).

The application of the interface program results in the production of 12 IC and 12 BC files, containing different concentration values for each month of the year.

6.2 Land-use based emission spatial disaggregation scheme

Accurate estimation of pollutant emissions is crucial to successful air quality modelling. The emissions inventories are subject to large uncertainties, including (1) the degree of completeness of the inventory; (2) the quality of emission factor estimates; and (3) the accuracy of the inventory's temporal and spatial patterns [Placet *et al.*, 2000; Sawyer *et al.*, 2000].

The national emission inventory used in the present study compiles total annual quantities of anthropogenic emissions to the air, which are assigned by municipality and SNAP (Selected Nomenclature for sources of Air Pollution) category. Table 6.1 lists and briefly describes each of the ten considered SNAP categories.

Table 6.1. SNAP categories considered in the study.

SNAP	NAME	DESCRIPTION
1	COMBUSTION IN ENERGY AND TRANSFORMATION INDUSTRIES	Public electricity and combined heat and power stations, district heating, transformation to solids and to gases, petroleum refineries.
2	NON-INDUSTRIAL COMBUSTION PLANTS	Heat generation in other sectors than industry and energy production and transformation (commercial, institutional and residential plants).
3	COMBUSTION IN MANUFACTURING INDUSTRY	Heat generation and production processes whose heat demand is met through combustion.
4	PRODUCTION PROCESSES	Non-combustion related sources only (petroleum, metal, chemical, pulp and paper, food, drink and other industries).
5	EXTRACTION AND DISTRIBUTION OF FOSSIL FUELS AND GEOTHERMAL ENERGY	Energy related non-combustion sources (extraction, treatment and loading of solid, liquid and gaseous fuels; liquid fuel, gasoline and gas distribution).
6	SOLVENT AND OTHER PRODUCT USE	Use of solvents through application of solvent containing products, as an agent, and in manufacturing and processing of products (paint application; degreasing and dry cleaning and electronics; others; use of HFC, N_2O, NH_3, PFC and SF_6).
7	ROAD TRANSPORT	Vehicles moving and parking.
8	OTHER MOBILE SOURCES AND MACHINERY	Operation of aircraft, ships, tractors, construction machinery, lawn movers, military and other equipment.
9	WASTE TREATMENT AND DISPOSAL	Waste incineration with or without heat recovery, solid waste disposal on land and other waste treatment.
10	AGRICULTURE	Non-energy processes in culture, and animal breeding (on-field burning is included).

In the reference setup, the inventory was further disaggregated at the sub-municipality level (freguesia), using population data given by Census 2001, concerning population and fuel consumption [Monteiro *et al.*, 2001]. For the improved setup the land use data is the corner stone of the disaggregation process.

Therefore in this section, spatial surrogates are presented to disaggregate 2005 national emission totals [URL10] onto a spatially resolved emission inventory, which can be used as input for any air quality model domain over Portugal, and specifically for the CAMx model domains already presented.

A spatial surrogate is a value greater than zero and less than or equal to one that specifies the fraction of the emissions of a particular country, in this case Portugal, which should be allocated to a particular grid cell of the air quality model domain of interest [Eyth and Habisak, 2003]. Typically, some type of geographic characteristic is used to weight the attributes into grid cells in a manner more specific than a simple uniform distribution. In this study, based on the methodology described in Maes *et al.* [2009], satellite derived CORINE land cover (CLC) data in combination with national statistics are applied as spatial surrogate variables for disaggregating non-point emission sources over Portugal. The surrogate value is calculated as the ratio of the attribute value in the intersection of the country and the grid cell to the total value of the attribute in the country; examples of such weight attributes are population, number of households or land use.

Several studies have also used CORINAIR data to produce spatially and temporally resolved emission inventories [Lenhart and Friedrich, 1995; Kluizenaar *et al.*, 2001; Friedrich and Reis, 2004; Monforti and Pederzoli, 2005; Poupkou *et al.*, 2007; Borge *et al.*, 2008; Maes *et al.* , 2009]. However, this type of study was never conducted before for the Portuguese emission inventory.

The methodology developed and applied is presented in Figure 6.1.

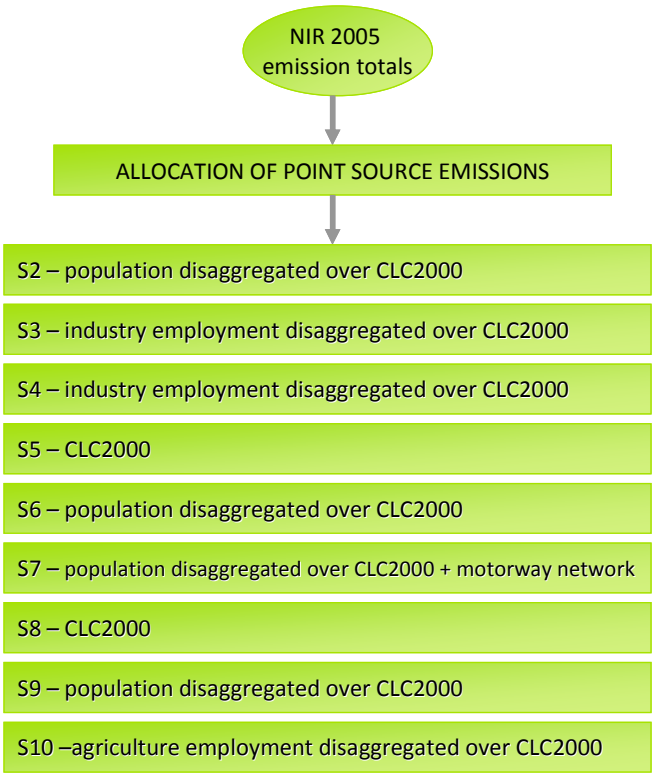

Figure 6.1 Methodology for the spatial disaggregation of the 2005 National Emission Inventory.

First, point source emissions (those already described for the reference setup) were allocated on the air quality domain of interest. Next, non-point emissions, for each SNAP category, were spatially distributed using specific quantitative spatial surrogate data, based on statistics from the National

Statistics Institute (INE), and other source specific activity data, and on CLC2000 data for Portugal, a dataset already described in §4.2.2. It is worth mentioning that SNAP1 emissions are all included as point sources; therefore no disaggregation was performed for this sector.

Figure 6.2 presents CLC2000 for Portugal, with a 250x250 m resolution, and its 44 classes, a dataset that will be extensively used in the disaggregation process. The two most representative land use classes are the agricultural areas (Class 2) and forest and semi-natural areas (Class 3), each one representing approximately 48%, therefore together 96% of the national territory; artificial areas (Class 1) only represents 2.7% of the territory [Painho and Caetano, 2006].

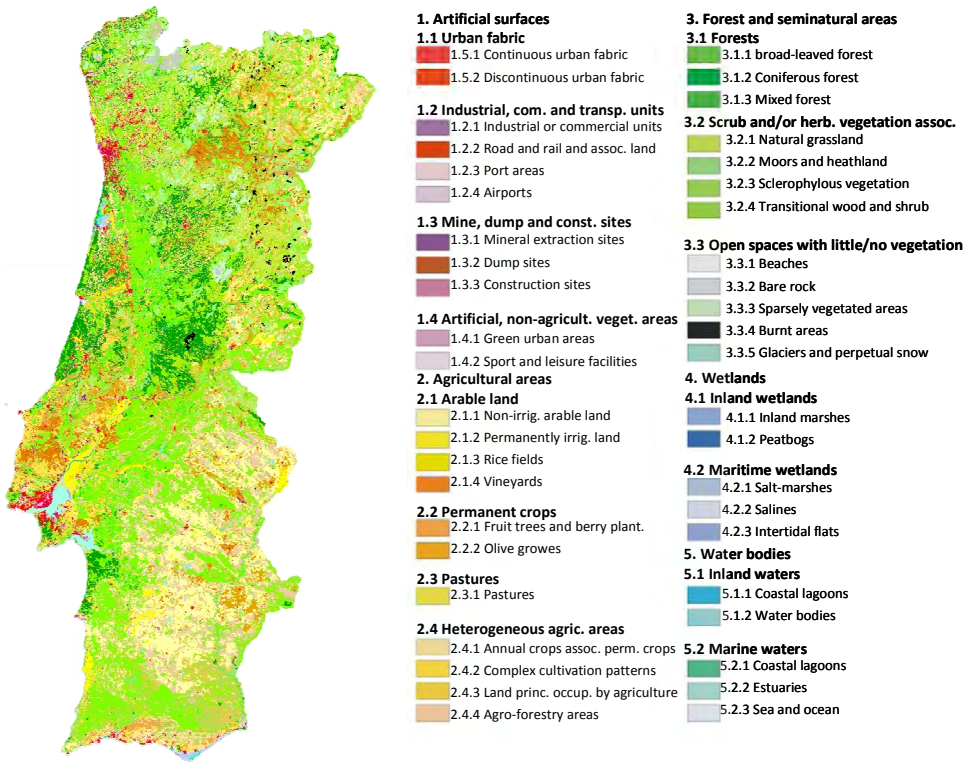

Figure 6.2 Corine Land Cover 2000 for Portugal [EAA, 2000].

The spatial disaggregation for each SNAP is described below.

6.2.1 Non-industrial combustion (SNAP2), solvent use (SNAP6) and waste treatment (SNAP9)

Area sources for these three categories were spatially distributed using the population disaggregated over the CLC2000 data, i.e., using the population density calculated for each land use category. S9 could have been disaggregated over CLC2000 land cover class dump sites. However, this class is not representative for Portugal (only 460 ha) and therefore it is not used.

Population density data are available in Portugal at the sub-municipality level, or communes (in Portugal, *freguesia*). The size of *freguesias* in Portugal is very heterogeneous, ranging from 4 ha to 42500 ha; hence this level of spatial resolution is insufficient for air quality modelling purposes.

Moreover, a certain *freguesia* may contain, for instance, parts of dense urban nucleus, agricultural land with some sparse population, and natural vegetation areas with very little or no population. CLC gives useful geo-referenced information for disaggregation, since its geographic database provides information that is spatially much more detailed than the *freguesia* limits (250 m x 250 m resolution). The objective is to disaggregate population data attributing different densities to different land cover categories, following the methodology developed by Gallego and Peedell [2001], hereafter briefly described.

According to Gallego and Peedell [2001], the population density attributable to land cover class *c* in commune *m* is computed as

$$Y_{cm} = U_c W_m$$

where Y_{cm} is the population density for land cover class *c* in commune *m*, U_c is the disaggregation coefficient for land cover type *c* (the same for every commune), and W_m is the adjustment factor to ensure that the total population commune *m* is matched (different for each commune).

Using highly detailed population datasets for a given region, Gallego and Peedell [2001] performed an iterative process, with the disaggregation being carried out with an initial set of coefficients provided by the EEA for an aggregated CORINE Land Cover nomenclature. After an optimization process, six final aggregated CLC classes were defined (Table 6.2).

Table 6.2 Final CLC grouped classes for population disaggregation [Gallego and Peedell, 2001].

Grouped class	CORINE classes
1 - Urban dense	111 -Continuous urban fabric
2- Other urban	112- Discontinuous urban fabric
	121 – Industrial or commercial units
	122 – Road and rail networks and associated land
	123 – Port areas
	124 – Airports
	141 – Green urban areas
	142 – Sport and leisure facilities
3 - Arable	211 – Non-irrigated arable land
	212 – Permanently irrigated land
	213 – Rice fields
4 - Permanent crops and complex cultivation	221 – Vineyards
	222 – Fruit trees and berry plantations
	223 – Olive groves
	241 – Annual and permanent crops associated…
	242 – Complex cultivation patterns
5 - Pastures	231 – Pastures
	243 – Agriculture, with natural vegetation
6 - Forest and natural vegetation	244 – Agro-forestry areas
	311 –Broad leaved forest
	312 – Coniferous forest
	313 – Mixed forest
	321 – Natural grassland
	322 – Moors and heathland
	323 – Sclerophyllous vegetation
	324 –Transitional woodland-shrub

Since the ratio between the density in different land cover classes is not the same in densely populated areas and in more rural areas, the authors suggest the stratification of communes in each region applying a very simple criterion: 1) dense communes: population density higher than twice the average density in its NUTS2 region; 2) less dense: population density lower than twice the average density in its NUTS2 region, and with urban area reported in CLC2000; 3) no urban: no urban area reported in CLC2000. The final coefficients obtained for the disaggregation of population data according to land use category (Table 6.3) were subject to quality assessment procedures, tested for regions with high-resolution population density data, and were judged approximately correct [Gallego and Peedell, 2001).

Table 6.3 Final disaggregation coefficients (Uc) with 6 aggregated CLC classes and three strata of communes [Gallego and Peedell, 2001).

	1. Urban dense	2. Other urban	3. Arable	4. Permanent crops and …	5. Pastures	6. Forest and natural …
Stratum 1	1445.9	619.1	10.2	15.4	5.1	3.3
Stratum 2	947.4	622.4	17.4	30.9	11.3	5.2
Stratum 3	-	-	32.0	69.3	22.8	8.6

The described methodology was then applied to the Portuguese continental territory, with population given by CENSUS 2001 [URL18] being disaggregated over the CLC distribution presented in Figure 6.2, and emissions disaggregated with population density. For that purpose a geographic information system, ArcGis, was used through the following steps:

i) intersection of CLC2000 data with the commune's limits;

ii) grouping of 44 CLC classes in the 6 aggregated CLC classes;

iii) classification of the communes in the three strata (dense, less dense and no urban area);

iv) attribution of U_c according to land use class and commune stratum;

v) determination of W_c for each commune in order to comply with the total population data;

vi) determination of population density for each CLC land use class in each commune;

vii) intersection of the population density with the domain grid and calculation of the population for each cell of the domain;

vii) disaggregation of municipality emission totals using the calculated population.

This procedure is illustrated in Figure 6.3, with a schematic of the spatial allocation of NO_x emissions from SNAP2, for domain 3 of the simulation: a) NO_x emissions (ton) per year and per municipality from the NIR are represented; b) CLC aggregated in 6 classes showing a large area of urbanized cells over Porto municipality and its surroundings; c) population distribution calculated according to land use classes; d) gridded NO_x emissions with 1 km resolution.

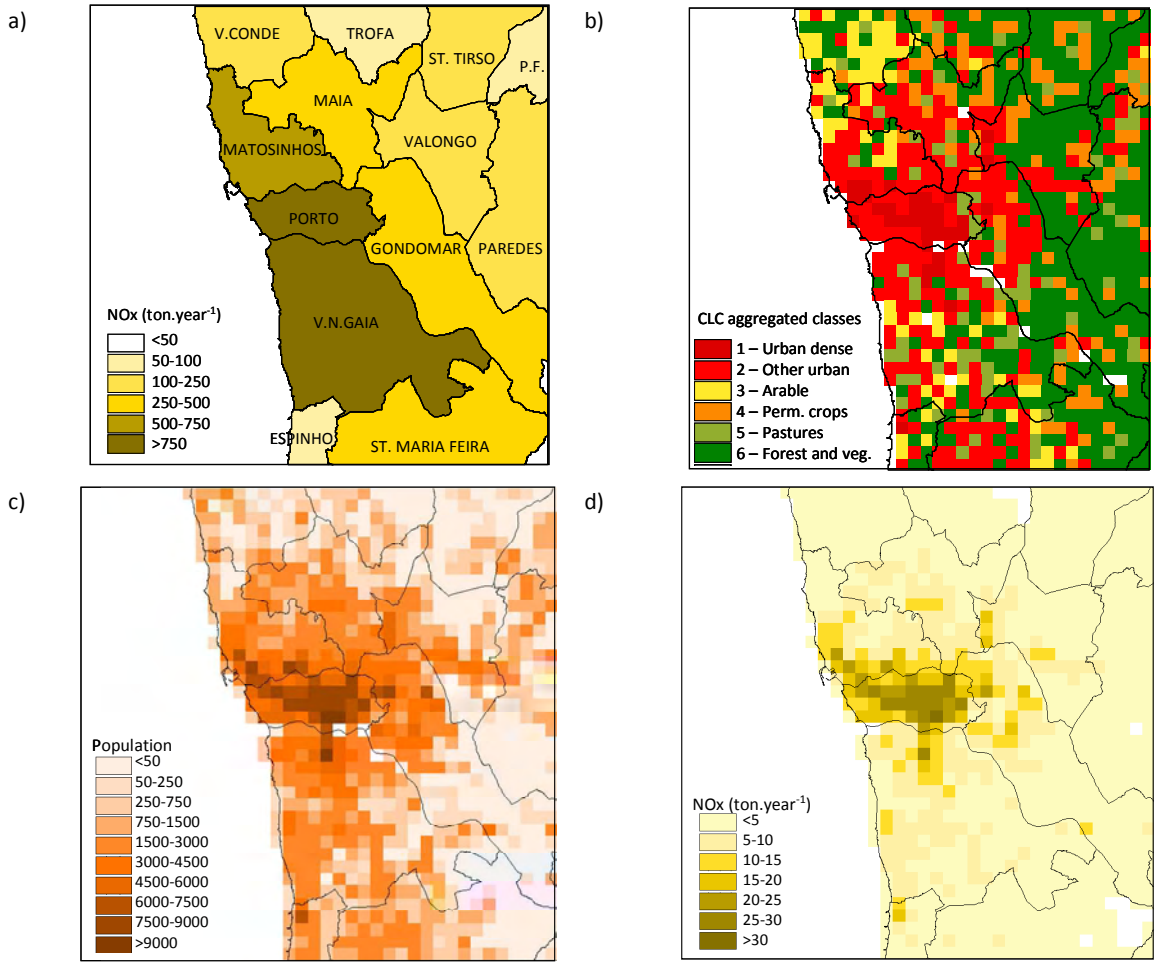

Figure 6.3 Spatial allocation of NOx emissions from SNAP2 for domain 3: a) Input data: emissions at municipality level; b) CLC aggregated classes; c) calculated population for each grid cell of the domain; d) gridded emissions at 1 km resolution.

Figure 6.4 shows an example of the differences between the methodology here developed and the methodology used for the disaggregation in the reference setup for NMVOC emissions from SNAP6, for the three simulation domains. The reference setup disaggregation presents higher NMVOC emission values per cell of the domain, for the three domains, as a result of a greater concentration of emissions in the cities / urban centres (Lisboa, Porto and Aveiro). For the improved setup urban areas show higher emission values, but when compared with surrounding cells the difference in the magnitude of emissions is not as high as for the reference setup. Concerning domain3, the distribution of emissions is quite different between setups: in the first, emissions are concentrated on the N/NW part of Porto, S of Matosinhos and North of Vila Nova de Gaia; while for the second, Porto presents higher emissions. The population disaggregation over the urban dense cells, which imply greater emissions, can explain these differences.

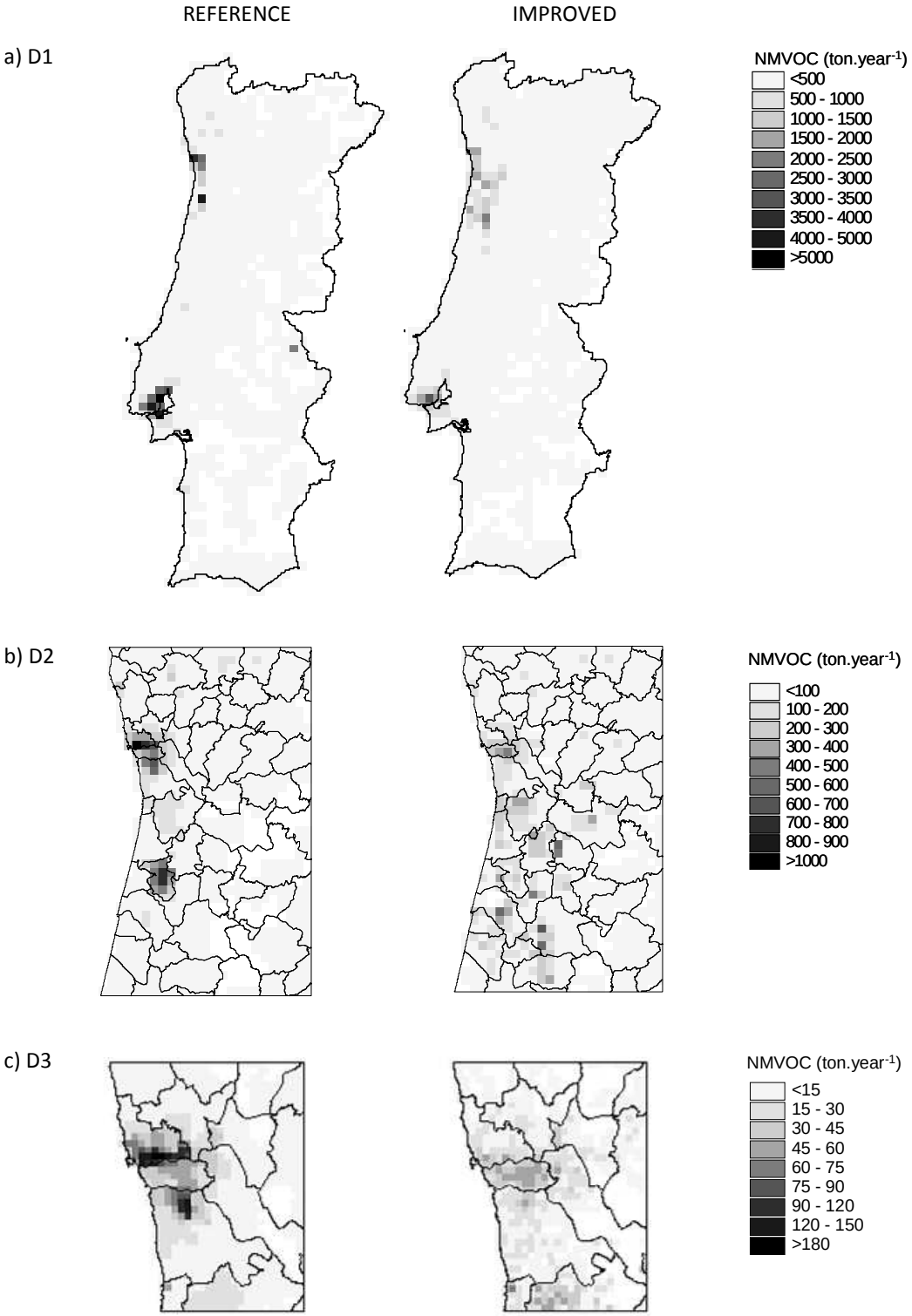

Figure 6.4 Reference and improved setup spatial allocation of NMVOC emissions from SNAP6, for the three simulation domains.

6.2.2 Industrial combustion (SNAP3) and industrial processes (SNAP4)

Non-point sources for these sectors were allocated using the CLC2000 land cover class industrial and commercial units (code 121) in combination with statistical activity data provided by INE on the

number of employees in industry at the municipality level. For those municipalities with CLC 121 classified areas, INE data with low spatial resolution were proportionally disaggregated on the high resolution CLC land cover map (250 m x 250 m) spreading the numbers of employees in the industry over the land cover class industrial and commercial units, again using ArcGis. For the municipalities with no commercial and industrial units classification under CLC2000, the numbers of employees in the industry were spread over the land cover classes corresponding to class 112 – discontinuous urban fabric. Emissions were then spread over the territory proportionally to the industry employment density. Figure 6.5 presents S3 PM10 emissions disaggregated over D1 using the reference setup methodology and the new methodology here described. For the improved setup emissions are not as concentrated as for the reference setup.

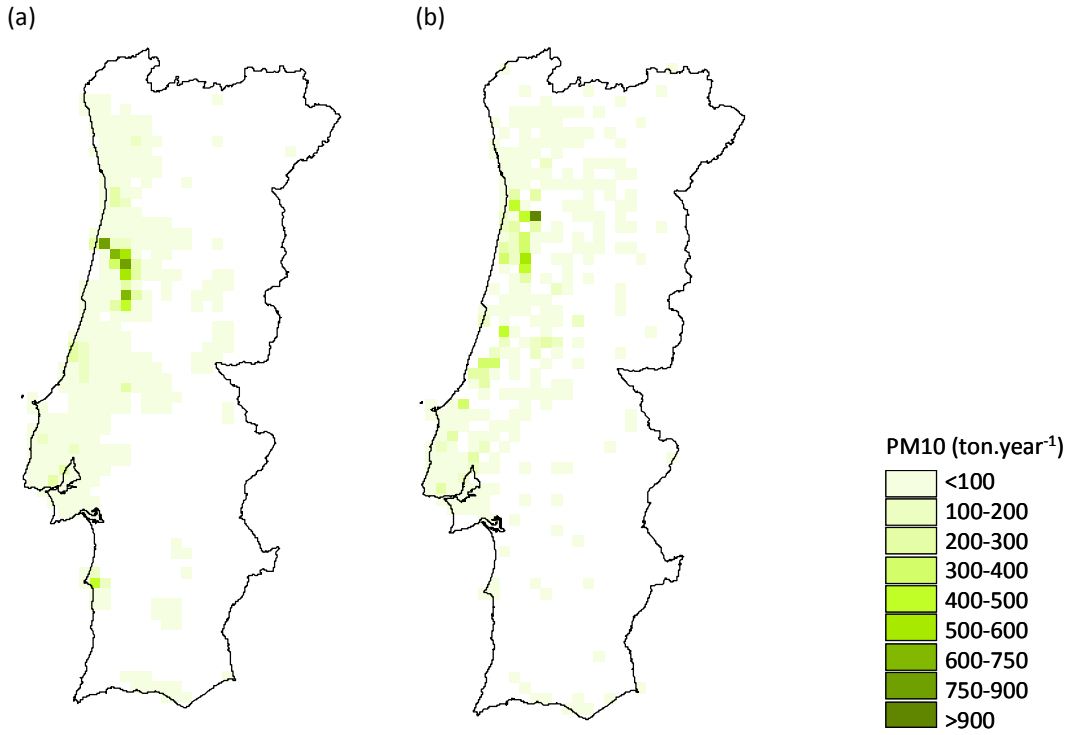

Figure 6.5 Spatial allocation of PM10 emissions from SNAP3 for domain 1 for (a) the reference setup and (b) the improved setup.

6.2.3 Extraction and distribution of fossil fuels (SNAP5)

Maes *et al.* [2009] disaggregated the emissions released during the extraction and distribution of fossil fuels using the CLC land class ports; on the other hand, Popkou *et al.* [2007] used population data. In Portugal, only a few municipalities have port areas identified in CLC2000, and even those have relatively small areas classified as such in CLC, therefore S5 emissions were disaggregated over the land cover classes corresponding to artificial surfaces (corresponding to class 1 in CLC level 1 – see Table 5.4), with a bigger weight being given to port areas where they exist.

6.2.4 Road transport (SNAP7)

The national emission inventory distinguishes road transport emissions in two sub-categories: motorway emissions and non-motorway emissions. Ideally non-motorway emissions should be further classified as urban roads and non-urban roads, and then disaggregated over the respective network; however, this distinction is not available from the national inventory. Therefore non-motorway emissions were spatially distributed using the population disaggregated over the CLC2000 data, as described for SNAP2, 6 and 9.

Motorway emissions were disaggregated over the 2005 motorway network, again using ArcGis as the geographical tool. Figure 6.6 presents SNAP7 CO emissions for domain 3 for the reference and for the improved setup.

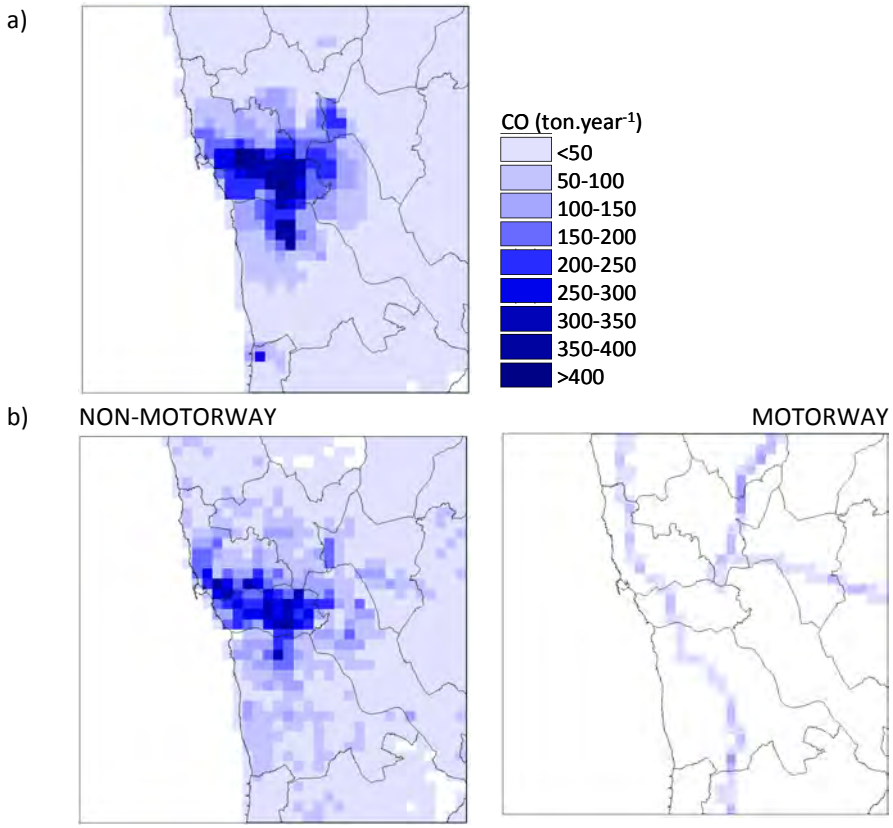

Figure 6.6 Spatial allocation of CO emissions from SNAP7 for domain 3 a) reference setup and b) improved set-up (non-motorways and motorway emissions).

Although both datasets present higher values over Porto municipality, southern Matosinhos and northern Vila Nova de Gaia, emissions from the reference setup are spatially more concentrated. Also the separate treatment of motorways emissions allows a better discrimination.

6.2.5 Other mobile sources (SNAP8)

This source category includes emissions from mobile off-road sources, such as emissions from civil aviation, national navigation, railways, military transport, gardening and agricultural practices. Here

navigation emissions were not considered. Emissions from agricultural equipments were treated separately, using a cut-off value of 58% to estimate the share of agriculture in S8; this value was calculated by Maes *et al.* [2009] as an European average based on NFR (Nomenclature For Reporting) source categories (more refined than SNAP categories). This share of emissions from off-road agricultural vehicles was disaggregated using the methodology described hereafter for SNAP10. The remaining S8 emissions (railways, gardening and military) were distributed over the land use categories 112 to 142 (discontinuous urban fabric, industrial or commercial units, road and rail networks and associated land, port areas, green urban areas and sport and leisure facilities) since more detailed data, such as geo-referenced railway network, is not available.

6.2.6 Agriculture (SNAP10)

Emissions caused by agricultural production processes were disaggregated combining the CLC2000 land cover classes concerning agriculture (corresponding to class 2 in CLC level 1 – see Table 5.4) with INE low resolution statistical data (municipality level) on the number of employees in agriculture. Figure 6.7 presents NH_3 emissions from SNAP10 for the reference setup and for the improved setup, for domain 3. The emission distribution is very different between setups; for the improved setup emissions are concentrated in the NW part of the domain corresponding to the land use class arable, with no emissions in the southern part of the domain in the urban areas.

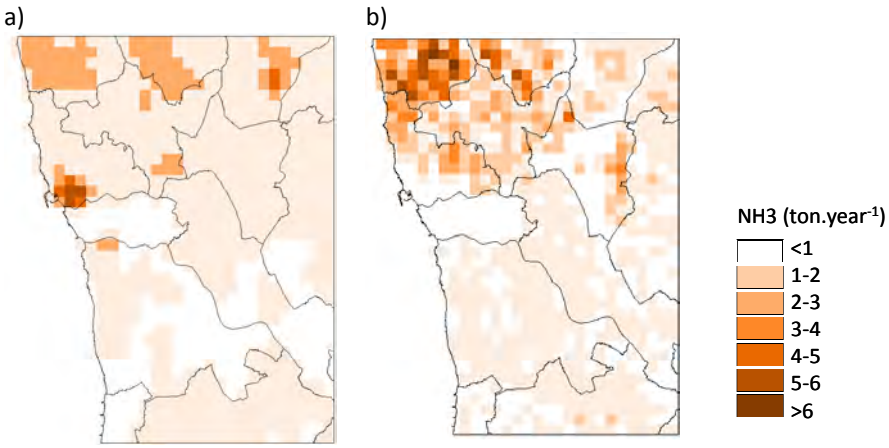

Figure 6.7 Spatial allocation of NH_3 emissions from SNAP10 for domain 3 for a) the reference setup and b) the improved setup.

6.3 Emissions temporal allocation

Emission inventories are generally compiled to report annual emission totals for regulatory purposes and legal requirements. Air quality models, however, require emissions at finer temporal resolution. To provide these, an emission model is needed to apportion the longer-term average values into hourly fluxes according to temporal profiles that specify how many emissions are hourly assigned. These temporal profiles are not based on actual temporal data for a specific time period, but on typical

temporal variations for the defined categories of sources [Orthofer and Winiwater, 1998; Tao *et al.*, 2004; Monforti and Pederzoli, 2005; Samaali *et al.*, 2009].

For CAMx improved setup, new time-varying profiles were developed, describing variations in monthly (12-element), daily (2-element, weekday and weekend) and hourly (24-element) anthropogenic emissions, transforming time-averaged man-made emissions into hourly fluxes. The application of these profiles yields different hourly emissions.

The information to construct representative and meaningful temporal profiles was taken from National official statistics (energy, industrial production, transport, etc). Whenever such data were not available, temporal profiles from IER (Institut fur Energiewirtschaft und Rationelle Energieanwendung, University of Stuttgart) were used [Schmidt *et al.*, 2001]. Table 6.4 presents the information used for the construction of temporal profiles for each SNAP activity, as well as its source.

Table 6.4 Data for the construction of temporal profiles

	MONTHLY profiles	DAILY and HOURLY profiles
SNAP2	Monthly energy consumption (REN - National Electric Network)	Load diagrams (REN - National Electric Network)
SNAP3 SNAP4	Industrial production statistics (INE – National Statistics Institute)	IER
SNAP5 SNAP7 SNAP8	Monthly fuels sales (DGEG -General Directorate for Energy and Geology)	Traffic counts [Oliveira *et al.*, 2004]
SNAP6	Monthly fuels sales	IER
SNAP9 SNAP10	IER	IER

If emissions were equally distributed along the year (the same emissions for every hour of every day of every month in the year) the temporal weight factors would always be the same and equal to 1. The consideration of the different weight factors results in distinct emission profiles, which yield considerable differences in emissions: the average daytime (8 am to 8 pm) emissions for the considered profiles ranged from 55% (for SNAP2) to 120% (for SNAP3 and 4) higher than when considering a uniform distribution of emissions; on the other hand, the average night time emissions ranged from 45% (for SNAP7) to 10% (for SNAP 2, 5, 9 and 10) smaller than when considering a uniform distribution of emissions.

Figures 6.8 and 6.9 illustrate some of the differences between the temporal profiles. Figure 6.8 presents the monthly profiles for three different activities – SNAPS 2, 3 and 7 – with evident and marked differences as expected: SNAP 2, representing energy consumption in the residential, service and commercial activities, presents higher values in the winter months; SNAP 3 (and SNAP4) reveals a clear decrease in August and December, translating the decrease in production in these two months due to the summer and Christmas seasons; SNAP7 presents higher values for the summer months.

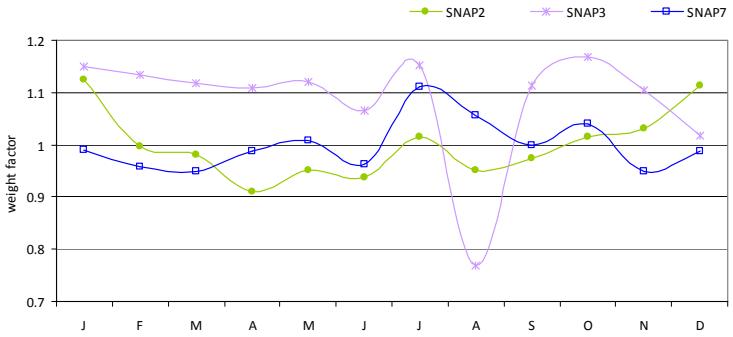

Figure 6.8 Monthly profiles (January to December) for SNAP 2 (non-industrial combustion), SNAP 3 (combustion in manufacturing industry) and SNAP 7 (road transport).

Figure 6.9 shows the importance of considering different daily profiles for motorways and non-motorways road traffic, since these two exhibit very different profiles: on weekdays, both profiles show peaks around 8:00–9:00 and 18:00–19:00, but for motorways these are much higher; on weekends motorways present a pronounced peak around 17:00, while non-motorways traffic flux present a very discrete maximum at 19:00. The figure also reveals the importance of considering different profiles for weekdays and weekends; profiles are particularly different for motorways, whose peaks assume very high values during the week.

a)

b)

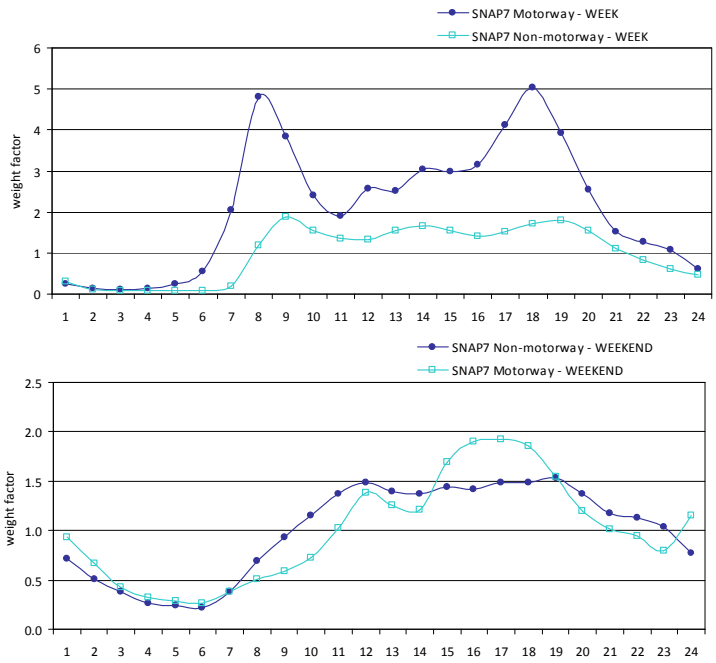

Figure 6.9 Hourly profiles for SNAP 7 a) week and b) weekend.

6.4 Chemical speciation

In this section, activity-specific chemical speciation profiles for NMVOC and PM are developed. For nitrogen oxides, given the lack of consistent information regarding speciation, a constant non-specific NO/NO_x ratio of 0.9 has been assumed for all the categories emitting nitrogen oxides, following USEPA defaults [USEPA, 2002].

6.4.1 Non-methane volatile organic compounds

The volatile organic compound's chemical category contains some hundreds of compounds that are crucial for modelling photochemical reactions in the atmosphere; the chemical speciation of NMVOC has been identified as a key issue when predicting ozone concentrations in areas dominated by urban sources [Vautard *et al.*, 2000].

While for the reference setup, a single NMVOC profile was used for every activity, for the improved setup activity-specific chemical speciation profiles were constructed, based on European references, such as EMEP/CORINAIR Guidebook [EEA, 2006b], when available. However, most of the speciation profiles were taken from a compilation by Passant [2002]. The speciation profiles are composed of tens to hundreds of NMVOC chemical compounds (for instance, the chemical industry profile has 224 species), therefore these had to be grouped in the NMVOC classes considered in the speciation process, all of them included in the selected chemical mechanism and presented in Table 6.5.

Table 6.5 NMVOC classes considered in CAMx mechanism 4.

NMVOC class	Description
PAR	Paraffin carbon bond (C-C)
TOL	Toluene (C6H4-CH3)
XYL	Xylene (C6H5-(CH3)2)
FORM	Formaldehyde
ALD2	Acetaldehyde and higher aldehydes
ETH	Ethene
OLE	Olefinic carbon bond (C=C)
MEOH	Methanol
ETOH	Ethanol
ISOP	Isoprene

Since each SNAP activity has contributions from different origins, e.g. non-industrial combustion emissions result from the contribution of wood and gas burning, additional data is needed to determine an average profile. Therefore, the selected profiles were combined with information from the national emission inventory and national energy balances from the DGEG (General Directorate for Energy and Geology) [URL19], allowing the determination of a weighed average profile for each SNAP.

Table 6.6 presents the profiles used in the construction of the final NMVOC profile for each SNAP activity, as well as its source and the source of additional data.

Table 6.6 NMVOC profiles construction for each SNAP category.

SNAP	PROFILES [SOURCE]	ADDITIONAL DATA [SOURCE]	FINAL PROFILE (%)	
2	36. Domestic comb. of gas 125. Domestic wood comb. [Passant , 2002]	Energy consumption in the domestic and service sector (fuel type %) [2005 national energy balance, DGGE]	PAR OLE ETH TOL XYL FORM ALD2 ETOH	36.7 1.4 12.0 1.0 0.3 1.6 5.6 9.2
3	31. Industrial comb. of oil 33. Industrial comb. of coal 95. Int. comb. engine - natural gas 126. Industrial wood comb. [Passant , 2002]	Energy consumption in industrial combustion (fuel type %) [2005 national energy balance, DGGE]	PAR OLE ETH TOL XYL FORM ETOH	48.0 6.2 5.8 3.5 3.6 10.8 4.9
4	15. Chemical industry 103. Cement industry 14. Oil refineries [Passant , 2002]	NMVOC emissions from industrial processes (industry type %) [NIR2005]	PAR OLE ETH TOL XYL FROM ALD2 MEOH ETOH	11.5 11.9 9.9 1.7 4.2 0.5 0.1 1.9 1.1
5	71.Petrol distribution – unleaded [Passant , 2002]	-	PAR OLE TOL XYL	91.4 7.3 0.5 0.2
6	3. Paint manufacture 6. Adhesives 11. Other solvent use 44. Decorative paint 53. Rubber processes 59. Printing 68. Cosmetics and toiletries 69. Household products [Passant , 2002]	NMVOC emissions from solvents (industry type %) [NIR2005]	PAR TOL XYL ETOH	39.8 9.1 10.6 6.2
7	Road transport Activities 070100 – 070500 [EMEP/CORINAIR]	Fuel consumption in transports (fuel type %) [2005 national energy balance, DGGE]	PAR OLE ETH TOL XYL FORM ALD2	10.3 7.1 10.1 6.4 6.6 8.6 11.7
8	Road transport Activities 070100 – 070500 [EMEP/CORINAIR]			
9	22. Landfill 115. Waste incineration [Passant , 2002]	NMVOC emissions from waste (treatment type %) [NIR2005]	PAR OLE ETH TOL MEOH ETOH	29.6 5.5 11.8 70.6 1.2 4.8
10	Agricultural Pesticide Application Open Fire Profiles – Agricultural [SPECIATE, Battye and Harris, 2005]	-	PAR OLE ETH TOL XYL FORM ALD2 ISOP MEOH ETOH	27.4 5.1 5.0 1.8 1.1 5.0 3.0 0.2 7.0 0.2

6.4.2 Particulate matter

Again, as for NMVOC, while for the reference setup, a single profile was used for every activity, for the improved setup activity-specific chemical speciation profiles were constructed, based on USEPA [2002] profiles, and also in a report by Battye and Harris [2005]. The selected profiles were then combined with information from national sources, allowing the determination of a weighed average profile for each SNAP. Table 6.7 presents the PM2.5 species considered for the speciation.

Table 6.7 PM2.5 classes considered in CAMx mechanism 4.

PM2.5 class	Description
PEC	Primary Elemental Carbon
PNO3	Particulate Nitrate
POA	Primary Organic Aerosol
PSO4	Sulfate
FCRS	Fine Crustal (≤2.5 µm)
FPRM	Fine Other Primary (≤2.5 µm)

Table 6.8 lists the profiles used in the construction of the final profile for each SNAP activity, as well as its source and the source of additional data, and the resulting weighed PM2.5 profile.

Table 6.8 PM2.5 profiles construction for each SNAP category.

SNAP	PROFILES [SOURCE]	ADDITIONAL DATA [SOURCE]	FINAL WEIGHED PROFILE (%)	
2	6.3.3. Residential wood combustion [Battye and Harris] 22004. Natural gas combustion 22002. Residual oil combustion [USEPA, 2002]	Energy consumption in the domestic and service sector (fuel type %) [2005 national energy balance, DGGE]	PEC PNO3 POA PSO4 FCRS FPRM	10.3 0.3 57.0 21.3 0.1 11.1
3	NCOAL.. Coal combustion 22004. Natural gas combustion 22002. Residual oil combustion NWWAS. Wood waste boiler [USEPA, 2002]	Energy consumption in industrial combustion (fuel type %) [2005 national energy balance, DGGE]	PEC PNO3 POA PSO4 FPRM	4.7 0.3 35.6 23.9 35.5
4	22015. Chemical manuf. average 22030. Secondary aluminium 22036. Asphalt roofing 22045. Pulp and paper average [USEPA, 2002]	PM25 emissions from industrial processes (industry type %) [NIR2005]	PEC PNO3 POA PSO4 FPRM	0.7 0.4 20.4 16.9 61.6
5	Default [USEPA, 2002]	-	FPRM	1
6	Default [USEPA, 2002]	-	FPRM	1
7 8	6.1.2. Light-duty Gasoline Vehicles 6.1.4. On-road diesel sources [Battye and Harris]	Fuel consumption in transports (fuel type %) [2005 national energy balance, DGGE]	PEC PNO3 POA PSO4 FPRM	44.0 2.3 48.6 2.1 3.0
9	Default [USEPA, 2002]	-	FPRM	1
10	NAGBN. [USEPA, 2002]	-	PEC PNO3 POA PSO4 FPRM	4.0 0.3 67.0 1.0 27.7

6.5 Results

For the improved setup, CAMx was initialized with MM5 data from Test2 for the summer episode, and from Test 3 for the winter episode.

6.5.1 Summer episode

Table 6.9 presents the statistical results for ozone for the summer episode, averaged for the air quality monitoring sites of each simulation domain, for the reference and the improved setup, with the best results highlighted in bold.

Table 6.9 CAMx statistical results obtained for ozone, summer episode.

	r	BIAS ($\mu g.m^{-3}$)	MQE ($\mu g.m^{-3}$)	MNBE (%)	MNGE (%)	UPA (%)
			Ozone 9 km resolution (D1)			
REFERENCE SETUP	0.65	27.4	3.67	-8.6%	18.8%	**-0.1%**
IMPROVED SETUP	**0.77**	**19.5**	**2.84**	**-4.6%**	**12.2**%	-10.7%
			Ozone 3 km resolution (D2)			
REFERENCE SETUP	0.66	31.4	3.93	-31.7%	19.9%	**-5.0%**
IMPROVED SETUP	**0.79**	**21.3**	**2.85**	**-25.8%**	**18.6%**	-11.1%
			Ozone 1 km resolution (D3)			
REFERENCE SETUP	0.64	33.2	4.00	-33.4%	17.9%	**-14.1%**
IMPROVED SETUP	**0.79**	**20.8**	**2.82**	**-32.5%**	**16.6%**	-15.4%
USEPA guidelines	-	-	-	± 5-15%	15-20%	± 30-35%

The highest skills are obtained with the improved setup, with the exception of UPA, as a consequence of the higher peak values obtained with the reference setup. The improved setup results in higher correlations (close to 0.8), smaller BIAS (reductions achieve 8 $\mu g.m^{-3}$ in D1 and 13 $\mu g.m^{-3}$ in D3) and smaller errors; the improvements are particularly felt for the higher resolutions simulations (3 km and 1 km). The 1 km resolution presents now the higher correlation coefficient and the lower MQE, in opposition to the verified for the reference setup; the 9 km resolution has the lowest BIAS. Regarding USEPA guidelines both setups meet the UPA and MNGE criteria; the MNBE criteria are met only for the 9 km resolution. Results from this statistical analysis indicate that the accuracy of the spatial and temporal disaggregation of emissions has increased, and consequently simulated air pollutants concentrations are closer to the observed ones.

Figure 6.10 presents the graphical analysis of the statistical parameters (r, BIAS and MQE) for each air quality monitoring site for D3. The correlation factor presents the greatest increases for traffic (ANT, BAG and VRM) and background (ERM, LB and VNT) stations; for the background/industrial stations (CST and PRF) the increase in *r* is much smaller, although these already presented high *r* values. Regarding the BIAS, traffic stations present the highest decreases and therefore, better results; for the

MQE all sites show similar improvements. Despite being reduced in the improved setup, the BIAS in Table 6.9 indicates that the modelling system is not able to simulate the ozone peaks.

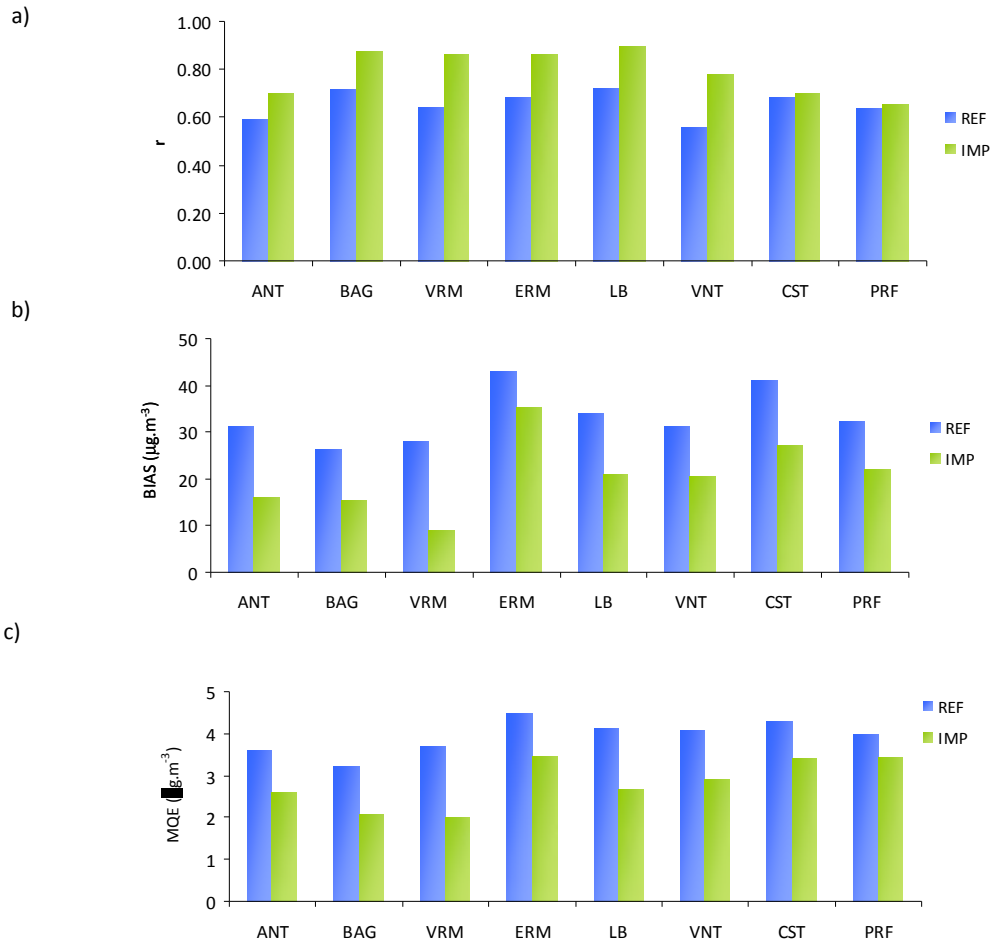

Figure 6.10 CAMx statistical results for ozone, for the summer episode 1 km simulation (D3) a) r, b) BIAS, and c) MQE, for the reference and improved setups.

The time series evolution of ozone concentrations for the six days of the summer episode are illustrated in Figure 6.11, for the observed values as well as for both setups. Only Baguim, Ermesinde and Perafita air quality stations are shown, representing the three types of monitoring stations (traffic, background and industrial). The first two days of the episode show a significant increase in ozone concentrations, and therefore an approximation to the observed values, for all sites. For the remaining days of the episode, the improved setup is also closer to the observed values. Both setups, reference and improved, are not able to simulate the peak concentrations, although the reference setup is able to better simulate the peaks.

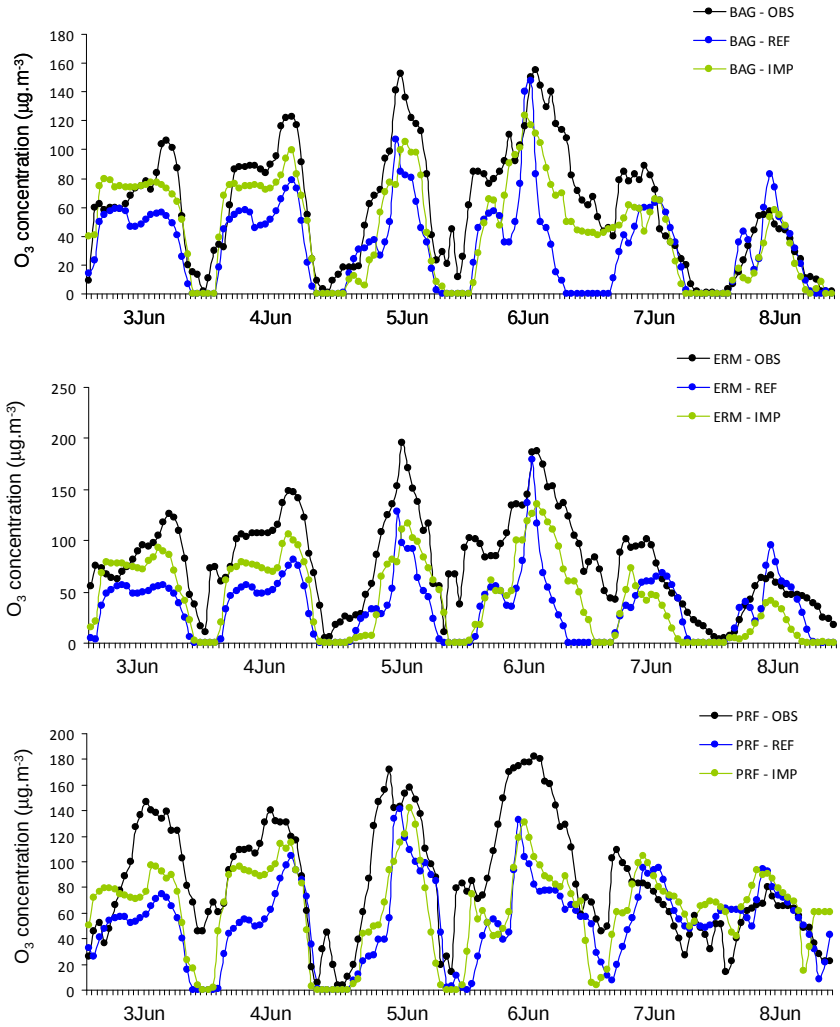

Figure 6.11 Time-series evolution of ozone observed, and reference and improved simulated concentrations, for D3, summer episode.

Table 6.10 presents the statistical results for PM10 for the summer episode, averaged for the air quality monitoring sites of each of the simulation domains, for the reference and the improved setup, with the best results highlighted in bold.

Table 6.10 CAMx statistical results obtained for PM10, summer episode.

	r	BIAS ($\mu g.m^{-3}$)	MQE ($\mu g.m^{-3}$)	r	BIAS ($\mu g.m^{-3}$)	MQE ($\mu g.m^{-3}$)	r	BIAS ($\mu g.m^{-3}$)	MQE ($\mu g.m^{-3}$)
	PM10 – 9 km resolution (D1)			PM10 – 3 km resolution (D2)			PM10 – 1 km resolution (D3)		
REFERENCE	0.22	21.5	2.61	0.21	20.5	2.72	0.22	19.3	2.67
IMPROVED	**0.42**	**16.9**	**2.42**	**0.41**	**14.1**	**2.45**	**0.41**	**12.3**	**2.46**

The correlation coefficients improve significantly, probably as a result of the use of more adequate time profiles. PM10 still is under-predicted, but the BIAS and MQE reveal improvements, resulting from the use of more accurate boundary and initial conditions as well as a better spatial distribution of emissions. The small differences found between the three simulation resolutions (9, 3 and 1 km) do

not allow the identification of a better overall resolution: the best correlation is obtained for the 9 km resolution and the lowest BIAS for the 1 km resolution, but the parameters are very similar for the three spatial resolutions.

Figure 6.12 shows the graphical analysis of the statistical parameters (r, BIAS and MQE) for each air quality monitoring site for D3.

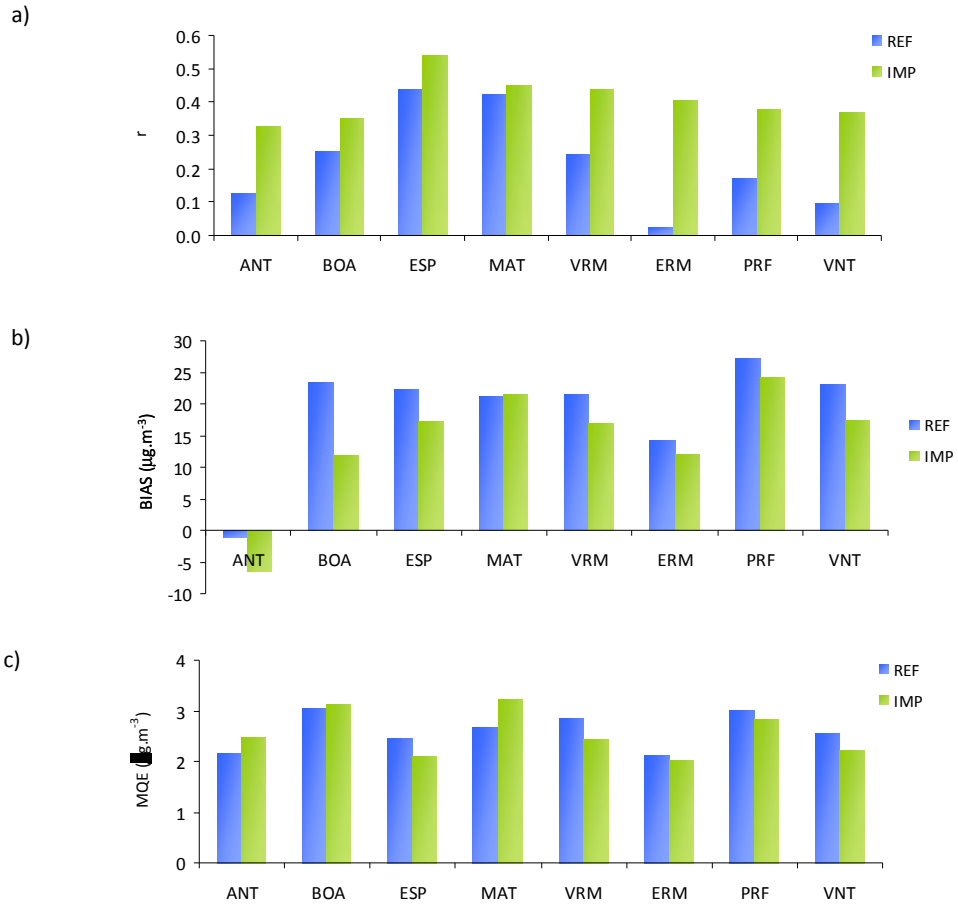

Figure 6.12 CAMx statistical results for PM10 for the summer episode 1 km simulation (D3) a) r, b) BIAS, c) MQE, for the reference and improved setups.

The correlation factor increases for all stations, with background and industrial stations presenting the greatest increases, due to the poorest performance of the model for this type of stations for the reference setup. With the exception of Matosinhos and Antas, all the stations present lower BIAS for the improved setup. Regarding the MQE, some of the traffic stations present higher values (ANT, BOA and MAT); the rest have similar improvements.

Figure 6.13 shows PM10 daily averages for the reference and improved setup simulations and for the observed values, for Boavista, Ermesinde and Vila Nova da Telha air quality stations, representing the three types of monitoring stations (traffic, background and industrial).

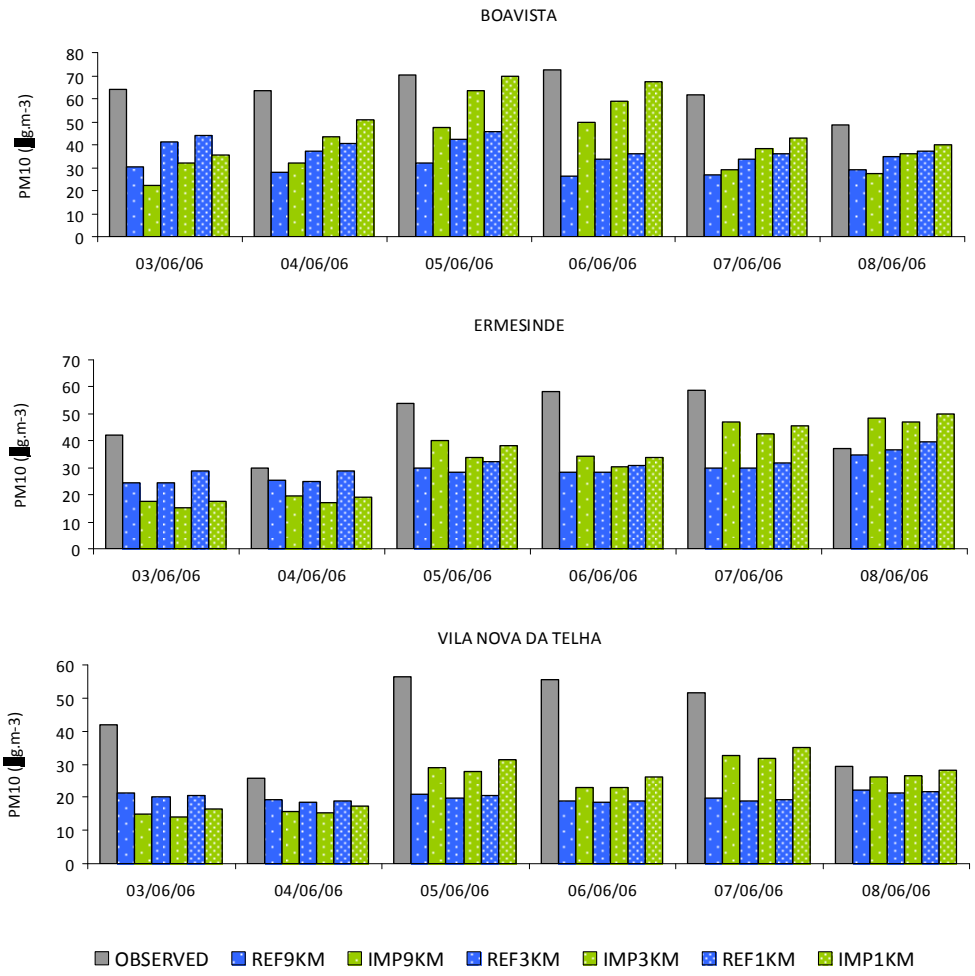

Figure 6.13 Observed, reference setup and improved setup, PM10 daily average concentrations, summer episode.

Figure 6.14 presents the spatial distribution of PM10 daily average differences between the improved and the reference setups for days 3, 5 and 7 of June. The analysis of the two figures reveal that for the first two days of the episode, the improved setup shows lower concentrations, resulting in a worst representation of the PM10 daily average. From the June 5 to 7, the greatest part of the domain presents positive differences, which in general translate an approximation to the observed daily average. Also from the 5 to 7 June, in Espinho, Vermoim, Matosinhos, Perafita and Vila Nova da Telha, the model was not able to simulate the observed PM10 concentration peaks. In the last day of simulation, a group of stations closer to the coast (ESP and PRF) present negative differences, while the rest still shows positive differences.

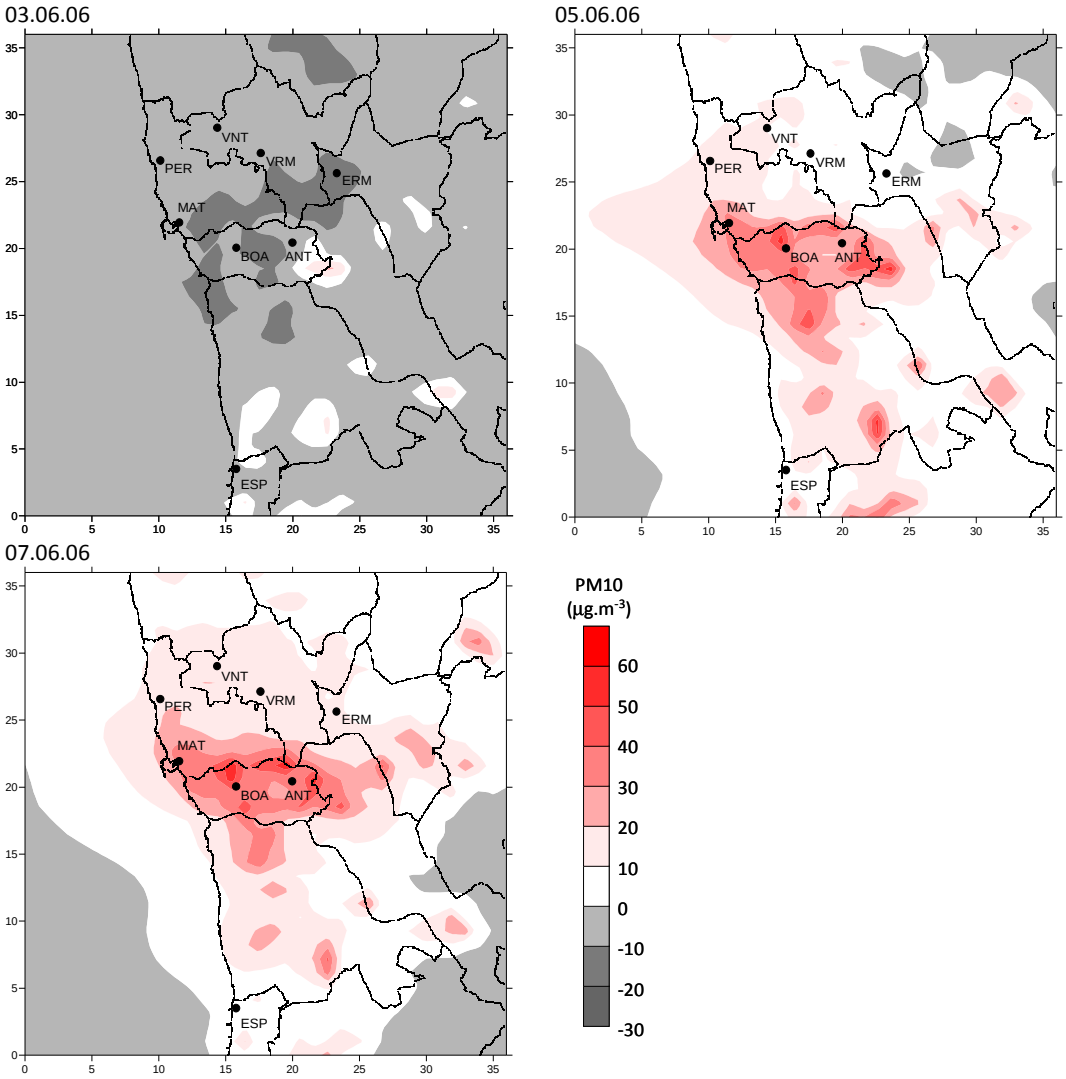

Figure 6.14 Spatial distribution of PM10 daily average differences between the improved and reference setups, summer episode.

6.5.2 Winter episode

Table 6.11 shows the statistical results for PM10 for the winter episode, averaged for the air quality monitoring sites of each of the simulation domains, for the reference and the improved setup, with the best results highlighted in bold.

Table 6.11 CAMx statistical results obtained for PM10, winter episode.

	r	BIAS ($\mu g.m^{-3}$)	MQE ($\mu g.m^{-3}$)	r	BIAS ($\mu g.m^{-3}$)	MQE ($\mu g.m^{-3}$)	r	BIAS ($\mu g.m^{-3}$)	MQE ($\mu g.m^{-3}$)
	PM10 – 9 km resolution (D1)			PM10 – 3 km resolution (D2)			PM10 – 1 km resolution (D3)		
REFERENCE	0.36	**0.1**	3.6	0.35	-4.6	4.2	0.33	-8.2	3.4
IMPROVED	**0.38**	-0.6	**2.6**	**0.37**	**-1.0**	**3.1**	**0.40**	**-2.0**	**3.0**

The correlation coefficients present a small increase for D1 and a more significant increase for D3; PM10 is slightly over predicted (small BIAS are obtained for both setups). The MQE reveal

improvements, resulting from the use of more accurate boundary and initial conditions as well as a better spatial distribution of emissions. The overall analysis reveals better results for the improved setup and for the 1 km resolution, which was the one who benefited the most from the improvements introduced in the modelling system.

Figure 6.15 shows the graphical analysis of the statistical parameters (r, BIAS and MQE) for each site for D3.

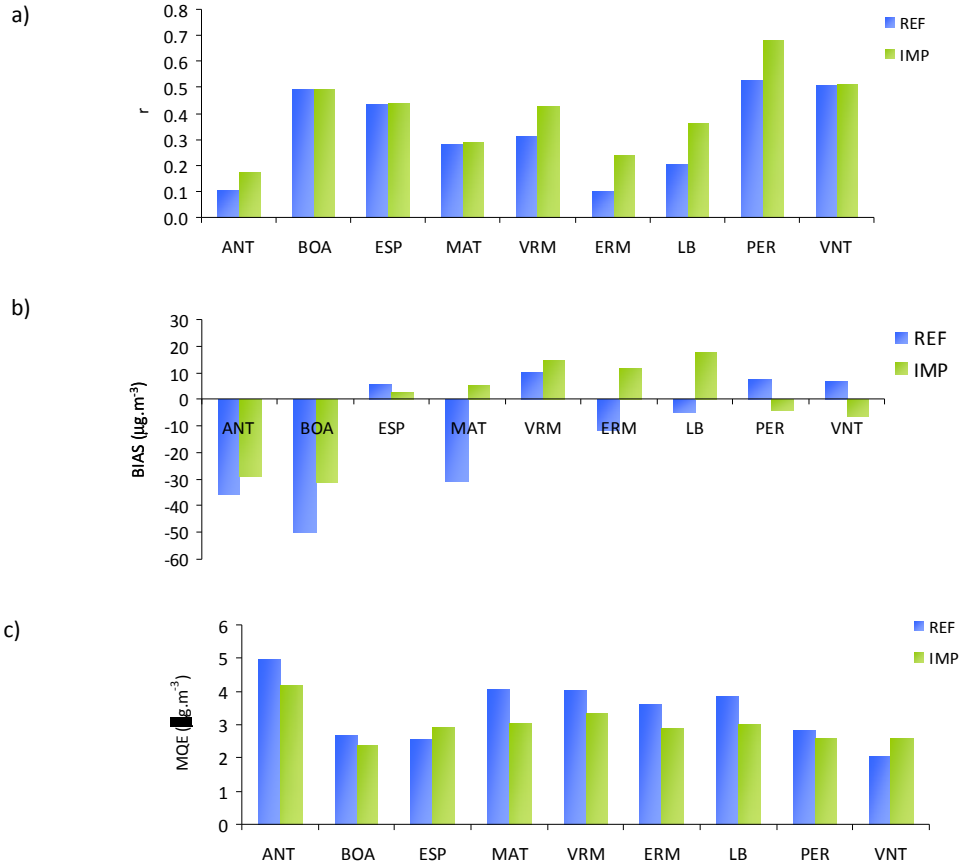

Figure 6.15 CAMx statistical results for PM10 for the winter episode 1 km simulation (D3) a) r, b) BIAS, c) MQE, for the reference and improved setups.

In the improved setup, all the sites present an increase of the correlation factor. Regarding the BIAS, distinct situations can be identified: Antas and Boavista reveal a decrease in concentrations, resulting in a smaller over–prediction of the observed values; in Matosinhos, Ermesinde and Leça do Balio the decrease in concentrations transforms the over-predictions of the reference setup in under-predictions for the improved setup; the background/industrial sites Vila Nova da Telha and Perafita present increases in concentrations, resulting in a slight over-prediction for the improved setup.

Figure 6.16 shows PM10 daily averages for the reference and improved setup simulations and for observed values, for Matosinhos (traffic site), Vermoim (suburban) and Vila Nova da Telha (industrial).

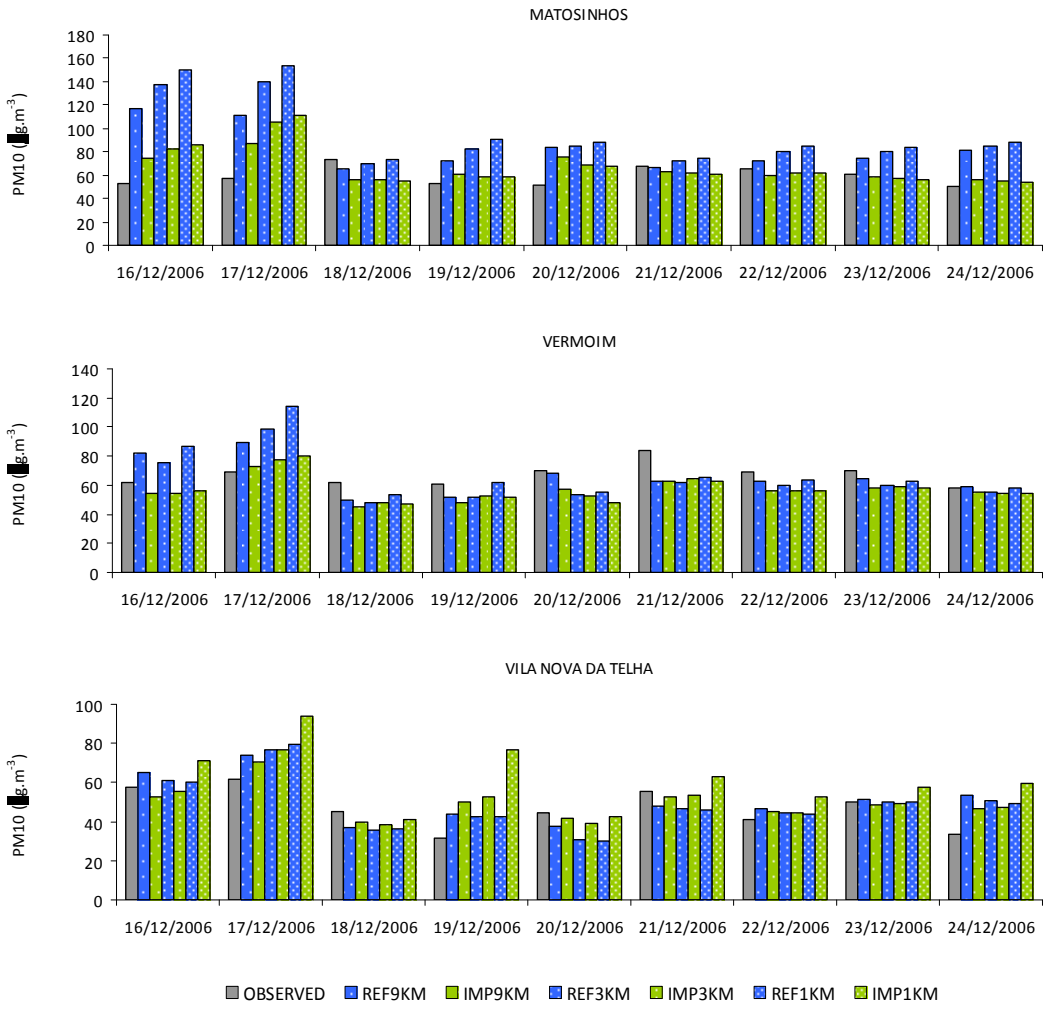

Figure 6.16 CAMx observed, reference setup and improved setup, PM10 daily average concentrations, winter episode.

Figure 6.17 presents the spatial distribution of PM10 daily average differences between the improved and reference setups for a group of days of the episode.

16.12.06 18.12.06

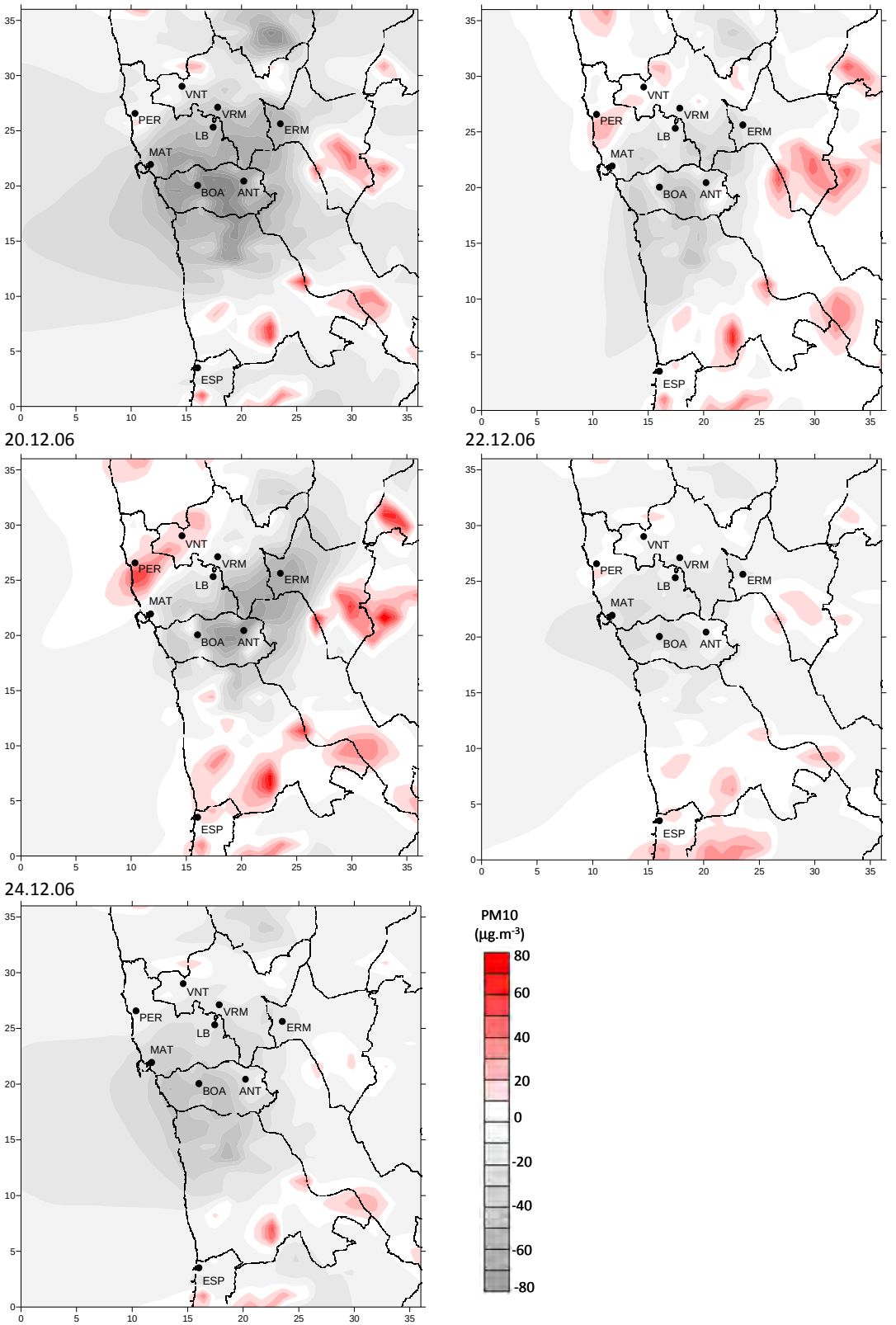

Figure 6.17 Spatial distribution of PM10 daily average differences between the improved and reference setups, winter episode.

The analysis of the two figures shows that for the majority of the sites the improved setup results in a decrease of simulated PM10 concentrations when compared to the reference setup. Only three sites present higher concentrations: Perafita and Vila Nova da Telha during the entire episode, and Espinho

in part of the episode; for the Perafita this means a better performance, while for the other two slightly worst results. For the remaining sites, the negative differences result in a better model performance.

6.6 Final remarks

From the presented above it is possible to conclude that the performance for ozone is better than for particulate matter, namely concerning correlation factors. This is explained by the fact that ozone is a photochemical pollutant, and therefore presents a well defined daily cycle that models are usually able to reproduce quite reasonably [Vautard *et al.*, 2007]. The improved setup also results in lower bias and lower errors; USEPA quality parameters are also better, except for the ability of the modelling system to predict peaks. This is coherent with the BIAS obtained for ozone which, although reduced in the improved setup, reached values around 20 $\mu g.m^{-3}$.

The new methodology for emissions spatial disaggregation improved the spatial distribution of emissions in each municipality, reducing the PM10 over-estimation for the improved setup. However the over-estimation was not eliminated. This may be explained by the over-estimation of PM10 emissions at the municipality level in the national emission inventory, already suggested by Monteiro *et al.* [2007b]. The improved setup also resulted in better correlation coefficients due to the consideration of region-specific emission temporal profiles.

The obtained statistical parameters both for ozone and PM10 are in accordance with those found for other modelling studies [Ferreira, 2007; Monteiro, 2007; Vautard *et al.*, 2007].

As a final remark, it is clear that the new, or improved, modelling system setup constitutes an adequate, valuable and improved tool for the study of urban air quality and its relation with land use in the study area.

7 URBAN DEVELOPMENT SCENARIOS FOR PORTO REGION – AIR QUALITY IMPLICATIONS

In the present chapter two alternative urban development scenarios for the Porto study region are developed and tested through the application of the atmospheric modelling system, which was previously selected and improved.

Firstly, it was necessary to clearly characterize the reference situation, or starting point, including the analysis of the recent urban expansion trends in the study area, the evolution of the population, and the mobility relations between the different urban centres that constitute the study region. This characterization was presented in chapter 4 and established the basis for the development of future scenarios.

Two different and opposite urban development scenarios are developed and simulated - *SPRAWL* and *COMPACT*. The first represents the continuation of the trend observed in the last decades, and can be described as a *business-as-usual scenario*; the second symbolizes the rupture with the current situation through urban containment. In addition, the reference situation, now on referred as *BASE*, is also simulated for comparison purposes.

Meteorological modelling for the three situations – *BASE*, *SPRAWL* and *COMPACT* - is performed for the year 2006; therefore, meteorological differences between the two scenarios, and between each of the scenarios and *BASE*, will steam solely from land use changes. New emission totals and their spatial distribution, resulting from the land use changes, are calculated for the two land use scenarios. Finally, meteorological outputs and new pollutant emissions are fed into the air quality model to determine the changes in air quality resulting from different land use scenarios related to different urban development pathways.

7.1 Scenarios definition

Here, the two scenarios - *SPRAWL* and *COMPACT* – are characterized in terms of land use, population, and pollutant emissions, having *BASE* as a reference.

7.1.1 Land use

The development of the two land use scenarios, is based in the aspects previously described, and is performed over the original CLC2000 land use map, through the alteration of land use type parcels, using the ArcGis software.

7.1.1.1 SPRAWL scenario

The *SPRAWL* scenario corresponds to the business-as-usual scenario, representing the continuation of the last decades trend, with urban areas continuing to expand at much faster rates than population, and urban development spreading throughout the study area, by filling up existing gaps and expanding the boundaries of existing urban areas. All the new residential areas (or urban fabric) take place in the form of discontinuous urban fabric. This urban sprawl scenario results in the smearing out of the region's inhabitants over a large area, thus effectively simulating the sprawl-related growth process.

The urban development process in the period 1987-2000 was analysed for each municipality separately and replicated for *SPRAWL*; the original CLC2000 land use map was changed through the creation of new artificial surface areas, which replaced natural and semi-natural areas.

To illustrate this process, Figure 7.1 and Table 7.1 present the land use changes obtained for Maia municipality.

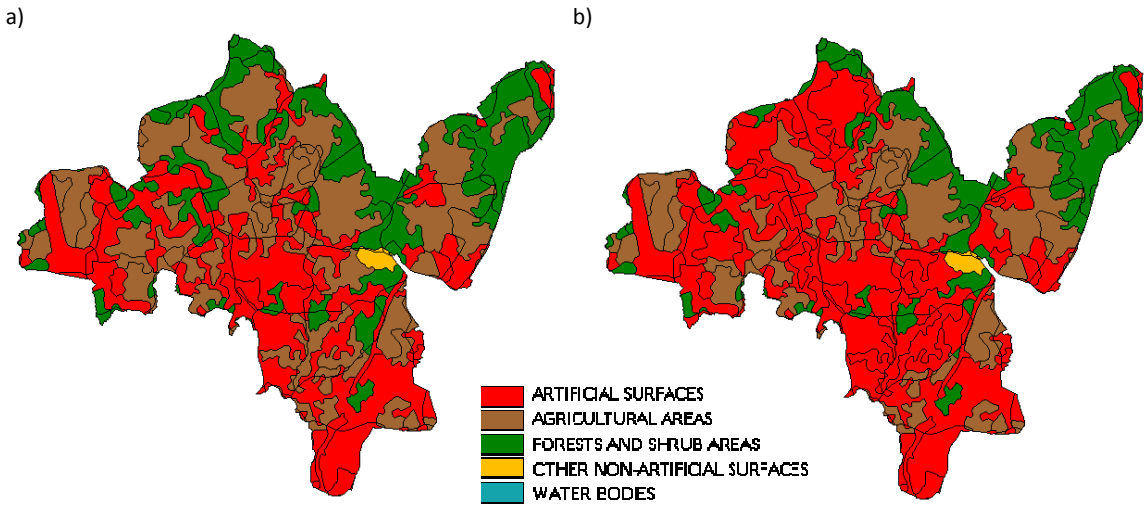

Figure 7.1 Maia land cover maps for a) *BASE* and b) *SPRAWL* scenario.

Maia continues the sprawling process verified between 1987 and 2000, with more than half of its territory composed of artificial surfaces, the great majority of it in the form of discontinuous urban fabric and with increasing areas of industrial and commercial activities. Land cover maps present the replacement of natural and semi-natural areas, not only in the already highly urbanized southern part, by filling up gaps between existing urbanized areas, but also in the less urbanized northern part of the municipality.

Table 7.1 Maia land cover data for the *BASE* and *SPRAWL* scenarios.

Land uses	BASE		SPRAWL		Change	
	hectares	%	hectares	%	hectares	%
Artificial surfaces	3094.3	37.1	4348.5	52.1	+ 1254.2	+40.5
Continuous urban fabric	154.7	5.0	154.7	3.6	0	0
Discontinuous urban fabric	2091.8	67.6	2661.9	61.2	+570.1	+27.3
Industrial or commercial units	520.9	16.8	1204.9	27.7	+684.0	+131.3
Other artificial surfaces	327.0	10.6	327.0	7.5	0	0
Agricultural areas	3138.2	37.6	2382.7	28.6	-755.5	-24.1
Forests and shrub areas	2054.1	24.6	1555.3	18.6	-498.8	-24.3
Other non-artificial surfaces	55.7	0.7	55.7	0.7	0	0

Analogous tables for the remaining municipalities can be found in Appendix F. Similar to the verified between 1987 and 2000, municipalities in the first metropolitan ring around Porto – Maia, Valongo and Vila Nova de Gaia – and Santa Maria da Feira, already highly urbanized (37%, 28%, 38% and 23% respectively), reveal the largest absolute increases of artificial surfaces, over 1000 hectares. Municipalities outside the first metropolitan ring, such as Lousada, Penafiel, Marco de Canavezes and Castelo de Paiva, which already presented the highest growth rates between 1987 and 2000, continue along the same path.

The combined *SPRAWL* land use from each municipality resulted in a new land use map for the study region presented in Figure 7.2, side-by-side with the *BASE* map (CLC2000). The built-up area (artificial surfaces) was increased from 18% to 25% of the total area; a number that can be considered realistic given current trends and the fact that in 1987 the share was 13%. The artificial areas expansion took over agricultural and forested landscapes located in the proximity of already existent urban areas.

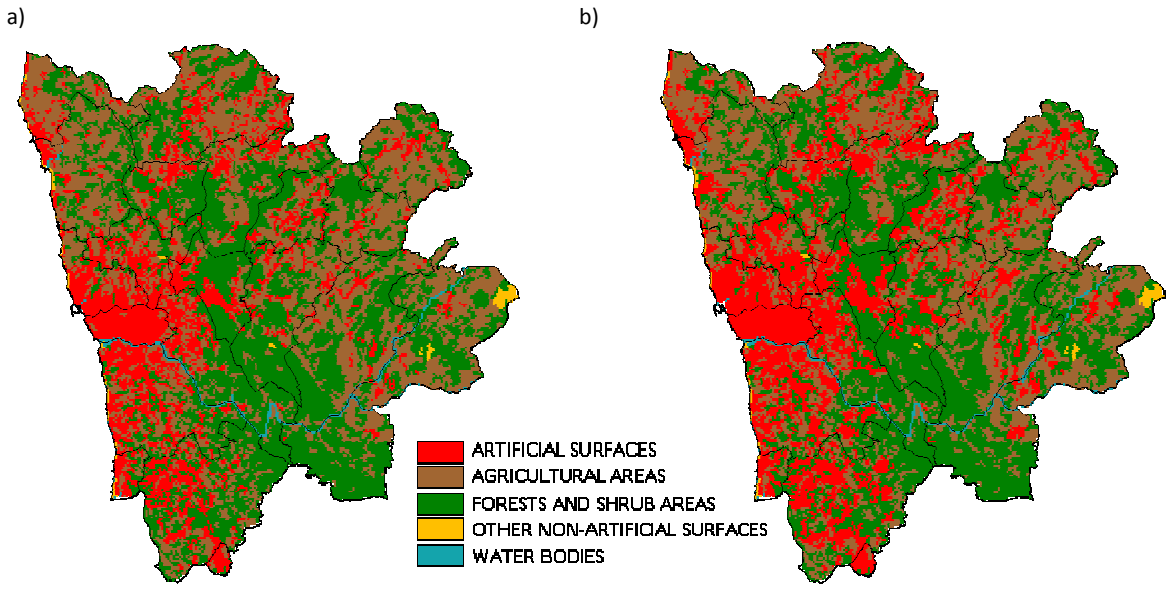

Figure 7.2 Study region land cover maps for a) *BASE* and b) *SPRAWL* scenario.

The land cover maps reveal the expansion of artificial areas not only in the urban centre of the region (Porto, Matosinhos, Gondomar and Vila Nova de Gaia), but also throughout the entire study region. Table 7.2 presents the comparison between the *BASE* and the *SPRAWL* scenario in terms of the total area for each of the 4 large land use categories, and sub-categories, and corresponding share (%), as well as the magnitude of the change.

Table 7.2 Study region land cover data for the *BASE* and *SPRAWL* scenario.

Land uses	BASE		SPRAWL		Change	
	hectares	%	hectares	%	hectares	%
Artificial surfaces	43727.9	18.3	60139.2	25.1	+ 16411.3	+37.5
Continuous urban fabric	4059.2	9.3	4059.2	6.7	0	0
Discontinuous urban fabric	32895.0	75.2	44647.7	74.2	+11752.7	+35.7
Industrial or commercial units	4973.1	11.4	9571.7	15.9	+4598.6	+92.5
Other artificial surfaces	1800.7	4.1	1860.6	3.1	0	0
Agricultural areas	93766.2	39.1	83201.4	34.7	-10564.8	-11.3
Forests and shrub areas	98319.4	41.0	92472.9	38.6	-5846.5	-5.9
Other non-artificial surfaces	3784.9	1.6	3784.9	1.6	0	0

In comparison with *BASE*, in the *SPRAWL* scenario built-up land uses increase 37.5%, with 16400 new hectares. Agricultural areas present the largest decrease, representing now less than 35% of the total area of the region; forest and shrub areas continue to be the dominant land use in the region, with a share around 39%. Regarding the composition of artificial surfaces, the continuous urban fabric loses importance, with no additional areas of this type being created, representing now less than 7% of the artificial surfaces. Discontinuous urban fabric presents the largest increase, almost 12 000 hectares;

industrial and commercial units continue the growth trend verified between 1987 and 2000, with the highest relative growth, almost doubling its presence in the study area.

7.1.1.2 COMPACT

In *COMPACT* the totality of urban growth is accommodated within already existent urban areas, i.e., no additional artificial surfaces are created. The only land-use changes implemented in this scenario concern changes from discontinuous to continuous urban fabric. Therefore, no spatial representation of the *COMPACT* scenario is presented here, since it coincides with the *BASE* maps. Table 7.3 presents the comparison between the *BASE* and the *COMPACT* scenario regarding the total area for each of the four large land use categories, and sub-categories, and corresponding share, as well as the magnitude of the change.

Table 7.3 Study region land cover data for the *BASE* and *COMPACT* scenario.

Land uses	BASE		COMPACT		Change	
	hectares	%	hectares	%	hectares	%
Artificial surfaces	43727.9	18.3	43727.9	18.3	0	0
Continuous urban fabric	4059.2	9.3	4092.1	9.4	+32.9	+0.8
Discontinuous urban fabric	32895.0	75.2	32862.0	75.1	-32.9	-1.0
Industrial or commercial units	4973.1	11.4	4973.1	11.4	0	0
Other artificial surfaces	1800.7	4.1	1800.7	4.1	0	0
Agricultural areas	93766.2	39.1	93766.2	39.1	0	0
Forests and shrub areas	98319.4	41.0	98319.4	41.0	0	0
Other non-artificial surfaces	3784.9	1.6	3784.9	1.6	0	0

7.1.2 Population

As already mentioned in Chapter 4, the population of the study region has been increasing; however, this increase has not been uniform along the region, with municipalities growing at different rates and even decreasing in Porto municipality. Figure 7.3 presents the number of residents per municipality and for the region, for the years 1981 (when available), 1991, 2001 and 2006.

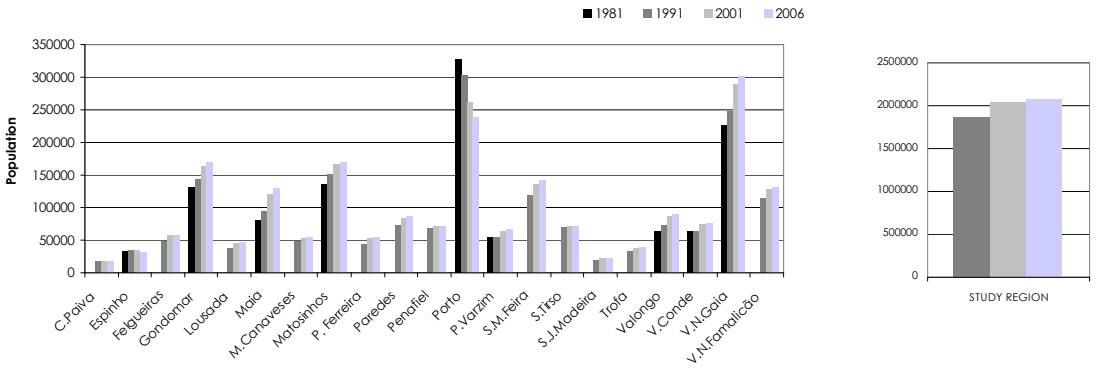

Figure 7.3 Population evolution in the study region.

The study region population increased from 1.86 million people in 1991 to 2.07 million in 2006 (11.3% growth); the rate of growth however has decreased from around +1% per year in 1991-2001, to 0.2% per year, in 2001-2006.

In the 25-years period under analysis, in Porto municipality population presented a decrease of 27%; an important feature of this decrease is that its rate has been accelerating: in the period 1981-1991 the rate was around -0.8%, in 1991-2001 the rate increased to -1.3%, and in 2001-2006 around -1.8%. As a result of this decrease, Vila Nova de Gaia is presently the most populated municipality of the region, with a growth of 33% between 1981 and 2006. The municipality with the highest population growth was Maia, with almost 60% between 1981 and 2006. Other municipalities with high population growth, all above 20% between 1991 and 2006 were: Lousada, Paços de Ferreira, Póvoa de Varzim, Santa Maria da Feira and Trofa.

Taking this into account, both scenarios are developed for a population of 2.2 million people, corresponding to an increase of 220'000 inhabitants (13% increase) in relation to the base year 2000, in what can be considered a 20-year period. This population increase is differently distributed through the municipalities, according to the land use scenario.

Since the *SPRAWL* scenario corresponds to the perpetuation of the past 20 years trend, the population will change accordingly in each of the municipalities, presenting the same growth rates as observed between 1991 and 2001.

In the *COMPACT* scenario however, the trend is interrupted; Porto municipality attracts new residents, and its population is increased. The remaining cities will continue to attract people, but at a rate 25% smaller than the verified in the last years (and therefore also in *SPRAWL*). Figure 7.4 presents the population observed in 1991 and 2000, and considered in *SPRAWL* and *COMPACT*.

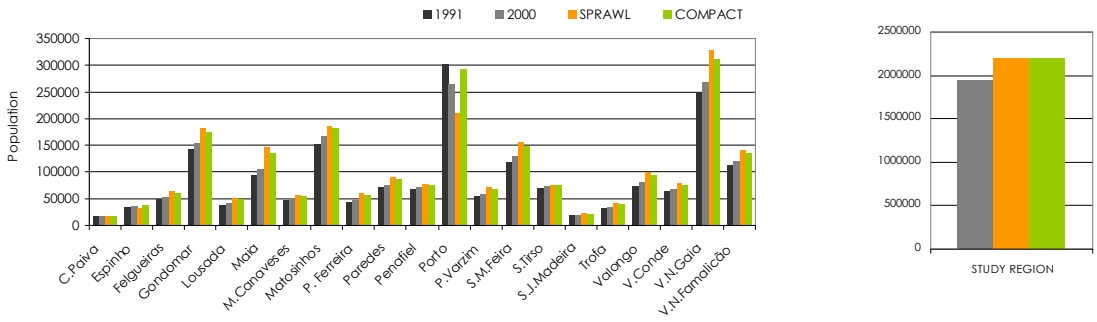

Figure 7.4 Population for the SPRAWL and COMPACT scenarios and its comparison with the population in 1991 and 2000.

In *COMPACT* all the municipalities present a growth in their population, but at a smaller rate than the verified for *SPRAWL*. The exception is Porto, with more inhabitants than those in 2000, but sill less than those registered in 1991.

The population in each municipality is distributed over the land use data for *BASE*, *COMPACT* and *SPRAWL*, according to the disaggregation methodology already described in §62.1. Figure 7.5 presents the results in terms of the number of inhabitants per grid cell of the 1 km resolution simulation domain. *SPRAWL* clearly presents the largest spread of population along the simulation domain and the lowest population density (maximum values are below 9000 inhab.km^{-2}). *BASE* and *COMPACT* show a similar situation, but higher densities are found in the later with maximum values of 11 000 inhab.km^{-2} in comparison with 10 000 inhab.km^{-2} in *BASE*.

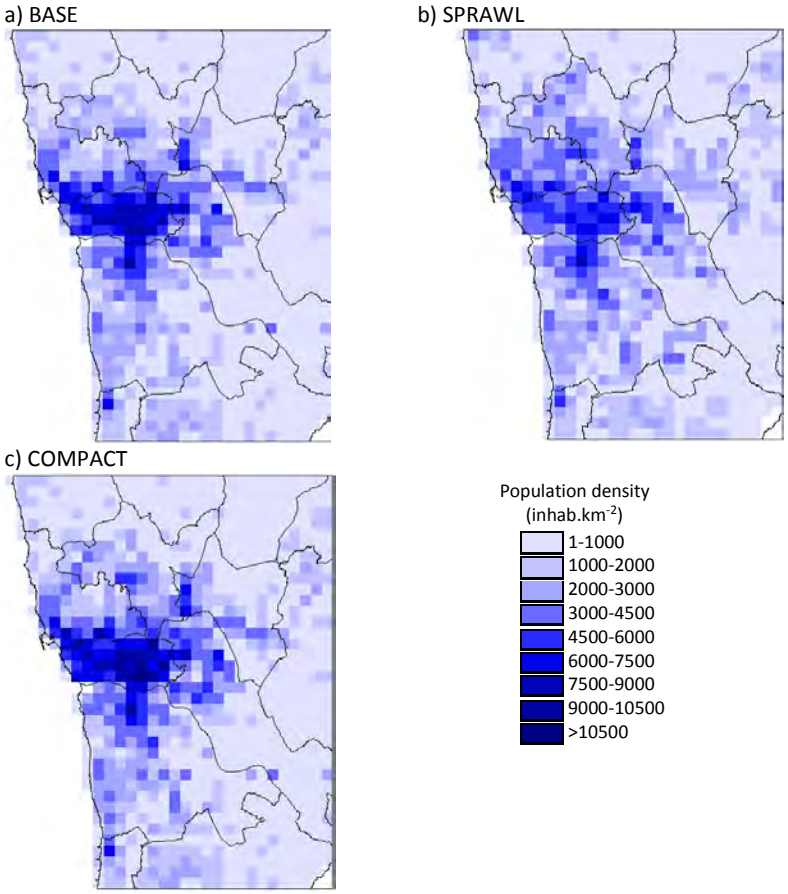

Figure 7.5 Population density for the 1 km resolution simulation domain for a) BASE, b) SPRAWL and c) COMPACT.

This data is fundamental for the further determination of the population affected by air pollutants concentrations in each of the studied scenarios.

Moreover, considering the new land use data and the population per municipality, the residential density, i.e., the number of residents per residential area (residential area is given by the sum of the

continuous and discontinuous urban fabric) is calculated. Figure 7.6 presents residential density for each municipality for 1987 (when available), 2000, *SPRAWL* and *COMPACT*.

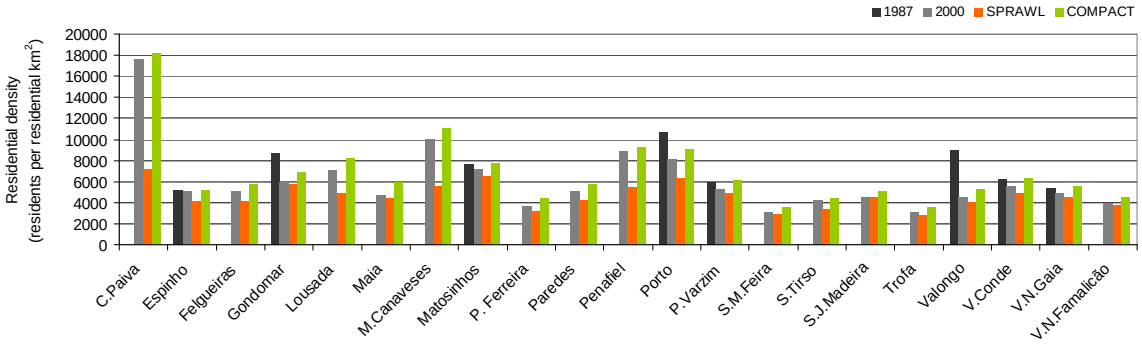

Figure 7.6 Residential density for 1987, 2000, *SPRAWL* and *COMPACT*.

In SPRAWL the residential density decreases for the entire study region, but especially in the municipalities of Porto, Marco de Canavezes and Penafiel; for the last two this is explained by the high increase in residential areas, while for Porto there is a decrease of the number of inhabitants. Castelo de Paiva presents an abnormally high residential density in 2000 (and also in COMPACT) which may result from the fact that a significant part of the population does not live in urban continuous and discontinuous urban land, but probably in agricultural or forested areas. In fact, the artificial surface in this municipality was still very low in 2000, as can be seen in Appendix F.

In the *SPRAWL* scenario, the urban sprawl process induces a population spreading in general, displacing a number of inhabitants from the urban centres to the surrounding areas, and decreasing the population density in the region.

The municipalities for which the population in 1987 was available allowed the calculation of the residential density for 1987 through the use of the CLC90, showing that it is completely pertinent to maintain the urban area at the 2000 levels; for these municipalities the *COMPACT* residential density remains smaller (for Porto, Espinho, Valongo and Goondomar) or slightly higher (Matosinhos, Póvoa de Varzim, Vila do Conde and Vila Nova de Gaia) than the residential density observed in 1987.

7.1.3 Pollutant emissions

As a result of the population growth and the land use changes established for each urban development scenario, new emission totals have to be calculated, as well as their spatial distribution. Land use differences are particularly important for three emission categories - mobile, agriculture and biogenic sources -, with the remaining categories presenting a greater dependence on population.

Available pollutant emission values for NOx, NMVOC, CO, NH_3, PM10 and PM2.5, i.e., the emissions for the *BASE* situation, are the basis for estimating the scenarios emissions. It should be noted that future

emissions do not take into account possible changes in emission factors, transportation patterns, or technology. However, these estimates do provide emission totals and spatial distributions which are consistent with increased urbanization given today's technology and travel behaviour.

7.1.3.1 Non industrial combustion (SNAP2), extraction and distribution of fossil fuels (SNAP5) and solvent use (SNAP6) emissions

New emissions for these three categories are recalculated for each scenario considering the new population in each municipality, and also the change in the artificial surfaces, since these categories represent emissions that related not only to the domestic sector, but also to the commercial and industrial areas. An equal weighting factor of 0.5 was given to each of these factors, population and artificial area. Emissions are calculated considering: i) the new population in each municipality, with emission rates per inhabitant per municipality kept equal to the *BASE* rates; and ii) the new artificial area in each municipality, with emission rates per artificial area per municipality kept equal to the *BASE* rate.

Figures 7.7 and 7.8 present for SNAP2 and for SNAPS 5 and 6, respectively, the yearly emission totals for a selection of pollutants for BASE and the two scenarios.

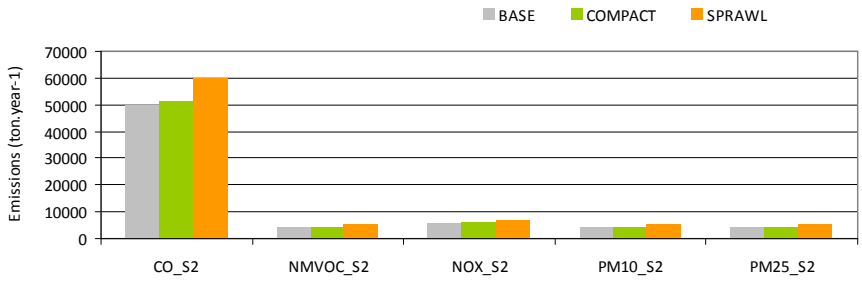

Figure 7.7 Study region SNAP 2 (non-industrial combustion) emissions for *BASE*, *COMPACT* and *SPRAWL*.

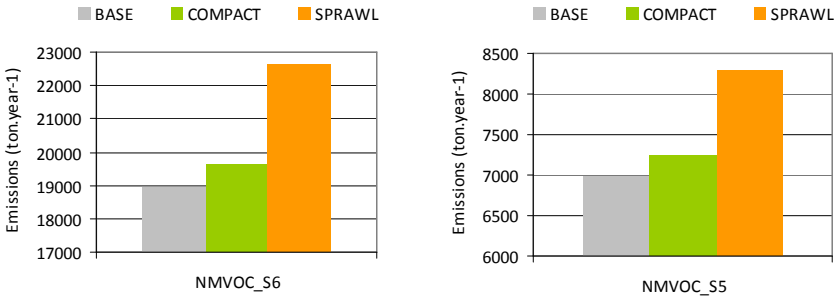

Figure 7.8 Study region SNAP 5 (fossil fuels distribution) and SNAP6 (solvent use) emissions for *BASE*, *COMPACT* and *SPRAWL*.

Emissions for the *COMPACT* and *SPRAWL* scenarios are 4% and 18% higher than the *BASE* emissions, respectively. Although emissions per municipality are not shown, while SPRAWL presents higher totals than *COMPACT* in the study region, in Porto municipality that is not the case. In COMPACT Porto

population increases while in SPRAWL population decreases and the increase in artificial area is insignificant. As a result, in Porto emissions from these three categories are 17% higher for *COMPACT*.

Next, emissions are spatially distributed using the population disaggregated over the *SPRAWL* and *COMPACT* land uses, as described in §6.2. The result is illustrated in Figure 7.10, for SNAP2 NO_x grid emissions at 1 km resolution (*BASE* emissions were already presented in §6.2 – Figure 6.3).

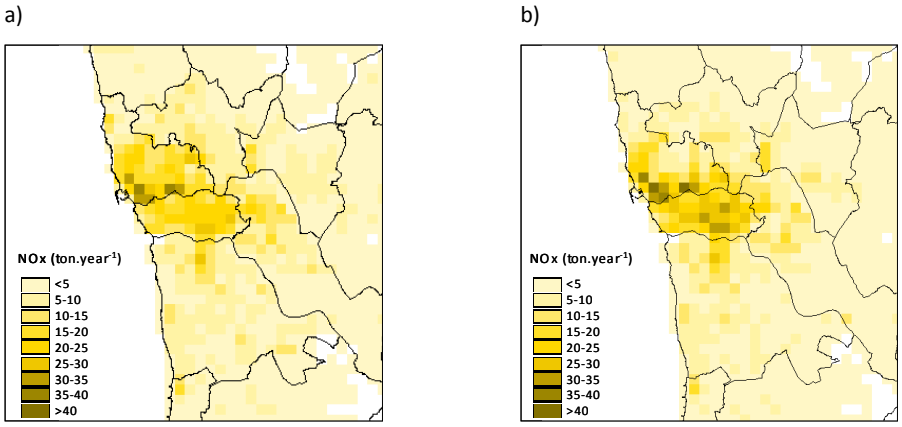

Figure 7.9 SNAP2 NOx grid emissions at 1 km resolution for a) *SPRAWL* and b) *COMPACT*.

For both scenarios emissions are concentrated in the Porto municipality and in the first metropolitan ring municipalities; however *SPRAWL* presents a greater spread of emissions, as a result of the urban growth. The highest emissions rates for grid cell are obtained for the *COMPACT* scenario and the lowest for *BASE*.

7.1.3.2 Industrial combustion (SNAP3) and industrial processes (SNAP4) emissions

Emissions for these two industrial source categories are recalculated for each scenario as follows: with the new population in each municipality and using the share of population employed in the industry of the *BASE*, the number of employees in the industry sector is calculated for each municipality; then, considering emission rates per number of employees in industry per municipality equal to the *BASE* rates, new emission totals are calculated. Figure 7.10 presents the yearly emission totals for SNAP3 and SNAP4; these are very similar for *COMPACT* and *SPRAWL*, and are around 7% higher than *BASE* emissions.

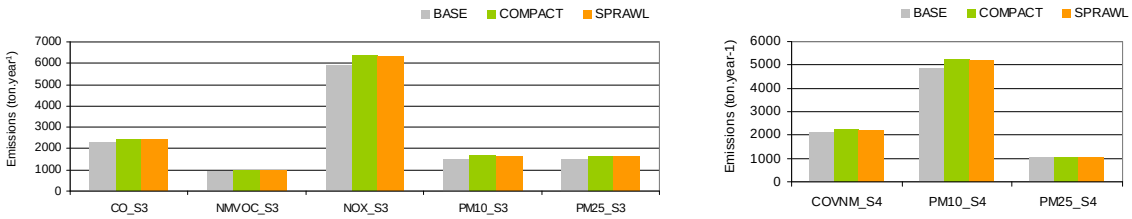

Figure 7.10 Study region SNAP3 (industrial combustion) and SNAP4 (industrial processes) emissions for *BASE*, *COMPACT* and *SPRAWL*.

Emissions were then spatially distributed over the land cover class industrial and commercial units in combination with the number of employees in industry at the municipality level, as described in §6.2. Although not presented, the resulting emissions spatial distribution is very similar for the three situations.

7.1.3.3 Road transport (SNAP7) emissions

Since road transport emissions are highly dependent not only on population distribution but mainly on the mobility of the population, ideally a traffic model should be applied to simulate the effect of urban sprawl on traffic volumes and their spatial distribution. These modelling techniques fall out of the scope of the present work and therefore are not used.

In the present work, to calculate transport emissions resulting from land use changes, a methodology is developed taking into account the population growth, the urban area expansion and the mobility attractiveness/repulsion rates between municipalities. These three factors influence emissions and are considered as follows:

i) The growth of the population causes an increase in the number of trips. For each municipality it was assumed that the emissions are proportional to the number of trips, which in turn is proportional to the number of residents.

ii) The growth of the urban area causes an increase in the mean distance from home to employments and leisure destinations. The residents in new urbanized areas find themselves more distant from locations where most employments are concentrated, while the residents in already existent urban areas will find possible employment and leisure destinations in the newly built areas in the periphery. For each municipality it was assumed that the emissions are proportional to the mean travel distance, which in turn is proportional to the urban area's radius. For example, in *SPRAWL* Maia's urban area increases by a factor of 1.4; therefore the mean travelled distance increased by a factor of $1.4^{1/2}=1.185$; in *COMPACT* the factor is 1 since no urban growth was verified.

iii) An additional factor related to attraction/repulsion rates between municipalities has to be considered since traffic emissions are not only dependent on the population and urban area, but also on the mobility of people between municipalities. The attraction/ repulsion rates calculated for *BASE*, presented in §4.3 are maintained and used for both scenarios.

The distribution of emissions between municipalities is very different for both scenarios, as illustrated in Figure 7.11, which presents CO yearly emission totals for non-motorways road transport emissions for each municipality and for the entire study area.

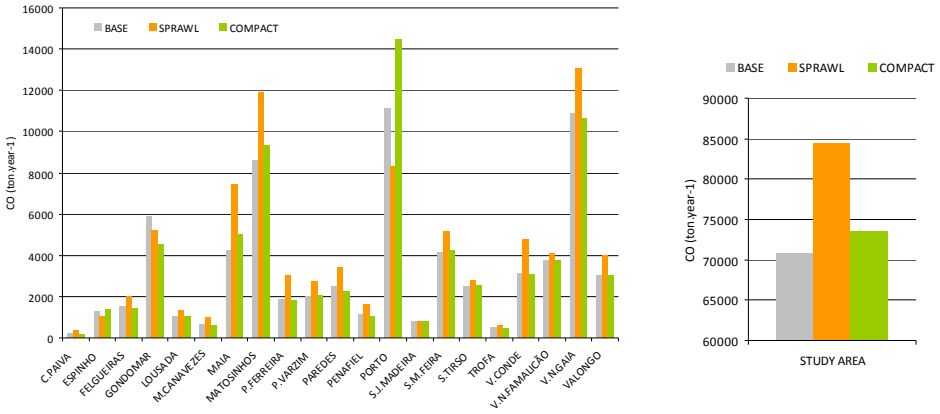

Figure 7.11 Study region SNAP7 (non-motorways road transport) CO emissions for *BASE*, *COMPACT* and *SPRAWL*, for each municipality and for the entire study area.

Resulting emissions are higher for *SPRAWL*, which are 19% higher than the *BASE* emissions, while *COMPACT* emissions are only 4% higher. The largest differences between scenarios are found for Porto (25% lower than the *BASE* emissions for *SPRAWL*, and 30% higher for *COMPACT*), Matosinhos (+38% for *SPRAWL*, +8% for *COMPACT*), Vila Nova de Gaia (+20% for *SPRAWL*, -2% for *COMPACT*) and Maia (+56% for *SPRAWL*, +9% for *COMPACT*).

Regarding the spatial distribution of emissions, Figure 7.12 presents SNAP7 non-motorway CO grid emissions at 1 km resolution for *SPRAWL* and *COMPACT* (*BASE* emissions were already presented in §6.2 – Figure 6.6). For both scenarios, emissions are concentrated in the Porto, Matosinhos, Maia, NW Gondomar and Vila Nova de Gaia municipalities; however *COMPACT* presents a greater concentration of emissions, as a result of the urban containment, and therefore higher emission rates.

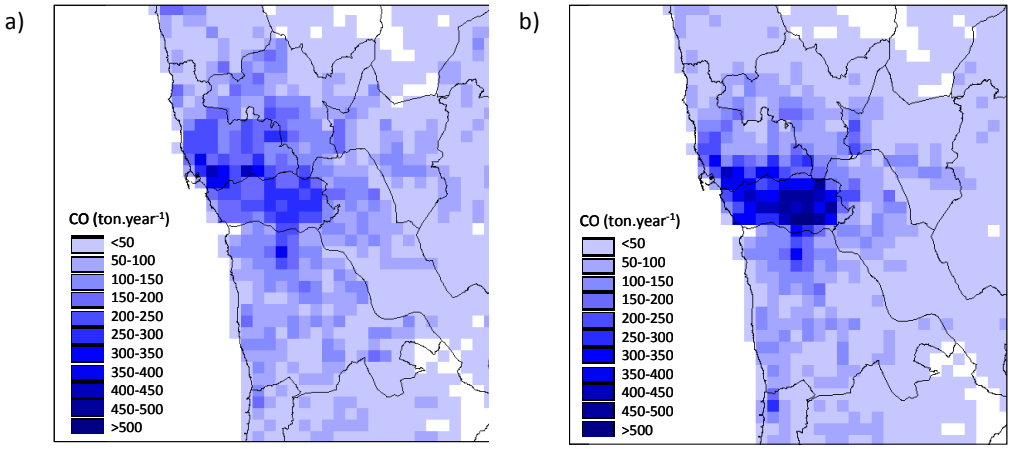

Figure 7.12 SNAP7 (non motorway road transport) CO grid emissions at 1 km resolution for a) *SPRAWL* and b) *COMPACT*.

7.1.3.4 Other mobile sources (SNAP8) and waste treatment (SNAP9) emissions

The estimation of new emissions for these categories took into account the new population in each municipality, with emission rates per inhabitant per municipality kept equal to the *BASE* rates, for each category. Figure 7.13 presents SNAP9 yearly emission totals for *BASE*, *COMPACT* and *SPRAWL*; emissions for the *COMPACT* and *SPRAWL* scenarios are 7% and 6% higher than the *BASE* emissions, respectively. The same analysis applies to SNAP8.

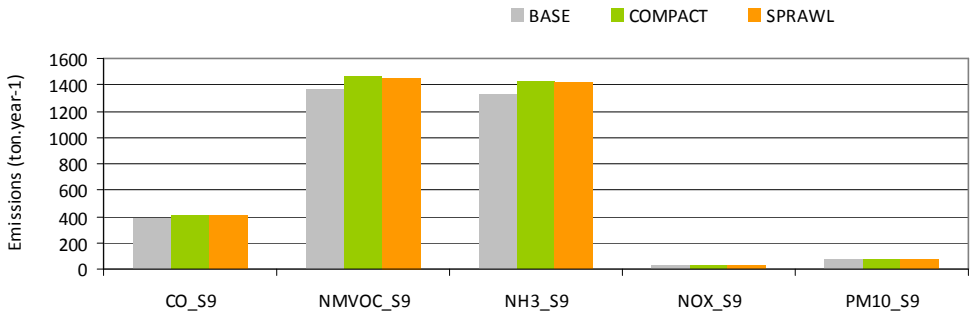

Figure 7.13 Study region SNAP9 (waste treatment and disposal) emissions for BASE, COMPACT and SPRAWL.

The resulting emissions spatial distribution is illustrated in Figure 7.14, for NH_3 SNAP9 grid emissions at 1 km resolution in *BASE*, *SPRAWL* and *COMPACT*.

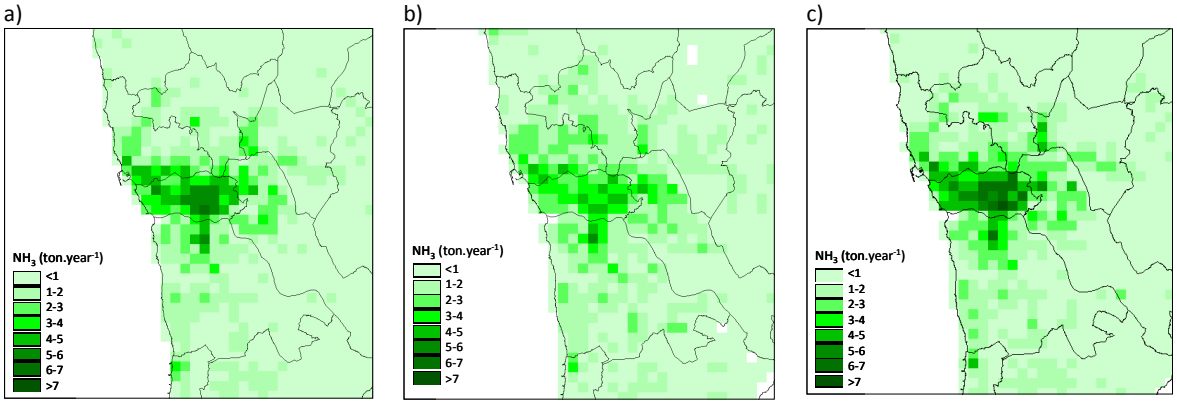

Figure 7.14 SNAP9 (waste treatment) NH_3 grid emissions at 1 km resolution for a) *BASE*, b) *SPRAWL* and c) *COMPACT*.

Similarly to the verified in other sectors, SPRAWL presents a higher dispersion of emissions and lower emission rates in comparison with BASE and COMPACT; on the other hand, the containment of urban expansion, and therefore of population in COMPACT results in the highest emission rates.

7.1.3.5 Agriculture (SNAP10) emissions

New emissions for the agriculture category were recalculated considering the new agricultural area in each scenario, with emission rates per agricultural area per municipality kept equal to the *BASE* rates.

Since the *COMPACT* scenario presents no changes in agricultural area in relation to the *BASE*, emission totals, as well as their spatial distribution are the same. Figure 7.15 presents the obtained results.

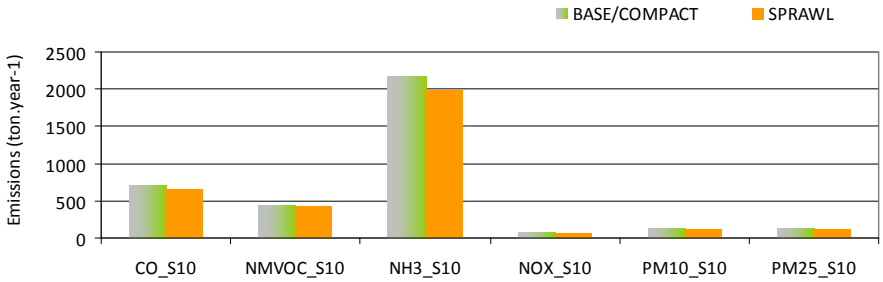

Figure 7.15 Study region SNAP10 (agriculture) emissions for BASE/COMPACT and SPRAWL.

As a result of the transformation of agricultural areas into artificial land use, agriculture emissions were reduced by almost 10% in SPRAWL. The resulting emissions spatial distribution is illustrated in Figure 7.16, for NH_3 grid emissions at 1 km resolution for BASE/COMPACT and SPRAWL scenarios.

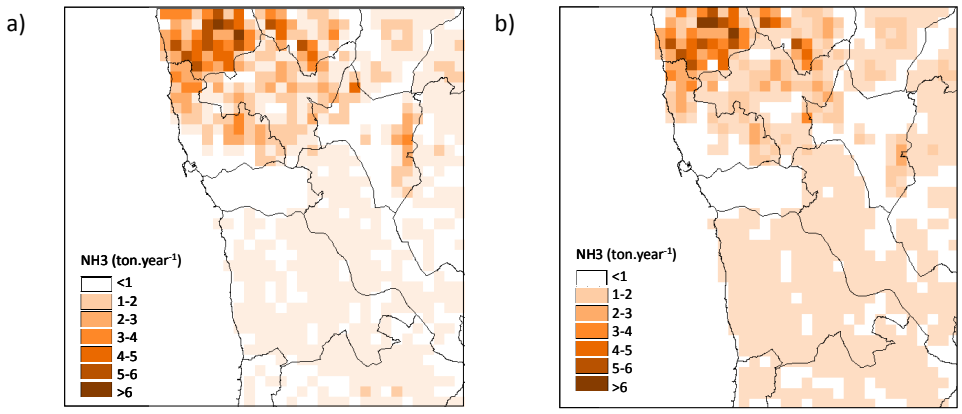

Figure 7.16 SNAP10 (agriculture) NH_3 grid emissions at 1 km resolution for a) *BASE/COMPACT* and b) *SPRAWL*.

The consumption of agricultural land for urbanization purposes in SPRAWL is clearly visible in the figure, in the form of a larger area occupied by blank grid cells (zero emissions from agriculture), in comparison with BASE and COMPACT.

7.1.3.6 Biogenic emissions

Biogenic emissions were calculated for the forested areas according to the methodology previously described in 5.3.1. Differences in relation to *BASE* result from the conversion of forested areas to artificial areas, and also from temperature changes induced by land use changes; these only take place in the *SPRAWL* scenario, since in *COMPACT*, the forest land use are not changed in relation to *BASE*. Therefore, as a result of land use changes biogenic *SPRAWL* emissions are lower when compared to *BASE* (and *COMPACT*): 20% lower for monotherpene and 16% lower for isoprene.

7.1.3.7 Total emissions

The above presented methodology results on different emission totals for both scenarios. Figure 7.17 shows emission totals for the study region for *SPRAWL* and *COMPACT* as well as for *BASE*.

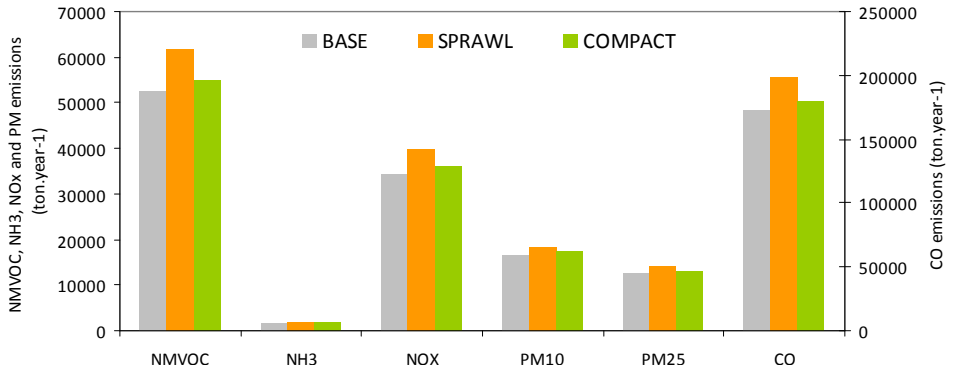

Figure 7.17 Study region total NMVOC, NH_3, NO_x, PM and CO emissions for *BASE*, *SPRAWL* and *COMPACT*.

Lower emissions are obtained for BASE and higher for SPRAWL; SPRAWL emissions are around 9% to 17% higher than BASE emissions (for NH_3 and NMVOC, respectively), while COMPACT emissions are 4% to 6% higher (for NH_3 and NMVOC, respectively).

Figure 7.18 shows the spatial distribution of CO, NMVOC, NOx and PM10 gridded emission totals for the 1 km resolution domain for *SPRAWL* and *COMPACT*. COMPACT emissions are more concentrated over Porto municipality and present higher emission rates per grid cell; SPRAWL presents more scattered emissions throughout the simulation domain, and therefore lower emission rates. Emissions of NMVOC constitute an exception, because they are highly related with the port activity in Matosinhos, and therefore present higher values for this municipality in both scenarios.

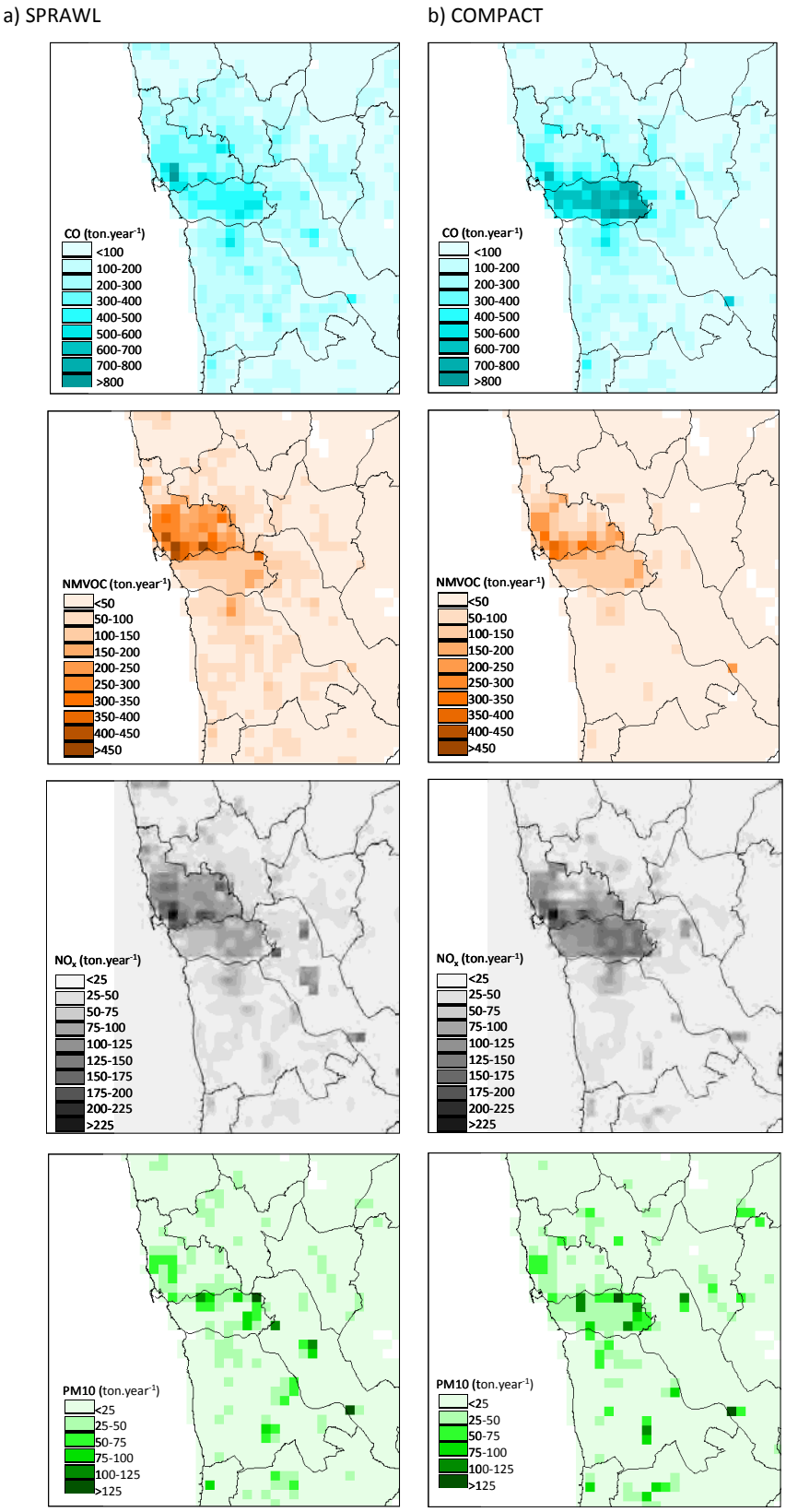

Figure 7.18 Spatial allocation of CO, NMVOC, NOx and PM10 total emissions at 1 km resolution for a) *SPRAWL* and b) *COMPACT*.

7.2 Base long-term simulations

Aiming to provide a thorough analysis of the air quality impacts of different urban land use scenarios, the atmospheric simulation of BASE and scenarios is performed for a one-year period, covering a wide range of air pollution conditions. The year of 2006 was the selected meteorological year to be simulated, as already discussed in 4.1. All the aspects regarding the meteorological model and its application were described in detail in Chapter 5, which allowed the choice and development of the most adequate model configuration for the study area.

7.2.1 Meteorological modelling

For *BASE* the simulation was performed with land use data from 2000 since no data is available for 2006. No extensive validation was performed since the model configuration was considered adequate in the sensitivity tests and validation procedures presented in the previous chapter. However, some results are presented here for Porto/Pedras Rubras meteorological station.

Figure 7.19 shows the time-series comparison of surface temperature and wind components for observed and *BASE* simulated values.

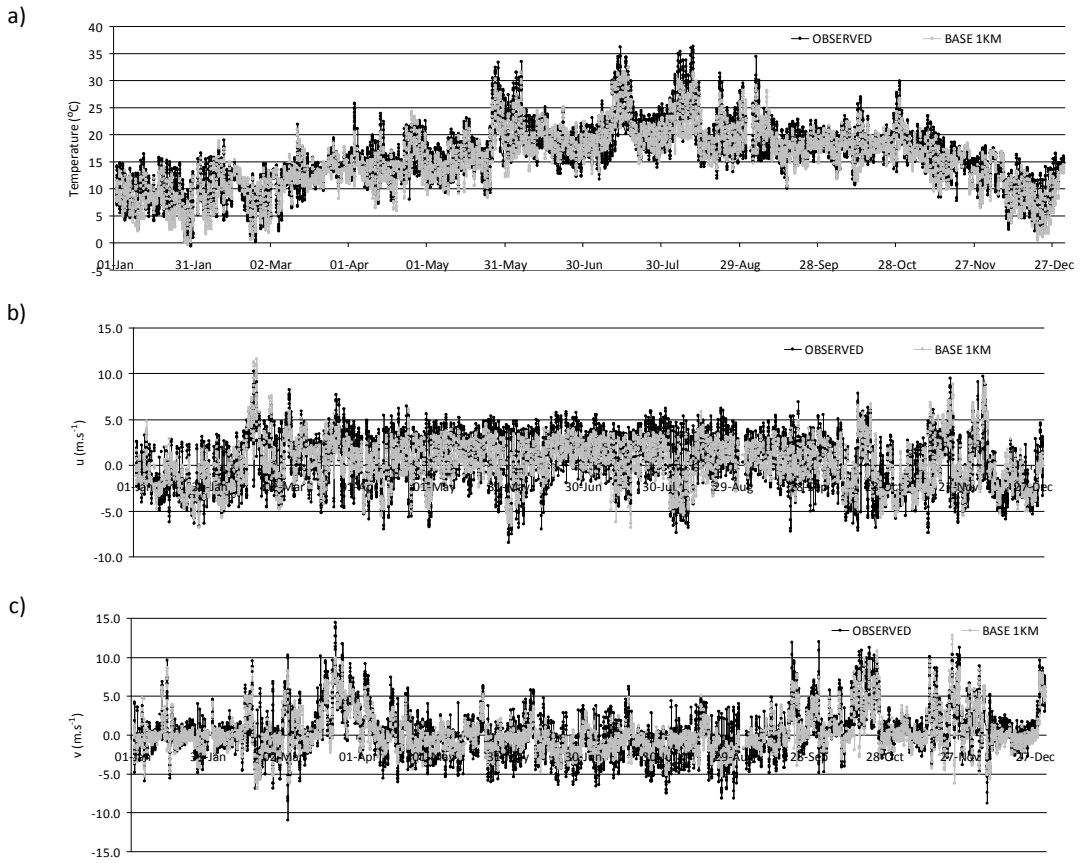

Figure 7.19 Observed and *BASE* (1-km resolution) time-series comparison of surface a) temperature, b) zonal wind component and c) meridional wind component, at Porto/Pedras Rubras meteorological station.

Concerning temperature, simulated values follow the distribution of the observed ones; a general under-estimation of temperature is visible, especially for the higher temperatures registered at the end of May / beginning of June, July and August. Simulated wind components present a smaller variability when compared with observed ones, but also follow the observed trend.

Figures 7.20 and 7.21 present the statistical analysis of BASE 1-km and 3-km resolution simulations, for Porto/Pedras Rubras, using the parameters already described in §5.2. For temperature (Figure 7.20) besides the referred statistical parameters, the average and the standard deviation (STD) are also shown. Results from both resolutions are similar, with the 3 km resolution presenting a better correlation and a better S/Sobs; the 1 km resolution has lower errors as expected by the smaller under-estimation. Average temperature and STD are lower than the observed; however, the 1 km resolution simulated temperature is slightly higher and therefore closer to the observed.

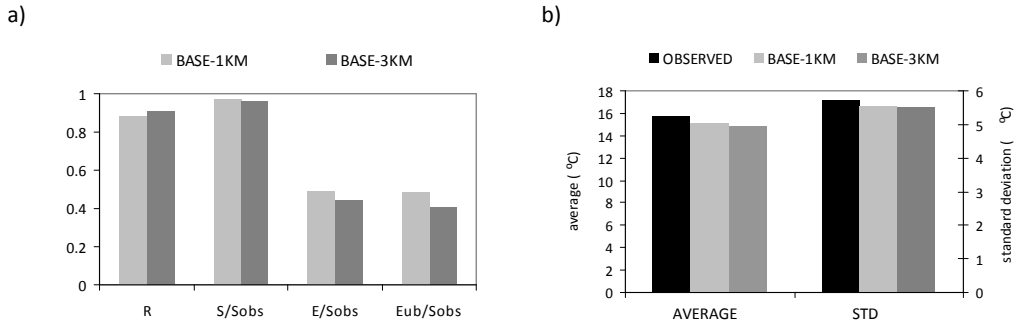

Figure 7.20 Surface temperature a) statistical parameters for *BASE* 1-km and 3-km resolution, and b) observed and simulated (*BASE* 1-km and 3-km resolution) average and standard deviation.

The obtained statistical parameters for the wind components are shown in Figure 7.21. As expected, results are not as good as for temperature, with lower correlation coefficients and higher errors. The meridional wind component is better simulated than the zonal one.

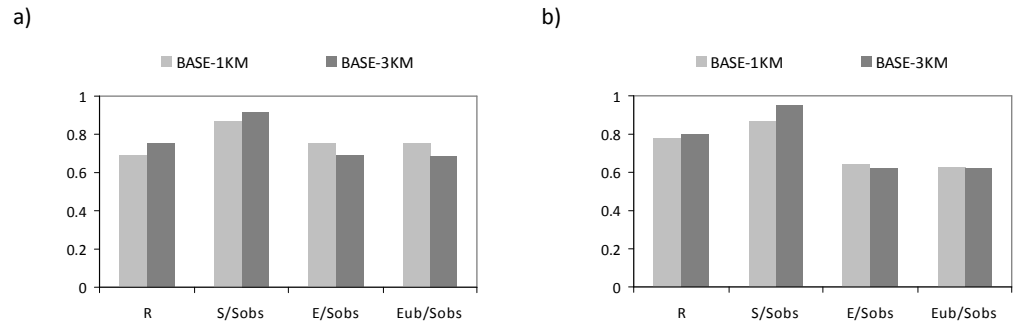

Figure 7.21 Statistical parameters for *BASE* 1-km and 3-km for surface a) zonal wind component and b) meridional wind component.

Overall, the meteorological simulation reveals a good performance for the three meteorological variables, with statistical parameters presenting a reasonable behaviour ($S \approx S_{obs}$, $E < S_{obs}$ and $E_{UB} < S_{obs}$).

7.2.2 Air quality modelling

Here the air quality results for the annual simulation of *BASE* are presented. The air quality model configuration and its application are described in detail in chapter 6.

For *BASE* the simulation used emissions data for 2005 (there are no emission estimates for 2006, since the national inventory is updated with a 2-year periodicity). No extensive validation was performed for the *BASE* simulation; however, some results are presented here.

Table 7.4 shows the statistical results for ozone and PM10, averaged over the air quality monitoring sites, for simulation domains 2 and 3. For ozone statistical parameters are given considering the entire year (from January to December) and considering only the summer months (April to September).

Table 7.4 CAMx statistical results obtained for O_3 and PM10.

	Ozone 3 km resolution (D2)			Ozone 1 km resolution (D3)		
	r	BIAS ($\mu g.m^{-3}$)	MQE ($\mu g.m^{-3}$)	r	BIAS ($\mu g.m^{-3}$)	MQE ($\mu g.m^{-3}$)
ANNUAL	0.64	-21.8	3.7	0.64	-22.9	4.0
SUMMER	0.66	-20.4	3.6	0.65	-23.0	3.1
	PM10 3 km resolution (D2)			PM10 1 km resolution (D3)		
	r	BIAS ($\mu g.m^{-3}$)	MQE ($\mu g.m^{-3}$)	r	BIAS ($\mu g.m^{-3}$)	MQE ($\mu g.m^{-3}$)
ANNUAL	0.53	-9.2	3.2	0.53	-7.7	3.1

The results show correlation factors in the order of 0.65 for O_3 and 0.53 for PM10, independent of the resolution considered. The BIAS for PM10 ranges from -7.7 (for the 1 km resolution) to -9.2 $\mu g.m^{-3}$ (for the 3 km resolution); for O_3 deviation are higher, around -20 $\mu g.m^{-3}$. The MQE for both pollutants varies from 3 to 4 $\mu g.m^{-3}$. These statistical parameters are within the range of statistical parameters obtained with this and other air quality modelling systems [Holmes and Morawska, 2006; Ferreira, 2007; Monteiro *et al.*, 2007a; Vautard *et al.*, 2007].

For ozone, differences between summer and annual statistics are not discernible. The obtained negative BIAS shows that the model is over-predicting O_3 and PM10 concentrations. The time-series analysis for the air quality monitoring stations reveals that the modelling system over-predicts ozone lower concentrations, and under-predicts the ozone and PM10 concentration peaks. The observed ozone under-prediction is intimately related with the temperature under-prediction in the summer months discussed in §7.2.1.

In addition to the statistical analysis of the model performance, another possible and interesting exercise is the comparison of observed and simulated BASE concentrations in terms of the legislated values for O_3 and PM10. In this scope, Figure 7.22 a) presents the number of exceedances to the PM10

daily limit value (50 µg.m^{-3}, not to be exceed more than 35 days along the year, indicated by the red line) observed and BASE simulated; Figure 7.22 b) shows the annual average observed and *BASE* simulated and their comparison with the annual limit value (40 µg.m^{-3}, indicated by the red line).

a) b)

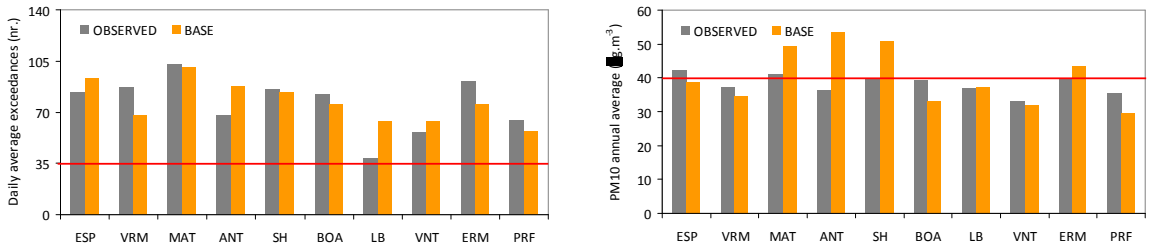

Figure 7.22 Observed and BASE a) number of exceedances to PM10 daily limit value, and b) PM10 annual average.

Regarding the number of daily average exceedances the model, although the higher over-prediction at Antas, and Leça do Balio, and the under-prediction at Vermoim and Ermesinde, correctly identifies that all the air quality monitoring sites are not in compliance with the legislation. Except for Espinho and Antas, the model successfully simulates the annual average, with Matosinhos, Senhora da Hora and Ermesinde presenting values above the allowed 40 µg.m^{-3}.

Figure 7.23 a) shows the number of annual exceedances to the ozone information threshold (180 µg.m^{-3}) observed and *BASE* simulated. Although not legislated, ozone daily maximum values are usually analysed in model validation exercises (Vautard *et al.*, 2007), therefore Figure 7.27 b) presents the ozone mean daily maxima, observed and *BASE* simulated, for the summer months (April to September).

a) b)

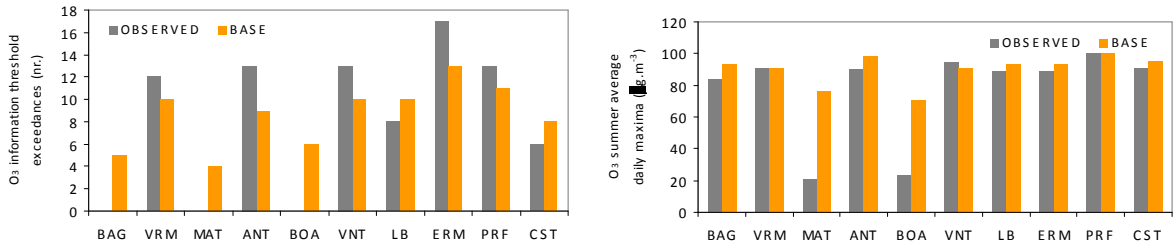

Figure 7.23 Observed and BASE a) number of exceedances to O_3 information threshold, and b) O_3 mean daily maxima for summer months.

Model results point to exceedances to the ozone information threshold in Baguim, Matosinhos and Boavista, while these have not been observed; for the remaining air quality sites, the model presents a good agreement with observations. The same is valid for ozone summer average daily maxima.

7.3 Scenarios long-term simulations

Here the scenarios above described and associated land use change maps and emissions files are used to assess the effects of urban structure on the urban air quality levels, through the application of the selected and improved air quality system. The results of the *BASE* simulation constitute the base-case against which the SPRAWL and *COMPACT* scenarios are compared.

7.3.1 Meteorological modelling

As for BASE, the *SPRAWL* and *COMPACT* meteorological simulations are performed for 2006 meteorological year, using the land use data produced according to the procedure described in §7.1.1. Since for *COMPACT* the land use is very similar to that of *BASE* (the only change concerned the conversion of a few hectares of discontinuous urban fabric to continuous urban fabric), meteorological results from *COMPACT* only present very small temperature differences in relation to *BASE*. Therefore, from now on, and for meteorological purposes, no distinction is made between *BASE* and *COMPACT*.

Taking into consideration that the most widely recognized meteorological effect of urbanization is the urban heat island effect and because of the recognized influence of urban temperatures on ozone formation, hereafter the meteorological analysis will be focused on surface temperature.

SPRAWL meteorological simulations produced a domain-averaged annual temperature increase of approximately 0.4 °C. This is attributed to the increased share of built-up areas in the domain, which convert incoming radiation to sensible heat rather than to latent heat (evaporation), owing to the limited water availability in artificial surfaces characterized by impervious materials. However, in some regions and for certain time-periods differences between scenarios reached significantly higher values than the average.

Figure 7.24 presents the differences between *COMPACT* and *SPRAWL* annual simulations for hourly surface temperature, at Porto/Pedras Rubras meteorological site, with 1 km and 3 km resolution. Although the land use in Porto/Pedras Rubras was not changed, there were temperature differences as high as 2.5°C between the two simulations. These differences indicate that changes in meteorological parameters are not necessarily confined to the cells where the land use pattern was modified.

a)

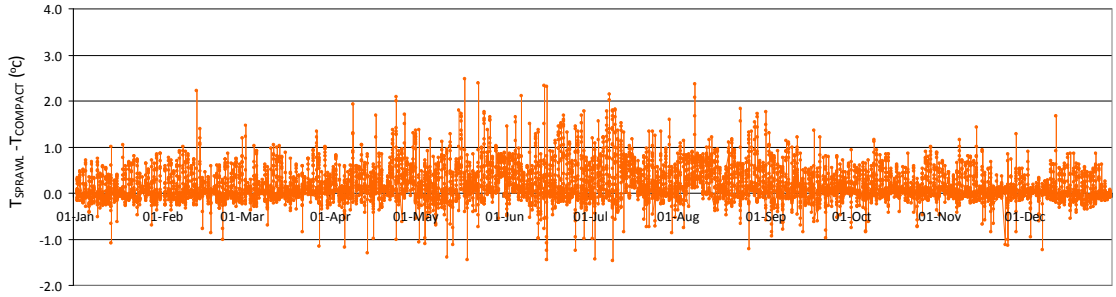

b)

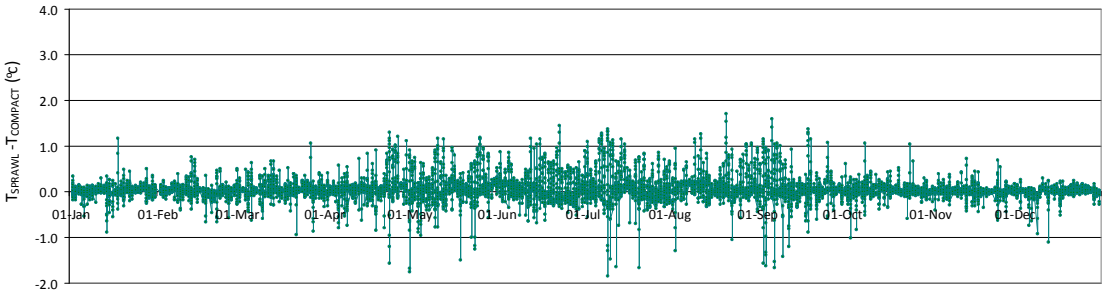

Figure 7.24 Hourly surface temperature differences between *SPRAWL* and *COMPACT* for Porto/Pedras Rubras meteorological site for a)1-km resolution, and b) 3-km resolution.

Higher differences (from -1.5°C to +2.5°C) are more frequently found for the 1km resolution, as expected from the higher resolution and therefore most detailed description of land use. For the 3 km differences go from -1.8°C to +1.8°C. Also, higher differences are found in the summer months, i.e., from April to September, since higher temperatures are also reached, and therefore meteorological differences are enhanced.

While temperature increases would be expected with increasing urbanization, due to the urban heat island effect, temperature decreases are also verified. Local temperature increases in grid cells with modified land use could have lead to higher wind speeds and increased instability which, downwind can lead to areas of increased vertical mixing and decreased surface temperatures.

As already mentioned in Chapter 5, the Porto/Pedras Rubras meteorological station is located in a rural environment, and consequently does not capture the features of an urban region, where differences between both scenarios are likely to be higher. Therefore, to capture the changes in an urban area, the same analysis was performed for Maia, one of the municipalities with a larger increase in artificial surface (Figure 7.25).

a)

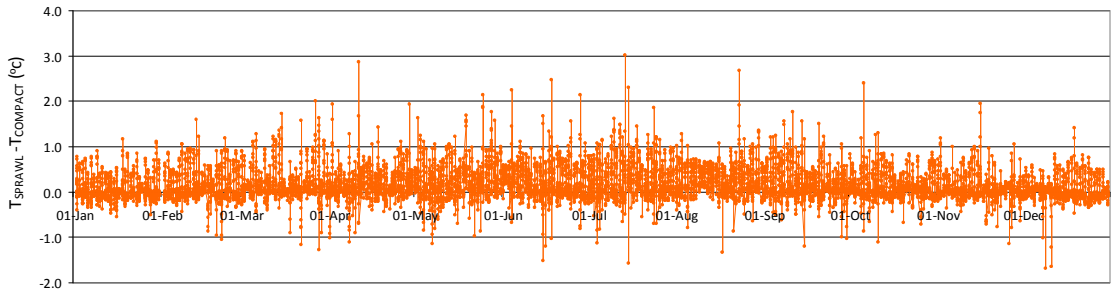

b)

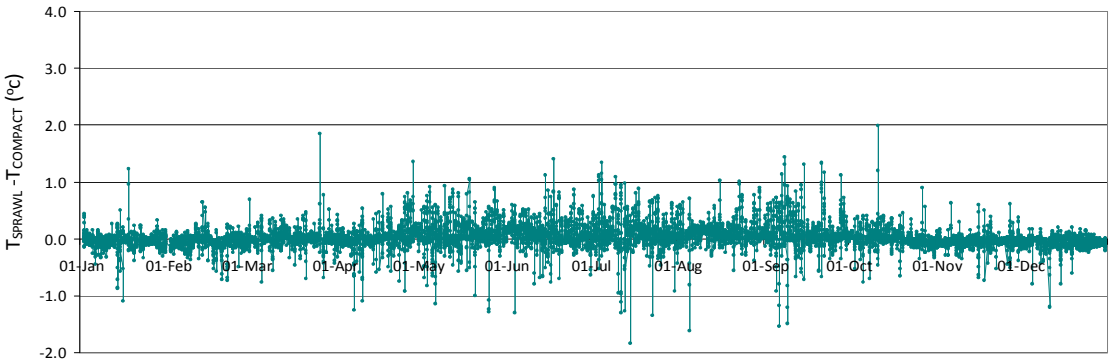

Figure 7.25 Hourly surface temperature differences between *SPRAWL* and *COMPACT* for Maia municipality for a)1-km resolution, and b) 3-km resolution.

For Maia municipality, temperature differences range from -1.5°C to +3°C, for the 1-km resolution, and from -1.8°C to 2°C for the 3-km resolution. Hence, while for the 3-km resolution no differences in the temperature range are found between the rural site (Porto/Pedras Rubras) and the urban site (Maia), for the 1-km resolution the urban site presents higher temperature increases. Again, the summer months present the largest differences, with July showing the highest temperature diference (+3°C in Jul 14th at 15:00).

To illustrate the spatial extent of effects of land use changes in temperature, the average afternoon (12:00 – 18:00) temperature differences for July are shown in Figure 7.26. For July, average afternoon temperature differences range from about -1.2°C to +1.4°C, with largest increases occurring over Vila do Conde, Maia, Matosinhos, Porto and Gondomar, i.e., municipalities in the first metropolitan ring, which present some of the largest urban expansion.

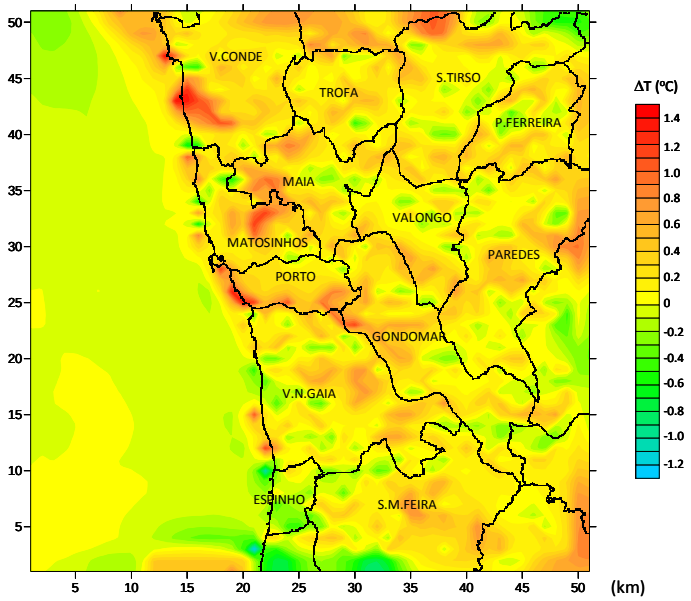

Figure 7.26 July differences between SPRAWL and COMPACT afternoon (12:00 – 18:00) average surface temperature fields between at 1 km resolution.

The observed changes are consistent with the substantial increases in urban surfaces across large parts of the model domain, and the spatial pattern of the temperature changes generally matches the area of increased urbanization. This is quite evident for the coastal part of Vila do Conde, NE Matosinhos and SE Vila Nova de Gaia.

The temperature differences obtained as a result of land use changes are consistent with previous research by Civerolo *et al.* [2000, 2007] and De Ridder *et al.* [2008b], although these authors conducted research only for episodic air pollution situations.

Although not presented, the SPRAWL scenario with its increased urban land cover also had a noticeable effect on surface layer winds across the metropolitan region, generally leading to a slight increase in wind speed.

7.3.2 Air quality modelling

For *SPRAWL* and *COMPACT*, simulations are performed with land use and emissions data produced according to the procedures previously described. Meteorological inputs are given by the respective MM5 annual simulation.

Results from the two scenarios are analysed against the *BASE* simulation and against each other in order to identify the main differences between them. The following analysis is performed separately for PM10 and ozone.

7.3.2.1 PM10

Figure 7.27 presents the spatial distribution of PM10 annual average concentrations calculated for *BASE*, *SPRAWL* and *COMPACT*, highlighting the areas for which the legislated annual limit value (40 µg.m^{-3}) is exceeded.

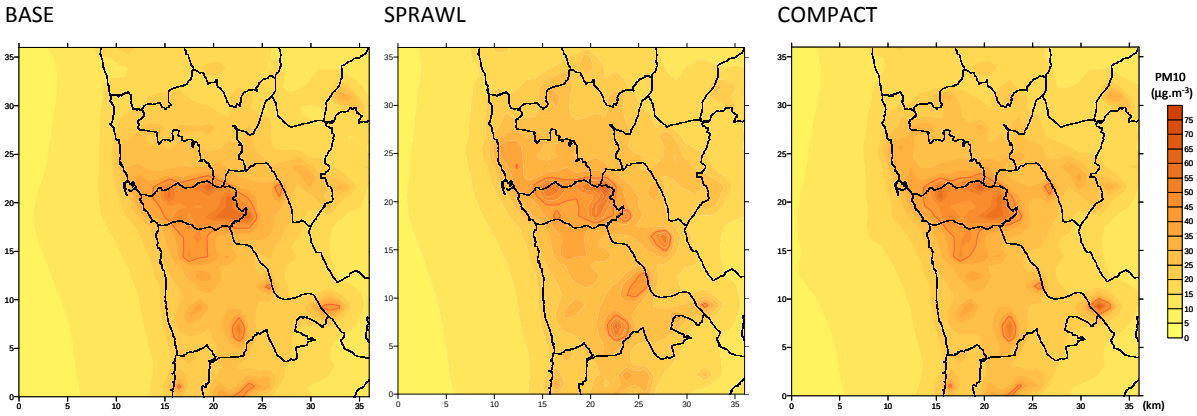

Figure 7.27 PM10 annual average for BASE, SPRAWL and COMPACT (the orange lines surround the areas for which the legislated annual limit value is exceeded).

BASE and *COMPACT* present a larger area of high PM10 annual averages (> 40 µg.m^{-3}) over Porto municipality and its immediate surroundings, in comparison to *SPRAWL*. This is because the *SPRAWL* scenario implies a further decrease in Porto's population, and therefore emissions, and a consequent increase in neighbouring municipalities. The result is a decrease of emissions in Porto and therefore in pollutants concentrations. Nevertheless, considering the entire simulation domain, *SPRAWL* shows the highest PM10 annual concentrations (> 70 µg.m^{-3}), and larger areas above the annual limit value in Gondomar and Vila Nova de Gaia. The comparison between *COMPACT* and *BASE* suggests that the higher concentrations take place in exactly the same areas, with *COMPACT* revealing higher concentrations (> 65 µg.m^{-3}, and >60 µg.m^{-3} for *BASE*). This is due to the population concentration in already urbanized areas, with the consequent increase of emissions.

To better analyse the differences between the scenarios, the spatial distribution of the concentration differences are presented in Figure 7.28. Air quality monitoring stations are also presented for further analysis. Differences between annual averages from *SPRAWL* and *BASE* range from -15 to +24 µg.m^{-3}, with negative values mainly over Porto, as a result of the decrease in emissions from traffic in this municipality. Higher positive differences are found over certain parts of the municipalities in the first metropolitan ring (Gondomar, Vila Nova de Gaia, Matosinhos, Maia and Valongo) corresponding to areas of urban expansion. Differences between *COMPACT* and *BASE* range from -5 to +8 µg.m^{-3}, with higher positive differences over Matosinhos, in areas previously urbanized but with a greater

population density in *COMPACT*. However, for the most part of the simulation domain differences are small, between -5 and +5 µg.m^{-3}.

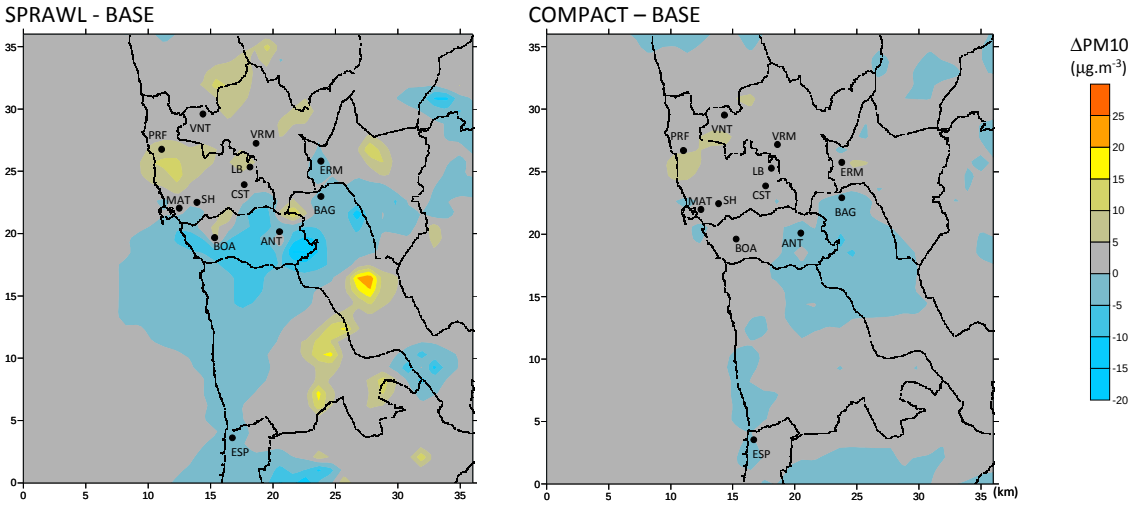

Figure 7.28 PM10 annual average differences between a) SPRAWL and BASE, and b) COMPACT and BASE.

Figure 7.29 presents the results for PM10 annual averages for *BASE, SPRAWL* and *COMPACT* for each air quality monitoring site located in the simulation domain. The sites are grouped by municipality in order to facilitate the analysis: Boavista and Antas (Porto); Vermoim and Vila Nova da Telha (Maia); Matosinhos, Senhora da Hora, Leça do Balio, Perafita and Custóias (Matosinhos); Baguim (Gondomar); Ermesinde (Valongo); and Espinho.

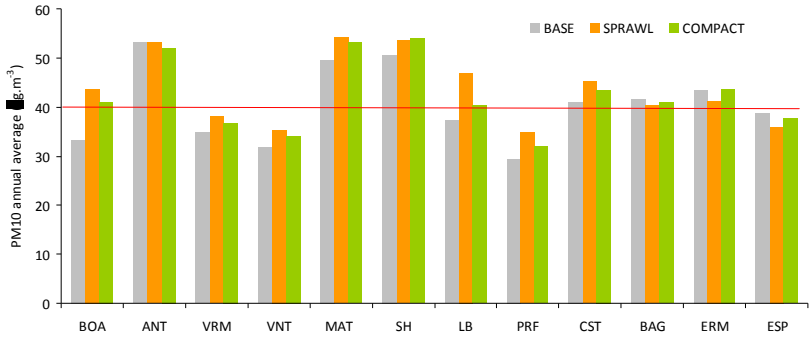

Figure 7.29 PM10 annual average for BASE, SPRAWL and COMPACT (the red line indicates the legislated annual limit value, 40µg.m^{-3}), at the air quality monitoring sites.

For the majority of the air quality sites, SPRAWL presents the highest annual average of the three simulations, with the exception of Senhora da Hora, Baguim, Ermesinde and Espinho. However, the results for Baguim and Ermesinde are not representative of the respective municipalities, since those also show areas of increased PM10 concentrations, not captured by the air quality monitoring sites, particularly in Gondomar where the highest increases are simulated.

Municipalities which in *BASE* did not exceed the legislated annual average, such as Boavista and Leça do Balio, now exceed the limit with *SPRAWL* and *COMPACT*. Other sites which were already in non-compliance show a deterioration of their situation (such as Matosinhos and Senhora da Hora). In Antas, Baguim, and Ermesinde both scenarios improve the PM10 levels.

Figure 7.30 shows the analysis of the number of exceedances to the PM10 daily limit value (50 µg.m^{-3}) obtained for *BASE, SPRAWL* and *COMPACT*.

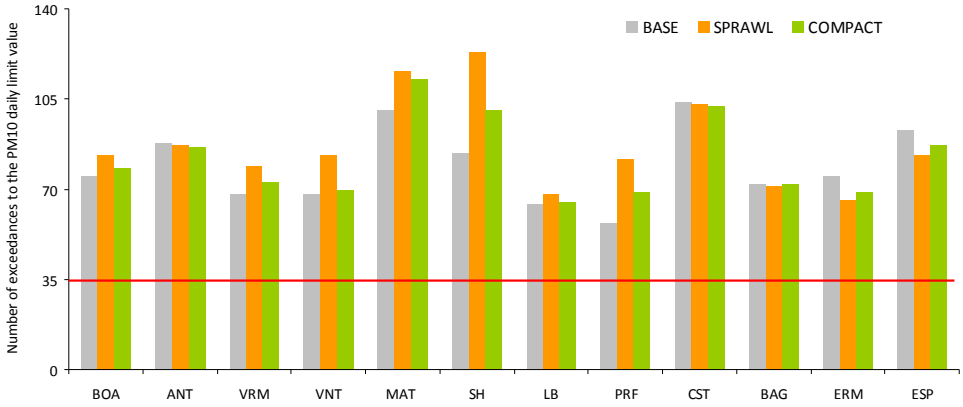

Figure 7.30 Number of exceedances to the PM10 daily limit value for BASE, SPRAWL and COMPACT (the red line indicates the allowed number of exceedances to the daily limit value, 35).

Results are very similar to those observed for the annual average, with the aggravation of the situation particularly for the sites of Matosinhos, Senhora da Hora and Perafita (in Matosinhos municipality), and Vila Nova da Telha (Maia). These correspond to areas of larger urban expansion in the case of SPRAWL and of population density increase in *COMPACT*.

The analysis performed so far concerns the annual average; however it is also interesting to look at particular PM10 pollution episodes, since differences between scenarios may be better depicted. A day with high PM10 concentrations, belonging to one of the episodes identified in Chapter 5 (Figure 5.3) is here analysed. On the 10th of February, high levels of PM10 were measured over the study area, with daily averages reaching more than 120 µg.m$^{-3,}$ and hourly values going up to 276 µg.m^{-3} in Matosinhos at 22:00. Figure 7.31 presents the evolution of PM10 concentrations along the 10th February and the daily averages at Matosinhos, for *BASE, SPRAWL* and *COMPACT,* as well as the measured values.

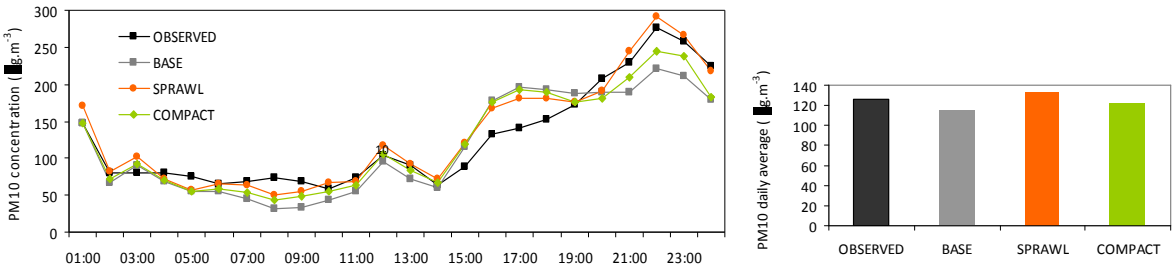

Figure 7.31 PM10 pollution episode of 10th February a) hourly concentrations evolution and b) daily averages at Matosinhos, for BASE, SPRAWL and COMPACT, and observed.

Although not reaching concentrations as high as the observed values, the BASE simulation is able to reproduce the PM10 air pollution episode. *SPRAWL* peak concentrations are higher reaching 290 µg.m^{-3}, while *COMPACT* maximum concentrations reaching almost 240 µg.m^{-3} in comparison with the 220 µg.m^{-3} for *BASE*. Simulated daily averages are also higher for *SPRAWL* and *COMPACT* with 133 and 122 µg.m^{-3}, respectively (17 µg.m^{-3} and 6 µg.m^{-3} higher than *BASE*).

Besides the obtained concentrations for each scenario it is also important to assess the number of individuals affected by high PM10 concentrations, since the population distribution across the study area is quite different for *BASE*, *SPRAWL* and *COMPACT*. Therefore, the maps of annual average concentrations (Figure 7.27) were crossed with population data per grid cell (Figure 7.5), to calculate the number of individuals affected by PM10 concentrations above the annual limit value. The results in terms of percentage of population (and not absolute since *BASE* has a lower population) are shown in Figure 7.32.

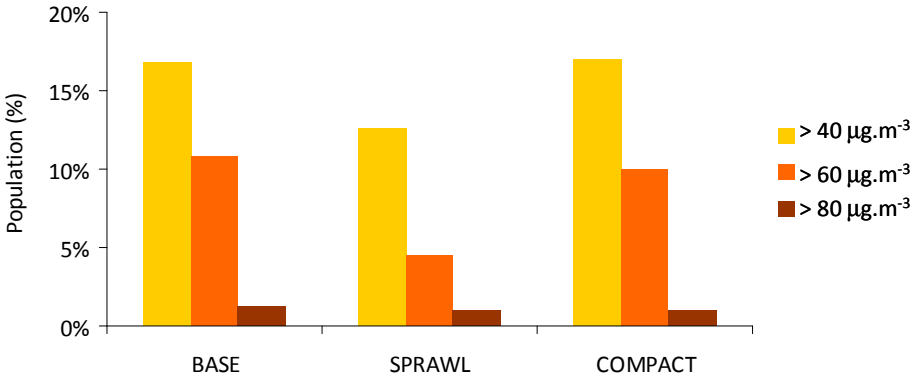

Figure 7.32 Population affected by PM10 concentrations above the annual limit value in BASE, SPRAWL and COMPACT.

COMPACT presents the greatest share of population affected by PM10 concentrations above 40 µg.m^{-3} (17%, corresponding to 370 000 inhabitants), while *SPRAWL* has the lowest number (12.5%, around 270 000 inhabitants). For the three considered concentration ranges, *SPRAWL* has the lowest share of people affected, while *BASE* and *COMPACT* show similar concentrations, although generally lower for

BASE. Notwithstanding the existence of higher PM10 concentrations in *SPRAWL*, results indicate that the dispersion of the population along the study region withdraws people from the areas of higher concentrations. In turn, the *COMPACT* scenario places a greater part of the region's population in areas of highest PM10 levels.

However, it is important to notice that the approach used to estimate the population affected by high PM10 concentrations is very simple and does not account with population daily dislocation between municipalities, as described for the idealized study case (Chapter 3). The calculation of exposure levels involves a complex methodology that also includes time activity patterns and the consideration of different micro-environments.

7.3.2.2 O_3

The combination of increased temperatures (for *SPRAWL*) and different emissions (for both scenarios) produces the ozone concentration pattern changes displayed in Figure 7.33. The spatial distribution of the ozone summer (April to September) average concentration differences between *BASE*, *SPRAWL* and *COMPACT* are shown. Air quality monitoring stations location is also depicted for further analysis.

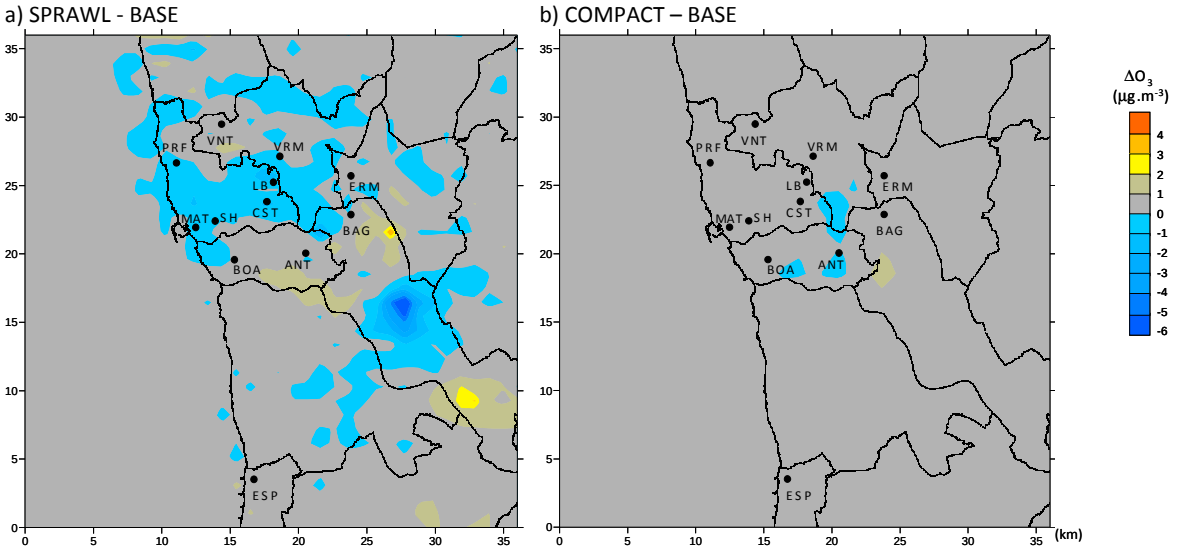

Figure 7.33 Ozone summer average differences between a) SPRAWL and BASE, and b) COMPACT and BASE.

The immediate analysis of the maps reveals that differences between the scenarios and *BASE* are much smaller than those obtained for PM10.

Differences between *SPRAWL* and *BASE* range from -6 to +4 µg.m^{-3}, with negative values mostly found over Matosinhos, Maia and Gondomar (centre), in areas where the population expanded and emissions increased. In fact, comparing this map with the one for PM10 (Figure 7.28), negative differences for ozone are found in the areas of positive PM10 differences. Still regarding *SPRAWL*, ozone increases occur over Porto and part of Gondomar (N and S) in areas downwind the largest

emission increase, such as Matosinhos, Maia and the centre of Gondomar municipality, as a result of air pollutants transport and consequent ozone formation. This is consistent with the prevailing NW wind direction in the region.

Differences between *COMPACT* and *BASE* range from -1.5 to +2 $\mu g.m^{-3}$. Negative differences take place in Porto municipality as an outcome of the population densification in that area and the corresponding emissions increase, which lead to the local consumption of ozone.

Under the combined effects of increased urbanization and increased emissions, ozone decreases are not completely unexpected and have been found in previous research works [Civerolo *et al.*, 2007; De Ridder *et al.*, 2008b]. This is probably due to the higher ozone removal by titration caused by higher anthropogenic emissions in an already emissions-dense region. Also, as investigated by Cohan *et al.* [2005], the non-linear response of ozone concentrations to changes in precursor emissions was found to increase with tonnage and emission density of the source region; this seems to be the case in the study region. According to the modelling study conducted by Tao *et al.* [2005], the synergy among precursor's emission source categories may sometimes suppress O_3, acting as negative source contributions. These authors concluded that the full potential of each source category in O_3 formation (the pure contribution) is not achieved when emissions from the other source categories are accounted for.

For both scenarios the largest part of the simulation domain presents very small positive differences, less than 1 $\mu g.m^{-3}$, meaning that average concentrations are slightly higher in comparison to BASE.

Figure 7.34 presents the number of exceedances to the hourly ozone information threshold (180 $\mu g.m^{-3}$), obtained for *BASE*, *SPRAWL* and *COMPACT*.

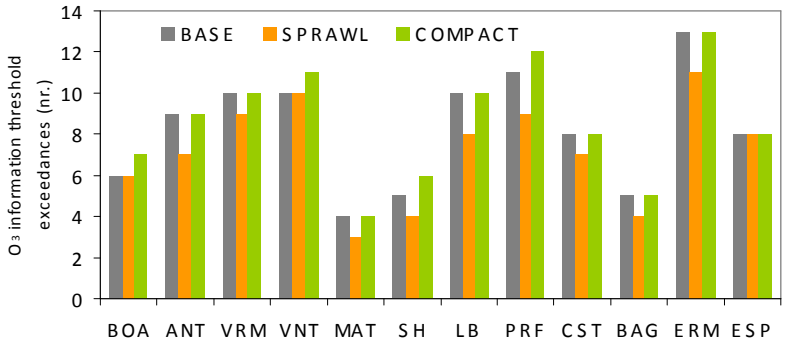

Figure 7.34 Number of exceedances to the ozone information threshold for BASE, SPRAWL and COMPACT.

SPRAWL presents the lowest number of exceedances, except in Espinho where the three simulations produced similar results. *COMPACT* is the worst scenario, with more exceedances than *BASE* for Boavista, Vila Nova da Telha, Senhora da Hora and Perafita.

The comparison of these results with the concentration patterns presented in Figure 7.33, reveals that there are no air quality sites in the areas of concentration increases, mainly for *SPRAWL*. However, if the same analysis is carried out for Gondomar in an area where no monitoring stations exist and for which higher positive differences are observed in the map of Figure 7.33, results are quite different: *SPRAWL* yields more exceedances (8) to the ozone information threshold in comparison with *BASE* (5) and *COMPACT* (6).

Regarding the maximum values, which are also important for ozone assessment, summer average daily maxima are presented in Figure 7.35 for the three simulations.

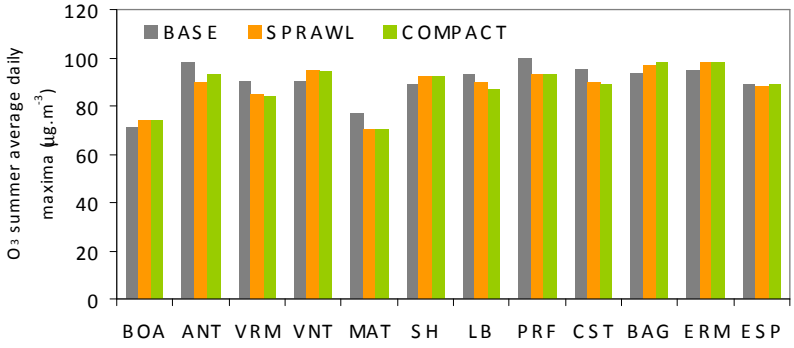

Figure 7.35 Ozone summer average daily maxima for BASE, SPRAWL and COMPACT.

Antas, Vermoim, Matosinhos, Leça do Balio, Perafita and Custóias, show a reduction in the ozone summer average daily maxima for both scenarios. The sites located in Matosinhos and Maia municipalities reflect the increase of precursors emissions and the titration effect already mentioned, resulting from the increase in urbanization and the intensification of population density in *SPRAWL* and *COMPACT*.

As for PM10, ozone air pollution episodes may show enhanced differences between scenarios. One day with high O_3 concentrations, belonging to one of the episodes identified in Chapter 5 is here analysed. In the 22nd of August, high levels of O_3 were measured over the study area, with the information threshold being exceeded in a group of monitoring stations; Antas registered the highest observed concentration with 188 µg.m^{-3} at 15:00. Figure 7.36 presents the evolution of O_3 concentrations along the 22nd of August at Antas, for *BASE*, *SPRAWL* and *COMPACT*, as well as the observed values.

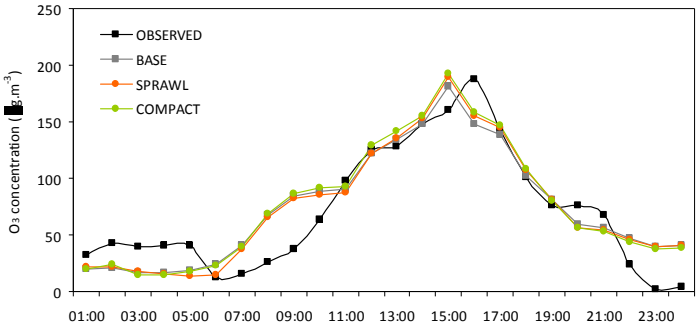

Figure 7.36 Ozone hourly concentrations evolution for the 22nd August at Matosinhos for BASE, SPRAWL and COMPACT, and observed.

Although reaching the peak concentration before the observed peak, the *BASE* simulation is able to reproduce the ozone air pollution episode. Differences between scenarios and BASE are small, with *COMPACT* peak concentration reaching 193 µg.m^{-3}, while *SPRAWL* reaches 190 µg.m^{-3}, in comparison with 182 µg.m^{-3} for *BASE*. Although not presented, other episodic situations were analysed, allowing the conclusion that ozone differences are always of this magnitude.

Regarding the number of persons affected by high ozone concentrations, the combination of the annual average concentrations maps with population data per grid cell, allows the determination of the number of individuals affected by ozone summer average concentrations above 70 µg.m^{-3}. This value was chosen because it is the concentration above which differences between the three situations are more substantial. The results are presented in Figure 7.37.

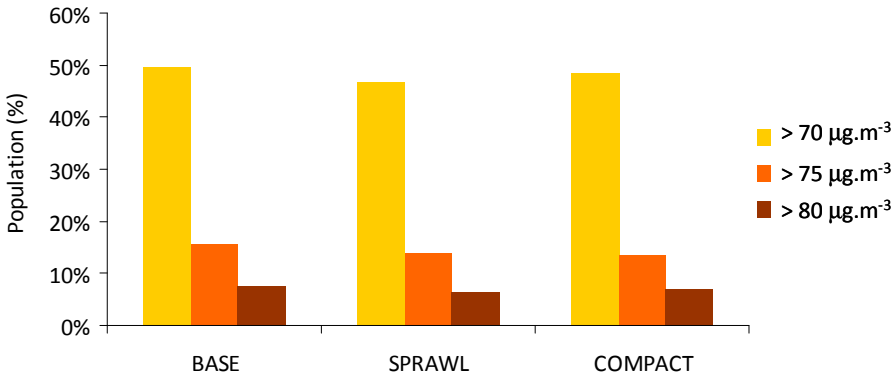

Figure 7.37 Population affected by ozone summer average concentrations above 70, 75 and 80 µg.m^{-3} in BASE, COMPACT and SPRAWL.

Once more, differences between scenarios and *BASE* are smaller than those observed for PM10. *COMPACT* presents the highest share of inhabitants affected by ozone summer average concentrations above 70 µg.m^{-3} (48.5%, corresponding to roughly 1 million people). However, looking at other concentration ranges the situation is different, since above 75 µg.m^{-3} *BASE* is the worst situation, with 21% of the population.

7.4 Final Remarks

The purpose of the work presented in this chapter was to investigate the effects of urban planning measures on air quality levels, namely on ozone and PM10 concentrations, through the application of a specifically developed methodology.

The selected working area is located in Portugal's Northern region, covering the Porto urban region, which is composed of a regional conglomerate of cities with a total population of over two million. Maps of land use and population parameters and an emission inventory were established for the situation as it is today (BASE). Moreover, two distinct future urban development scenarios - *COMPACT* and *SPRAWL* - were created, based on population and land use changes. The population of the study region was increased, to reflect a 20-years period, and differently distributed among municipalities according to each scenario. The land use patterns of the area were modified following a scenario of urban sprawl (*SPRAWL*) and maintained through the concentration of people in already existent urban areas (*COMPACT*). New emissions were estimated for each scenario, taking into account population growth and land use changes. The air quality modelling system was applied to *BASE, SPRAWL* and *COMPACT*, using as input the modified spatial distributions of land use and emissions. The three situations were evaluated and compared based on the effects of the urban growth scenarios on temperature, emissions, pollutant concentrations, and affected population.

The main findings can be summarised as follows. The averaged temperature increased by 0.4°C due to the land use changes in SPRAWL scenario. However, local increases reached 3°C, even in areas where land use changes were not implemented. Regarding emissions, the larger number of inhabitants, together with the conversion of forests and agricultural areas to urbanized land, and the increase of the average distance between people's homes and working places (these last two only for *SPRAWL*), were responsible for a higher pollutant emissions. In particular, emissions of NOx, VOCs, and PM10 increased by 11% to 17% in *SPRAWL*, and 4% to 6% in *COMPACT*.

Concerning the air quality changes associated to these different scenarios, PM10 concentration changes range from -15 to +24 $\mu g.m^{-3}$ in SPRAWL, and -5 to +8 $\mu g.m^{-3}$ in *COMPACT*; when expressed as relative changes this is of the order of -12% to +19%, and -4% to +7%, respectively. *SPRAWL* presents the highest PM10 annual concentrations (> 70 $\mu g.m^{-3}$), especially over areas of urban expansion and increasing emissions. *COMPACT* has slightly higher PM10 concentrations than *BASE*, due to the population concentration in already urbanized areas, and consequent increase of emissions in those areas.

For ozone, summer averaged changes were relatively modest, ranging from -6 to +4 $\mu g.m^{-3}$ in *SPRAWL*, and -1.5 to +2 $\mu g.m^{-3}$ in *COMPACT* (-8% to +5%, and -2% to +2.5%, respectively). While the largest part

of the domain shows positive differences under 1 $\mu g.m^{-3}$, negative differences are found mostly in areas where the population expanded and emissions increased. On the other hand, higher ozone increases occur over areas downwind the greatest emission increases, as a result of air pollutants transport and chemical transformation.

Findings for ozone illustrate the complex and often counteracting effects of substantial growth in urban cover on surface O_3 concentrations. On one hand, higher temperatures lead to enhanced photochemical production; however, higher anthropogenic emissions associated with higher urbanization rates have the potential to increase the spatial extent of VOC-limited conditions typically associated with core urban areas. In such areas, NOx emissions contribute to decreased O_3 concentrations while they can lead to augmented O_3 formation in downwind areas [Sillman, 1999].

Finally, the population affected by higher pollutants concentrations in each scenario, and its comparison with the base situation, revealed that although the existence of higher PM10 concentrations in *SPRAWL*, the concentration of the population in *COMPACT* places a greater part of the inhabitants in areas of highest PM10 levels. For ozone results are not so clear, with *BASE* and *COMPACT* sharing the highest number of affected individuals.

In conclusion, this study demonstrated that changes in land use patterns in metropolitan areas lead to changes in meteorology, air quality and population exposure.

8 CONCLUSIONS

The main aim of this study was to explore the relationship between the structure of the urban area and its air quality. Several research studies had demonstrated already that compact cities with mixed land uses are energetically more efficient and are responsible for lower emissions of atmospheric pollutants in comparison with sprawling cities. But a fundamental question remained unanswered: do compact cities promote a better air quality when compared to sprawling cities? And, given the ever-growing concentration of population in urban areas, do compact cities promote a healthier atmospheric environment? Given the signs provided by the energy and emissions aspects, the answers may seem obvious and straight forward but, as it was demonstrated along this study, they are not.

To answer these questions a strategy was drawn. The strategy, or approach, relied on the use of advanced atmospheric modelling tools for the evaluation of different urban development scenarios.

Aiming to assure a correct and complete analysis, a step-by-step methodology was defined and applied. First, it was necessary to characterize the current state of knowledge on the subject, including the genesis and growth of the problem, the policies adopted so far to address it, the tools available to tackle it, and gain insight from the studies previously conducted by several researchers on the field.

People in general have imagined ideal cities since ever and planners in particular have devoted their attention to the search of the most sustainable urban structure. In the last decades, the growing awareness of urban problems related to the depletion of resources (including energy), atmospheric pollution and waste, has re-ignited the attention to the role of urban planning in urban sustainability. Discussion has been focused on density and land use function related aspects, with opinions classified in two main groups: those in favour of urban dispersion and those who believe in the virtues of urban compaction.

Throughout Europe, but especially in Southern countries, the dispersed urban form is replacing traditionally compact urban areas, with urban land cover increasing much faster than population. This fact however does not result from a conscious attitude or planning option, but instead is the outcome of the lack of planning and disregard of the inclusion of environmental aspects in the planning process. Although the European Commission's initiatives and support towards a European strategy on the urban environment, and the recognition of sprawl as one of the most urgent urban issues to be tackled, no Directives on the subject have been adopted. The EC strategy is limited and despite sending the right signs to the Member States, it relies on voluntary initiatives to promote sustainable urban areas.

By nature, cities concentrate people, material and activities, therefore, together with major industry, they are responsible by the largest levels of pollution, namely at the atmospheric level. In Europe, while the population growth has remained minimal, the number of households and motorized vehicles, and consequently, energy consumption has increased. Although pollutant emissions in Europe have decreased substantially in the last two decades, as a result of technology and fuel improvements many times enforced through legislative initiatives, the ambient concentrations of PM10 and ozone have not shown any improvement. Approximately 20% of the European population is exposed to ozone concentrations above the target value; for PM10, 50% of the population is potentially exposed to ambient concentrations higher than the limit set for the protection of human health.

The above mentioned values were obtained through the use of two important air quality management tools - air quality monitoring networks and numerical air quality models -, that are nowadays widely used over Europe and North America. Numerical air quality models are recognized and recommended by EU air quality legislation as powerful tools for the evaluation and management of air quality, since they are able to estimate air pollutants concentrations in any point of a given study area.

While the environmental implications of transport and industrial activities have been recognized and studied for decades, the study of the influence of urban structure on air quality is still in its early steps. The few studies that integrate air quality modelling with urban structure aspects were conducted for episodic (a few days to a few weeks) air pollution situations and lack to compare different urban development pathways, instead comparing urban sprawl development with a reference starting point.

Having characterized the scientific and policy state of knowledge, a first modelling approach for an idealized urban area was performed. For that purpose three idealized and distinct city structures were created - DISPERSE, COMPACT and CORRIDOR – and a mesoscale photochemical modelling system was applied to an episodic air pollution situation. The simulations performed revealed lower ozone concentrations for the COMPACT city, but a higher number of people exposed to higher pollutant

levels. The idealized case-study confirmed the importance of the city spatial structure on the urban air quality, and also that atmospheric modelling systems are adequate tools for the study of the topic.

However, for a deeper analysis of the air quality consequences of different urban land use scenarios the study of a real urban area was necessary, as well as the extension of the modelling along an entire year to assure that the full range of air pollution conditions would be covered. Two essential steps were taken to do so: i) an adequate study area was identified and characterized, and ii) a modelling system able to perform long term simulations for the identified critical pollutants (O_3 and PM10) was selected and improved to correctly simulate the air quality outcomes resulting from land use changes.

The Porto urban region was identified as a suitable area for this study. The sprawling development model is evident in the Porto metropolitan region: extensive land occupation, high losses in agricultural and forest covers and the decrease in urban densities are the main signs of the current urban transformation and robust indicators of the direction taken by the urbanization process. Also, the Porto urban region presents a poor air quality, with ozone thresholds and daily and annual PM10 limit values exceeded. The region is currently under the obligation of developing and implementing *Plans and Programs for the Improvement of the Air Quality*, as mandated by the European legislation on air quality.

An adequate modelling system, composed by the meteorological model MM5 and the air quality model CAMx, was selected. The meteorological model was evaluated through a series of sensitivity tests, whose outputs were then fed as inputs to the air quality model aiming to define the most adequate setup for the purpose of the study. This task resulted in two important outcomes:

i) It was found that the model presented a poor land use data-set for the Portuguese territory, particularly for coastal and urban areas (which is the case of the study area). The existing dataset was then replaced by the more detailed and accurate CLC2000 data, yielding improved meteorological results.

ii) Two distinct setups, based on two different PBL parameterizations, were identified as adequate for the simulation of summer and winter air pollution episodes.

Notwithstanding the reasonable performance of the modelling system, and based on previous modelling studies which identified aspects to be improved in the air quality model configuration, it was decided that further actions were to be taken. Of particular importance to the purpose of the study, intimately related to land use and population distribution across the study area, was the refinement of the spatial distribution of emissions, for which the corner stone was the improved land use dataset. Also of significance was the development of region-specific temporal profiles for the temporal distribution of emissions, and the development of region-specific chemical speciation profiles. As a

result of these actions, an improved modelling system configuration was obtained, able to adequately simulate the air quality impacts of land use changes over the study region.

Finally, and making use of the knowledge and tools produced along this study, two urban development scenarios for the Porto area were defined and tested, with the objective of thoroughly assessing the implications of land use changes on the air quality levels of the Porto urban region. *SPRAWL* and *COMPACT* symbolize two different and alternative development paths. *SPRAWL* represents the perpetuation of the last decade's trend: urban areas continue to expand throughout the study region, at a faster rate than population growth, and Porto municipality continues to be emptied of its population while still remaining the most important attracting pole in the region for employment, education and other activities. *COMPACT* represents the rupture with the current trend, and all urban growth is accommodated in already existent urban areas, therefore raising the population density in the study area.

A methodology was developed for the estimation of pollutant emissions for both scenarios, devoting special attention to transport emissions since not only the population growth and urban area growth had to be taken into account, but also the mobility of the population throughout the Porto region. As a result the total amount of pollutant emissions increased in relation to the reference situation, *BASE*. In particular, emissions of NOx, VOCs, and PM10 increased by 11% to 17% in *SPRAWL*, and 4% to 6% in *COMPACT*.

The modelling system was then applied for *SPRAWL* and *COMPACT,* and also *BASE*, for a full-year simulation. The analysis of the meteorological results revealed that, owing to the land use changes in *SPRAWL*, the average temperature increased by 0.4°C. However local increases reaching 3°C were also detected; and some were even estimated in areas where land use changes were not implemented.

Regarding air quality, *SPRAWL* presented the highest PM10 concentrations, with an aggravation of the annual average values especially over areas of urban expansion and increasing emissions. Also, in the sites corresponding to the current monitoring stations, an increase in the number of exceedances to the daily limit value was found. Differences between each scenario and *BASE* were considerable, ranging from -15 to +24 $\mu g.m^{-3}$ in *SPRAWL*, and -5 to +8 $\mu g.m^{-3}$ in *COMPACT*. For *COMPACT* slightly higher PM10 concentrations than *BASE* were estimated, due to the population increase in already urbanized areas, and consequent increase of emissions in those same areas.

For ozone, while the largest part of the domain had small concentration increases (< 1 $\mu g.m^{-3}$) for both scenarios, smaller concentrations are found in areas where the population expanded and emissions increased, as a result of ozone titration by NO in the polluted atmosphere. Instead higher ozone levels are estimated for areas downwind the greatest emission increases, as a result of air pollutants

transport and consequent ozone formation. Differences between scenarios and *BASE* were smaller than those found for PM10, ranging from -6 to +4 $\mu g.m^{-3}$ in *SPRAWL*, and -1.5 to +2 $\mu g.m^{-3}$ in *COMPACT*.

Finally, the population affected by higher PM10 and O_3 concentrations was determined for each scenario and for *BASE*. The analysis revealed that although the existence of higher PM10 concentrations in *SPRAWL*, the increase of the population density in *COMPACT* places a greater part of the inhabitants in areas of highest PM10 levels. This means that individually each inhabitant is exposed to lower PM10 concentrations in *COMPACT*, however, looking to the population as a whole, in terms of public health, the situation is inverted and *SPRAWL* presents a lower number of people affected by the highest concentrations. For ozone, results are not so clear, with *BASE* and *COMPACT* sharing the highest number of individuals affected, and *SPRAWL* clearly presenting the lowest number of total inhabitants affected by higher concentrations.

In conclusion, it seems clear that changes in land use patterns in urban areas lead to changes in meteorology, emissions, air quality, and population exposure. The signal of the change is evident: sprawling urban areas, when compared to contained urban development, are responsible by higher temperatures, higher emissions of pollutants to the atmosphere, higher atmospheric pollutants concentrations, and higher levels of individual exposures to air pollutants. However, if the population is considered as a whole, compact urban developments imply a higher number of individuals exposed to the higher concentrations.

According to the review of the literature on this thesis subject, this was the first time a long term study was performed to analyse the impacts of urban growth, and consequent land use changes, on air quality, through the development of alternative urban development scenarios and the application of an air quality modelling system. Also, the methodology can be applied to any city or urban area for which the required data is available. However, the methodology presented here can be improved. Future work shall focus on the use of land use models for the simulation of land use changes, and traffic modelling to simulate the effect of land use changes on traffic volumes and their spatial distribution.

Along the next decade, it is expected that changes in the land use will take place. More likely, as revealed by the current trends, urban sprawl, the destruction of agricultural lands, and forestation and deforestation are expected to alter the landscape. These patterns will, in turn, lead to changes in population, energy consumption, traffic and anthropogenic and biogenic emissions. The results of this thesis suggest that changing land use patterns should be taken into consideration when using models to evaluate changes in quality levels (in particular ozone and PM10) stemming from various emissions reduction scenarios in urban areas. This is the case of the Porto urban region, for which *Plans and*

Programs for the Improvement of the Air Quality are now being developed for PM10 and soon starting to be conducted for ozone.

Also, it is important to note that, such as technology alone has not been able to tackle the air quality problems, more compact urban development patterns alone will not be sufficient to fully address urban air quality problems. Technological advances in emissions control have proven to be highly effective in reducing emissions over the last decades, and emerging technologies, such as hybrid vehicles and alternative fuels, are expected to continue these reductions. The importance of land use-oriented approaches to air quality management lies in the potential for these strategies to limit the dramatic growth in traffic, which has greatly diluted the benefits of technological improvements so far, and also in addressing the local meteorological drivers of air pollution, such as temperature.

European legislation has successfully managed to drive technology improvements with visible results in terms of emission reductions. A high quality and healthy urban environment is unlikely to emerge spontaneously from the multitude of decisions taken independently by the multitude of urban actors (public authorities, private institutions and companies, and individuals). It is my conviction that legislation is required to drive urban development in the right direction and to guide daily management decisions, namely through the establishment of clear guidelines and obligations for environmental management and sustainable urban transport plans, and even limitations to urban expansion. Therefore the strategy for addressing urban air quality problems must include land use policies that promote more compact urban forms, complemented by technological emission controls.

In the years to come, cities will continue to be the main centres of economic activity, innovation and culture. Therefore, managing the urban environment and the quality of life of its inhabitants goes well beyond the concern for the well-being of the urban population, affecting instead the well-being of humanity as a whole.

REFERENCES

Alley, E.R., Stevens, L.B., Cleland, W.L., 1998. Air Quality Control Handbook. McGrawHill.

Anderlini, F., 2003. Dopo l'urbanizzazione. In: Sprawl Suburbano e Dinamica Sociale. Bologna e Altre Metropolis. CLUEB, Bologna.

Anderson, H.R., Atkinson, R.W., Peacock, J.L., Sweeting, M.J., Marston, L., 2005. Ambient particulate matter and health effects: publication bias in studies of short-term associations. *Epidemiology* 16 (2), 155–163.

Anderson, H.R., 2009. Air pollution and mortality: A history. *Atmospheric Environment* 43,142–152.

Ambiente Italia, 2003. European Common Indicators Towards a Local Sustainability Profile. Ambiente Italia, Milano.

André , M., Hammarstrom, U., Reynaud, I., 1999. Driving statistics for the assessment of air pollutant emissions from road transport. INRETS report, LTE9906, Bron, France.

Appel, K. W., Gilliland, A. B., Sarwar, G., Gilliam, R. C., 2007. Evaluation of the Community Multiscale Air Quality (CMAQ) model version 4.5: Sensitivities impacting model performance Part I Ozone. *Atmospheric Environment* 41, 9603-9615.

Aquilina, N., Dudek, A.V., Carvalho, A., Borrego, C., Nordeng, T.E., 2005. MM5 high resolution simulations over Lisbon. *Geophysical Research Abstracts*. SRef-ID: 1607-792/gra/EGU05-a-08685. European Geosciences Union. 7:08685.

APA – Agência Portuguesa do Ambiente, 2007. Identificação e Avaliação de Eventos Naturais no ano de 2006. APA (Ed.), Lisboa, Portugal.

APA – Agência Portuguesa do Ambiente, 2008. Evolução da qualidade do ar em Portugal entre 2001 and 2005. APA (Ed.), Lisboa, Portugal.

APA – Agência Portuguesa do Ambiente, 2009. Portuguese Informative Inventory Report 1990 – 2007: Submitted under the UNECE Convention on long-range transboundary air pollution. APA (Ed.), Lisboa, Portugal.

Atkinson, R., Lloyd, A. C. , Winges, L., 1982. An updated chemical mechanism for hydrocarbon/NOx/SO_2 photo-oxidations suitable for inclusion in atmospheric simulation models. *Atmospheric Environment* 16, 1341-1355.

Baek, S., Kim, Y., Perry, R., 1997. Indoor air quality in homes, offices and restaurants in Korean urban area – indoor/outdoor relationships. *Atmospheric Environment* 31 (4), 529-544.

Ballard, S. P., B. W. Golding, and R. N. Smith, 1991. Mesoscale model experimental Forecasts of the Haar of Northeast Scotland. *Monthly Weather Review* 119, 2107-2123.

Barna, M., Lamb, B., 2000. Improving ozone modeling in regions of complex terrain using observational nudging in a prognostic meteorological model. *Atmospheric Environment* 34, 4889–4906.

Barret, G., 1996. The transport dimension, in The compact city a sustainable urban form? Jenks, M., Burton, E., Williams, K. (Eds.). Taylor and Francis Group, Oxford, 350 p.

Barros, N., 1999. Poluição atmosférica por foto-oxidantes: o ozono troposférico na região de Lisboa. Departamento de Ambiente e Ordenamento, Universidade de Aveiro, Aveiro. Dissertação apresentada à Universidade de Aveiro para obtenção do grau de Doutor em Ciências Aplicadas ao Ambiente.

Barros, N., Borrego, C., Toll, I.,Soriano, C., Jiménez, J., Baldasano, J.M., 2003. Urban photo-chemical pollution in the Iberian Peninsula: Lisbon and Barcelona Airsheds. *Air & Waste Management* 53, 347–359.

Battye, W., Harris, J., 2005. Improving modeling inventory data: speciation profiles. EC/R Incorporated Technical Report, Chapel Hill, NC, 27517.

Berge, E., Huang, H-C., Chang, J., Liu, T-H. 2001. A study of the importance of initial conditions for photochemical oxidant modeling. *Journal of Geophysical Research* 106, 1347–1363.

Bessagnet, B., Hodzic, A., Vautard, R., Beekmann, M., Cheinet, S., Honoré, C., Liousse, C., Rouil, L., 2004. Aerosol modelling with CHIMERE – Preliminary evaluation at the continental scale. *Atmospheric Environment* 38, 2803-2817.

Borge, R., Lumbreras, J., Rodríguez, E., 2008. Development of a high-resolution emission inventory for Spain using the SMOKE modelling system: a case study for the years 2000 and 2010. *Environmental Modelling and Software* 123, 1026–1044.

Borrego, C., Costa, M.J., Martins, J.M., Barros, N., Coutinho, M., Conceição, M., Miranda, A.I., Thomaz, S.F., 1994. Desenvolvimento de metodologias para o estudo da qualidade do ar em zonas costeiras. In: Actas da 4ª Conferência Nacional Sobre a Qualidade do Ambiente, 6-8 Abril, Universidade Nova de Lisboa, Portugal, Vol. II, M108-M117.

Borrego, C., Carvalho, A.C., Miranda, A.I., 1999. Numerical simulation of wind field over complex terrain. In: San Jose, R. (Ed.), Measuring and Modelling Investigation of Environmental Processes. WIT Press, United Kingdom.

Borrego, C., Tchepel, O., Costa, A.M., Amorim, J.H., Miranda, A.I., 2003. Emission and dispersion modelling of Lisbon air quality at local scale. *Atmospheric Environment* (37), 5197-5205.

Borrego, C., Martins, H., Carvalho, A., Carvalho, A.C., Lopes, M., Valente, J., Miranda, A.I., 2004. Portuguese power plants impact on air quality. In Air Pollution 2004, Rhodes, Greece, 30 June – 2 July 2004 – Air Pollution XII, Eds. C.A. Brebbia, WIT Press, Southampton, UK, pp. 201 – 211.

Borrego, C., Miranda, A.I., Ginga, J., Coutinho, M., 2005. Estado da qualidade do ar na região norte - 2004. Rede de monitorização da região norte. Universidade de Aveiro, Aveiro, Portugal.

Borrego, C., Martins, H., Tchepel, O., Salmim, L., Monteiro, A., Miranda, A.I., 2006a. How urban structure can affect city sustainability from an air quality perspective. *Journal of Environmental Modeling and Software* 21, 461-467.

Borrego, C., Miranda, A.I, Sousa, M., Sousa, S., Coutinho, M., 2006b. Estado da Qualidade do Ar na Região Norte – 2005, Identificação de medidas para a melhoria da qualidade do ar na Região Norte no que respeita ao ozono e seus precursores, Relatório R1, Departamento de Ambiente e Ordenamento da Universidade de Aveiro e IDAD, Portugal.

Borrego, C., Monteiro, A., Ferreira, J., Miranda, A.I., Costa, A.M., Carvalho, A.C., Lopes, M., 2008a. Modelling uncertainty estimation procedures for air quality assessment. *International Environmental Journal* 34(5), 613-620.

Borrego, C., Miranda, A.I, Sousa, S., 2008b. Estado da Qualidade do Ar na Região Norte - 2006. Departamento de Ambiente e Ordenamento da Universidade de Aveiro, Portugal.

Borrego, C., Miranda, A.I, Sousa, S., Carvalho, A., Sá, E., Martins, H., Valente, J., Varum C., Jorge, S., 2008c. Planos e Programas para a Melhoria da Qualidade do Ar na Região Norte - Uma visão para o período 2001-2006. Departamento de Ambiente e Ordenamento da Universidade de Aveiro, Portugal.

Borrego, C., Lopes, M., Valente, J., Tchepel, O., Miranda, A.I. ,Ferreira, J., 2008d. The role of PM10 in air quality and exposure in urban areas. Air Pollution 2008 Conference, 22-24 Setembro, Skyathos, Grécia. Eds. C.A. Brebbia, J.W.S. Longhurst. WIT Transactions on Ecology and the Environment, vol. 116, WIT Press, Southampton, UK, pp 511-520. doi:10.2495/AIR08521

Bottenheim, J. W., Strausz, O. P., 1982. Modelling study of a chemically reactive power plant plume. *Atmospheric Environment* 16, 85-106.

Breheny, M., 1992a. Sustainable development and urban form. Pion, London.

Breheny, M., 1992b. The contradictions of the compact city: a review, in Sustainable development and urban form. Breheny, M. (Ed.). Pion, London.

Breheny, M., 1996. Centrists, decentrists and compromisers, in The compact city a sustainable urban form? Jenks, M., Burton, E., Williams, K. (Eds.). Taylor and Francis Group, Oxford, 350 p.

Breheny, M., Gordon, I., Archer, S., 1998. Building densities and sustainable cities. Project Outline 5, Engineering and Physical Sciences Research Council Sustainable Cities Programme, Swindon, UK.

Burchell, R., Shad, N., Listokin, D., Phillips, H., Downs, A., Seskin, S., Davis, J., Moore, T., Helton, D., Gall, M., 1998. The costs of sprawl - revisited. Washington, DC, National Academy Press.

Burchell, R., Lowenstein, G., Dophin, W., 2002. Costs of Sprawl- 2000. Transportation Research Board, National Academy Press, Washington, DC.

Burnett, R.T., Brook, J., Dann, T., Delocla, C., Philips, O., Cakmak, S., Vincent, R., Goldberg, M.S., Krewski, D., 2000. Association between particulate- and gas-phase components of urban air pollution and daily mortality in eight Canadian cities. *Inhalation Toxicology* 12 (Suppl. 4), 15–39.

Byun, D.W., Schere, K.L., 2006. Review of the governing equations, computational algorithms, and other components of the models—3/Community Multiscale Air Quality (CMAQ) modelling system. *Applied Mechanics Review* 59, 51–77.

Cagmani, R., Gibelli, M.C., Rigamonti, P., 2002. Urban mobility and urban form: the social and environmental costs of different patterns of urban expansion. *Ecological Economics* 40 (2), 199–216.

Camalier, L., Cox, W., Dolwick, P., 2007. The effects of meteorology on ozone in urban areas and their use in assessing ozone trends. *Atmospheric Environment* 41, 7127–7137.

Cameron, I., Kenworthy, J.R. Lyons, T.J., 2003. Understanding and Predicting Private Motorised Urban Mobility. *Transportation Research* D 8, 267–283.

Cameron, I., Lyons, T.J., Kenworthy, J.R., 2004. Trends in vehicle kilometres of travel in world cities, 1960–1990: underlying drivers and policy responses. *Transport Policy* 11, 287–298.

Carter, W.P.L. 2001. Programs and Files Implementing the SAPRC-99 Mechanism and its Associates Emissions Processing Procedures for Models-3 and Other Regional Models. Available at: http://pah.cert.ucr.edu/~carter/SAPRC99.htm.

Carvalho, A.C., 2005. A qualidade do ar e as alterações climáticas. Departamento de Ambiente e Ordenamento, Universidade de Aveiro, Aveiro. Dissertação apresentada à Universidade de Aveiro para obtenção do grau de Doutor em Ciências Aplicadas ao Ambiente.

Carvalho, A.C., Carvalho, A., Gelpi, I., Barreiro, M., Borrego, C., Miranda, A.I., Perez-Munuzuri, V., 2006. Influence of topography and land use on pollutants dispersion in the Atlantic coast of Iberian Peninsula. *Atmospheric Environment* 40, 3969-3982.

Catalán, B., Saurí, D. , Serra, P., 2008. Urban sprawl in the Mediterranean? Patterns of growth and change in the Barcelona Metropolitan Region 1993–2000. *Landscape and Urban Planning* 85, 174-184.

Cervero, R., 1988. Land use mixing and suburban mobility. *Transportation Quarterly* 42 (3), 428-446.

Cervero, R., 2000. Transport and Land Use: Key Issues in Metropolitan Planning and Smart Growth. UCTC Report #436, University of California Transportation Center, Berkeley, CA. Available from http://www.uctc.net/papers/436.pdf

Chaline, C., 2001. Urbanisation and town management in the Mediterranean countries. Evaluation and Perspective for Sustainable urban development, Plan Bleu. Paper prepared for the Mediterranean Meeting on Urban Management and Sustainable Development, 3–5 September 2001, Barcelona. Available from http://www.planbleu.org/publications/chaline_eng.pdf

Cheng, C.S., Campbell, M., Li, Q., Li, G., Auld, H., Day, N., Pengelfly, D., Gingrich, S., Yap, D., 2007. A synoptic climatological approach to assess climatic impact on air quality in south-central Canada. Part II: future estimates. *Water Air and Soil Pollution* 182, 117–130.

Civerolo, K.L., Sistla, G., Rao, S.T., Nowak, D.J., 2000. The effects of land use in meteorological modeling: implications for assessment of future air quality scenarios. *Atmospheric Environment* 34, 1615–1621.

Civerolo, K., Hogrefe, C., Lynn, B., Rosenthale, J., Ku, J-Y, Solecki, W., Cox, J., Small, C., Rosenzweig, C., Goldberg, R., Knowlton, K., Kinney, P., 2007. Estimating the effects of increased urbanization on surface meteorology and ozone concentrations in the New York City metropolitan region. *Atmospheric Environment* 41, 1803-1818.

Cohan, D.S., Hakami, A., Hu, Y., Russell, A.G., 2005. Nonlinear response of ozone to emissions: source apportionment and sensitivity analysis. *Environmental Science and Technology* 39, 6739-6748.

COM(90) 218 final, 27 June, Comunication from the Commission to the Council and Parliament, Green Paper on the Urban Environment.

COM(97) 197 final, 6 May, Communication from the Commission Towards an urban agenda in the European Union.

COM(98) 605 final, 28 October, Communication from the Commission to the Council, the European Parliament, the Economic and Social Committee and the Committee of the Regions. Sustainable Urban Development in the European Union: a Framework for Action.

COM(2001)60 final, 11 February, Communication from the Commission to the Council, the European Parliament, the Economic and Social Committee and the Committee of the Regions. Towards a thematic strategy on the urban environment.

COM(2001) 245 final, 4 May, , Communication from the Commission. The Clean Air for Europe (CAFE) Programme: Towards a Thematic Strategy for Air Quality.

COM(2004)60 final, 11 February, Communication from the Commission to the Council, the European Parliament, the Economic and Social Committee and the Committee of the Regions. Towards a thematic strategy on the urban environment.

COM(2005)718 final, 11 January, Communication from the Commission to the Council and the European Parliament. Thematic Strategy on the Urban Environment.

COST Action 728 - Enhancing Mesoscale Meteorological Modelling Capabilities for Air Pollution and Dispersion Applications, 2005. Memorandum of Understanding.

Council Directive 96/62/EC of 27 September 1996 on ambient air quality assessment and management.

Council Directive 1999/30/EC of 22 April 1999 relating to limit values for sulphur dioxide, nitrogen dioxide and oxides of nitrogen, particulate matter and lead in ambient air.

Cousin, F., Liousse, C., Cachier, H., Bessagnet, B., Guillaume, B., Rosset, R., 2005. Aerosol modelling and validation during ESCOMPTE 2001. *Atmospheric Environment* 39 (8), 1539-1550.

Coutinho, M., Borrego, C., 1991. Photochemical production on coastal areas of Portugal. In: Proceedings of the 19th International Technical. Meeting of NATO - CCMS on Air Pollution Modeling and Its Applications, 29 September - 4 October, Ierapetre, Crete, 129 - 136.

Coutinho, M., Rocha, A., Borrego, C., 1994. Numerical simulation of meso-meteorological circulations in the Lisbon region. In: Gryning, S.E., Millan, M.M. (Eds.), Air Pollution Modelling and Its Applications X. Plenum Press, New York and London.

Crane, R., 2000. The influence of urban form on travel: an interpretative review. *Journal of Planning Literature* 15 (1), 3-23.

De Ridder, K., Lefebre, F., Adriaensen, S., Arnold, U., Beckroege, W., Bronner, C., Damsgaard, O., Dostal, I., Dufek, J., Hirsch, J., IntPanis, L., Kotek, Z., Ramadier, T., Thierry, A., Vermoote, S., Wania, A., Weber, C., 2008a. Simulating the impact of urban sprawl on air quality and population exposure in the German Ruhr area. Part I: Reproducing the base state. *Atmospheric Environment* 42 (30), 7059-7069.

De Ridder, K., Lefebre, F., Adriaensen, S., Arnold, U., Beckroege, W., Bronner, C., Damsgaard, O., Dostal, I., Dufek, J., Hirsch, J., IntPanis, L., Kotek, Z., Ramadier, T., Thierry, A., Vermoote, S., Wania, A., Weber, C., 2008b. Simulating the impact of urban sprawl on air quality and population exposure in the German Ruhr

area. Part II: Development and evaluation of an urban growth scenario. *Atmospheric Environment* 42 (30), 7070-7077.

Decision 1600/2002/EC of the European Parliament and of the Council of 22 July 2002 laying down the Sixth Community Environment Action Program.

Derwent, R.G., 1999. Atmospheric Chemistry. In Air Pollution and Health, Holgate, S., Samet, J., Koren, H., Maynard, R. (Ed.) London Academic Press, 51-62.

Directive 2000/69/EC of the European Parliament and of the Council of 16 November 2000 relating to limit values for benzene and carbon monoxide in ambient air.

Directive 2002/3/EC of the European Parliament and of the Council of 12 February 2002 relating to ozone in ambient air.

Directive 2004/107/EC of the European Parliament and of the Council of 15 December 2004 relating to arsenic, cadmium, mercury, nickel and polycyclic aromatic hydrocarbons in ambient air.

Directive 2008/50/EC of the European Parliament and of the Council of 21 May 2008 on ambient air quality and cleaner air for Europe.

Dodge, M.C., 2000. Chemical oxidant mechanisms for air quality modeling: critical review. *Atmospheric Environment* 34, 2103–2130.

Downs, A., 1992. Stuck in Traffic: Coping with Peak-hour Traffic Congestion. The Brookings Institution, Washington, DC.

Draxier, R., Hess, G.D., 1998. An overview of the HYSPLIT_4 modelling system for trajectories, dispersion and deposition. *Australian Meteorological Magazine*, 47 (4), 295-308.

Dudhia, J., 1993. A nonhydrostatic version of the Penn State/NCAR mesoscale model: Validation tests and simulation of an Atlantic cyclone and clod front. *American Meteorological Society - Monthly Weather Review* 121, 1493-1513.

Dudhia, J., 1996: A multi-layer soil temperature model for MM5. Preprints, The Sixth PSU/ NCAR Mesoscale Model Users' Workshop, 22-24 July 1996, Boulder, Colorado, 49-50. Available from http://www.mmm.ucar.edu/mm5/mm5v2/whatisnewinv2.html.

Dudhia, J., Gill, D., Manning, K., Wang, W., Bruyere, C., 2005. PSU/NCAR Mesoscale Modelling System Tutorial Class Notes and Users' Guide (MM5 Modelling System Version 3) (updated for MM5 Modelling System Version 3.7 - Released January 2005).

Eastman, J.L., Pielke, R. A., McDonald, D. J., 1998. Calibration of Soil Moisture for Large-Eddy Simulations over the FIFE Area. *Journal of the Atmospheric Sciences* 55 (7), 1131–1140.

EC Expert Group on the Urban Environment, 1998. Response of the EC Expert Group on the Urban Environment on the Communication 'Towards an Urban Agenda in the European Union'. EC, Brussels.

ECOTEC, 1993. Reducing Transport Emissions Through Planning. HMSO, London.

EEA – European Environment Agency, 2000. CORINE land cover technical guide – Addendum 2000. M. Bossard, J. Feranec and J. Otahel Technical report No 40. European Environment Agency, Copenhagen.

EEA – European Environment Agency, 2006a. Urban sprawl in Europe – the ignored challenge. EEA Report No. 10/2006. European Environment Agency, Copenhagen.

EEA – Environment European Agency, 2006b. EMEP/CORINAIR Emission Inventory Guidebook – 2006. Technical report No 11/2006. European Environment Agency, Copenhagen.

EEA – European Environment Agency, 2007. Air pollution in Europe 1990-2004. EEA Report No. 2/2007. European Environment Agency, Copenhagen.

EEA – European Environment Agency, 2008. Annual European Community LRTAP Convention emission inventory repport 1990-2006. European Environment Agency, Copenhagen.

EEA – European Environment Agency, 2009. Ensuring quality of life in Europe's cities and towns: Tackling the environmental challenges driven by European and global change. EEA Report No. 5/2009. European Environment Agency, Copenhagen.

EEA-JRC, 2002. Towards an urban atlas: assessment of spatial data on 25 European cities and urban areas. Environmental Issue Report No. 30. European Environment Agency and European Commission DG Joint Research Centre. Office for Official Publications of the European Communities, Luxembourg. ISBN 92-9167-470-2. 131 pp.

Elbir, T., 2003. Comparison of model predictions with the data of an urban air quality monitoring network in Izmir, Turkey. *Atmospheric Environment* 37, 2149–2157.

Emison, G., 2001. The relationships of sprawl and ozone air quality in United States' metropolitan areas. *Regional Environmental Change* 2, 118-127.

ENVIRON, 2008. CAMx v4.5.1 User's Guide. ENVIRON International Corporation, Novato, California, EUA. June 2008.

Evtyugina, M., Nunes, T., Pio, C., Costa, C., 2006. Photochemical pollution under sea breeze conditions, during summer, at the Portuguese West Coast. *Atmospheric Environment* 40, 6277-6293.

Ewing, R., Pendall, R., Chen, D., 2003. Measuring sprawl and its transportation impacts. *Transportation Research Record* 1831, 175–183.

Eyth, A.M., Habisak, K., 2003. The MIMS spatial allocator: a tool for generating emission surrogates without a geographic information system. In: 12th International Emission Inventory Conference – Emission Inventories – Applying New Technologies San Diego, April 29–May 1, 2003. Available from:<http://www.epa.gov/ttn/chief/conference/ei12/modeling/eyth.pdf>.

Fenger, J., 1999. Urban air quality. *Atmospheric Environment* 33, 4877-4900.

Ferreira, J., 2007. Relação Qualidade do Ar e Exposição Humana a Poluentes Atmosféricos. Departamento de Ambiente e Ordenamento, Universidade de Aveiro, Aveiro. Dissertação apresentada à Universidade de Aveiro para obtenção do grau de Doutor em Ciências Aplicadas ao Ambiente.

Ferreira, J., Carvalho, A., Carvalho, A.C., Monteiro, A., Martins, H., Miranda, A.I., Borrego, C., 2003. Chemical Mechanisms in two photochemical modelling systems: a comparison procedure. In Int. Tech. Meeting of NATO-CCMS on "Air Pollution Modelling and its Application", 26th, Istanbul, Turkey, 26-30 May 2003 - Air Pollution Modelling and its Application XVI, Eds Carlos Borrego and Selahattin Incecik, Kluwer Academic/ Plenum Publishers, New York, p. 87-96.

Ferreira J., Salmim, L.; Monteiro, A., Miranda, A.I., Borrego, C., 2004. Avaliação de episódios de ozono em Portugal através da modelação fotoquímica. In 8ª Conferência Nacional de Ambiente, 27-29 de Outubro 2004, Lisboa, Portugal – Actas da 8ª Conferência Nacional de Ambiente: Lisboa, p. 383-384.

Ferreira, J., Martins, H., Miranda, A.I., Borrego, C., 2005. Population Exposure to Atmospheric Pollutants: the influence of Urban Structure. In 1st International Conference Environmental Exposure and Health, Atlanta, EUA, 5-7 October 2005 - Environmental Exposure and Health. Eds. M.M. Aral, C.A. Brebbia, M.L. Masila and T. Sinks. WITPress, p. 13-22.

Fiore, A.M., Dentener, F.J, Wild. O., Cuvelier, C., Schultz, M.G., Hess, P., et al., 2009. Multimodel estimates of intercontinental source-receptor relationships for ozone pollution. *Journal of Geophysical Research* 114, D04301, doi:10.1029/2008JD010816.

Flassak Th., Kessler Ch. and Moussiopoulos N., 1992. The chemical reaction model RADM2 in MARS (Model for the Atmospheric Dispersion of Reactive Species), in EUROTRAC Annual Report1991, Part 5, 53-57.

Frank, L.D., Stone, B., Bachman, W., 2000. Linking land use with household vehicle emissions in he central puget sound: methodological framework and findings. *Transportation Research Part D* 5, 173-196.

Friedrich, R., Reis, S. (Eds.), 2004. Emissions of Air Pollutants – Measurements, Calculations and Uncertainties. Springer-Verlag, Berlin, Heidelberg, New York.

Frumkin, H., Frank, L., Jackson, R., 2004. Urban Sprawl and Public Health: Designing, Planning, and Building for Healthy Communities. Island Press,Washington, DC.

Gallego, J., Peedell, S., 2001. Using CORINE Land Cover to Map Population Density. Towards Agri-Environmental Indicators. Topic Report 6/2001. EEA, Copenhagen. Available at: <http://reports.eea.europa.eu/topic_report_2001_06/en/Topic_6_2001.pdf>, pp. 92–103.

Gayno. G., 1994. Development of a high-order, fog producing boundary layer model suitable for use in numerical weather predictions. M.S. Thesis, Pennsylvania State University, 104p.

Gery, M.W., Whitten, G.Z., Killus, J.P., Dodge, M.C., 1989. A Photochemical Kinetics Mechanism for Urban and Regional Scale Computer Modeling. *Journal of Geophysical Research* 94, 925-956.

Ginoux, P., Chin, M ., Tegen, I., Prospero, J. M., Holben, B., Dubovik, O., Lin., S. J., 2001. Sources and distributions of dust aerosols simulated with the GOCART model, *Journal of Geophysical Research* 106, 20255-20274.

Gomez-Ibanez, 1991. J.A. Gomez-Ibanez, A Global View of Automobile Dependence (book review). *Journal of the American Planning Association* 57, 376–379.

Grell, G.A., Dudhia, J., Stauffer, D.R., 1994. A description of the fifth-generation Penn State/NCAR Mesoscale Model (MM5), Tech. Rep. NCAR/TN-398+STR, Natl. Cent. for Atmos. Res., Boulder, Colorado.

Grell, G.A., Peckham, S. E., Schmitz, R., McKeen, S.A., Frost, G., Skamarock, W.C., Eder, B., 2005. Fully coupled “online” chemistry within the WRF model. *Atmospheric Environment* 39 (37), 6957-6975.

Guenter, A., Hewwit, C., Erikson, D., Fall, R., Geronc, C., 1997. A global model of natural volatile organic compound emissions. *Journal of Geophysical Research* 100, 63–70.

Hass, H., Van Loon, M. Kessler, C., Matthijsen, J., Sauter, F., Stern, R., Zlatev, R., Langner, J., Fortescu, V., Schaap, M., 2003. Aerosol modeling: results and intercomparison from European Regional-scale Modeling Systems. A contribution to the EUROTRAC-2 subproject GLOREAM. EUROTRAC report.

Han, Z., Ueda, H., An, J., 2008. Evaluation and intercomparison of meteorological predictions by five MM5-PBL parameterizations in combination with three land-surface models. *Atmospheric Environment* 42, 233-249.

Handy, S., 1996. Methodologies for exploring the link between urban form and travel behaviour. *Transportation Research D* 1 (2), 151-165.

Handy, S., Xinyu, C., Mokhtarian, P., 2005. Correlation or Causality between the Built Environment and Travel Behavior? Evidence from Northern California. *Transportation Research Part D* 10 (6), 427-444.

Hanna, S.R., Chang, J.C., Strimaitis, D.G., 1993. Hazardous gas model evaluation with field observations. *Atmospheric Environment* 27A, 2265-2285.

Hanna, S. R., Chang, J. C., Fernau, M. E., 1998. Monte Carlo Estimates of Uncertainties in Predictions by a Photochemical Grid Model (UAM-IV) due to Uncertainties in Input Variables. *Atmospheric Environment* 32 (21), 3619-3628.

Hauglustaine, D. A., Hourdin, F., Walters, S., Jourdain, L., Filiberti, M., Larmarque, J., Holland, E., 2004. Interactive chemistry in the Laboratoire de Météorologie Dynamique general circulation model : description and background tropospheric chemistry evaluation, *Journal of Geophysical Research* 109, D04314, doi:10.1029/2003JD003957.

Heimlich, R., Anderson, W., 2001. Development at the urban fringe and beyond: Impacts on agriculture and rural land. Agriculture Economic Report (AER803). United States Department of Agriculture.

Herala, N., 2003. Regulating traffic with land use planning. *Sustainable Development* 11, 91-102.

Hertel, O., De Leeuw, F., Raaschou-Nielsen, O., Jensen, S., Gee, D., Herbarth, O., Pryor, S., Palmgren, F., Olsen, E., 2001. Human exposure to outdoor air pollution. *Pure and Applied Chemistry* 73 (6), 933-958.

Hogrefe, C., Rao, S.T., Kasibhatla, P., Hao, W., Sistla, G., Mathur, R., McHenry, J., 2001. Evaluating the performances of regional-scale photochemical modelling systems: Part II - ozone predictions. *Atmospheric Environment* 35, 4175-4188.

Hogrefe, C., Biswas, J., Lynn, B., Civerolo, K., Ku, J.Y., Rosenthal, J., Rosenzweig, C., Goldberg, R., Kinney, P.L., 2004. Simulating regional-scale ozone climatology over the eastern United States: model evaluation results. *Atmospheric Environment* 38, 2627– 2638.

Hogrefe C., Porter, P.S., Gego, E., Gilliland, A., Gilliam, R., Swall, J., Irwin, J., Rao, S.T., 2006. Temporal features in observed and simulated meteorology and air quality over the eastern United States. *Atmospheric Environment* 40, 5041–5055.

Hoinka, K.P. and Castro, M., 2003. The Iberian Peninsula thermal low. *The Quarterly Journal of the Royal Meteorological Society* 129, 1491 - 1511. (Corrigendum, Q. J. R. Meteorol. Soc. 132 (2006), 1377).

Holloway, T., Fiore, A., Galanter Hastings, M., 2003. Intercontinental transport of air pollution: will emerging science lead to a new hemispheric treaty? *Environmental Science and Technology* 37, 4535–4542.

Holmes, N., Morawska, L., 2006. A review of dispersion modelling and its application to the dispersion of particles: an overview of different dispersion models available. *Atmospheric Environment* 40 (30), 5902-5928.

Hong, S.-Y., and H.-L. Pan, 1996. Nonlocal boundary layer vertical diffusion in a medium-range forecast model. *Monthly Weather Review* 124, 2322-2339.

Houyoux, M.R., Vukovich, J.M., Coats Jr., C.J., Wheeler, N.J.M., Kasibhatla, P., 2000. Emission inventory development and processing for the seasonal model for regional air quality (SMRAQ) project. *Journal of Geophysical Research* 105, 9079–9090.

Hurley, P., Manins, P., Lee, S., Boyle, R., Leung., Y., Dewundege, P., 2003. Year-long, high-resolution, urban airshed modelling: verification of TAPM predictions of smog and particles in Melbourne, Australia. *Atmospheric Environment* 37 (14), 1899-1910.

IA - Instituto do Ambiente , 2001. Delimitação de Zonas e Aglomerações para Avaliação da Qualidade do Ar em Portugal, Instituto do Ambiente, Lisboa.

Indovina, F. (Ed.), 1990. La Città diffusa. DAEST-IUAV, Venice.

INE – Instituto Nacional de Estatística, 2003. Movimentos pendulares e organização do território metropolitano – Área Metropolitana de Lisboa e Área Metropolitana do Porto: 1991/2001. Instituto Nacional de Estatística, Lisboa.

Irving, P., Moncrieff, I., 2004. Managing the environmental impacts of land transport: integrating environmental analysis with urban planning. *Science of the Total Environment* 334-335, 47-59.

ITT - Institut fur Technische Thermodynamik, 1994. The nonhydrostatic mesoscale model MEMO: version 5.0 – A technical reference. Karlsruhe.

Jacob, D.J., Winner, D.A., 2009. Effect of climate change on air quality. *Atmospheric Environment* 43, 51-63.

Jacobson, M.Z., 1999. Fundamentals of Atmospheric Modeling. Cambridge University Press, Cambridge, 656 p.

Jacobson, M.Z. 2002. Atmospheric Pollution: History, Science and Regulation. Cambridge University Press, Cambridge, 375 p.

Janjic, Z. I., 1990. The step-mountain coordinate: Physical package. *Monthly Weather Review* 118, 1429-1443.

Janjic, Z. I., 1994. The step-mountain eta coordinate model: Further development of the convection, viscous sublayer, and turbulent closure schemes. *Monthly Weather Review* 122, 927-945.

Jenks, M., Burton, E., Williams, K. (Eds.), 1996. The compact city a sustainable urban form? Taylor and Francis Group, Oxford, 350 p.

Jenks, M., 2000. The acceptability of urban intensification, in Achieving Sustainable Urban Form. Williams, K., Burton, E., Jenks, M. (Eds.), E & FN Spon, London, 388 p.

Jiménez P., Jorba, O., Parra, R., Baldasano, J. M., 2006. Evaluation of MM5-EMICAT2000-CMAQ performance and sensitivity in complex terrain: High-resolution application to the northeastern Iberian Peninsula. *Atmospheric Environment* 40 (26), 5056-5072.

Jiménez, P., Parra, R., Baldasano, J.M., 2007. Influence of initial and boundary conditions for ozone modeling in very complex terrains: A case study in the northeastern Iberian Peninsula. *Environmental Modelling & Software* 22, 1294–1306.

Kasanko, M., Barredo, J.I., Lavalle, C., McCormick, N., Demicheli, L., Sagris, V. Brezger, A., 2006. Are European cities becoming dispersed? A comparative analysis of fifteen European urban areas. *Landscape and Urban Planning* 77, 111–130.

Kenworthy, J., Laube, F., 1996. Automobile dependence in cities: an international comparison of urban transport and land use patterns with implications for sustainability. *Environmental Impact Assessment Review* 16, 279-308.

Keyser, D., Anthes, R.A., 1977. The applicability of a mixed-layer model of the planetary boundary layer to real-data forecasting. *Monthly Weather Review* 105, 1351-1371.

Kluizenaar, Y., Aherne, J., Farrell, E.P., 2001. Modelling the spatial distribution of SO_2 and NO_x emissions in Ireland. *Environmental Pollution* 112, 171-182.

Kühn, M., 2003. Greenbelt and Green Heart: separating and integrating landscapes in European city regions. *Landscape and Urban Planning* 64, 19–27.

Lenhart, L., Friedrich, R., 1995. European Emission Data with High Temporal and Spatial Resolution. *Water, Air and Soil Pollution* 85, 1897-1902.

Leontidou, L., 1990. The Mediterranean City in Transition: Social Change and Urban Development. Cambridge University Press, Cambridge.

Liu, T.H., Jeng, F.T., Huang, H.C., Berge, E., Chang, J.S., 2001. Influences of initial conditions and boundary conditions on regional and urban scale Eulerian air quality transport model simulations. *Chemosphere-Global Change Science* 3, 175–183.

Lopes, M., 1997. Poluição fotoquímica no litoral Português: modelação de mesoscala. Departamento de Ambiente e Ordenamento, Universidade de Aveiro, Aveiro. Dissertação apresentada à Universidade de Aveiro para obtenção do grau de Mestre em Poluição Atmosférica.

Maes, J., Vliegen, J., Vel, K.V., Janssen, S., Deutsch, F., Ridder, K., Mensink, C., 2009. Spatial surrogates for the disaggregation of CORINAIR emission inventories. *Atmospheric Environment* 43,1246–1254.

Mallet, V., Sportisse, B., 2006. Uncertainty in a chemistry-transport model due to physical parameterizations and numerical approximations: An ensemble approach applied to ozone modeling. *Journal of Geophysical Research* 111, D01302.

Mao, Q., Gautney, L.L., Cook, T.M., Jacobs, M.E., Smith, S.N., Kelsoe, J.J., 2006. Numerical experiments on MM5-CMAQ sensitivity to various PBL schemes,. *Atmospheric Environment* 40, 3092–3110.

Marquez, L., Smith, N., 1999. A framework for linking urban form and air quality. *Journal of Environmental Modelling & Software* 14 (6), 541-548.

Marshall, S., Lamrani, Y., 2003. PLUME Synthesis Report: Land Use Planning Measures.

Marshall, J.D., McKoneb, T.E., Deakind, E., Nazaroff, W.W., 2005. Inhalation of motor vehicle emissions: effects of urban population and land area. *Atmospheric Environment* 39, 283–295.

Martín, F., Palacios, M., Crespi, S., 2001. Simulations of mesoscale circulations in the centre of the Iberian Peninsula for thermal low pressure conditions. Part I: Evaluation of the topography vorticity-mode mesoscale model. *Journal of Applied Meteorology* 40, 880–904.

Martins, H., Carvalho, A., Miranda, A.I., Salmim, L., Sousa, M. , 2004. Incêndios florestais periurbanos e qualidade do ar.In 8ª Conferência Nacional de Ambiente, Lisboa, Portugal, 27-29 Outubro 2004 - Actas da 8ª Conferência Nacional de Ambiente. Lisboa: Universidade Nova de Lisboa, p. 408-409.

Martins, H., Miranda, A.I., Borrego, C., 2007a. Linking urban structure and air quality. Transportation Land Use, Planning, and Air Quality 2007, 9-11 July, Orlando, Florida, USA., p. 219-227.

Martins, H., Ferreira, J., Sousa, S., Miranda, A.I., Borrego, C., 2007b. Caracterização e avaliação de episódios de partículas no ar ambiente da aglomeração do Porto Litoral. In 9ª Conferência Nacional de Ambiente, 18-20 de Abril 2007, Aveiro, Portugal – Actas da 9ª CNA Um futuro sustentável Ambiente, Sociedade e Desenvolvimento: Dep de Ambiente, Univ. de Aveiro, p. 840-846 (vol 3).

Masnavi, M.R., 2000. The new millennium and the new urban paradigm: the compact city in practice, in Achieving Sustainable Urban Form. Williams, K., Burton, E., Jenks, M. (Eds.), E & FN Spon, London, 388 p.

Mensink, C., De Ridder, K., Lewyckyj, N., Delobbe, L., Janssen, L., Van Haver, P., 2001. Computational aspects of air quality modelling in urban regions using an optimal resolution approach (AURORA). *Large-scale scientific computing – lecture notes in computer science* 2179, 299–308.

Millan, M., Artiñano, B., Alonso, L., Castro, M., Fernandez-Patier, R., Goberna, J., 1992. Mesometeorological Cycles of air pollution in the Iberian Peninsula. Air Pollution Research Report 44, European Community Commission, Brussels.

Minguzzi, E., Bedogni, M., Carnevale, C., Pirovano, G., 2005. Sensitivity of CTM simulations to meteorological input. *International Journal of Environment and Pollution* 24, No. 1/2/3/4.

Minnery, J., 1992. Urban Form and Development Strategies: Equity, Environmental and Economic Implications. The National Housing Strategy Background, Paper 7. AGPS, Canberra.

Miranda, A.I, Martins, H., Monteiro, A., Ferreira, J., Carvalho, A.C., Borrego, C., 2002. Evaluation of two mesoscale modelling systems using different chemical mechanisms. 4th Symposium on the Urban Environment, 20–24 May, Virginia, USA.

Miranda, A.I.; Ferreira, F.; Borrego, C.; Kuhlbusch, T.; Viana, M.; Winiwarter, W. and Ketzel, M., 2006. Modelling Particulate Matter in European COST633 Action Member States. In COST633 International Conference on Similarities and Differences in Airborne Particulate Matter: Exposure and Health Effects over Europe. 3-5 Abril 2006, Vienna, Austria - Proceedings of the international conference. Eds Thomas Kuhlbusch & Flemming Cassee. p. 96 - (poster presentation).

Mlawer, E. J., S. J. Taubman, P. D. Brown, M. J. Iacono, and S. A. Clough, 1997: Radiative transfer for inhomogeneous atmosphere: RRTM, a validated correlated-k model for the longwave. *Journal of Geophysical Research* 102 (D14), 16663-16682.

Monforti, F., Pederzoli, A., 2005. THOSCANE: a tool to detail CORINAIR emission inventories. *Environmental Modelling and Software* 20, 505–508.

Monn, C., 2001. Exposure assessment of air pollutants: a review on spatial heterogeneity and indoor/outdoor/personal exposure to suspended particulate matter, nitrogen dioxide and ozone. *Atmospheric Environment* 35, 1-32.

Monteiro, A., Borrego, C., Tchepel, O., Santos, P., Miranda, A.I., 2001. Inventário de Emissões Atmosféricas – base de dados POLAR2. Aplicação à modelação atmosférica. In: Actas da 7ª Conferência Nacional sobre a Qualidade do Ambiente, 18-20 Abril, Universidade de Aveiro, Aveiro, Portugal, 954-958.

Monteiro, A., Vautard, R., Borrego, C., Miranda, A.I., 2005. Long-term simulations of photo-oxidant pollution over Portugal using the CHIMERE model. *Atmospheric Environment* 39, 3089–3101.

Monteiro, A., 2007. Desenvolvimento de um sistema de avaliação e previsão da qualidade do ar para Portugal. Departamento de Ambiente e Ordenamento, Universidade de Aveiro, Aveiro. Dissertação apresentada à Universidade de Aveiro para obtenção do grau de Doutor em Ciências Aplicadas ao Ambiente.

Monteiro, A., Miranda, A.I., Borrego, C., Vautard, R., 2007a. Air quality assessment for Portugal. *Science of the Total Environment* 373, 22-31.

Monteiro, A., Borrego, C., Miranda, A.I., Gois, V., Torres, P., Perez, A.T., 2007b. Can air quality modelling improve emission inventories? In 6th Int. Conference of Urban Air Quality 2007 (UAQ), 27-30 March 2007, Limassol, Cyprus – Proceedings of International Conference on Urban Air Quality. Published in CD-Rom.

Morris, R.E., Yarwood, G., Emery, C., Koo., B., 2004. Development and Application of the CAMx Regional One-Atmosphere Model to Treat Ozone, Particulate Matter, Visibility, Air Toxics and Mercury. Presented at 97th Annual Conference and Exhibition of the A&WMA, June 2004, Indianapolis.

Moussiopoulos, N., 1995. MARS: Version 2.0 – User's Guide. Aristotle University, Thessaloniki.

Moussiopoulos, N., 1996. State of art of air pollution modelling – needs and trends. In: Eds Caussade, B., Power, H. and Brebbia, C.A.: Proceedings of the 4th International Conference on Air Pollution, 26-28 July, California, USA, Computational Mechanics Publications, Southampton, Boston, 47-56.

Moussiopoulos, N., Sahm, P., Proyou, A., 1994. Numerical simulation of the wind field in Athens with the non-hydrostatic mesoscale model MEMO. *Environment Software*, 8–29.

Nemery, B., Hoet, P., Nemmar, A., 2001. The Meuse Valley fog of 1930: an air pollution disaster. *The Lancet* 357 (9257), 704-708.

Neuman, M., 2005. The compact city fallacy. *Journal of Planning Education and Research* 25, 11 – 26.

Newman, P., 1992. The compact city – an Australian perspective. *Built Environment* 18, 285-300.

Newman, P., Kenworthy, J.R., 1989a. Gasoline consumption and cities: a comparison of US cities with a global survey. *Journal of the American Planning Association* 55, 24–37.

Newman, P., Kenworthy, J.R., 1989b. Cities and automobile dependence: An international sourcebook. Gower, England.

Newman, P., Kenworthy, J. R., 1999. Sustainability and Cities: overcoming automobile dependence. Island Press, Washington DC.

Newton, P.W., 1997. Re-shaping cities for a more sustainable future – Exploring the link between urban form, air quality, energy and emissions. Report of the Australian Academy of Technological Sciences and Engineering, Melbourne, Australia.

Oke T.R., 1988. The urban energy balance. *Progress in Physical Geography* 12, 471-508.

Olesen, HR., 2001. Ten years of harmonization activities: past, present and future. Proceedings of the 7th Int. Conf. On Harmonization within Atmospheric Dispersion Modelling for Regulatory Purposes, Belgirate, Italy.

Oliveira, C., Santos, P., Nunes, T., Pio, C., Caseiro, A., Wahlin, P., 2004. Contribuição das emissões rodoviárias na qualidade do ar da cidade do Porto. In 8ª Conferência Nacional de Ambiente, 27-29 de Outubro 2004, Lisboa, Portugal – Actas da 8ª Conferência Nacional de Ambiente: Lisboa, p. 365-366.

Ordonez, C., Mathis, H., Furger, M., Henne, S., Hoglin, C., Staehelin, J., Prevot, A.S.H., 2005. Changes of daily surface ozone maxima in Switzerland in all seasons from 1992 to 2002 and discussion of summer 2003. *Atmospheric Chemistry and Phy*sics 5, 1187– 1203.

Orthofer, R., Winiwarter, W., 1998. Spatial and Temporal Disaggregation of Emission Inventories. In H. Power and J. M. Baldasano (Eds.). Air Pollution Emissions Inventory, Chapter 2. Southampton, UK: Computational Mechanics Publications, p.51-70.

Painho, M., Caetano, M., 2006. Cartografia de ocupação do solo - Portugal continental 1985-2000: Corine Land Cover 2000. Instituto do Ambiente, Amadora, 56p.

Passant, N. R., 2002. Speciation of UK emissions of non-volatile organic, AEA Technology, NETCEN, AEAT/ENV/R/0545, Culham, UK.

PBL — Netherlands Environmental Assessment Agency, 2008. Urbanisation dynamics and quality of place in Europe, EURBANIS report 1. Planbureau voor de Leefomgeving (NEAA), Bilthoven, the Netherlands.

Pielke, R.A., 1984. Mesoscale Meteorological Modeling. 1st Edition, Academic Press, New York.

Pielke, R.A., Cotton, W.R., Walko, R.L., Tremback, C.J., Lyons, W.A., Grasso, L.D., Nicholls, M.E., Moran, M.D., Wesley, D.A., Lee, T.J., Copeland, J.H., 1992. A comprehensive meteorological modelling system - RAMS. *Meteorology and Atmospheric Physics* 49, 69–91.

Pielke, R. A., Uliasz, M. 1998. Use of meteorological models as input to regional and mesoscale air quality models - limitations and strengths. *Atmospheric Environment* 32, 1455-1466.

Pinson, D., Thomann, S., 2001. La Maison et ses territories. In: De la villa a la ville diffuse. L'Harmattan, Paris.

Pio, C. A., Legrand, M., Oliveira, T., Afonso, J., Santos, C., Caseiro, A., Fialho, P., Barata , F., Puxbaum, H., Sanchez-Ochoa, A., Kasper-Giebl, A., Gelencsér, A., Preunkert, S., Schock, M., 2007. Climatology of aerosol composition (organic versus inorganic) at nonurban sites on a west-east transect across Europe. *Journal of Geophysical Research* 112, D23S02, doi:10.1029/2006JD008038.

Placet, M., Mann, C.O., Gilbert, R.O., Niefer, M.J., 2000. Emissions of ozone precursors from stationary sources: a critical review. *Atmospheric Environment* 34, 2183–2204.

Poupkou, A., Symeonidis, P., Ziomas, I., Melas, D., Markakis, K., 2007. A spatially and temporally disaggregated anthropogenic emission inventory in the southern Balkan region. *Water, Air and Soil Pollution* 185, 335–348.

Pun, B., Wu, S., Seigneur, C., 2007. Investigative modelling of new pathways for secondary organic aerosol formation. *Atmospheric Chemistry and Physics* 7 (9), 2199-2216.

Rao, T., Sistia, G., Henry, R., 1992. Statistical analysis of trends in urban ozone air quality. *Journal of the Air and Waste Management Association* 42, 1204–1211.

Rao, T., Zalewsky, E., Zurbenko, I., 1995. Determining temporal and spatial variations in ozone air quality. *Journal of the Air and Waste Management Association* 45, 57–61.

Reid, N., Misra, P.K., Amman, M., Hales, J., 2007. Air quality modelling for policy development. *Journal of Toxicology and Environmental Health* - Part A, 70 (3-4), 295-310.

Reisner, J., Rasmussen, R. J., Bruintjes, R.T., 1998. Explicit forecasting of supercooled liquid water in winter stroms using the MM5 mesoscale model. *Quarterly Journal of the Royal Meteorological Society* 124B, 1071-1107.

Rickaby, P. and De la Barra, T., 1989. A theoretical comparison of strategic spatial options for city-regional development using the TRANUS model. In: Lundquist, L., Mattson, L. and Eriksson, E. Editors, 1989. Spatial Energy Analysis Avebury, Aldershot.

Rickaby, P., 1991. Energy and urban development in an archetypal English town. *Environment and Planning* B 18 2, 153–176.

Rosenfeld, A., Akbari, H., Romm, J., Pomerantz, M., 1998. Cool communities: strategies for heat island mitigation and smog reduction. *Energy and Buildings* 28, 51–62.

Rotach, M. , 1999. On the influence of urban roughness sub-layer on turbulence and dispersion. *Atmospheric environment* 33, 4001-4008.

Salmim, L., Ferreira, J., Monteiro, A., Miranda, A.I., Borrego, C., 2005. Emissions reduction scenarios for 2010: impact on air quality in Portuguese urban areas. In 5th Int. Conference of Urban Air Quality 2005 (UAQ), 29-31 March 2005, Valencia, Espanha – Proceedings of International Conference on Urban Air Quality, Eds. Ranjeet Sokhi e Nicolas Moussiopoulos, pp. 172 – poster preentation.

Samaali, M., Moran, M.D., Bouchet, V.S., Pavlovic, R., Cousineau, S., Sassi, M., 2009. On the influence of chemical initial and boundary conditions on annual regional air quality model simulations for North America. *Atmospheric Environment*, doi: 10.1016/j.atmosenv.2009.07.019

Samet, J.M., Zeger, S.L., Dominici, F., Curriero, F., Coursac, I., Dockery, D.W., Schwartz, J., Zanobetti, A., 2000. The National Morbidity, Mortality, and Air Pollution Study. Part II: Morbidity and mortality from air pollution in the United States, Research Report of the Health Effect Institute 94 (Part 2), p. 5–70 discussion 71–79.

Saraiva, A.P., 2007. Princípios de Arquitectura Paisagista e de Planeamento do Território. João Azevedo Editor. Mirandela, Portugal.

Sawyer, R.F., Harley, R.A., Cadle, S.H., Norbeck, J.M., Slott, R., Bravo, H.A., 2000. Mobile sources critical review: 1998 NARSTO assessment. *Atmospheric Environment* 34, 2161–2181.

Schmidt, H., Derognat, C., Vautard, R., Beekmann, M., 2001. A comparison of simulated and observed ozone mixing ratios for the summer of 1998 in Western Europe. *Atmospheric Environment* 35, 2449- 2461.

Schlünzen, H. K., 1988. Das mesoskalige Transport- und Strömungsmodell METRAS – Grundlagen, Validierung, Anwendung (The mesoscale transport and Fluid Model 'METRAS' – Basics, Validation, Application). In: Wittenborn Söhne, G.M.L (Ed.), Hamburger Geophysikalische Einzelschriften, Heft 88. Hamburg, p. 139.

Schoffman, E., Vale,B., 1996. How compact is sustainable - how sustainable is compact?, in The compact city a sustainable urban form? Jenks, M., Burton, E., Williams, K. (Eds.). Taylor and Francis Group, Oxford, 350p.

Seaman, N., 2000. Meteorological modeling for air-quality assessments. *Atmospheric Environment* 34, 2231-2259.

Seinfeld J.H., Pandis S.N., 1998. Atmospheric chemistry and physics – From air pollution to climate change. ISBN 0-471-17816-0. John Wiley & Sons, inc. Wiley Interscience.

Shafran, P.C., Seaman, N. L., Gayno, G.A., 2000. Evaluation of numerical predictions of boundary layer structure during the Lake-Michigan Ozone Study. *Journal of Applied Meteorology* 39, 412-426.

Sillman, S., 1999. The relation between ozone, NOx, and hydrocarbons in urban and polluted rural environments. *Atmospheric Environment* 33, 1821–1845.

Sillman, S., Samson, P.J., 1995. The impact of temperature on oxidant formation in urban, polluted rural and remote environments. *Journal of Geophysical Research* 100, 11497–11508.

Simpson, D., Andersson-Sköld, Y. A., Jenkin M. E., 1993. Updating the chemical scheme for the EMEP MSC-W Note 2/93. The Norwegian Meteorological Institute. Oslo, Norway.

Smith, N., 2002. New globalism, New urbanism: Gentrification as Global Urban Strategy. *Antipode* 34(3), 427-450.

Steadman, P., Barrett, M., 1991. The Potential Role of Town and Country Planning in Reducing Carbon Dioxide Emissions. Report to the Department of the Environment, London.

Stone, B., 2005. Urban heat and air pollution: an emerging role for planners in the climate change debate. *Journal of the American Planning Association* 71 (1), 13–25.

Stone, B., Bullen, J.L., 2006. Urban form and watershed management: how zoning influences residential stormwater volumes. *Environment and Planning B: Planning and Design* 33(1), 21 – 37.

Stone, B., 2008. Urban sprawl and air quality in large US cities. *Journal of Environmental Management* 86 (4), 688-698.

Stull, 1998. Boundary layer meteorology. Kluwer Academic Press.

Tanaka, P.L., Allen, D.T., McDonald-Buller, E.C., Chang, S., Kimura, Y., Mullins, C.B., Yarwood, G., Neece, J.D., 2000. Development of a chlorine mechanism for use in the carbon bond IV chemistry model. *Journal of Geophysical Research* 108(D4), 4145.

Tao, Z., Larson, S. M., Williams, A., Caughey, M., Wuebbles, D. J., 2004. Sensitivity of regional ozone concentrations to temporal distribution of emissions. *Atmospheric Environment* 38, 6279-6285.

Tao, T, Larson, S. M., Williams, A., Caughey, M., Wuebbles, D. J., 2005. Area, mobile, and point source contributions to ground level ozone: a summer simulation across the continental USA. *Atmospheric Environment* 39, 1869-1877.

Tchepel, O., 1997. Application of Geographical Information Systems to Mesoscale Atmospheric Pollution Modelling. MsC Thesis. University of Aveiro, Portugal.

Tesche, T.W., Morris, R., Tonnesen, G., McNally, D., Boylan, J., Brewer, P., 2006. CMAQ/CAMx annual 2002 performance evaluation over the Eastern US. *Atmospheric Environment* 40 (26), 4906-4919.

Thunis, P., Rouil, L., Cuvelier, C., Stern, R., Kerschbaumer, A., Bessagnet, B., Schaap, M., Builtjes, P., Tarrason, L., Douros, J., Moussiopoulos, N., Pirovano, G., Bedogni, M., 2007. Analysis of model responses to emission-reduction scenarios within the City Delta project. *Atmospheric Environment* 41, 208-220.

Titheridge, H., Hall, S., Banister, D., 2000. Assessing the sustainability of urban development policies, in Achieving Sustainable Urban Form. Williams, K., Burton, E., Jenks, M. (Eds.), E & FN Spon, London, 388 p.

Thinh, N. X., Arlt, G., Heber, B., Hennersdorf, J., Lehmann, I., 2002. Evaluation of urban land-use structures with a view to sustainable development. *Environmental Impact Assessment Review* 22, 475- 492.

Thomas, L., Cousins, W., 1996. The compact city: a successful, desirable and achievable urban form?, in The compact city a sustainable urban form? Jenks, M., Burton, E., Williams, K. (Eds.). Taylor and Francis Group, Oxford, 350p.

TNS Opinion & Social, 2005. Special Eurobarometer 217 - Attitudes of Europeans towards the Environment, European Commission.

Trigo, R.M., Pereira, J.M.C., Pereira, M.G., Mota, B., Calado, T.J., DaCamara, C., Santo, F.E., 2006. Atmospheric conditions associated with the exceptional fire season of 2003 in Portugal. *International Journal of Climatology* 26, 1741-1757.

UN- United Nations, 2001. World urbanization prospects: The 1999 revision. UN Department of Economic and Social Affairs, New York.

UN-United Nations, 2004. World urbanization prospects: The 2003 revision. UN Department of Economic and Social Affairs, New York.

UNEC -United Nations Economic Commission for Europe, 2007. Hemispheric Transport of Air Pollution 2007. Air Pollution Studies No. 16. United Nations, New York and Geneva.

USEPA - United States Environmental Protection Agency, 1990. User's Guide for the Urban Airshed Model-Volume I; User's Manual for UAM(CBIV). U.S. Environmental Protection Agency, Research Triangle Park, NC, EPA-450/4- 90-007a.

USEPA - United States Environmental Protection Agency, 1991. Guideline for regulatory application of the urban airshed model. USEPA Report No. EPA-450/4-91-013. U.S. EPA, Office of Air Quality Planning and Standards, Research Triangle Park, North Carolina.

USEPA - United States Environmental Protection Agency, 2001. Our Built and Natural Environments: A Technical review of the interactions between land use, transportation and environmental quality. USEPA, 231-R-01–002, Washington.

USEPA - United States Environmental Protection Agency, 2002. SPECIATE 3.2. Available at: http://www.epa.gov/ttn/chief/software/speciate.

Van Dingenen, R., Raes, F., Putaud, J.P., Baltensperger, U., Charron, A., Facchini, M.C., Decesari, S., Fuzzi, S., Gehrig, R., Hansson, H.C., 2004. A European aerosol phenomenology-1: physical characteristics of particulate matter at kerbside, urban, rural and background sites in Europe. *Atmospheric Environment* 38, 2561-2577.

Van Loon, M., 2004. Model intercomparison in the framework of the review of the unified EMEP model. Technical report TNO-MEP R2004/282, Apeldoorn, The Netherlands.

Vautard, R., Beekmann, M., Menut, L., 2000. Applications of adjoint modelling in atmospheric chemistry: sensitivity and inverse modelling. *Environmental Modelling & Software* 15 (6-7), 703-709.

Vautard, R., Beekmann, M., Roux, J., Gombert, D., 2001. Validation of a deterministic forecasting system for the ozone concentrations over the Paris area. *Atmospheric Environment* 35, 2449-2461.

Vautard, R., Beekmann, M., Bessagnet, B., Blond, N., Hodzic, A., Honoré, C., Malherbe, L., Menut, L., Rouil, L., Roux, J., 2004. The use of MM5 for operational ozone/NOx/aerosols prediction in Europe: strengths and weaknesses of MM5. Paper 5th WRF /14th MM5, Users' Workshop NCAR, June 22-25, 2004.

Vautard, R., Builtjes, P., Thunis, P., Cuvelier, K., Bedogni, M., Bessagnet, B., Honoré, C., Moussiopoulos, N., Pirovano G., Schaap, M., Stern, R., Tarrason, L., Van Loon, M., 2007. Evaluation and intercomparison of ozone and PM10 simulations by several chemistry-transport models over 4 European cities within the City-Delta project, *Atmospheric Environment* 41, 173-188.

Veloso, B., Azevedo, R., Monteiro, A., Borrego, C. (2004). Métodos estatísticos na previsão da qualidade do ar para os centros urbanos do Porto e Lisboa. In: Actas da 8ª Conferência Nacional de Ambiente, 27-29 de Outubro, Lisboa, Portugal, 381-382.

Viegas, D.X., Abrantes, T., Palheiro, P., Santo, F.E., Viegas, M.T., Silva, J., Pessanha, L., 2006. Fire weather during the 2003, 2004 and 2005 fire seasons in Portugal. In V International Conference on Forest Fire Research. Ed D.X. Viegas, Figueira-da-Foz, 2006. Proceedings in CD.

Vukovich, F.M. and Sherwell, J., 2003. An examination of the relationship between certain meteorological parameters and surface ozone variations in the Baltimore–Washington corridor. *Atmospheric Environment* 37, 971–981.

WCED - World Commission on Environment and Development, 1987. Our Common Future, Oxford University Press, Oxford.

Webster, M., Nam, J., Kimura, Y., Jeffries, H., Vizuete, W., Allen, D.T., 2007. The effect of variability in industrial emissions on ozone formation in Houston, Texas. *Atmospheric Environment* 41, 9580-9593.

Welbank, M., 1996. The search for a sustainable urban form, in The compact city a sustainable urban form? Jenks, M., Burton, E., Williams, K. (Eds.). Taylor and Francis Group, Oxford, 350p.

WHO - World Health Organization, 1999. Monitoring Ambient Air Quality for Health Impact Assessment. World Health Organization Regional Publications, European Series, No.85, Copenhagen.

Wilkins, E. T., 1954. Air pollution and the London fog of December 1952. *Journal of the Royal Sanitary Institute* 74, 1-21.

Williams, K., Burton, E., Jenks, M. (Eds.), 2000. Achieving Sustainable Urban Form. E & FN Spon, London, 388p.

Wise, E. and Comrie, A., 2005. Meteorologically adjusted urban air quality trends in the Southwestern United States. *Atmospheric Environment* 39, 2969–2980

Wu, J., Lurmann, F., Winer, A., Lu, R., Turco, R. & Funk, T., 2005. Development of an individual exposure model for application to the Southern California children's health study. *Atmospheric Environment* 39, 259-273.

Xue, M., Droegemeier, K.K., Wong, V., 2000. The Advanced Regional Prediction System (ARPS) – a multiscale nonhydrostatic atmospheric simulation and prediction tool. Part I: model dynamics and verification. *Meteorology and Atmospheric Physics* 75, 161–193.

Young, W., Bowyer, D., 1996. Modelling the environmental impact of changes in urban structure. *Comput., Environ. and Urban Systems* 20 (4/5), 313-326.

Zhang, D.L., Zheng, W.Z., 2004. Diurnal Cycles of surface winds and temperatures as simulated by five boundary layer parameterizations. *Journal of Applied Meteorology* 43, 157–169.

Zlatev, Z., Christensen, J., Eliassen, A., 1993. Studying high ozone concentrations by using the Danish Eulerian model. *Atmospheric Environment* 27 A (6), 845-865.

Web pages (consulted between 2008 and 2009):

URL 1: European Environment Agency: http://www.eea.europa.eu

URL2: University of Chicago Oriental Institute: http://oi.uchicago.edu/OI/MUS/ED/TRC/MESO/cities.html

URL3: Athenaeum Institute for Architecture and Design:
http://www.athenaeum.ch/images/Corbusier%20ville%203millionsg.JPG

URL4: Architektur Theorie:
http://medienarchitektur.at/architekturtheorie/broadacre_city/2007_broadacre_city_image_13.shtml

URL5: London Borough of Hackney home page: www.hackney.gov.uk/ep-ebenezer-howard.htm

URL6: F that S blog: http://fthats.files.wordpress.com/2009/04/20071018-garden_city_detail.jpg

URL7: European Commission: http://ec.europa.eu/environment/

URL8: Yale School of Forestry and Environmental Studies: research.yale.edu/.../london_smog_1952.html

URL9: Hungarian Meteorological Service: http://www.met.hu/en/hmshp.php

URL10: Agência Portuguesa do Ambiente – Inventário 2005
http://www.apambiente.pt/politicasambiente/Ar/InventarioNacional/Documents/Alocacao_Espacial_Emissoes_2005.xls

URL11: Lisbon Metropolitan Area: http://www.aml.pt

URL12: Instituto de Meteorologia: http://www.meteo.pt

URL13: Base de dados on-line sobre a qualidade do ar : http://www.qualar.org

URL14: MM5 Community Model Homepage: http://www.mmm.ucar.edu/mm5

URL15: TOMS homepage: http://jwocky.gsfc.nasa.gov/

URL16: University Corporation for Atmospheric Research: http://dss.ucar.edu/datasets/ds083.2/data

URL17: CAMx Homepage: http://www.camx.com/

URL18: Instituto Nacional de Estatística: http://www.ine.pt/

URL19: Direcção Geral de Energia e Geologia: http://www.dgge.pt/

APPENDICES

Appendix A - Land use evolution in the study region 1987 – 2000

Appendix B – Mobility in the study region: attraction and repulsion rates

Appendix C – Ozone and PM10 episodes in the study region in 2006

Appendix D – Air pollution episodes - meteorological characterization

Appendix E – Meteorological sensitivity tests

Appendix F – SPRAWL land use scenario in the study region

Appendix A
Land use evolution in the study region 1987 – 2000

Table A.1 Castelo de Paiva municipality land cover data for 1987 and 2000.

Land uses	CLC90 (1987 data)		CLC2000		Change	
	hectares	%	hectares	%	hectares	%
Artificial surfaces	42.5	0.4%	123.7	1.%	+ 81.3	+191.3%
Continuous urban fabric	0	0%	0	0%	0.0	0.0%
Discontinuous urban fabric	42.5	100%	93.8	75.8%	+51.4	+120.9%
Industrial or commercial units	0	0%	29.9	24.2%	+29.9	-
Other artificial surfaces	0	0%	0	0%	0.0	0.0%
Agricultural areas	3340.5	30.2%	2782.1	25.2%	-558.4	-16.7%
Forests and shrub areas	7575.6	68.6%	8052.7	72.9%	+477.2	+6.3%
Other non-artificial surfaces	87.9	0.8%	87.9	0.8%	0.0	0.0%

Table A.2 Espinho municipality land cover data for 1987 and 2000.

Land uses	CLC90 (1987 data)		CLC2000		Change	
	hectares	%	hectares	%	hectares	%
Artificial surfaces	803.0	41.9%	873.5	46.6%	+70.5	+8.8%
Continuous urban fabric	174.6	21.7%	174.6	20.0%	0.0	0.0%
Discontinuous urban fabric	477.5	59.5%	548.0	62.7%	+70.5	+14.8%
Industrial or commercial units	47.2	5.9%	47.2	5.4%	0.0	0.0%
Other artificial surfaces	103.7	12.9%	103.7	11.9%	0.0	0.0%
Agricultural areas	458.8	24.0%	436.8	23.2%	-21.9	-4.8%
Forests and shrub areas	474.8	24.8%	470.5	25.1%	-4.3	-0.9%
Other non-artificial surfaces	136.3	7.1%	92.0	4.9%	-44.3	-32.5%

Table A.3 Santa Maria da Feira land cover data for 1987 and 2000.

Land uses	CLC90 (1987 data)		CLC2000		Change	
	hectares	%	hectares	%	hectares	%
Artificial surfaces	3236.8	15.3%	4827.7	22.8%	+1590.9	+49.2%
Continuous urban fabric	0.0	0.0%	0.0	0.0%	0.0	0.0%
Discontinuous urban fabric	2849.0	88.0%	4130.0	85.6%	+1281.9	+45.0%
Industrial or commercial units	322.8	10.0%	618.9	12.8%	+296.1	+91.7%
Other artificial surfaces	65.0	2.0%	77.8	1.6%	+12.9	+19.8%
Agricultural areas	6405.4	30.3%	5502.8	26.0%	-902.6	-14.1%
Forests and shrub areas	11407.9	54.0%	10799.2	51.1%	-608.7	-5.3%
Other non-artificial surfaces	86.1	0.4%	6.5	0.0%	-79.6	-92.4%

Table A.4 Felgueiras municipality land cover data for 1987 and 2000.

Land uses	CLC90 (1987 data)		CLC2000		Change	
	hectares	%	hectares	%	hectares	%
Artificial surfaces	669.7	5.9%	1115.5	9.8%	+445.8	+66.6%
Continuous urban fabric	0.0	0.0%	0.0	0.0%	0.0	0.0%
Discontinuous urban fabric	669.7	100.0%	1057.9	94.8%	+388.2	+58.0%
Industrial or commercial units	0.0	0.0%	57.6	5.2%	+57.6	-
Other artificial surfaces	0.0	0.0%	0.0	0.0%	0.0	0.0%
Agricultural areas	6900.2	60.9%	6618.5	58.4%	-281.6	-4.1%
Forests and shrub areas	3737.4	33.0%	3603.6	31.8%	-133.8	-3.6%
Other non-artificial surfaces	30.4	0.3%	0.0	0.0%	-30.4	-100.0%

Table A.5 Gondomar municipality land cover data for 1987 and 2000.

Land uses	CLC90 (1987 data)		CLC2000		Change	
	hectares	%	hectares	%	hectares	%
Artificial surfaces	1637.6	12.2%	2701.8	20.2%	+1064.2	+65.0%
Continuous urban fabric	0.0	0.0%	117.0	4.3%	117.0	-
Discontinuous urban fabric	1601.5	97.8%	2441.0	90.3%	+839.6	+52.4%
Industrial or commercial units	10.7	0.7%	95.5	3.5%	+84.8	+792.5%
Other artificial surfaces	25.4	1.6%	48.4	1.8%	+23.0	+90.6%
Agricultural areas	3881.6	29.0%	3155.3	23.6%	-726.3	-18.7%
Forests and shrub areas	5023.2	37.5%	6908.9	51.6%	1885.6	37.5%
Other non-artificial surfaces	2852.5	21.3%	618.1	4.6%	-2234.3	-78.3%

Table A.6 Lousada municipality land cover data for 1987 and 2000.

Land uses	CLC90 (1987 data)		CLC2000		Change	
	hectares	%	hectares	%	hectares	%
Artificial surfaces	199.4	2.1%	676.2	7.1%	+476.8	+239.1%
Continuous urban fabric	0.0	0.0%	0.0	0.0%	0.0	0.0%
Discontinuous urban fabric	154.4	77.4%	590.6	87.3%	+436.2	+282.5%
Industrial or commercial units	45.0	22.6%	85.6	12.7%	+40.6	+90.2%
Other artificial surfaces	0.0	0.0%	0.0	0.0%	0.0	0.0%
Agricultural areas	5454.0	56.5%	5095.9	53.5%	-358.1	-6.6%
Forests and shrub areas	3759.1	39.0%	3753.1	39.4%	-6.0	-0.2%
Other non-artificial surfaces	234.7	2.4%	0.0	0.0%	-234.7	-100.0%

Table A.7 Maia municipality land cover data for 1987 and 2000.

Land uses	CLC90 (1987 data)		CLC2000		Change	
	hectares	%	hectares	%	hectares	%
Artificial surfaces	1767.7	21.2%	3094.3	37.1%	+1326.7	+75.1%
Continuous urban fabric	91.3	5.2%	154.7	5.0%	+63.4	+69.5%
Discontinuous urban fabric	1211.6	68.5%	2091.8	67.6%	+880.2	+72.7%
Industrial or commercial units	72.8	4.1%	520.9	16.8%	+448.1	+615.8%
Other artificial surfaces	392.1	22.2%	327.0	10.6%	-65.1	-16.6%
Agricultural areas	4204.6	46.6%	3138.2	37.6%	-1066.4	-25.4%
Forests and shrub areas	2623.6	31.4%	2054.1	24.6%	-569.5	-21.7%
Other non-artificial surfaces	63.2	0.8%	55.7	0.7%	-7.5	-11.8%

Table A.8 Marco de Canaveses municipality land cover data for 1987 and 2000.

Land uses	CLC90 (1987 data)		CLC2000		Change	
	hectares	%	hectares	%	hectares	%
Artificial surfaces	276.6	1.4%	695.0	3.4%	+418.3	+151.2%
Continuous urban fabric	0.0	0.0%	0.0	0.0%	0.0	0.0%
Discontinuous urban fabric	169.7	61.3%	503.6	72.5%	+334.0	+196.8%
Industrial or commercial units	0.0	0.0%	31.9	4.6%	+31.9	-
Other artificial surfaces	107.0	38.7%	159.5	22.9%	+52.5	+49.1%
Agricultural areas	10513.1	51.8%	9988.1	49.3%	-525.0	-5.0%
Forests and shrub areas	8502.2	41.9%	8241.6	40.6%	-260.5	-3.1%
Other non-artificial surfaces	984.5	4.9%	1351.7	6.7%	+367.2	+37.3%

Table A.9 Matosinhos municipality land cover data for 1987 and 2000.

Land uses	CLC90 (1987 data)		CLC2000		Change	
	hectares	%	hectares	%	hectares	%
Artificial surfaces	2775.8	44.9%	3421.4	55.3%	+645.6	+23.3%
Continuous urban fabric	355.5	12.1%	495.6	14.5%	+160.1	+47.7%
Discontinuous urban fabric	1565.9	56.4%	1837.1	53.7%	+271.2	+17.3%
Industrial or commercial units	524.8	18.9%	897.1	26.2%	+372.3	+70.9%
Other artificial surfaces	349.6	12.6%	191.7	5.6%	-157.9	-45.2%
Agricultural areas	2368.0	38.3%	1979.2	32.0%	-388.8	-16.4%
Forests and shrub areas	900.7	14.6%	651.9	10.5%	-248.8	-27.6%
Other non-artificial surfaces	140.8	2.3%	132.8	2.1%	-8.1	-5.7%

Table A.10 Póvoa de Varzim municipality land cover data for 1987 and 2000.

Land uses	CLC90 (1987 data)		CLC2000		Change	
	hectares	%	hectares	%	hectares	%
Artificial surfaces	935.9	11.9%	1259.5	16.0%	+323.6	+34.6%
Continuous urban fabric	245.0	26.2%	235.7	20.1%	+8.7	+3.5%
Discontinuous urban fabric	664.2	71.0%	858.3	68.2%	+194.2	+29.2%
Industrial or commercial units	26.7	2.9%	54	4.3%	+27.2	102.0%
Other artificial surfaces	0	0.0%	93.5	7.4%	+93.5	-
Agricultural areas	4745.7	60.5%	4775.4	60.8%	+29.7	+0.6%
Forests and shrub areas	1968.4	25.1%	1675.6	21.3%	-292.7	-14.9%
Other non-artificial surfaces	200.4	2.6%	139.9	1.8%	-60.6	-30.2%

Table A.11 Paredes municipality land cover data for 1987 and 2000.

Land uses	CLC90 (1987 data)		CLC2000		Change	
	hectares	%	hectares	%	hectares	%
Artificial surfaces	800.6	5.1%	1777.0	11.4%	+976.4	+122.0%
Continuous urban fabric	0.0	0.0%	0.0	0.0%	0.0	0.0%
Discontinuous urban fabric	684.5	85.5%	1521.3	85.6%	+836.8	+122.3%
Industrial or commercial units	54.3	6.8%	193.9	10.9%	+139.6	+256.9%
Other artificial surfaces	61.8	7.7%	61.8	3.5%	0	0%

Agricultural areas	5794.1	37.1%	5356.5	34.3%	-437.6	-7.6%
Forests and shrub areas	7615.0	48.7%	8491.5	54.3%	+876.5	+11.5%
Other non-artificial surfaces	1415.3	9.1%	0.0	0.0%	-1415.3	-100.0%

Table A.12 Paços de Ferreira municipality land cover data for 1987 and 2000.

Land uses	CLC90 (1987 data)		CLC2000		Change	
	hectares	%	hectares	%	hectares	%
Artificial surfaces	554.7	7.6%	1408.0	19.4%	+853.3	153.8%
Continuous urban fabric	0.0	0.0%	0.0	0.0%	0.0	0.0%
Discontinuous urban fabric	533.8	96.2%	1316.8	93.5%	+783.0	+146.7%
Industrial or commercial units	0.0	0.0%	70.3	5.0%	+70.3	-
Other artificial surfaces	20.9	3.8%	20.9	1.5%	0.0	0.0%
Agricultural areas	3441.3	47.4%	2866.7	39.5%	-574.6	-16.7%
Forests and shrub areas	3259.7	44.9%	2981.1	41.1%	-278.7	-8.5%
Other non-artificial surfaces	0.0	0.0%	0.0	0.0%	0.0	-

Table A.13 Penafiel municipality land cover data for 1987 and 2000.

Land uses	CLC90 (1987 data)		CLC2000		Change	
	hectares	%	hectares	%	hectares	%
Artificial surfaces	338.4	1.8%	1129.2	5.2%	+790.8	+233.7%
Continuous urban fabric	0.0	0.0%	0.0	0.0%	0.0	0.0%
Discontinuous urban fabric	242.7	71.7%	822.5	72.8%	+579.8	+238.9%
Industrial or commercial units	0.0	0.0%	91.9	8.1%	+91.9	-
Other artificial surfaces	95.6	28.3%	214.7	19.0%	+119.1	+124.6%
Agricultural areas	9967.7	51.9%	9559.0	44.4%	-408.7	-4.1%
Forests and shrub areas	8367.0	43.6%	10458.4	48.6%	+2091.4	+25.0%
Other non-artificial surfaces	533.7	2.8%	391.6	1.8%	-142.1	-26.6%

Table A.14 Porto municipality land cover data for 1987 and 2000.

Land uses	CLC90 (1987 data)		CLC2000		Change	
	hectares	%	hectares	%	hectares	%
Artificial surfaces	3181.1	82.6%	3525.5	91.5%	+344.4	+10.8%
Continuous urban fabric	1591.0	50.0%	1763.3	50.0%	+172.3	+%
Discontinuous urban fabric	1319.5	41.5%	1462.4	41.5%	+142.9	+10.8%
Industrial or commercial units	109.3	3.4%	121.1	3.4%	+11.8	+10.8%
Other artificial surfaces	161.3	5.1%	178.7	5.1%	+17.4	+10.8%
Agricultural areas	567.4	14.7%	265.7	6.9%	-301.7	-53.2%
Forests and shrub areas	57.5	1.5%	14.7	0.4%	-42.8	-74.4%
Other non-artificial surfaces	46.6	1.2%	46.6	1.2%	0.0	0.0%

Table A.15 São João da Madeira municipality land cover data for 1987 and 2000.

Land uses	CLC90 (1987 data)		CLC2000		Change	
	hectares	%	hectares	%	hectares	%
Artificial surfaces	601.2	71.7%	601.2	71.7%	0.0	0.0%
Continuous urban fabric	96.9	16.1%	96.9	16.1%	0.0	0.0%
Discontinuous urban fabric	327.6	54.5%	327.6	54.5%	0.0	0.0%
Industrial or commercial units	176.7	29.4%	176.7	29.4%	0.0	0.0%
Other artificial surfaces	0	0.0%	0	0.0%	0.0	0.0%
Agricultural areas	162.1	19.3%	162.1	19.3%	0.0	0.0%
Forests and shrub areas	75.3	9.0%	75.3	9.0%	0.0	0.0%
Other non-artificial surfaces	0.0	0.0%	0.0	0.0%	0.0	-

Table A.16 Santo Tirso municipality land cover data for 1987 and 2000.

Land uses	CLC90 (1987 data)		CLC2000		Change	
	hectares	%	hectares	%	hectares	%
Artificial surfaces	1371.8	10.3%	1916.5	14.3%	+544.7	+39.7%
Continuous urban fabric	60.3	4.4%	60.3	3.1%	+0.0	0%
Discontinuous urban fabric	1298.0	94.6%	1673.3	87.3%	+375.3	+28.9%
Industrial or commercial units	0.0	0.0%	129.5	6.8%	+129.5	-
Other artificial surfaces	13.5	1.0%	53.4	2.8%	+39.9	+295.2%
Agricultural areas	5446.6	40.7%	5096.7	38.1%	-349.9	-6.4%
Forests and shrub areas	6374.5	47.6%	6211.6	46.4%	-162.9	-2.6%
Other non-artificial surfaces	185.8	1.4%	153.8	1.1%	-32.0	-17.2%

Table A.17 Vila Nova de Famalicão municipality land cover data for 1987 and 2000.

Land uses	CLC90 (1987 data)		CLC2000		Change	
	hectares	%	hectares	%	hectares	%
Artificial surfaces	2562.9	12.6%	3486.1	17.2%	+923.2	+36.0%
Continuous urban fabric	51.8	2.0%	69.6	2.0%	+17.9	+34.5%
Discontinuous urban fabric	2228.7	87.0%	2941.8	84.4%	+713.0	+32.0%
Industrial or commercial units	244.9	9.6%	410.9	11.8%	+166.0	+67.8%
Other artificial surfaces	37.5	1.5%	63.7	1.8%	+26.3	+70.1%
Agricultural areas	10570.0	52.0%	10204.9	50.2%	-365.1	-3.5%
Forests and shrub areas	7109.2	35.0%	6633.2	32.6%	-476.0	-6.7%
Other non-artificial surfaces	82.1	0.4%	0.0	0.0%	-82.1	-100.0%

Table A.18 Valongo municipality land cover data for 1987 and 2000.

Land uses	CLC90 (1987 data)		CLC2000		Change	
	hectares	%	hectares	%	hectares	%
Artificial surfaces	801.9	10.9%	2029.9	27.7%	+1228.0	+153.1%
Continuous urban fabric	59.2	7.4%	143.8	7.1%	+84.6	+142.9%
Discontinuous urban fabric	729.5	91.0%	1689.0	83.2%	+959.5	+131.5%
Industrial or commercial units	0	0.0%	184.0	9.1%	+184.0	-
Other artificial surfaces	13.2	1.6%	13.2	0.6%	0.0	0.0%
Agricultural areas	1789.5	24.4%	1078.6	14.7%	-710.9	-39.7%
Forests and shrub areas	4089.8	55.7%	4231.3	57.6%	141.6	3.5%
Other non-artificial surfaces	658.7	9.0%	0.0	0.0%	-658.7	-100.0%

Table A.19 Vila do Conde municipality land cover data for 1987 and 2000.

Land uses	CLC90 (1987 data)		CLC2000		Change	
	hectares	%	hectares	%	hectares	%
Artificial surfaces	1093.0	7.5%	1429.5	9.8%	+336.6	+30.8%
Continuous urban fabric	141.9	13.0%	141.9	9.9%	0	0.0%
Discontinuous urban fabric	888.8	81.3%	1067.0	74.6%	+178.2	+20.0%
Industrial or commercial units	42.0	3.8%	175.1	12.2%	+133.2	+317.4%
Other artificial surfaces	20.3	1.9%	45.5	3.2%	+25.2	+124.1%
Agricultural areas	8189.5	55.9%	8155.1	55.7%	-34.4	-0.4%
Forests and shrub areas	5029.6	34.3%	4816.9	32.9%	-212.7	-4.2%
Other non-artificial surfaces	333.6	2.3%	244.2	1.7%	-89.4	-26.8%

Table A.20 Vila Nova de Gaia municipality land cover data for 1987 and 2000.

Land uses	CLC90 (1987 data)		CLC2000		Change	
	hectares	%	hectares	%	hectares	%
Artificial surfaces	4921.3	29.3%	6391.3	38.0%	+1470.0	29.9%
Continuous urban fabric	329.7	6.7%	386.4	6.0%	+56.7	+17.2%
Discontinuous urban fabric	4158.5	84.5%	5166.6	80.8%	+1008.1	+24.2%
Industrial or commercial units	300.2	6.1%	657.6	10.3%	+357.4	+119.1%
Other artificial surfaces	39.4	0.8%	180.7	2.2%	+141.3	+358.6%
Agricultural areas	6333.2	37.7%	5386.6	32.0%	-946.6	-14.9%
Forests and shrub areas	4800.2	28.5%	4347.0	25.8%	-453.2	-9.4%
Other non-artificial surfaces	762.3	4.5%	692.1	4.1%	-70.2	-9.2%

Table A.21 Trofa municipality land cover data for 1987 and 2000.

Land uses	CLC90 (1987 data)		CLC2000		Change	
	hectares	%	hectares	%	hectares	%
Artificial surfaces	838.2	11.5%	1251.3	17.1%	+413.1	+49.3%
Continuous urban fabric	33.4	4.0%	33.4	2.7%	0	0.0%
Discontinuous urban fabric	762.9	91.0%	1093.7	87.4%	+330.8	+43.4%
Industrial or commercial units	29.4	3.5%	111.7	8.9%	+82.3	+279.9%
Other artificial surfaces	12.4	1.5%	12.4	1.0%	0	+0.0%
Agricultural areas	2308.1	31.6%	2162.0	29.6%	-146.1	-6.3%
Forests and shrub areas	4013.5	55.0%	3887.7	53.2%	-125.8	-3.1%
Other non-artificial surfaces	141.2	1.9%	0.0	0.0%	-141.2	-100.0%

Appendix B
Mobility in the study region: attraction and repulsion rates

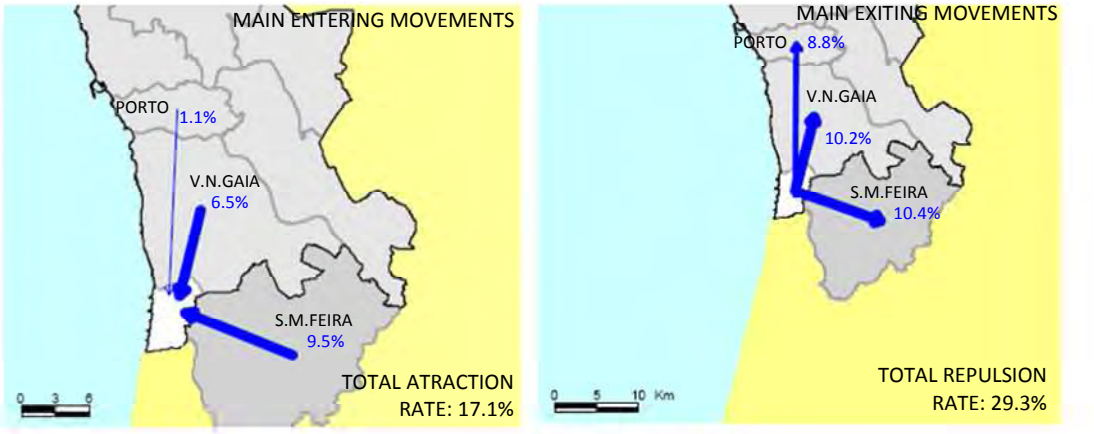

Figure B.1 Espinho main entering and exiting movements and attraction and repulsion rates for 2001 (maps from INE[2003]; numbers computed by manipulation of INE data).

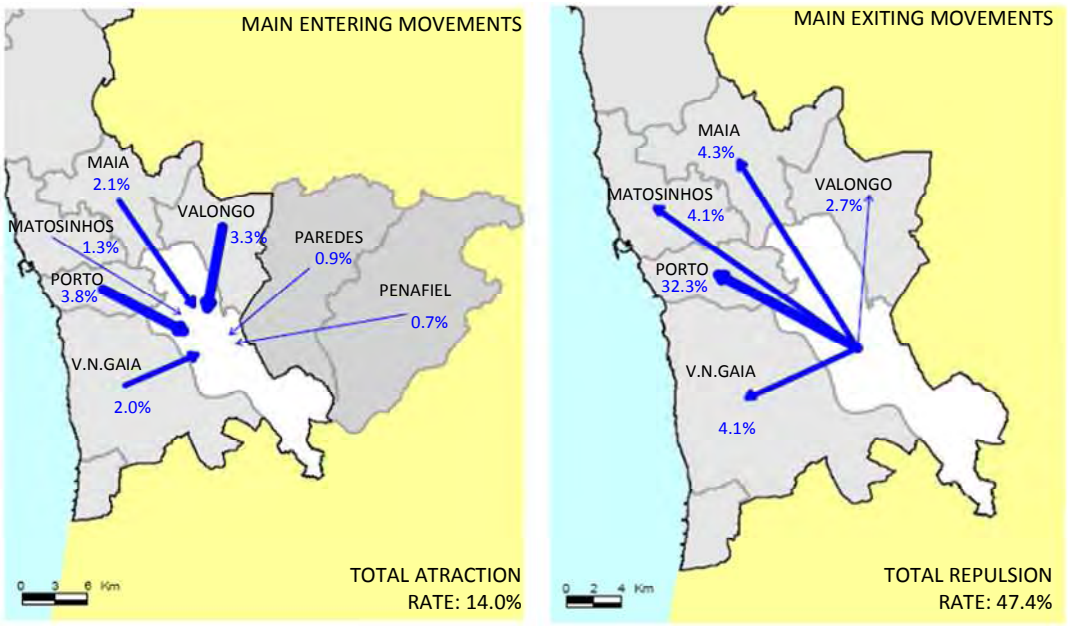

Figure B.2 Gondomar main entering and exiting movements and attraction and repulsion rates for 2001 (maps from INE[2003]; numbers computed by manipulation of INE data).

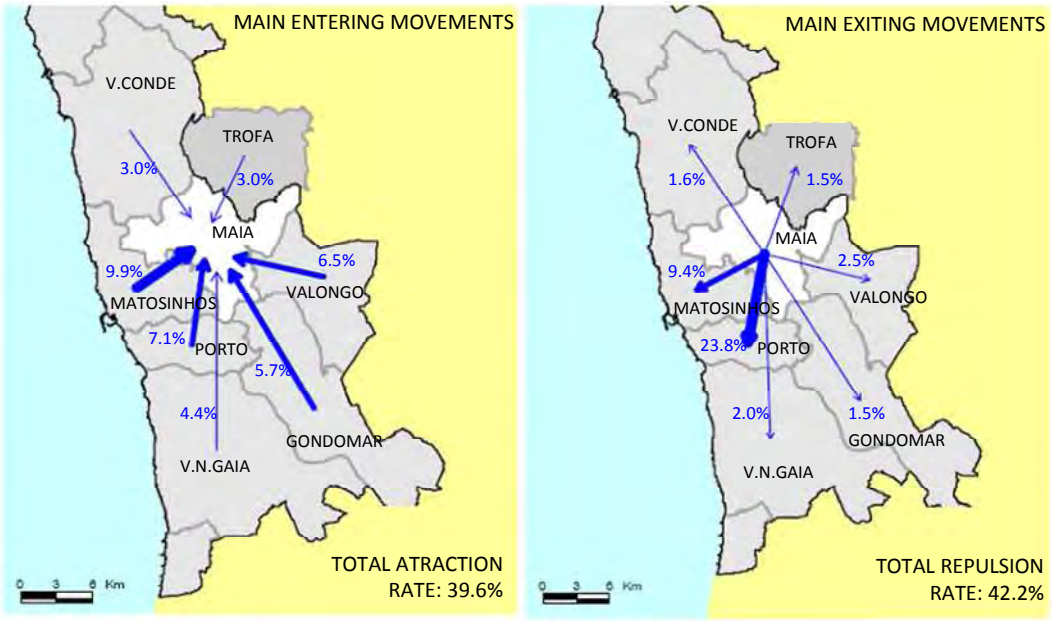

Figure B.3 Maia main entering and exiting movements and attraction and repulsion rates for 2001 (maps from INE[2003]; numbers computed by manipulation of INE data).

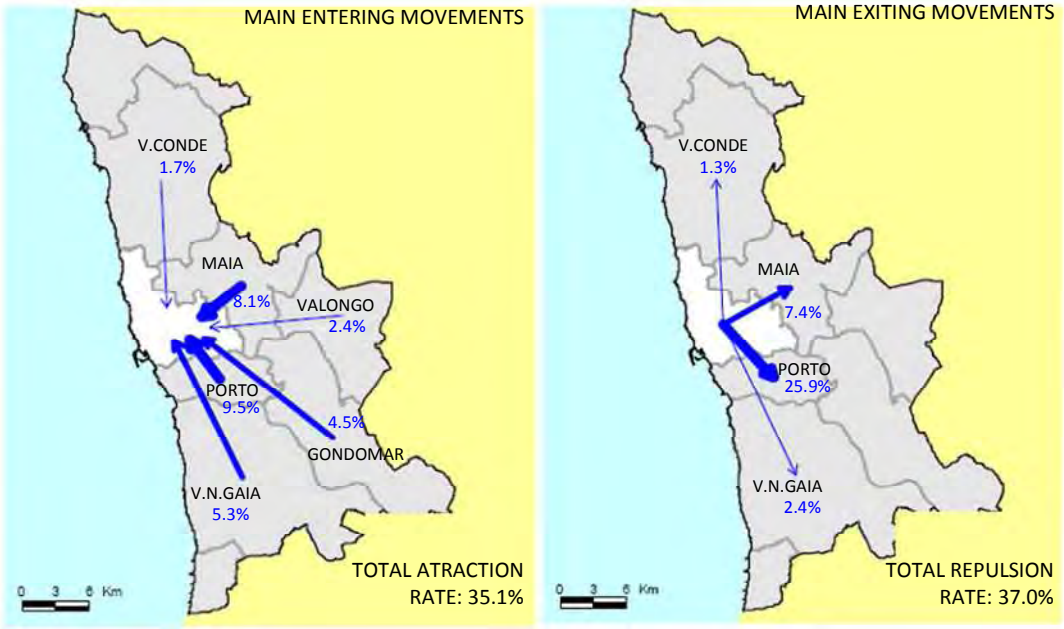

Figure B.4 Matosinhos main entering and exiting movements and attraction and repulsion rates for 2001 (maps from INE[2003]; numbers computed by manipulation of INE data).

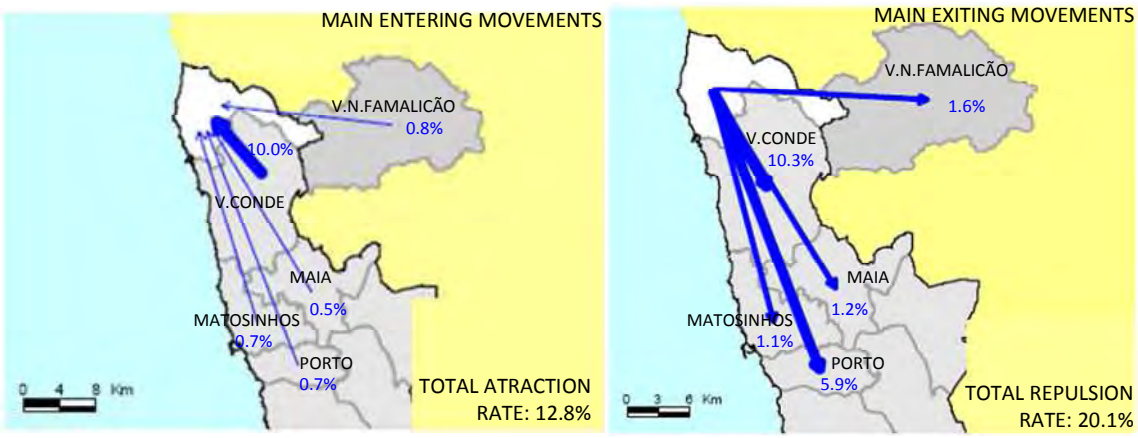

Figure B.5 Póvoa de Varzim main entering and exiting movements and attraction and repulsion rates for 2001 (maps from INE[2003]; numbers computed by manipulation of INE data).

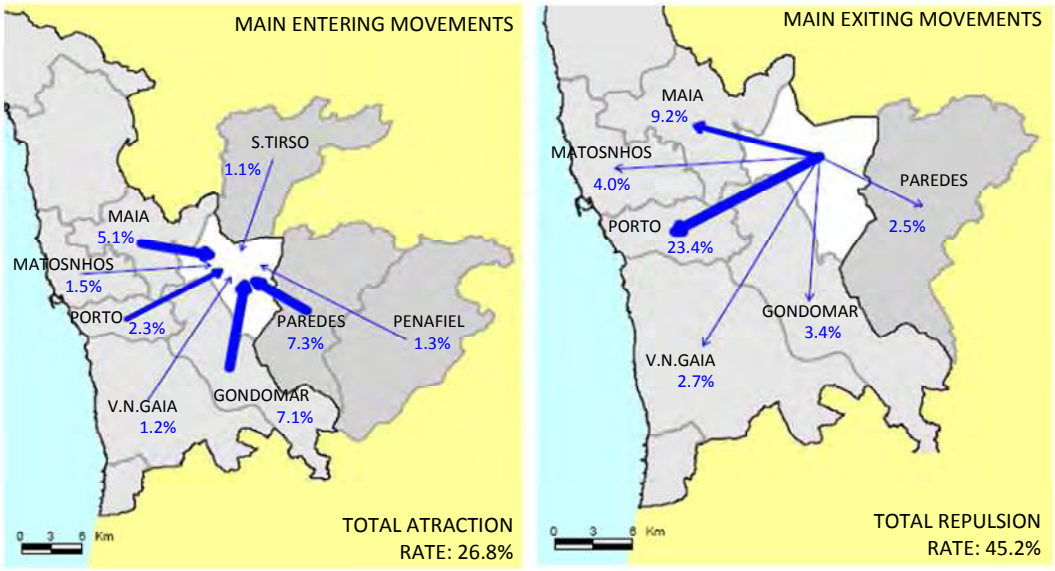

Figure B.6 Valongo main entering and exiting movements and attraction and repulsion rates for 2001 (maps from INE[2003]; numbers computed by manipulation of INE data).

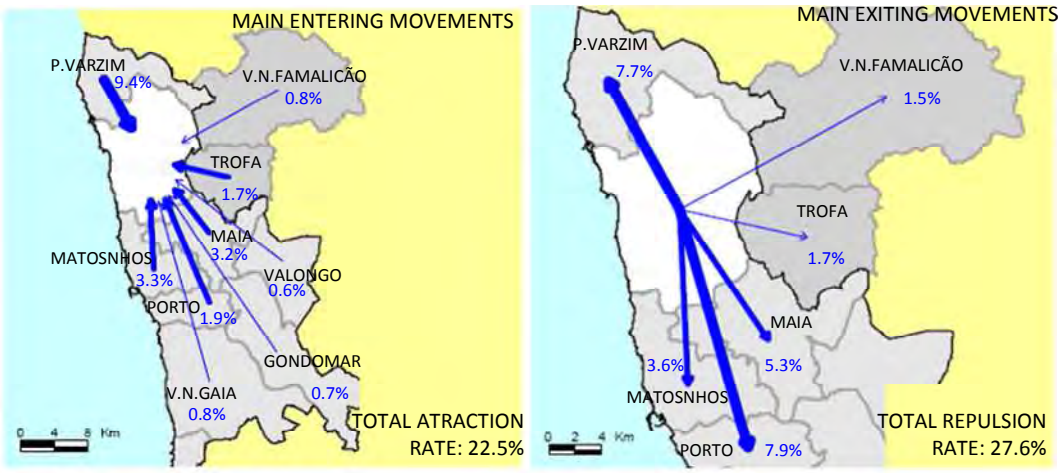

Figure B.7 Vila do Conde main entering and exiting movements and attraction and repulsion rates for 2001 (maps from INE[2003]; numbers computed by manipulation of INE data).

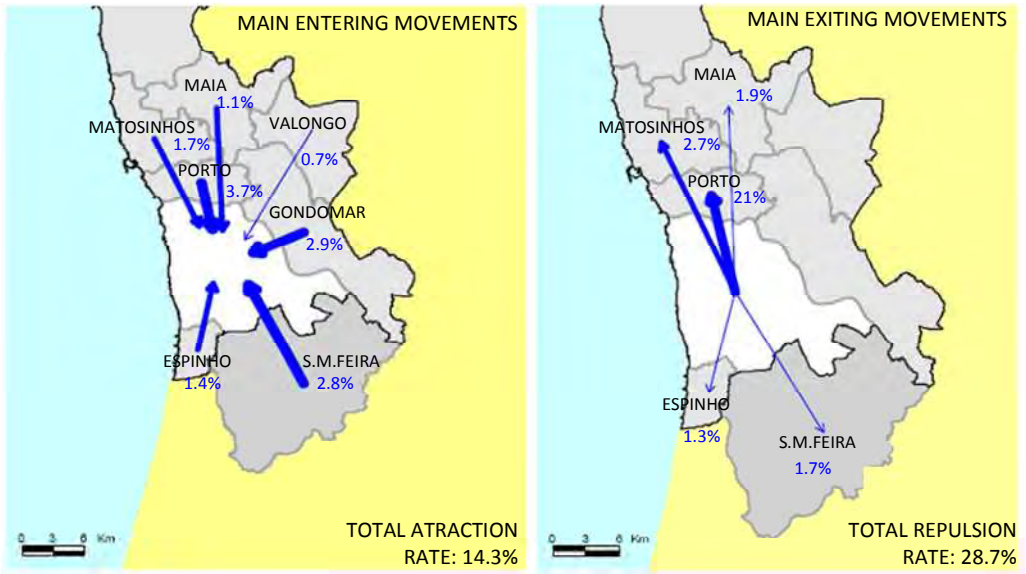

Figure B.8 Vila Nova de Gaia main entering and exiting movements and attraction and repulsion rates for 2001 (maps from INE[2003]; numbers computed by manipulation of INE data).

Appendix C
Ozone and PM10 episodes in the study region in 2006

Table C.1 Ozone episodes in the study region in 2006

Day	Hour	Air quality stations	Hourly concentrations (µg.m^{-3})
05-06-2006	14:00	VNT, ST, CLD	201, 186, 195
	15:00	ERM, VRM, VNT, LB, ST, CLD	196, 186, 195, 200, 183, 184
	16:00	VNT	183
06-06-2006	16:00	ERM, VNT, LB, ST, CLD	186, 183, 195, 184, 195
	17:00	ERM, LB, CLD	188, 184, 187
	18:00	PRF	182
13-07-2006	14:00	ANT	183
	15:00	ERM, ST, CLD	191, 194, 182
	16:00	ERM, VRM, ANT, VNT, LB, ST, CL, CLD	209, 187, 200, 189, 186, 193, 189, 186
	17:00	CST, ERM, ANT, VNT, LB, ST, CL	184, 188, 196, 187, 198, 188, 183
	18:00	LB	182
06-08-2006	15:00	PRF	202
	16:00	VRM, VNT	187, 189
	17:00	ANT	185
08-08-2006	15:00	PRF	200
	16:00	CST, VRM, PRF, VNT	185, 181, 198, 187
	17:00	VRM	181
09-08-2006	15:00	PRF	181
	16:00	PRF, CLD	216, 198
	17:00	PRF, ST, CL, CLD	209, 201, 187, 205
	18:00	CST, VRM, PRF, LB, ST, CL, CLD	190, 192, 183, 189, 192, 192 193
	19:00	ERM, ANT	184, 182
11-08-2006	14:00	CLD	190
	15:00	VNT,ST, CLD	184, 189, 196
	16:00	CST, ERM, VRM, PRF, LB, CL	191, 188, 186, 202, 183, 210
	17:00	ERM, ANT	182, 184
22-08-2006	13:00	ST, CLD	182, 201
	14:00	ST, CLD	192, 227
	15:00	PRF, ST, CLD	192, 214, 207
	16:00	VRM, VNT, CL	186, 187, 194
	17:00	ERM, ANT	203, 188
05-09-2006	12:00	ST, CLD	193, 224
	13:00	ST, CL, CLD	269, 208, 231
	14:00	CST, VRM, ANT, VNT, ST, CL, CLD	182, 182, 225, 189, 227, 323, 226
	15:00	CST, ERM, VRM, PRF, ANT, VNT, ST, CL, CLD	211, 189, 187, 191, 213, 234, 219, 279, 198
	16:00	ERM, VRM, PRF, ANT, VNT, ST, CL	240, 217, 185, 240, 195, 187, 225
	17:00	ERM	189

Table C.2 PM10 episodes in the study area in 2006.

Days	Air quality stations	Maximum daily average concentrations ($\mu g.m^{-3}$)
3-5 Jan 06	ERM, BV, ANT, MAT, VNT, VRM, PRF, ESP, LB, SH, VC, CST, ST, CLD, PRD	95, 63, 71, 84, 70, 75, 71, 58, 67, 77, 79, 59,64, 58, 96
7-12 Jan 06	ERM, BV, ANT, MAT, VNT, VRM, PRF, ESP, LB, SH, VC, ST, CLD, PRD, CL	87, 56, 72, 86, 65, 89, 59, 78, 75, 80, 77, 72, 51, 97, 52
17-20 Jan 06	ERM, BV, ANT, MAT, VNT, VRM, ESP, LB, SH, VC, ST, PRD	65, 60, 59, 76, 50, 71, 55, 72, 60, 75, 57, 71
23-24 Jan 06	ERM, ANT, MAT, VNT, VRM, PRF, ESP, LB, SH, VC, CST, ST, CLD, PRD	73, 56, 62, 53, 71, 54, 54, 69, 61, 62, 74, 55, 57, 99
26 Jan 06	MAT, VRM, VC, ST, PRD	55, 51, 58, 64, 61
30 Jan-14 Fev 06	ERM, BV, ANT, MAT, VNT, VRM, PRF, ESP, LB, SH, VC, CST, CLD, PRD, CL	134, 103, 99, 136, 118, 148, 117, 112, 153, 122, 137, 65, 108, 134, 93
17-18 Fev 06	PRF, ESP, VC	63, 72, 63
24 Fev 06	ERM, ANT, MAT, VRM, LB, SH, PRD	61, 52, 59, 53, 58, 54, 93
10 Mar 06	MAT, PRF, ESP	51, 55, 61
13-16 Mar 06	ERM, BV, ANT, MAT, VNT, VRM, PRF, ESP, LB, SH, VC, CLD, PRD, CL	81, 80, 70, 81, 65, 83, 79, 78, 92, 85, 80, 69, 84, 73
24 Mar 06	BV, MAT, PRF, ESP, SH, VC, ST	53, 52, 70, 74, 52, 69, 57
27 Mar 06	PRF, ESP, VC	58, 67, 66
12 Abr 06	MAT, VRM, LB, SH	66, 55, 58, 54
23-27 Abr 06	ERM, BV, ANT, MAT, VNT, VRM, PRF, ESP, LB, SH, VC, CST, ST, CLD, PRD	67, 65, 58, 76, 60, 62, 76, 89, 60, 83, 69, 68, 76, 55, 74
10 Mai 06	BV, ANT, MAT, VRM, SH, CL	77, 51, 60, 57, 57, 60
26 Mai-7 Jun 06	ERM, BV, ANT, MAT, VNT, VRM, PRF, ESP, SH, VC, CST, ST, CLD, PRD, CL	59, 118, 90, 129, 79, 88, 100, 101, 114, 104, 79, 87, 65, 82, 137
13 Jun 06	ERM, BV, ANT, MAT, VRM, ESP, VC	64, 60, 62, 65, 65, 72, 59
18 Jun 06	ERM, MAT, VRM, VC	52, 52, 53, 60
22-23 Jun 06	ERM, BV, ANT, MAT, VRM, SH, VC, ST, CLD, PRD, CL	60, 60, 60, 50, 61, 58, 51, 60, 52, 59, 63
27 Jun-1 Jul 06	ERM, BV, ANT, VNT, VRM, SH, VC, CST, ST, CLD, PRD, CL	60, 54, 56, 55, 58, 65, 55, 79, 77, 53, 68, 68
7 Jul 06	ERM, BV, ANT, MAT, VRM, SH, VC, CST	56, 58, 62, 51, 50, 68, 60, 68
10-18 Jul 06	ERM, BV, ANT, MAT, VNT, VRM, PRF, ESP, SH, VC, CST, ST, CLD, PRD, CL	92, 97, 96, 89, 87, 89, 80, 118, 99, 121, 64, 73, 64, 67, 77
2 Ag 06	BV, SH, VC	50, 51, 50
4-14 Ag 06	ERM, BV, ANT, MAT, VNT, VRM, PRF, ESP, SH, VC, ST, CLD, PRD, CL	122, 116, 102, 121, 179, 125, 112, 162, 125, 132, 101, 80, 88, 97
22 Ag 06	MAT, ESP, SH	53, 52, 57
29 Ag 06	BV, MAT, ESP, SH	51, 57, 67, 57
31 Ag 06	ERM, BV, VNT, VRM, SH, CST	59, 57, 58, 68, 52, 57
4-9 Set 06	ERM, BV, ANT, MAT, VNT, VRM, PRF, ESP, SH, VC, CST, ST, CLD, PRD, CL	90, 84, 73, 100, 89, 98, 74, 100, 77, 82, 50, 86, 65, 117, 83
10 Out 06	BV, ANT, PRF, SH, VC	52, 50, 51, 51, 51
23 Out 06	MAT, PRF, ESP, CST	57, 52, 70, 53
28 Out-1 Nov 06	ERM, BV, ANT, MAT, VNT, VRM, PRF, ESP, SH, VC, ST, CLD, PRD, CL	64, 62, 66, 77, 63, 66, 55, 71, 65, 66, 62, 54, 75, 74
11-14 Nov 06	ERM, BV, ANT, MAT, VNT, VRM, PRF, ESP, SH, VC, ST, PRD, CL	66, 58, 56, 59, 58, 69, 56, 61, 57, 66, 60, 63, 67
12 Dez 06	ERM, ANT, MAT, VC, PRD	61, 50, 55, 57, 66
16-24 Dez 06	ERM, BV, ANT, MAT, VNT, VRM, PRF, ESP, LB, SH, VC, ST, CLD, PRD, CL	74, 58, 66, 73, 61, 84, 81, 59, 82, 89, 77, 103, 61, 83, 82
31 Dez 06	PRF, ESP, VC	65, 54, 59

(Abbreviations: ANT-Antas, BV-Boavista, CL- Centro de Lacticínios, CLD-Calendário, CST-Custóias, ERM-Ermesinde,ESP-Espinho, LB-Leça do Balio, MAT-Matosinhos, PRD-Paredes, PRF-Perafita, ST-Santo Tirso, SH - Senhora da Hora, VC-Vila do Conde, VNT-Vila Nova da Telha, VRM –Vermoim)

Appendix D
Air pollution episodes - meteorological characterization

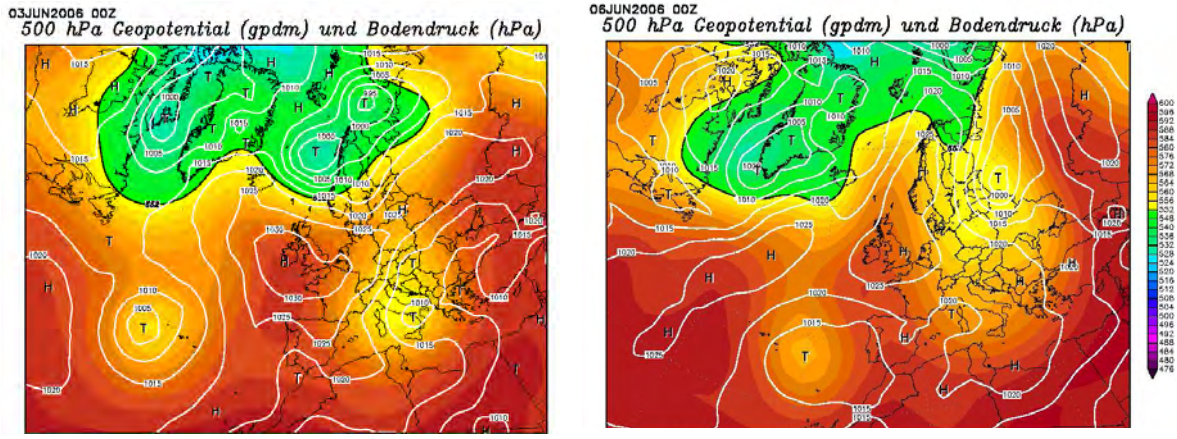

Figure D.1 Summer episode 500 hPa pressure maps – 3 and 6 June 2006 (www.weterzentrale.de).

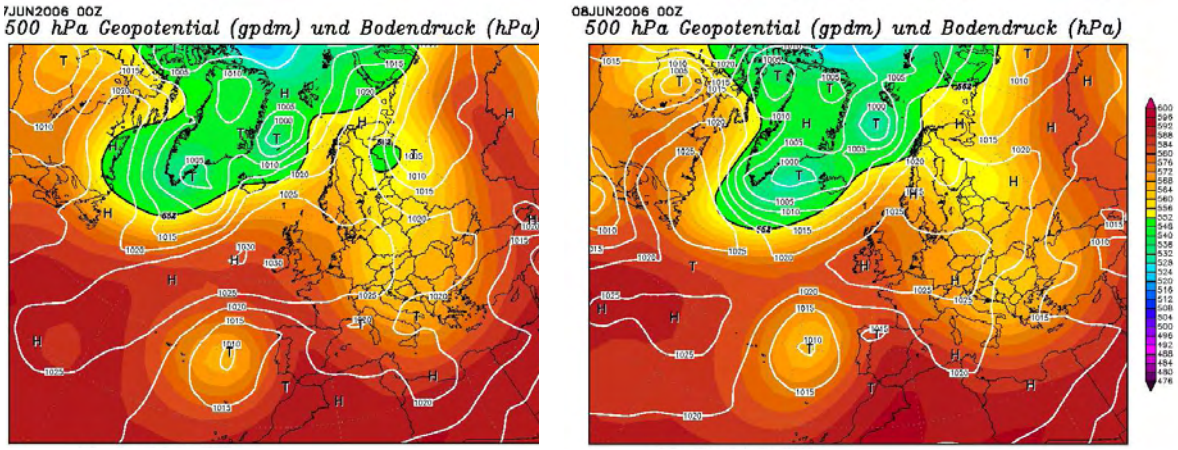

Figure D.2 Summer episode 500 hPa pressure maps – 7 and 8 June 2006 (**www.weterzentrale.de**).

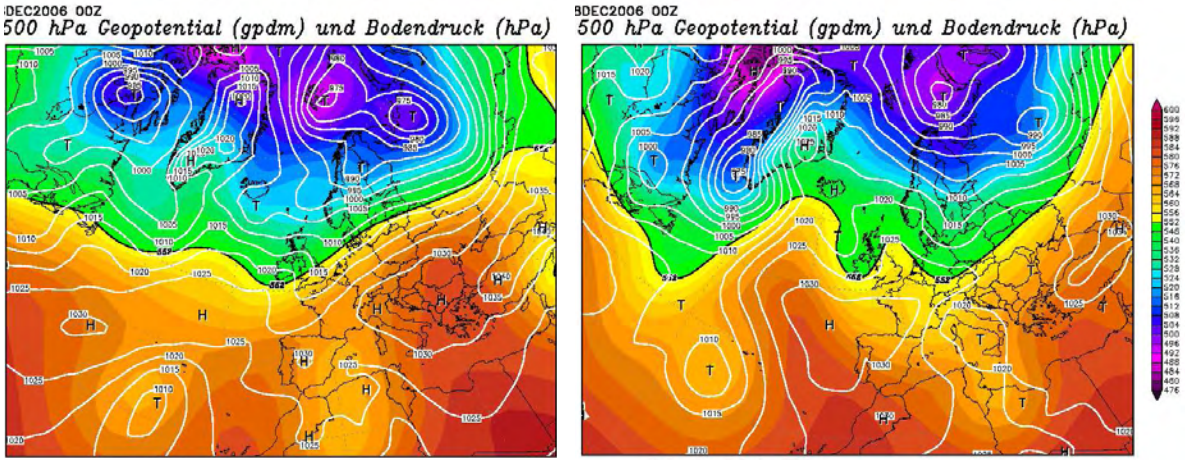

Figure D.3 Winter episode 500 hPa pressure maps – 16 and 18 December 2006 (www.weterzentrale.de).

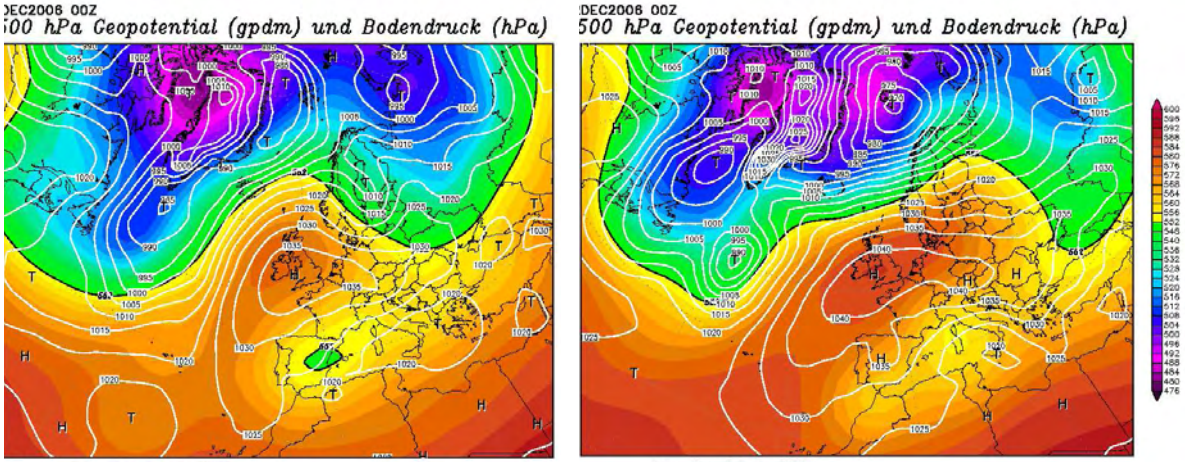

Figure D.4 Winter episode 500 hPa pressure maps – 20 and 22 December 2006 (www.weterzentrale.de).

Appendix E
Meteorological sensitivity tests

Table E.1 Statistical measures for temperature and wind components obtained for MM5 – test1 simulation - summer (3-8 June 2006) and winter (16-24 December 2006) episodes

	T				u				v			
	r	S/S_{obs}	E/S_{obs}	E_{ub}/S_{obs}	R	S/S_{obs}	E/S_{obs}	E_{ub}/S_{obs}	r	S/S_{obs}	E/S_{obs}	E_{ub}/S_{obs}
VS	0.95	0.68	0.60	0.42	0.86	0.49	0.67	0.63	0.34	0.45	1.11	0.95
9km	0.88	0.92	0.62	0.47	0.76	0.59	0.79	0.69	0.12	0.53	2.21	1.36
3km	0.92	0.80	0.62	0.41	0.88	0.42	0.66	0.64	0.83	0.60	0.61	0.61
	0.72	1.00	1.30	0.75	0.78	0.42	0.76	0.72	0.51	0.40	0.87	0.87
BR	0.44	0.42	0.96	0.90	0.10	1.99	2.14	2.14	0.16	1.33	1.53	1.53
9km	0.22	0.74	1.91	1.14	0.13	1.43	3.15	1.74	0.11	2.51	2.64	2.60
3km	0.89	0.73	0.66	0.48	0.45	1.39	1.61	1.22	0.08	0.51	1.07	1.07
	0.61	0.82	1.13	0.83	0.16	0.72	1.97	2.09	0.20	0.83	1.24	1.17
VC	0.43	0.39	1.05	0.95	0.84	0.93	0.56	0.55	0.56	2.72	2.35	2.33
9km	0.42	0.64	1.22	0.94	0.30	1.94	2.27	1.91	0.25	7.62	7.45	7.43
VR	0.92	0.72	0.74	0.44	0.71	1.61	1.58	1.14	0.48	0.60	0.90	0.88
9km	0.47	0.88	1.01	0.97	0.28	1.47	3.00	1.64	0.02	0.51	1.13	1.13
CBR	0.91	0.74	0.71	0.45	0.80	0.77	0.60	0.60	0.42	0.95	1.06	1.05
9km	0.79	1.16	1.08	0.72	0.34	0.79	1.05	1.04	0.38	1.27	1.89	1.32
CB	0.95	0.66	1.05	0.43	0.63	0.71	0.81	0.78	0.72	0.69	0.70	0.69
9km	0.90	0.89	1.21	0.48	0.63	1.12	1.10	0.92	0.63	0.55	0.79	0.78
LS	0.91	0.92	1.02	0.47	0.77	0.83	0.94	0.78	0.78	1.17	0.80	0.91
9km	0.78	1.15	2.29	0.72	0.56	0.92	1.51	0.90	0.41	1.13	1.78	1.17
SN	0.34	0.55	1.04	0.96	0.67	1.06	0.93	0.84	0.71	1.25	0.91	0.89
9km	0.54	0.83	0.97	0.89	0.52	1.03	2.36	0.99	0.65	1.31	1.11	1.01
EV	0.91	0.47	0.69	0.60	0.73	0.66	0.74	0.69	0.64	0.78	0.80	0.79
9km	0.71	0.70	1.31	0.71	0.48	0.58	1.11	0.90	0.53	0.85	1.56	0.95
BJ	0.92	0.55	0.70	0.53	0.59	0.71	1.02	0.82	0.74	0.79	0.81	0.67
9km	0.75	0.81	1.73	0.69	0.65	0.48	0.93	0.78	0.56	0.58	0.83	0.83
FR	0.83	1.16	0.96	0.65	0.94	0.61	0.53	0.49	0.54	1.27	1.13	1.12
9km	0.74	1.13	1.78	0.78	0.45	0.49	1.18	0.89	0.50	1.17	1.97	1.10

Table E.2 Statistical measures for temperature and wind components obtained for MM5 – Test2 simulation - summer (3-8 June 2006) and winter (16-24 December 2006) episodes.

	T				u				v			
	r	S/S_{obs}	E/S_{obs}	E_{ub}/S_{obs}	r	S/S_{obs}	E/S_{obs}	E_{ub}/S_{obs}	r	S/S_{obs}	E/S_{obs}	E_{ub}/S_{obs}
VS	0.95	0.71	0.53	0.39	0.85	0.54	0.64	0.61	0.38	0.50	1.10	0.93
9km	0.89	0.96	0.58	0.47	0.77	0.61	0.77	0.66	0.13	0.53	2.19	1.36
3km	0.92	0.80	0.62	0.41	0.88	0.44	0.67	0.66	0.83	0.58	0.62	0.62
	0.73	1.01	1.28	0.74	0.78	0.41	0.78	0.73	0.53	0.38	0.87	0.86
BR	0.42	0.43	0.97	0.91	0.1	1.97	2.12	2.11	0.13	1.31	1.55	1.54
9km	0.24	0.74	1.91	1.13	0.12	1.40	3.12	1.72	0.12	2.48	2.60	2.56
3km	0.89	0.76	0.66	0.47	0.44	1.28	1.22	1.62	0.12	0.52	1.09	1.09
	0.61	0.82	1.12	0.84	0.16	0.82	1.97	1.38	0.19	0.85	1.29	1.19

VC	0.43	0.40	1.04	0.94	0.85	0.92	0.56	0.55	0.60	2.71	2.30	2.28
9km	0.43	0.64	1.22	0.93	0.29	1.93	2.28	1.91	0.25	7.61	7.44	7.42
VR	0.93	0.74	0.70	0.41	0.72	2.05	2.06	1.49	0.51	0.76	0.91	0.90
9km	0.48	0.93	1.02	0.99	0.27	1.99	3.99	2.12	0.03	0.65	1.18	1.18
CBR	0.91	0.74	0.70	0.44	0.81	0.77	0.58	0.58	0.42	0.94	1.05	1.05
9km	0.80	1.14	1.08	0.69	0.32	0.72	1.05	1.03	0.38	1.24	1.83	1.29
CB	0.95	0.66	1.05	0.43	0.63	0.72	0.81	0.78	0.72	0.69	0.69	0.69
9km	0.90	0.88	1.21	0.48	0.63	1.12	1.10	0.92	0.63	0.55	0.79	0.78
LS	0.91	0.92	1.02	0.47	0.77	0.83	0.94	0.78	0.78	1.17	0.80	0.91
9km	0.78	1.14	2.27	0.72	0.58	0.91	1.50	0.88	0.42	1.13	1.75	1.15
SN	0.34	0.55	1.04	0.96	0.67	1.07	0.94	0.84	0.70	1.24	0.91	0.89
9km	0.53	0.83	0.97	0.90	0.52	1.05	2.35	1.00	0.66	1.31	1.10	1.00
EV	0.91	0.47	0.69	0.60	0.73	0.66	0.74	0.69	0.74	0.79	0.81	0.67
9km	0.72	0.70	1.31	0.70	0.47	0.57	1.12	0.90	0.54	0.84	1.55	0.94
BJ	0.92	0.55	0.70	0.53	0.59	0.71	1.02	0.82	0.64	0.78	0.80	0.78
9km	0.75	0.81	1.73	0.69	0.65	0.48	0.93	0.78	0.56	0.58	0.84	0.83
FR	0.83	1.16	0.96	0.65	0.94	0.61	0.53	0.49	0.54	1.27	1.13	1.12
9km	0.74	1.13	1.78	0.78	0.45	0.49	1.18	0.89	0.51	1.16	1.95	1.09

Table E.3 Statistical measures for temperature and wind components obtained for MM5 – Test3 simulation - summer (3-8 June 2006) and winter (16-24 December 2006) episodes.

	T				u				v			
	r	S/S_{obs}	E/S_{obs}	E_{ub}/S_{obs}	R	S/S_{obs}	E/S_{obs}	E_{ub}/S_{obs}	r	S/S_{obs}	E/S_{obs}	E_{ub}/S_{obs}
VS	0.95	0.82	0.35	0.35	0.82	0.65	0.63	0.59	0.21	0.56	1.15	1.04
9km	0.88	1.01	0.50	0.49	0.76	0.73	0.73	0.67	0.11	0.59	2.16	1.40
	0.93	0.94	0.38	0.36	0.76	0.49	0.76	0.70	0.77	0.53	0.68	0.68
3km	0.89	1.06	0.91	0.48	0.71	0.44	0.80	0.75	0.53	0.43	0.86	0.85
BR	0.39	0.45	0.96	0.92	0.07	1.98	2.16	2.16	0.01	1.26	1.61	1.60
9km	0.49	0.54	2.13	0.94	0.01	1.42	2.80	1.81	0.09	2.32	2.49	2.44
	0.92	0.84	0.43	0.40	0.23	1.43	1.54	1.54	0.07	0.60	1.25	1.24
3km	0.64	0.80	1.42	0.82	0.16	1.06	1.15	1.45	0.13	1.14	1.59	1.43
VC	0.39	0.41	1.04	0.95	0.75	0.81	0.67	0.67	0.67	2.34	1.82	1.82
9km	0.59	045	1.37	0.83	0.41	1.43	1.51	1.37	0.28	6.81	6.63	6.60
VR	0.94	0.88	0.44	0.35	0.62	2.37	2.36	1.92	0.37	0.85	1.13	1.04
9km	0.54	1.04	0.98	0.98	0.30	2.40	4.29	2.45	0.15	0.79	1.20	1.18
CBR	0.92	0.81	0.48	0.40	0.79	0.81	0.62	0.62	0.39	0.98	1.11	1.09
9km	0.77	1.29	1.07	0.83	0.29	0.80	1.10	1.08	0.37	1.33	1.83	1.37
CB	0.93	0.82	0.71	0.39	0.60	0.86	0.84	0.84	0.62	0.78	0.80	0.80
9km	0.88	1.03	0.97	0.52	0.60	1.18	1.27	1.00	0.59	0.70	0.82	0.82
LS	0.79	1.06	0.80	0.75	0.72	0.94	0.88	0.89	0.74	1.18	0.81	0.98
9km	0.89	1.24	1.39	0.57	0.48	0.93	1.45	0.98	0.31	1.27	1.55	1.35
SN	0.32	0.32	1.02	0.95	0.81	0.95	0.61	0.60	0.74	1.14	0.80	0.79
9km	0.55	0.72	0.97	0.85	0.65	0.82	1.17	0.79	0.71	1.17	0.85	0.84
EV	0.89	0.58	0.59	0.55	0.66	0.67	0.77	0.75	0.62	0.85	0.83	0.82
9km	0.87	0.88	0.75	0.52	0.42	0.71	1.16	0.96	0.49	0.95	1.43	1.01
BJ	0.95	0.70	0.43	0.40	0.57	0.79	0.97	0.85	0.70	0.83	0.84	0.72
9km	0.89	1.11	1.05	0.52	0.63	0.67	0.90	0.78	0.59	0.72	0.83	0.82
FR	0.81	1.40	0.86	0.83	0.88	0.65	0.57	0.55	0.52	1.28	1.15	1.14
9km	0.85	1.09	1.19	0.57	0.43	0.55	1.18	0.90	0.59	1.17	1.76	1.01

Table E.4 Statistical measures for temperature and wind components obtained for MM5 – Test4 simulation - summer (3-8 June 2006) and winter (16-24 December 2006) episodes.

	T				u				v			
	r	S/S_{obs}	E/S_{obs}	E_{ub}/S_{obs}	r	S/S_{obs}	E/S_{obs}	E_{ub}/S_{obs}	r	S/S_{obs}	E/S_{obs}	E_{ub}/S_{obs}
VS	0.95	0.82	0.35	0.35	0.82	0.65	0.63	0.59	0.22	0.55	1.14	1.03
9km	0.88	1.01	0.50	0.50	0.75	0.72	0.74	0.67	0.12	0.60	2.17	1.41
	0.93	0.94	0.38	0.36	0.77	0.49	0.75	0.70	0.77	0.53	0.68	0.68
3km	0.89	1.05	0.91	0.48	0.71	0.44	0.80	0.75	0.53	0.43	0.86	0.86
BR	0.40	0.45	0.96	0.92	0.06	1.98	2.16	2.16	0.01	1.26	1.62	1.60
9km	0.50	0.54	2.12	0.94	0.01	1.41	2.79	1.81	0.10	2.32	2.50	2.44
	0.92	0.84	0.43	0.40	0.24	1.35	1.48	1.48	0.07	0.59	1.24	1.23
3km	0.64	0.80	1.41	0.82	0.15	1.02	1.20	1.60	0.13	1.11	1.57	1.40
VC	0.39	0.41	1.04	0.95	0.74	0.82	0.68	0.68	0.67	2.33	1.82	1.82
9km	0.58	045	1.37	0.83	0.42	1.42	1.49	1.35	0.28	6.82	6.64	6.61
VR	0.94	0.87	0.44	0.35	0.62	2.37	2.38	1.92	0.37	0.87	1.15	1.06
9km	0.54	1.04	0.98	0.98	0.30	2.40	4.30	2.45	0.14	0.79	1.20	1.19
CBR	0.92	0.81	0.48	0.40	0.78	0.80	0.62	0.62	0.39	0.97	1.11	1.09
9km	0.90	1.06	0.48	0.46	0.24	0.84	1.15	1.14	0.44	1.47	1.88	1.40
CB	0.93	0.82	0.70	0.39	0.60	0.86	0.84	0.84	0.62	0.78	0.80	0.80
9km	0.88	1.03	0.97	0.52	0.59	1.18	1.27	1.01	0.59	0.70	0.82	0.82
LS	0.79	1.06	0.80	0.75	0.72	0.94	0.88	0.89	0.75	1.19	0.81	0.98
9km	0.89	1.24	1.39	0.57	0.48	0.93	1.45	0.99	0.32	1.30	1.55	1.36
SN	0.32	0.32	1.02	0.95	0.81	0.95	0.61	0.60	0.74	1.14	0.80	0.79
9km	0.55	0.72	0.97	0.85	0.65	0.84	1.16	0.79	0.72	1.19	0.85	0.84
EV	0.94	0.62	0.48	0.47	0.70	0.72	0.73	0.71	0.53	0.86	0.91	0.91
9km	0.87	0.88	0.76	0.52	0.41	0.70	1.17	0.97	0.49	0.95	1.44	1.02
BJ	0.95	0.70	0.43	0.40	0.57	0.79	0.97	0.85	0.70	0.83	0.84	0.72
9km	0.89	1.10	1.05	0.51	0.63	0.67	0.91	0.78	0.58	0.72	0.84	0.83
FR	0.81	1.40	0.86	0.83	0.88	0.65	0.57	0.55	0.52	1.28	1.15	1.14
9km	0.85	1.09	1.19	0.57	0.43	0.55	1.18	0.90	0.59	1.16	1.75	1.01

a)

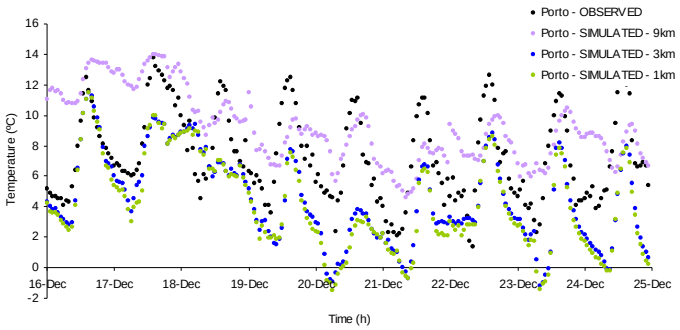

b)

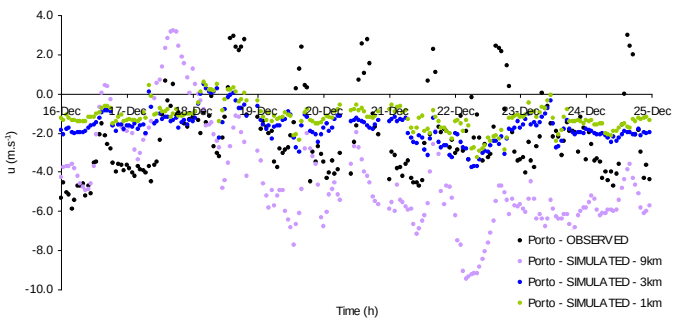

c)

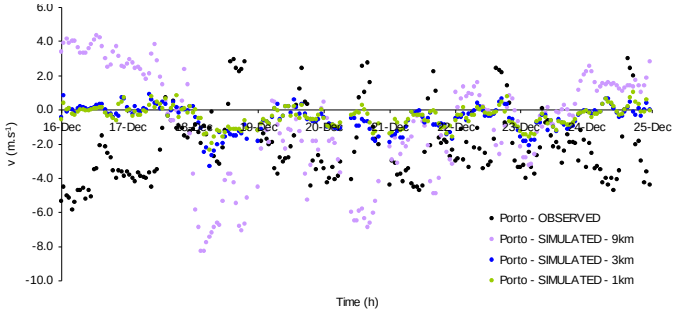

Figure E.1 Winter episode time series comparison of surface a) temperature, b) zonal wind component, and c) meridional wind component from MM5-test1 simulations at 9 km, 3 km and 1 km, and surface measurements at Porto.

a)

b)

c)

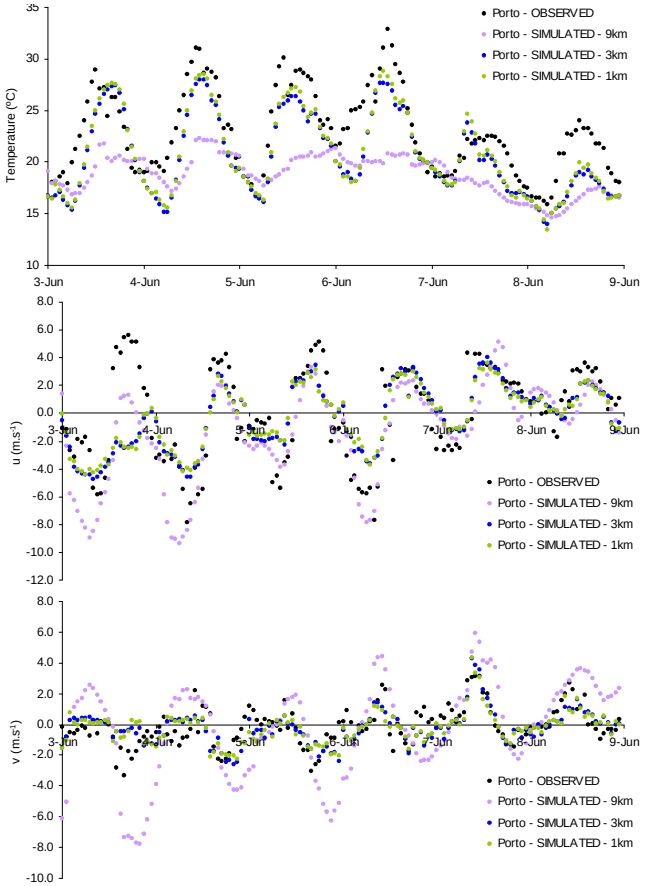

Figure E.2 Summer episode time series comparison of surface a) temperature, b) zonal wind component, and c) meridional wind component MM5-Test2 simulations at 9, 3 and 1 km, and surface measurements at Porto.

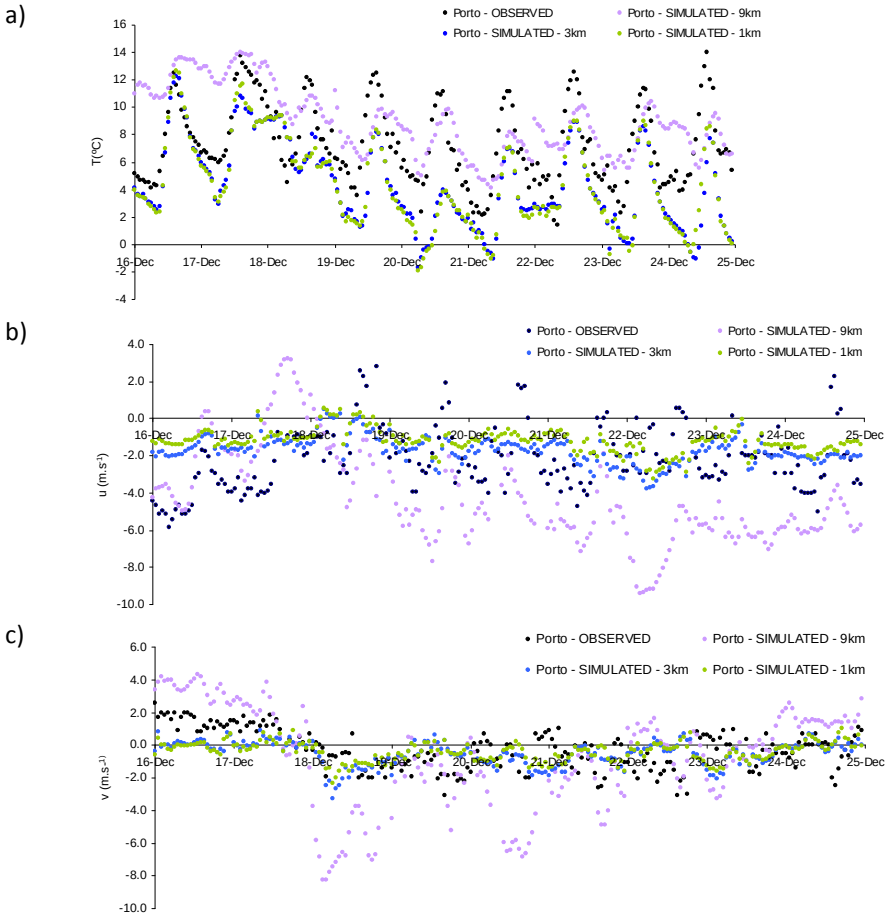

Figure E.3 Winter episode time series comparison of surface a) temperature, b) zonal wind component, and c) meridional wind component from MM5-Test2 simulations at 9, 3 and 1 km, and surface measurements at Porto.

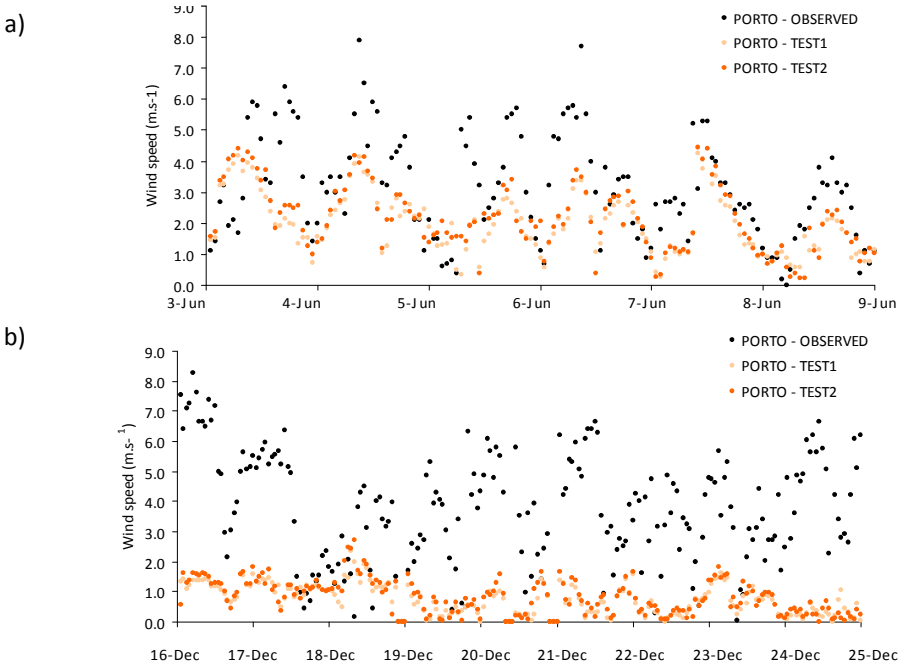

Figure E.4 a) Summer and b) winter, episode time series comparison of wind speed for test2 and test1 in Porto, for D3 (1 km resolution).

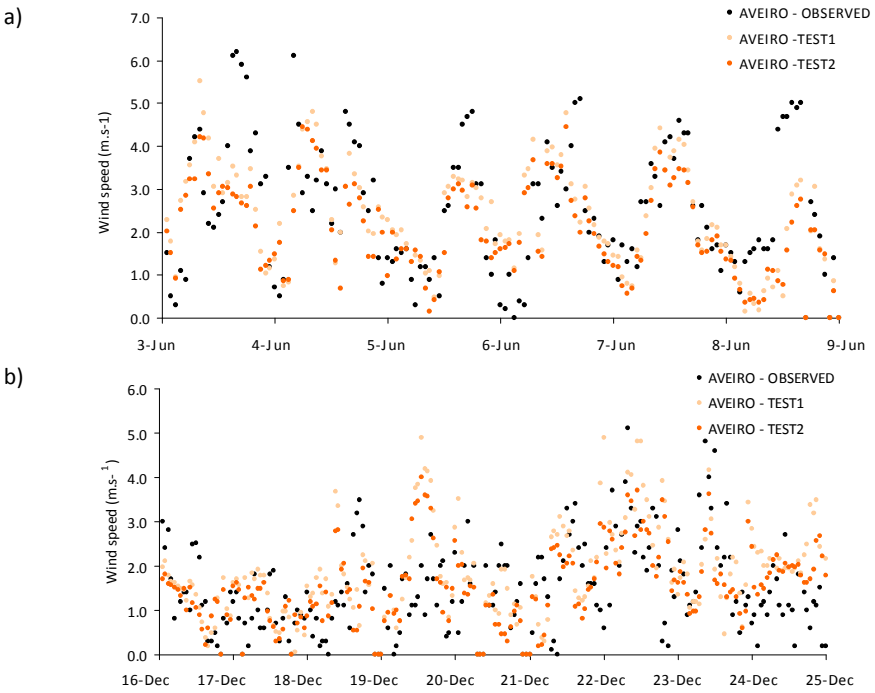

Figure E.5 a) Summer and b) winter, episode time series comparison of wind speed for test2 and test1 in Aveiro, for D4 (1 km resolution).

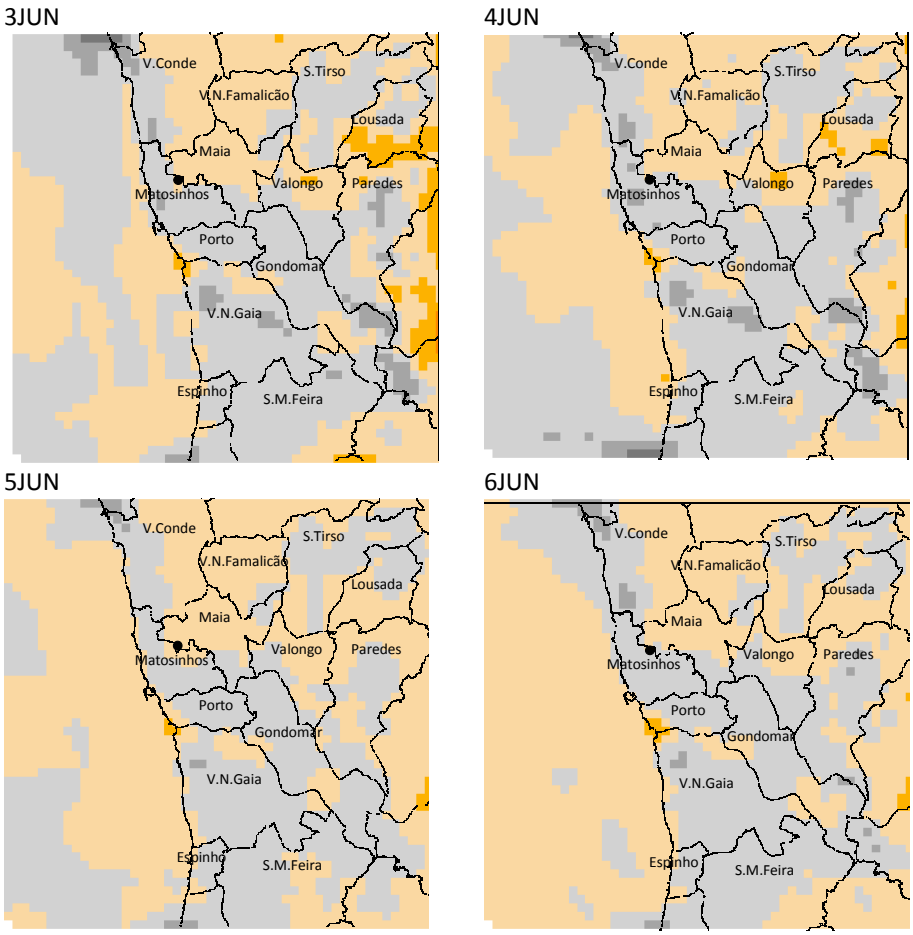

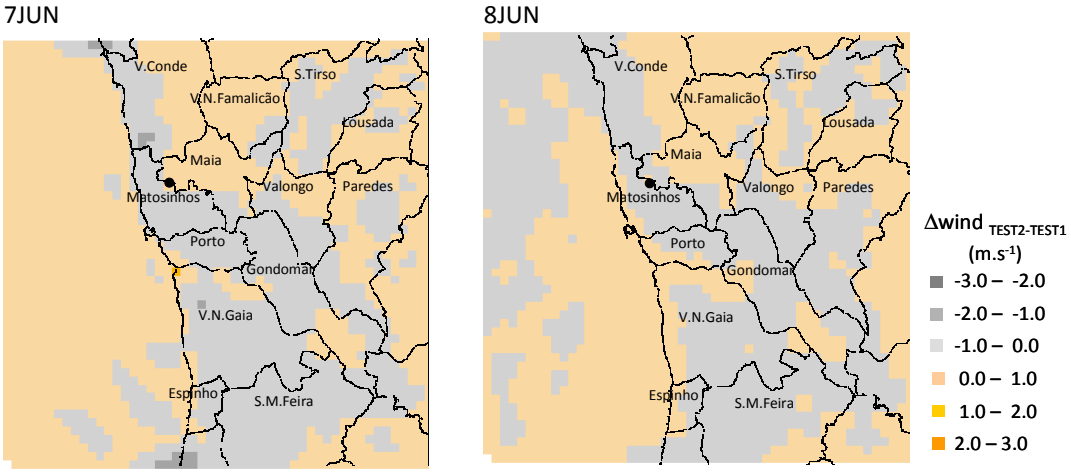

Figure E.6 Spatial plot of daily average wind speed differences (test2 minus test1) between model simulations, for the summer episode.

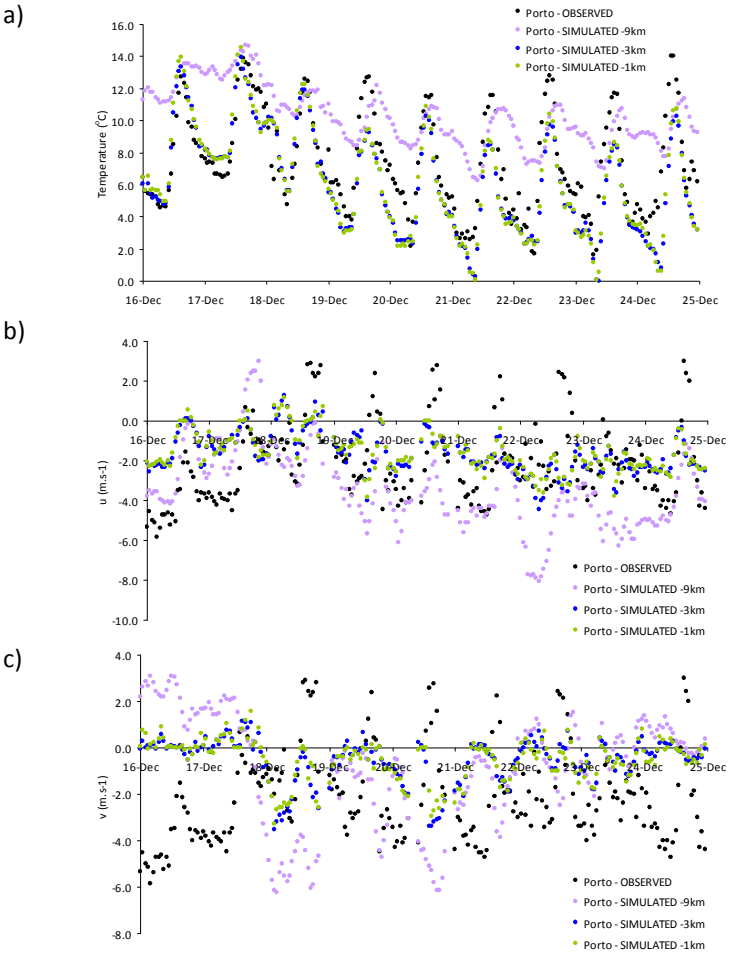

Figure E.7 Winter episode time series comparison of surface a) temperature, b) zonal wind component, and c) meridional wind component from MM5-Test3 simulations at 9 km, 3 km and 1 km, and surface measurements at Porto.

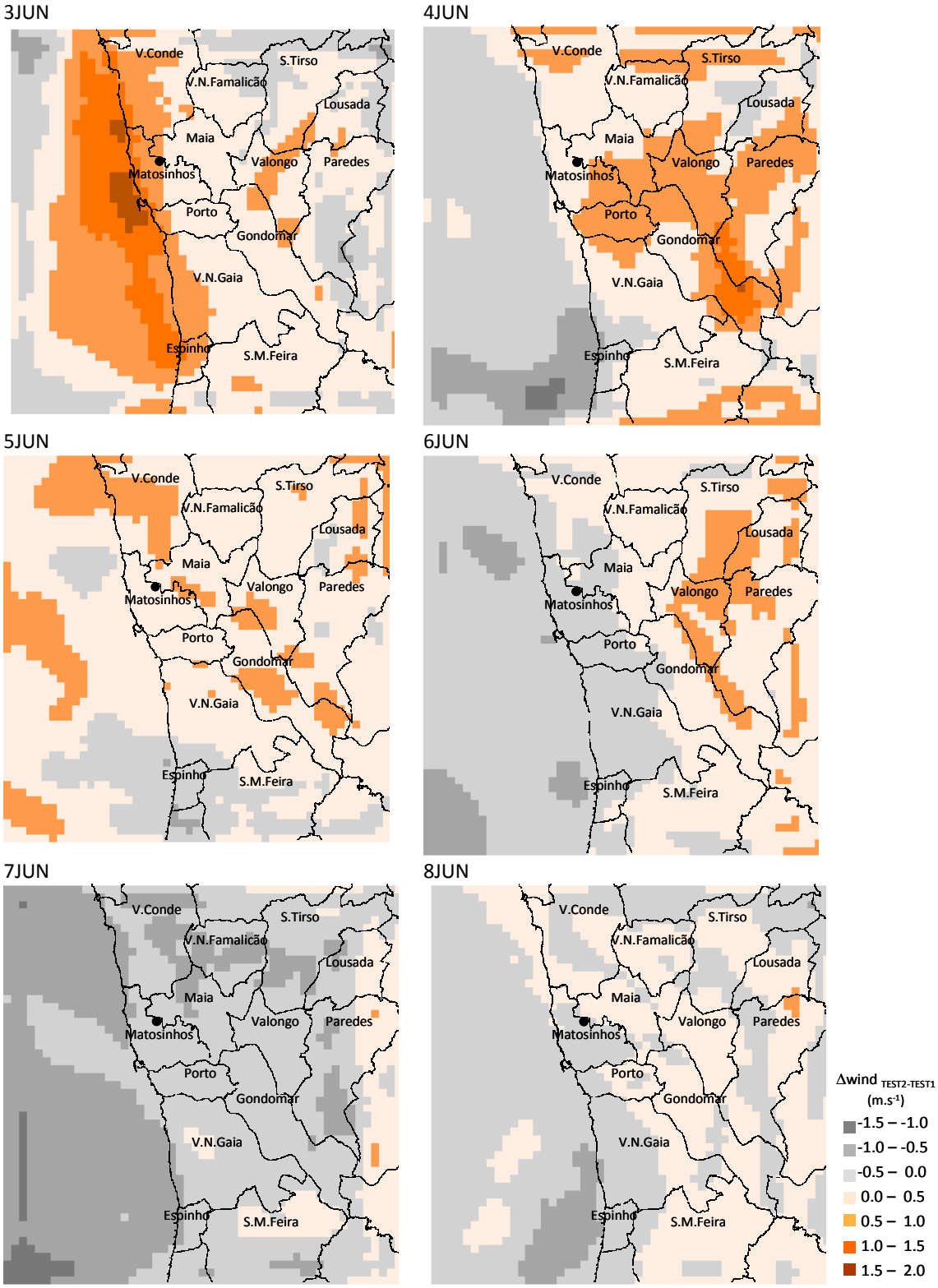

Figure E.8 Spatial plot of daily average wind speed differences (test3 minus test2) between model simulations, for the summer episode.

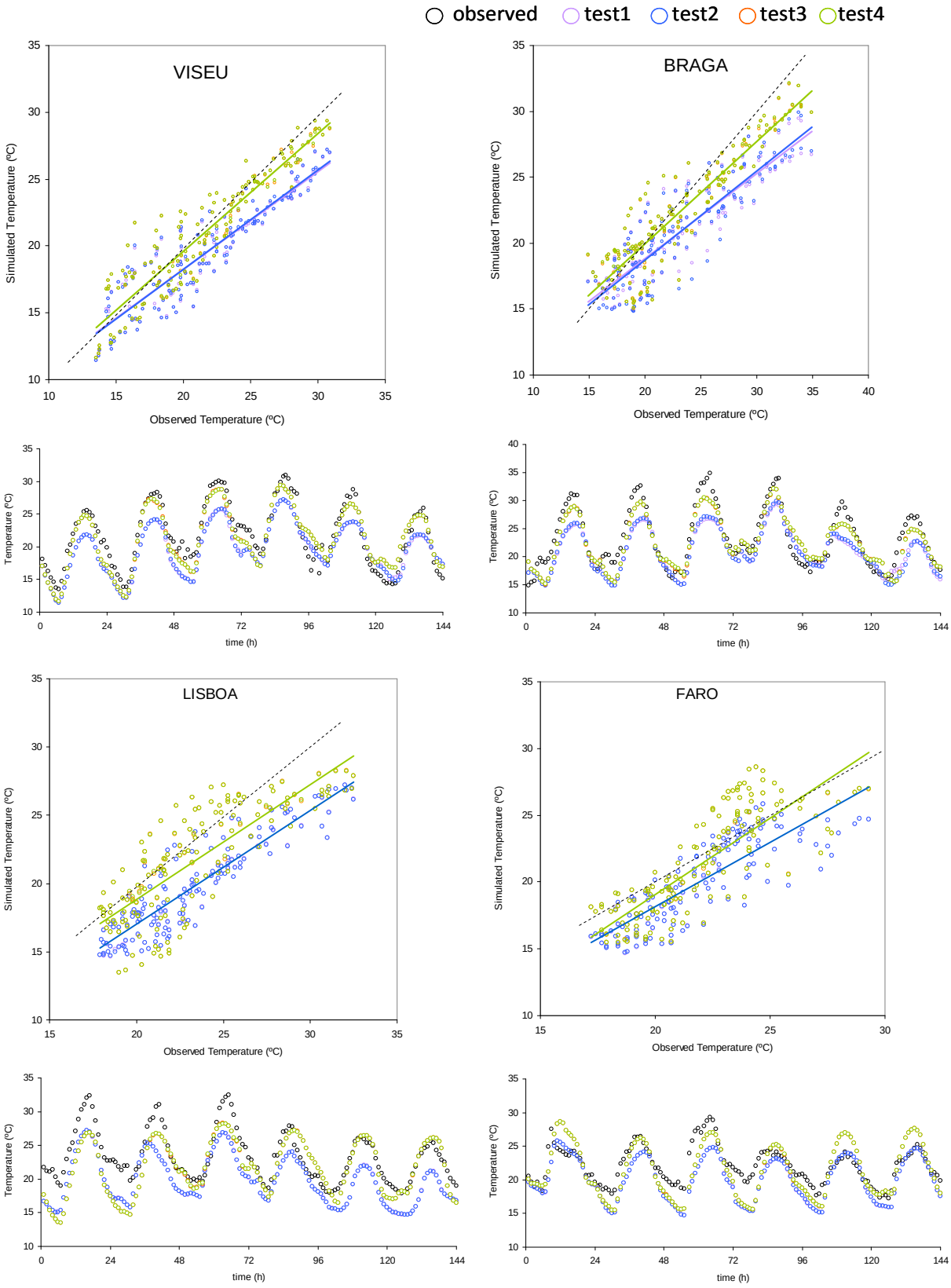

Figure E.9 Scatter diagram of observed versus modelled temperature Viseu and Braga (3 km resolution), and Lisboa and Faro (9 km resolution), summer episode.

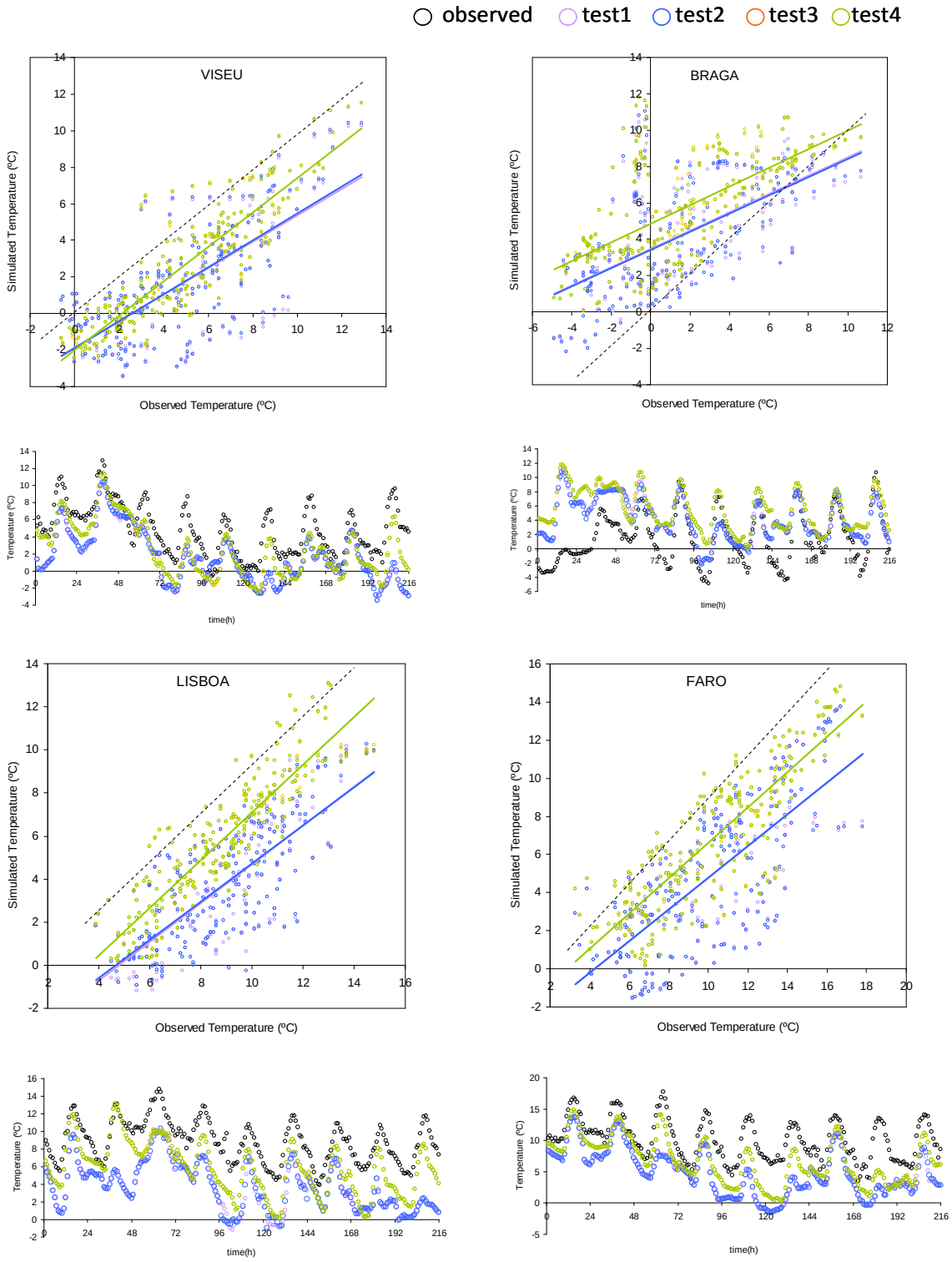

Figure E.10 Scatter diagram of observed versus modelled temperature Viseu and Braga (3 km resolution), and Lisboa and Faro (9 km resolution), winter episode

Appendix F
SPRAWL land use scenario in the study region

Table F.1 Castelo de Paiva municipality land cover data for BASE and SPRAWL.

Land uses	BASE		SPRAWL		Change	
	hectares	%	hectares	%	hectares	%
Artificial surfaces	123.7	1.1%	338.8	3.1%	+215.1	+173.8%
	0	0%	0	0.0%	0.0	0.0%
Continuous urban fabric	93.8	75.8%	239.5	70.7%	+145.6	+155.2%
Discontinuous urban fabric	29.9	24.2%	99.3	29.3%	+69.4	+232.2%
Industrial or commercial units	0	0%	0.0	0.0%	0.0	0.0%
Other artificial surfaces						
Agricultural areas	2782.1	25.2%	2674.6	24.2%	-107.5	-3.9%
Forests and shrub areas	8052.7	72.9%	7945.2	71.9%	-107.6	-1.3%
Other non-artificial surfaces	87.9	0.8%	87.9	0.8%	0.0	0.0%

Table F.2 Espinho municipality land cover data for BASE and SPRAWL.

Land uses	BASE		SPRAWL		Change	
	hectares	%	hectares	%	hectares	%
Artificial surfaces	873.5	46.6%	930.8	49.7%	+57.3	+6.6%
Continuous urban fabric	174.6	20.0%	174.6	18.4%	0.0	0.0%
Discontinuous urban fabric	548.0	62.7%	625.8	65.8%	+57.3	+10.5%
Industrial or commercial units	47.2	5.4%	47.2	5.0%	0.0	0.0%
Other artificial surfaces	103.7	11.9%	103.7	10.9%	0.0	0.0%
Agricultural areas	436.8	23.2%	385.8	20.6%	-51.0	-11.7%
Forests and shrub areas	470.5	25.1%	427.0	22.8%	-43.5	-9.2%
Other non-artificial surfaces	92.0	4.8%	131.1	7.0%	+39.1	+42.5%

Table F.3 Santa Maria da Feira land cover data for BASE and SPRAWL.

Land uses	BASE		SPRAWL		Change	
	hectares	%	Hectares	%	hectares	%
Artificial surfaces	4827.7	22.8%	6619.4	31.3%	+1791.8	+37.1%
Continuous urban fabric	0.0	0.0%	0	0.0%	0.0	0.0%
Discontinuous urban fabric	4130.0	85.6%	5450.6	82.3%	+1319.7	31.9%
Industrial or commercial units	618.9	12.8%	1091.0	16.5%	+472.1	+76.3%
Other artificial surfaces	77.8	1.6%	77.8	1.2%	0.0	0.0%
Agricultural areas	5502.8	26.0%	4556.5	21.6%	-946.3	-17.2%
Forests and shrub areas	10799.2	51.1%	9953.7	47.1%	-845.5	-7.8%
Other non-artificial surfaces	6.5	0.0%	6.5	0.0%	0.0	0.0%

Table F.4 Felgueiras municipality land cover data for BASE and SPRAWL.

Land uses	BASE		SPRAWL		Change	
	hectares	%	hectares	%	hectares	%
Artificial surfaces	1115.5	9.8%	1673.9	14.8%	+558.4	+50.1%
Continuous urban fabric	0.0	0.0%	0.0	0.0%	0.0	0.0%
Discontinuous urban fabric	1057.9	94.8%	1541.8	92.1%	+483.9	+45.7%
Industrial or commercial units	57.6	5.2%	132.2	7.9%	+74.5	+129.3%
Other artificial surfaces	0.0	0.0%	0.0	0.0%	0.0	0.0%
Agricultural areas	6618.5	58.4%	6263.6	55.2%	-354.9	-5.4%
Forests and shrub areas	3603.6	31.8%	3400.1	30.0%	-203.5	-5.6%
Other non-artificial surfaces	0.0	0.0%	0.0	0.0%	0.0	-

Table F.5 Gondomar municipality land cover data for BASE and SPRAWL.

Land uses	BASE		SPRAWL		Change	
	hectares	%	hectares	%	hectares	%
Artificial surfaces	2701.8	20.2%	3449.4	25.8%	+747.6	+27.7%
Continuous urban fabric	117.0	4.3%	117.0	3.4%	0.0	0.0%
Discontinuous urban fabric	2441.0	90.3%	3060.6	88.7%	+619.6	+25.4%
Industrial or commercial units	95.5	3.5%	223.5	6.5%	+128.0	+134.1%
Other artificial surfaces	48.4	1.8%	48.4	1.4%	0.0	0.0%
Agricultural areas	3155.3	23.6%	2766.2	20.7%	-389.1	-12.3%
Forests and shrub areas	6908.9	51.6%	6550.3	48.9%	-358.5	-5.2%
Other non-artificial surfaces	618.1	4.6%	618.1	4.6%	0.0	0.0%

Table F.6 Lousada municipality land cover data for BASE and SPRAWL.

Land uses	BASE		SPRAWL		Change	
	hectares	%	hectares	hectares	hectares	%
Artificial surfaces	676.2	7.1%	1206.6	12.7%	+530.4	+78.4%
Continuous urban fabric	0.0	0.0%	0.0	0.0%	0.0	0.0%
Discontinuous urban fabric	590.6	87.3%	1045.0	86.6%	+454.4	+76.9%
Industrial or commercial units	85.6	12.7%	161.5	13.4%	+75.9	+88.7%
Other artificial surfaces	0.0	0.0%	0.0	0.0%	0.0	0.0%
Agricultural areas	5095.9	53.5%	4820.5	50.6%	-275.4	-5.4%
Forests and shrub areas	3753.1	39.4%	3498.1	36.7%	-255.0	-6.8%
Other non-artificial surfaces	0.0	0.0%	0.0	0.0%	0.0	0.0%

Table F.7 Marco de Canaveses municipality land cover data for BASE and SPRAWL.

Land uses	BASE		SPRAWL		Change	
	hectares	%	hectares	%	hectares	%
Artificial surfaces	695.0	3.4%	1286.5	6.4%	+591.6	+85.1%
Continuous urban fabric	0.0	0.0%	0.0	0.0%	0.0	0.0%
Discontinuous urban fabric	503.6	72.5%	1026.9	79.8%	+523.3	+103.9%
Industrial or commercial units	31.9	4.6%	100.2	7.8%	+68.3	214.4%
Other artificial surfaces	159.5	22.9%	159.5	12.4%	0.0	0.0%
Agricultural areas	9988.1	49.3%	9567.6	47.6%	-420.5	-4.2%
Forests and shrub areas	8241.6	40.6%	8070.5	40.1%	-171.1	-2.1%
Other non-artificial surfaces	1351.7	6.7%	1193.4	5.9%	-158.3	-11.7%

Table F.8 Matosinhos municipality land cover data for BASE and SPRAWL.

Land uses	BASE		SPRAWL		Change	
	hectares	%	hectares	%	hectares	%
Artificial surfaces	3421.4	55.3%	4219.7	68.2%	+798.3	+23.3%
Continuous urban fabric	495.6	14.5%	495.6	11.7%	0.0	0.0%
Discontinuous urban fabric	1837.1	53.7%	2376.6	56.3%	+539.5	+29.4%
Industrial or commercial units	897.1	26.2%	1155.9	27.4%	+258.8	+28.8%
Other artificial surfaces	191.7	5.6%	191.7	4.5%	0.0	0.0%
Agricultural areas	1979.2	32.0%	1361.8	22.0%	-617.4	-31.2%
Forests and shrub areas	651.9	10.5%	471.0	7.6%	-180.9	-27.8%
Other non-artificial surfaces	132.8	2.1%	132.8	2.1%	0.0	0.0%

Table F.9 Póvoa de Varzim municipality land cover data for BASE and SPRAWL.

Land uses	BASE		SPRAWL		Change	
	hectares	%	hectares	%	hectares	%
Artificial surfaces	1259.5	16.0%	1553.3	19.8%	+293.8	+23.3%
Continuous urban fabric	235.7	20.1%	253.7	16.3%	0.0	0.0%
Discontinuous urban fabric	858.3	68.2%	1094.2	70.4%	+235.8	+27.5%
Industrial or commercial units	54	4.3%	111.9	7.2%	+58.0	+107.5%
Other artificial surfaces	93.5	7.4%	93.5	6.0%	0.0	0.0%
Agricultural areas	4775.4	60.8%	4599.3	58.6%	-176.2	-3.7%
Forests and shrub areas	1675.6	21.3%	1558.0	19.8%	-117.7	-7.0%
Other non-artificial surfaces	139.9	1.8%	139.9	1.8%	0.0	0.0%

Table F.10 Paredes municipality land cover data for BASE and SPRAWL.

Land uses	BASE		SPRAWL		Change	
	hectares	%	hectares	%	hectares	%
Artificial surfaces	1777.0	11.4%	2572.8	16.5%	+795.8	+44.8%
Continuous urban fabric	0.0	0.0%	0.0	0.0%	0.0	0.0%
Discontinuous urban fabric	1521.3	85.6%	2106.6	81.9%	+585.4	+38.5%
Industrial or commercial units	193.9	10.9%	404.3	15.7%	+210.4	+108.5%
Other artificial surfaces	61.8	3.5%	61.8	2.4%	0.0	0.0%
Agricultural areas	5356.5	34.3%	4877.4	31.2%	-479.1	-8.9%
Forests and shrub areas	8491.5	54.3%	8174.8	52.3%	-316.7	-3.7%
Other non-artificial surfaces	0.0	0.0%	0.0	0.0%	0.0	0.0%

Table F.11 Paços de Ferreira municipality land cover data for BASE and SPRAWL.

Land uses	BASE		SPRAWL		Change	
			hectares	%	hectares	%
Artificial surfaces	1408.0	19.4%	2169.3	29.9%	+761.3	+54.1%
Continuous urban fabric	0.0	0.0%	0.0	0.0%	0.0	0.0%
Discontinuous urban fabric	1316.8	93.5%	1924.0	88.7%	+607.2	+46.1%
Industrial or commercial units	70.3	5.0%	224.4	10.3%	+154.1	+219.3%

Other artificial surfaces	20.9	1.5%	20.9	1.0%	0.0	0.0%
Agricultural areas	2866.7	39.5%	2347.1	32.3%	-519.6	-18.1%
Forests and shrub areas	2981.1	41.1%	2739.4	37.8%	-241.6	-8.1%
Other non-artificial surfaces	0.0	0.0%	0.0	0.0%	0.0	0.0%

Table F.12 Penafiel municipality land cover data for BASE and SPRAWL.

Land uses	BASE		SPRAWL		Change	
	hectares	%	hectares	%	hectares	%
Artificial surfaces	1129.2	5.2%	1958.0	9.1%	+828.8	+73.4%
Continuous urban fabric	0.0	0.0%	0.0	0.0%	0.0	0.0%
Discontinuous urban fabric	822.5	72.8%	1416.9	72.4%	+594.3	+72.3%
Industrial or commercial units	91.9	8.1%	326.4	16.7%	+234.5	+255.2%
Other artificial surfaces	214.7	19.0%	214.7	11.0%	0.0	0.0%
Agricultural areas	9559.0	44.4%	9098.9	42.2%	-460.0	-4.8%
Forests and shrub areas	10458.4	48.6%	10089.6	46.8%	-368.8	-3.5%
Other non-artificial surfaces	391.6	1.8%	391.6	1.8%	0.0	0.0%

Table F.13 Porto municipality land cover data for BASE and SPRAWL.

Land uses	BASE		SPRAWL		Change	
	hectares	%	hectares	%	hectares	%
Artificial surfaces	3525.5	91.5%	3790.6	98.4%	+265.0	+7.5%
Continuous urban fabric	1763.3	50.0%	2076.5	54.8%	+313.2	+17.8%
Discontinuous urban fabric	1462.4	41.5%	1206.7	31.8%	-255.7	-17.5%
Industrial or commercial units	121.1	3.4%	358.1	9.4%	+236.9	+195.6%
Other artificial surfaces	178.7	5.1%	149.4	3.9%	-29.3	-16.4%
Agricultural areas	265.7	6.9%	0.7	0.0%	-265.0	-99.7%
Forests and shrub areas	14.7	0.4%	14.7	0.4%	0.0	0.0%
Other non-artificial surfaces	46.6	1.2%	46.6	1.2%	0.0	0.0%

Table F.14 São João da Madeira municipality land cover data for BASE and SPRAWL.

Land uses	BASE		SPRAWL		Change	
	hectares	%	hectares	%	hectares	%
Artificial surfaces	601.2	71.7%	677.2	80.8%	+76.1	+12.7%
Continuous urban fabric	96.9	16.1%	96.9	14.3%	0.0	0.0%
Discontinuous urban fabric	327.6	54.5%	336.9	49.8%	+9.3	+2.8%
Industrial or commercial units	176.7	29.4%	243.4	35.9%	+66.7	+37.8%
Other artificial surfaces	0	0.0%	0.0	0.0%	0.0	0.0%
Agricultural areas	162.1	19.3%	95.4	11.4%	-66.7	-41.2%
Forests and shrub areas	75.3	9.0%	66.0	7.9%	-9.3	-12.4%
Other non-artificial surfaces	0.0	0.0%	0.0	0.0%	0.0	0.0%

Table F.15 Santo Tirso municipality land cover data for BASE and SPRAWL.

Land uses	BASE		SPRAWL		Change	
	hectares	%	hectares	%	hectares	%
Artificial surfaces	1916.5	14.3%	2653.3	20.1%	+736.7	+38.4%
Continuous urban fabric	60.3	3.1%	60.3	2.3%	0.0	0.0%
Discontinuous urban fabric	1673.3	87.3%	2177.3	82.1%	+504.0	+30.1%
Industrial or commercial units	129.5	6.8%	362.3	13.7%	+232.8	+179.8%
Other artificial surfaces	53.4	2.8%	53.4	2.0%	0.0	0.0%
Agricultural areas	5096.7	38.1%	4553.2	34.4%	-543.5	-10.7%
Forests and shrub areas	6211.6	46.4%	6018.4	45.5%	-193.3	-3.1%
Other non-artificial surfaces	153.8	1.1%	0.0	0.0%	-153.8	-100.0%

Table F.16 Vila Nova de Famalicão municipality land cover data for BASE and SPRAWL.

Land uses	BASE		SPRAWL		Change	
	hectares	%	hectares	%	hectares	%
Artificial surfaces	3486.1	17.2%	4369.9	21.5%	+883.8	+25.4%
Continuous urban fabric	69.6	2.0%	69.6	1.6%	0.0	0.0%
Discontinuous urban fabric	2941.8	84.4%	3651.9	83.6%	+710.1	+24.1%
Industrial or commercial units	410.9	11.8%	584.6	13.4%	+173.7	+42.3%
Other artificial surfaces	63.7	1.8%	63.7	1.5%	0.0	0.0%
Agricultural areas	10204.9	50.2%	9817.1	48.3%	-387.8	-3.8%
Forests and shrub areas	6633.2	32.6%	6137.2	30.2%	-435.1	-6.6%
Other non-artificial surfaces	0.0	0.0%	0.0	0.0%	0.0	0.0%

Table F.17 Valongo municipality land cover data for BASE and SPRAWL.

Land uses	BASE		SPRAWL		Change	
	hectares	%	hectares	%	hectares	%
Artificial surfaces	2029.9	27.7%	3087.3	42.1%	+1057.4	+52.1%
Continuous urban fabric	143.8	7.1%	143.8	4.7%	0.0	0.0%
Discontinuous urban fabric	1689.0	83.2%	2353.7	76.2%	+664.6	+39.3%
Industrial or commercial units	184.0	9.1%	576.7	18.7%	+392.7	+213.5%
Other artificial surfaces	13.2	0.6%	13.2	0.4%	0.0	0.0%
Agricultural areas	1078.6	14.7%	587.3	8.0%	-491.2	-45.5%
Forests and shrub areas	4231.3	57.6%	3665.2	49.9%	-566.1	-13.4%
Other non-artificial surfaces	0.0	0.0%	0.0	0.0%	0.0	0.0%

Table F.18 Vila do Conde municipality land cover data for BASE and SPRAWL.

Land uses	BASE		SPRAWL		Change	
	hectares	%	hectares	%	hectares	%
Artificial surfaces	1429.5	9.8%	2055.1	14.0%	+625.6	+43.8%
Continuous urban fabric	141.9	9.9%	141.9	6.9%	0.0	0.0%
Discontinuous urban fabric	1067.0	74.6%	1487.1	72.4%	+420.1	+39.4%
Industrial or commercial units	175.1	12.2%	407.1	19.8%	+232.1	+132.5%
Other artificial surfaces	45.5	3.2%	19.0	0.9%	-26.5	-58.3%
Agricultural areas	8155.1	55.7%	7686.2	52.5%	-468.8	-5.7%
Forests and shrub areas	4816.9	32.9%	4660.2	31.8%	-156.8	-3.3%
Other non-artificial surfaces	244.2	1.7%	244.2	1.7%	0.0	0.0%

Table F.19 Vila Nova de Gaia municipality land cover data for BASE and SPRAWL.

Land uses	BASE		SPRAWL		Change	
	hectares	%	hectares	%	hectares	%
Artificial surfaces	6391.3	38.0%	7531.3	44.8%	+1140.1	+17.8%
Continuous urban fabric	386.4	6.0%	412.0	5.5%	+25.7	+6.6%
Discontinuous urban fabric	5166.6	80.8%	5956.5	79.1%	+189.9	+15.3%
Industrial or commercial units	657.6	10.3%	970.1	12.9%	+312.5	+47.5%
Other artificial surfaces	180.7	2.2%	192.7	2.6%	+12.0	+6.6%
Agricultural areas	5386.6	32.0%	4730.5	28.1%	-656.1	-12.2%
Forests and shrub areas	4347.0	25.8%	3863.0	23.0%	-484.0	-11.1%
Other non-artificial surfaces	692.1	4.1%	692.1	4.1%	0.0	0.0%

Table F.20 Trofa municipality land cover data for BASE and SPRAWL.

Land uses	BASE		SPRAWL		Change	
	hectares	%	hectares	%	hectares	%
Artificial surfaces	1251.3	17.1%	1691.5	23.2%	+440.2	+35.2%
Continuous urban fabric	33.4	2.7%	33.4	2.0%	0.0	0.0%
Discontinuous urban fabric	1093.7	87.4%	1448.6	85.6%	+354.9	+32.4%
Industrial or commercial units	111.7	8.9%	203.2	12.0%	+91.5	+81.9%
Other artificial surfaces	12.4	1.0%	6.2	0.4%	-6.2	-50.0%
Agricultural areas	2162.0	29.6%	2017.1	27.7%	2017.1	-6.7%
Forests and shrub areas	3887.7	53.2%	3586.1	49.2%	3586.1	-7.8%
Other non-artificial surfaces	0.0	0.0%	0.0	0.0%	0.0	0.0%